

School of Civil and Mechanical Engineering

**Properties of Concrete using Ferronickel Slag
as Fine Aggregate**

Ashish Kumer Saha

**This thesis is presented for the Degree of
Doctor of Philosophy
of
Curtin University**

December 2018

Dedicated

to my parents and sister for their encouragement and inspiration

&

to my lovely wife for her patience and sacrifices

DECLARATION

To the best of my knowledge and belief this thesis contains no material previously published by any other person except where due acknowledgment has been made.

This thesis contains no material that has been accepted for the award of any other degree or diploma in any university.

Signature:  _____

Date: 10/12/2018

ACKNOWLEDGEMENT

First of all, I would like to express my gratitude to God, the source of all energy and blessings that lead this study to fulfilment and kept me free from any major injuries in past three and a half years.

I would like to express my best regards to Associate Professor Prabir Sarker for trust in me. I am grateful for his steady invaluable support, encouragement and guidance throughout this research project.

I would like to thank Associate Professor Faiz Shaikh for his keen support in this research and guidance as my co-supervisor.

I gratefully thank SLN, New Caledonia for providing funding for my study and Curtin University for providing an ERAMET/CIPRS scholarship.

I would like to acknowledge the valuable comments and advices that I received in different stages from Professor Abhijit Mukherjee, Professor Vladimir Golovanevskiy, Dr Dipok Chandra Sarker, Md. Ashiqur Rahman, MNN Khan and Subhra Majhi.

I gratefully acknowledge the helps of laboratory technical staff Mr Robert Cutter, Mr Ashley Hughes, Mr Mick Elliss, Mr Mark Whittaker, Mr Luke English and Mr Craig Gwyther.

I acknowledge the use of equipment, scientific and technical assistance of the Microscopy and Microanalysis Facility, John de Laeter Centre and Chemical Engineering laboratory, Curtin University.

ABSTRACT

Application of various industrial by-products has been extensively studied in the past few decades in order to enhance the sustainability of construction industry. A large quantity of granulated ferronickel slag (FNS) is generated as a by-product during production of nickel alloy. Application of FNS as a replacement of sand in concrete will bring major benefits towards sustainable constructions. A series of experimental works were conducted in this study in order to evaluate the effects of using FNS fine aggregate in cement mortar and concrete.

Various properties of FNS aggregate were determined first. The grain size distribution of the slag was found to be suitable for using as a fine aggregate in concrete. Density and water absorption of FNS aggregates were within the allowable limits according to the Australian Standard 2758.1. It was found that flow of fresh mortar increased with the increase of FNS up to 50% replacement of natural sand and then declined with further increase of FNS. Compressive strength of hardened mortar specimens increased with the increase of FNS up to 50% and then declined with further increase of FNS. Use of fly ash as 30% cement replacement together with FNS as replacement of sand increased the flow of fresh mortar and decreased the strength of hardened specimens. Workability, compressive strength, splitting tensile strength, flexural strength, modulus of elasticity and leaching characteristics of concrete containing FNS aggregates were then evaluated. It was found that the use of 50% FNS with natural sand resulted in a well-graded fine aggregate and thus maximized the strength development. The 28-day compressive strengths of the concrete mixtures containing 50% FNS were 66 MPa and 51 MPa for no fly ash and 30% fly ash, respectively. The splitting tensile strength, flexural strength and modulus of elasticity of concrete containing 50% and 100% FNS correlated well with the compressive

strength, which is similar to the correlation for concrete containing 100% natural sand. The equations of design Codes and Standards are found conservative in the prediction of these properties from a specified compressive strength when FNS is used as a replacement of natural sand. The FNS was found environmentally compatible since leaching of heavy metals was far below the regulatory limits.

The potential alkali silica reaction (ASR) of ferronickel slag (FNS) aggregate was investigated by accelerated mortar bar test (AMBT) method. The test results indicated potential alkali silica reactivity of FNS when no supplementary cementitious material (SCM) was used with cement. There were visible surface cracks on the specimens using no fly ash or 10% fly ash. Use of 20% fly ash reduced expansion by 45% as compared to that with 10% fly ash. In accordance with the expansion limits of Australian Standard, the mixtures using 20% and 30% fly ash were categorised as slowly-reactive and non-reactive, respectively. Thermogravimetric analysis (TGA) and microstructural observations confirmed the effectiveness of fly ash to reduce portlandite that helped reduce the ASR expansion.

Durability related properties of concrete using FNS aggregate up to 100% replacement of natural sand and fly ash as 30% replacement of cement were studied. The volume of permeable voids (VPV) of concrete was found to increase with the increase of FNS aggregate. As a result, sorptivity and chloride permeability showed increasing trends with the increase of FNS aggregate. However, the pozzolanic reaction of fly ash reduced porosity of concrete as evidenced by scanning electron microscopy and energy-dispersive X-ray spectroscopy. The specimens with FNS aggregate and fly ash were classified as “excellent” in terms of VPV, “low” in terms of the chloride permeability and “good” in terms of sorptivity. Use of fly ash also reduced the strength losses of FNS aggregate concrete subjected to alternate wet-dry cycles. Furthermore, no explosive spalling was

observed in concrete using FNS aggregate after exposure to temperatures up to 800 °C for 2 hours. The use of FNS aggregate did not affect the residual compressive strength of concrete. Increase of thermal conductivity of concrete was observed with the increase of FNS aggregate. This is attributed to the increase of void content by the high volumes of FNS aggregate.

Overall, the use of FNS fine aggregate together with other by-product SCMs such as fly ash or ground FNS was found as a promising alternative for the production of green concrete.

LIST OF PUBLICATIONS

Journal:

1. Saha, A. K., Khan, M. N. N., & Sarker, P. K. (2018). Value added utilization of by-product electric furnace ferronickel slag as construction materials: A review. *Resources, Conservation and Recycling*, 134, 10-24.
2. Saha, A. K., Sarker, P. K., & Majhi, S. (2018). Effect of elevated temperatures on concrete incorporating ferronickel slag as fine aggregate. *Fire and Materials*. Doi: 10.1002/fam.2664
3. Saha, A. K., & Sarker, P. K. (2018). Durability of Mortar Incorporating Ferronickel Slag Aggregate and Supplementary Cementitious Materials Subjected to Wet–Dry Cycles. *International Journal of Concrete Structures and Materials*, 12(1), 29.
4. Saha, A. K., & Sarker, P. K. (2018). Potential alkali silica reaction expansion mitigation of ferronickel slag aggregate by fly ash. *Structural Concrete*. Doi:10.1002/suco.201700273
5. Saha, A. K., & Sarker, P. K. (2017). Sustainable use of ferronickel slag fine aggregate and fly ash in structural concrete: mechanical properties and leaching study. *Journal of Cleaner Production*, 162, 438-448.
6. Saha, A. K., & Sarker, P. K. (2017). Durability characteristics of concrete using ferronickel slag fine aggregate and fly ash. *Magazine of Concrete Research*, 70(17), 865–874
7. Saha, A. K., & Sarker, P. K. (2017). Compressive strength of mortar containing ferronickel slag as replacement of natural sand. *Procedia engineering*, 171, 689-694.
8. Saha, A. K., & Sarker, P. K. (2016). Expansion due to alkali-silica reaction of ferronickel slag fine aggregate in OPC and blended cement mortars. *Construction and Building Materials*, 123, 135-142.

Conference:

1. Saha, A. K., & Sarker, P. K. (2017). Effect of fly ash on the potential alkali silica reaction of ferronickel slag aggregate. One Curtin International Postgraduate Conference (OCPC) 2017, Miri, Sarawak, Malaysia.
2. Saha, A. K., & Sarker, P. K. (2017). Sorptivity and chloride permeability of concrete using ferronickel slag as fine aggregate. 28th Biennial National Conference of the Concrete Institute of Australia, Adelaide, South Australia.

TABLE OF CONTENTS

DECLARATION	i
ACKNOWLEDGEMENT	ii
ABSTRACT	iii
LIST OF PUBLICATIONS	vi
TABLE OF CONTENTS	vii
LIST OF FIGURES	xii
LIST OF TABLES	xv
NOMENCLATURE	xvi
ABBREVIATIONS	xvii

PART I: INTRODUCTION AND LITERATURE REVIEW

Chapter 1: INTRODUCTION	1
1.1 Background	1
1.2 Problem statement	4
1.3 Research objectives	4
1.4 Research approach and thesis organisation	5
1.5 References	7
Chapter 2: USE OF FERRONICKEL SLAG (FNS) IN CONCRETE	9
2.1 Overview	9
2.2 Properties of FNS	11
2.3 Performance of FNS as aggregate in concrete	13
<i>2.3.1 Fresh properties</i>	13
2.3.1.1 Workability	13
2.3.1.2 Bleeding	14
<i>2.3.2 Hardened properties</i>	15
2.3.2.1 Compressive strength	15

2.3.2.2 Modulus of elasticity	16
2.3.2.3 Flexural and tensile strengths	16
2.3.3 <i>Durability properties</i>	17
2.3.3.1 Alkali-silica reaction	17
2.3.3.2 Freezing and thawing resistance	20
2.3.3.3 Drying shrinkage	21
2.3.3.4 Air permeability and carbonation	22
2.3.4 <i>Applications in pavement construction</i>	23
2.4 Ground FNS as a supplementary binder in concrete	24
2.5 Use of FNS in geopolymers	27
2.6 Environmental effects	31
2.7 Limitations and challenges	33
2.8 Summary	35
2.9 References	37

PART II: MECHANICAL PROPERTIES

Chapter 3: WORKABILITY & STRENGTH PROPERTIES OF MORTAR USING FNS AGGREGATE	45
3.1 Overview	45
3.2 Materials and Methods	47
3.3 Results and Discussion	49
3.3.1 <i>Workability of mortar</i>	49
3.3.2 <i>Compressive strength</i>	50
3.4 Summary	53
3.5 References	54

Chapter 4: MECHANICAL PROPERTIES AND LEACHING STUDY OF CONCRETE USING FNS AGGREGATE	56
4.1 Overview	56
4.2 Experimental Work	58

4.2.1 <i>Materials</i>	58
4.2.2 <i>Mixture proportions and test methods</i>	60
4.3 Results and Discussion	63
4.3.1 <i>Workability & Air content</i>	63
4.3.2 <i>Compressive strength</i>	66
4.3.3 <i>Splitting tensile strength</i>	68
4.3.4 <i>Flexural strength</i>	71
4.3.5 <i>Modulus of elasticity</i>	72
4.3.6 <i>Leaching characteristics of hardened concrete</i>	74
4.4 Correlation of the mechanical properties with compressive strength	76
4.5 Summary	82
4.6 References	84

PART III: DURABILITY RELATED PROPERTIES

Chapter 5: POTENTIAL ALKALI SILICA REACTION OF FNS AGGREGATE	86
5.1 Overview	87
5.2 Experimental Work	88
5.2.1 <i>Materials</i>	88
5.2.2 <i>Mixture proportions and test methods</i>	89
5.3 Results	91
5.3.1 <i>Compressive strength</i>	91
5.3.2 <i>Porosity</i>	91
5.3.3 <i>AMBT results</i>	92
5.3.4 <i>Effect of AMBT exposure on compressive strength</i>	95
5.3.5 <i>Thermogravimetric analysis</i>	96
5.3.6 <i>Microstructure analysis by SEM and EDS</i>	99
5.4 Discussion	103
5.5 Summary	104
5.6 References	106

Chapter 6: USE OF FLY ASH AND BLAST FURNACE SLAG TO MITIGATE POTENTIAL ASR OF FNS AGGREGATE	109
6.1 Overview	109
6.2 Experimental Work	111
<i>6.2.1 Materials</i>	111
<i>6.2.2 Mixture proportions and test methods</i>	112
6.3 Results and Discussion	114
<i>6.3.1 Mortar bar expansion</i>	114
<i>6.3.2 Microstructural investigation by SEM and EDS</i>	120
6.4 Summary	123
6.5 References	125
Chapter 7: RESISTANCE OF CONCRETE USING FNS AGGREGATE TO ALTERNATE WET-DRY CYCLES	127
7.1 Overview	127
7.2 Experimental Work	129
<i>7.2.1 Materials</i>	129
<i>7.2.2 Mixture proportions and test methods</i>	130
7.3 Results and Discussion	133
<i>7.3.1 Volume of permeable voids</i>	133
<i>7.3.2 Sorptivity coefficient</i>	134
<i>7.3.3 Chloride permeability</i>	136
<i>7.3.4 Effect of wet–dry cycles</i>	137
7.3.4.1 Strength and mass variations due to wet–dry cycles	137
7.3.4.2 Microstructural observation after wet–dry cycles	142
7.4 Summary	144
7.5 References	146
Chapter 8: EFFECT OF ELEVATED TEMPERATURES ON CONCRETE INCORPORATING FNS AGGREGATE	148

8.1 Overview	148
8.2 Experimental Work	153
<i>8.2.1 Materials</i>	153
<i>8.2.2 Mixture proportions and test methods</i>	153
8.3 Results and Discussion	156
<i>8.3.1 Core temperature of concrete</i>	156
<i>8.3.2 Mass loss of concrete after elevated temperature exposure</i>	158
<i>8.3.3 Strength of concrete after heat exposure</i>	159
<i>8.3.4 Ultrasonic pulse velocity after elevated temperature exposure</i>	164
<i>8.3.5 Relationship between compressive strength and UPV</i>	167
<i>8.3.6 Microstructural observation</i>	169
8.4 Summary	171
8.5 References	173

PART IV: CONCLUSIONS AND RECOMMENDATIONS

Chapter 9: CONCLUDING REMARKS	175
9.1 Research impacts	175
9.2 Main research findings	176
9.3 Recommendations for future study	180
APPENDICES	181
APPENDIX A: Images of experiments	182
APPENDIX B: Mortar results	189
APPENDIX C: Concrete results	194
APPENDIX D: Attribution of research outputs	198
APPENDIX E: Copyright permission	201

LIST OF FIGURES

Fig. 1.1 Flow chart of concrete production	2
Fig. 1.2 Effect of Sand Dragging on Aquatic ecosystem	3
Fig. 2.1 FNS (a) air-cooled and (b) water-cooled (Choi & Choi, 2015)	11
Fig. 2.2 Bleeding of FNS concrete	15
Fig. 2.3 Microstructure of ASR affected FNS specimen (Choi & Choi, 2015)	18
Fig. 2.4 Influence of class F fly ash in FNS samples as an ASR mitigation technique (Choi & Choi, 2015)	19
Fig. 2.5 Phase analysis of raw FNS and FNS blended cement pastes (Rahman et al., 2017)	26
Fig. 2.6 Microstructure of fly ash geopolymer with (a) 0% FNS and (b) 20% FNS. (F-fly ash particles, H-HMNS particles, G-gel phase formed.) (Yang et al., 2014)	29
Fig. 2.7 XRD analysis of geopolymers with FNS under various conditions (A: 60 °C–24 h–7 d; B: 60 °C–24 h–28 d; C: 60 °C–48 h–28 d; D: 80 °C–48 h–28 d; 1: Kaolinite, 2: Maghemite, 3: Magnetite, 4: Quartz, 5: Sodalite) (Komnitsas et al., 2007)	30
Fig. 3.1 Gradation of fine aggregates	47
Fig. 3.2 Flow test (a) 100% sand; (b) 50% FNS and 50% sand (c) 100% FNS	49
Fig. 3.3 Flow value of mortar mixes	50
Fig. 3.4 Compressive strength of the mixtures with 100% OPC (Series A)	51
Fig. 3.5 Compressive strength of the mixtures with 30% fly ash and 70% OPC (series B)	52
Fig. 3.6 Effect of fly ash on compressive strength development (50% FNS as aggregate)	52
Fig. 4.1 Concrete breakwaters using ferronickel slag aggregates as 30% replacement of natural sand	58
Fig. 4.2 (a) FNS aggregate; (b) sand and (c) Coarse aggregate	60
Fig. 4.3 Slump of concrete with different percentages of FNS aggregate	64
Fig. 4.4 Air content of concrete with different percentages of FNS aggregate	65

Fig. 4.5 Samples after compressive strength test (left: PC-FNS0, middle: PC-FNS50 right: PC-FNS100)	66
Fig. 4.6 Mean compressive strengths (Error bars at one standard deviation)	67
Fig. 4.7 Mean splitting tensile strengths (Error bars at one standard deviation)	69
Fig. 4.8 Cracking pattern after splitting tensile strength test; (a) 100% sand (b) 100% FNS	70
Fig. 4.9 Mean flexural strengths of concrete (Error bars at one standard deviation)	71
Fig. 4.10 Mean modulus of elasticity (Error bars at one standard deviation)	73
Fig. 4.11 Relationship between splitting tensile strength and compressive strength	79
Fig. 4.12 Relationship between flexural strength and compressive strength	80
Fig. 4.13 Relationship between compressive strength and Modulus of elasticity	81
Fig. 5.1 Volume of permeable voids of mortar with respect to fly ash percentage	92
Fig. 5.2 ASR expansion of mortar bars containing different percentages of fly ash	93
Fig. 5.3 Visual inspection of AMBT samples after 21 days exposure	94
Fig. 5.4 Thermogravimetric mass changes of paste samples exposed to AMBT condition	98
Fig. 5.5 SEM and EDS of specimens after 21 days of NaOH exposure	102
Fig. 6.1 Length measurement of a mortar bar specimen	113
Fig. 6.2 ASR expansions of the mixtures of 100% OPC (Series A)	115
Fig. 6.3 ASR expansions of the mixtures of 70% OPC and 30% fly ash (Series B)	117
Fig. 6.4 ASR expansions of the mixtures of 70% OPC and 30% GGBFS (Series C)	118
Fig. 6.5 Variation of expansion with the percentage of FNS	119
Fig. 6.6 SEM and EDS data of, (a) Mix A1; (b) Mix A5; (c) Mix B1; (d) Mix B5; (e) Mix C1 and (f) Mix C5	122
Fig. 7.1 Variation of the volume of permeable voids with FNS content in concrete	133

Fig. 7.2 Variation of sorptivity with FNS content	135
Fig. 7.3 Charged passed during rapid chloride permeability test	136
Fig. 7.4 Physical appearance of PC-FNS100 samples after wet dry cycles	138
Fig. 7.5 Compressive strengths comparison due to wet-dry cycles exposure	138
Fig. 7.6 Percentage of strength change by the wet-dry cycles	139
Fig. 7.7 Mass loss due to wet dry cycle exposure	141
Fig. 7.8 SEM and EDS data of the samples after wet-dry cycles	143
Fig. 8.1 Temperature variation with time inside the furnace	155
Fig. 8.2 Variation of core temperature with time	157
Fig. 8.3 Mass loss of concrete due to fire exposure	159
Fig. 8.4 Specimens of mixture FA-FNS50 after different temperature exposures	160
Fig. 8.5 Residual strength after exposure to different temperatures	162
Fig. 8.6 Ultrasonic waveform of FA-FNS50 after different stages of fire exposure	164
Fig. 8.7 Residual UPV of samples after fire exposure	166
Fig. 8.8 Relationship between residual compressive strength and UPV	168
Fig. 8.9 SEM images of samples after 400 °C temperature exposure	170

LIST OF TABLES

Table 2.1 Chemical compositions of nickel slag (mass %)	12
Table 2.2 Physical Properties of FNS aggregate	13
Table 2.3 Freeze and thaw resistance of FNS concrete	20
Table 2.4 Drying shrinkage of FNS concrete	22
Table 3.1 Mix proportions of mortar	48
Table 4.1 Chemical compositions and loss on ignition (LOI) of OPC, FNS & fly ash (mass %)	59
Table 4.2 Physical properties of aggregates	60
Table 4.3 Mix proportions	61
Table 4.4 Mechanical properties of concrete at the age of 28 days	68
Table 4.5 Total dissolved metals in the leachates of concrete containing FNS aggregate and regulatory limits	74
Table 4.6 Relationship between the mechanical properties and compressive strength	76
Table 4.7 Ratio of the experimental to calculated mechanical properties	78
Table 5.1 Mortar mixture proportions	89
Table 5.2 Compressive strength of mortars containing 50% FNS fine aggregate	91
Table 5.3 Effect of AMBT exposure on compressive strength of mortar samples	96
Table 6.1 Mixture proportions of mortars	113
Table 6.2 Limits of AMBT expansion for reactivity classification as per AS1141.60.1	115
Table 6.3 Expansion of mortar bars after 21 days in 1M NaOH solution at 80 °C	116
Table 7.1 Flow time of the fine aggregates	130
Table 7.2 Concrete mix proportions	131
Table 8.1 Concrete mix proportions	154
Table 8.2 Compressive strength and residual strength percentage after fire exposure	161
Table 8.3 UPV results after high-temperature exposure	165

NOMENCLATURE

ρ	Density of concrete	kg/m ³
E / E_c	Modulus of elasticity	MPa
F_c	Compressive strength	MPa
f'_c	Characteristic compressive strength at 28 days	MPa
f_{cf}	Modulus of rupture	MPa
f_{ck}	Characteristic cylinder compressive strength (Eurocode 2)	MPa
f_{ct}	Indirect/uniaxial tensile strength	MPa
f'_{ct}	Characteristic uniaxial tensile strength	MPa,
$f_{ct,f}$	Measured flexural tensile strength	MPa
$f'_{ct,f}$	Mean characteristic flexural tensile strength	MPa
$f_{ct,sp}$	Indirect split tensile strength	MPa
f_{cm}	Mean cylinder compressive strength	MPa
f_{cmi}	Mean in-situ concrete compressive strength	MPa
f_{ctm}	Mean tensile strength (Eurocode 2)	MPa
f_t	Tensile strength	MPa
I	Absorption in sorptivity test	mm
V	Ultrasonic pulse velocity	km/sec

ABBREVIATIONS

ACI	American Concrete Institute
AS	Australian Standards
ASR	Alkali Silica Reaction
ASTM	American Society for Testing and Materials
AVPV	Apparent Volume of Permeable Voids
EDX / EDS	Energy Dispersive X-ray Spectrometer
FNS	Ferronickel slag
GGBFS	Ground Granulated Blast Furnace Slag
LOI	Loss on Ignition
OPC	Ordinary Portland Cement
RH	Relative Humidity
SCM	Supplementary Cementitious Materials
SEM	Scanning Electron Microscope
SH	Sodium Hydroxide (NaOH)
SSD	Saturated Surface Dry
TGA	Thermogravimetric Analysis
UPV	Ultrasonic pulse velocity
VCA	Volume fraction of (oven-dry rodded) Coarse Aggregate
VPV	Volume of Permeable Voids
XRD	X-Ray Diffraction
XRF	X-Ray Florescence

PART I: INTRODUCTION AND LITERATURE REVIEW

Chapter 1: INTRODUCTION

1.1 Background

Manufactured goods are becoming an integral part of our society because of rapid technological progress. However, productions of these goods have adverse environmental impacts. Similarly, civil engineering infrastructures are also one of the manufactured goods, which require a significant amount of resources and energy. In addition, continuous maintenance and repairs are required to ensure the prolonged longevity of these structures. Therefore, sustainable infrastructure development is a matter of great importance for our future existence (Ohno, 2017). Concrete has been the most popular construction material around the world due to the availability of materials, freedom of casting into any shape and high resistance to weathering action. The demand for concrete is rising rapidly due to massive infrastructure developments, especially in countries like China and India.

Concrete production requires a significant quantity of our natural resources including sand, water and stone. An overview of raw materials generally used for concrete production is shown in Fig. 1.1. Among these materials, sand acts as a filler, which occupies about 25 to 35% of the total volume of concrete. Sand also contributes to density, strength and durability properties of concrete. Therefore, good quality sand is essential to produce good quality concrete (Olonade et al., 2018).



Fig. 1.1 Flow chart of concrete production

Generally, river sand is found to be the most suitable and popular for construction purpose because of the presence of crystalline silica, which is chemically inert and stable. The increasing demand of concrete leads to excessive and uncontrolled dredging in various parts of the world (Davis et al., 2000). Uncontrolled dredging causes severe damage to the aquatic environment (Padmalal et al., 2008). Fig. 1.2 represents an overview of the damage, which is caused due to excessive sand extraction from the riverbed. Furthermore, unplanned river dredging can also cause significant damage to the waterfront structures (Liu et al., 1991). On the other hand, quality sand is not radially available due to topographical variations and transportation of sand from distant locations can be expensive. As a result, it is essential to evaluate the alternative materials, which can be used as a partial or full replacement of sand. Recent studies point out that different industrial by-products such as blast furnace slag, steel slag, ferronickel slags (FNS) and copper slag have the potential for use as an alternative to sand (Valcuende et al., 2015; Anastasiou et al., 2014; Mithun & Narasimhan, 2016).

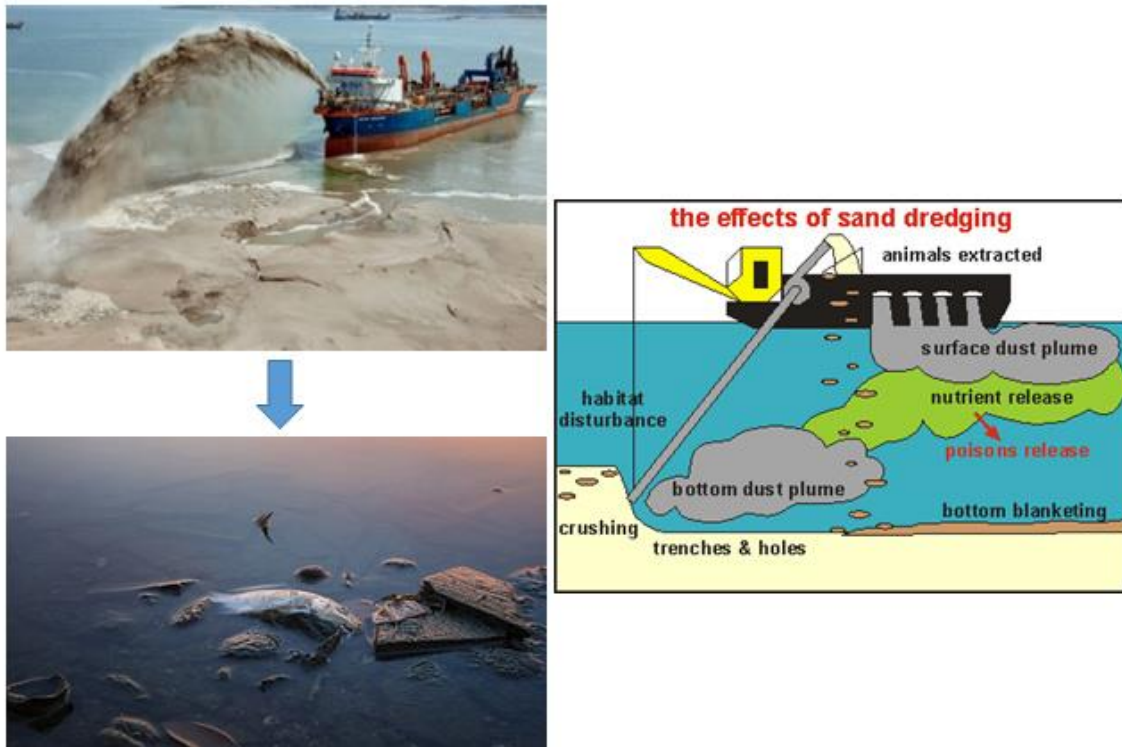


Fig. 1.2 Effect of Sand Dragging on Aquatic ecosystem (Seafriends, 2005)

Ferronickel slag (FNS) is an industrial waste, which is generated from electric arc furnace at a high temperature. This molten slag is cooled by either air or water (Choi & Choi, 2015). Nickle ores consist of a very low percentage of Nickle, as a result, a massive quantity of slag is generated during the production of nickel alloy (Coey et al., 1999). According to past literature, the physical properties of this slag are suitable to use as a fine aggregate in concrete. This particular slag has high density, harness and low water absorption compared to natural sand (JSCE, 2016; Sakoi et al., 2013). FNS aggregates may contain amorphous silica and show potential alkali silica reaction with a cementitious binder (Maragkos et al., 2009). However, this aggregate has been utilised as an alternative of sand in various field applications, for example, gravity retaining walls, cable anchors, wave-dissipating blocks and rockfill dams (Choi & Choi, 2015).

1.2 Problem statement

A considerable amount of by-product FNS is generated in the production process of nickel alloy because of the low-grade of the nickel ores available in the earth. About 12 to 14 tonnes of FNS is generated during the production of one-tonne nickel alloy. As a result, a significant quantity of slag is accumulated around the nickel plant premises. For example, one nickel manufacturer in New Caledonia has a current deposition of about 25 million tonnes of FNS, which can be used as a fine aggregate. The safe disposal of industrial slags requires land, labour and resources. Thus, utilizing this slag as a fine aggregate in the manufacture of concrete can reduce the cost of the disposal, as well as reduce the sand consumption and bring sustainability to the concrete industry. However, it is of utmost importance to investigate the short and long-term properties of concrete using any new material. Therefore, this study aimed at investigation of various fresh and hardened properties of cement mortar and concrete utilising FNS fine aggregate.

1.3 Research objectives

The aim of this study is to expand the knowledge related to the use of FNS as a fine aggregate in concrete. Specific objectives of this research are summarised below.

- Evaluate the current state of the art of FNS usage in concrete and determination of the properties of FNS in comparison to natural sand.
- Evaluation of the effects of FNS aggregate on fresh properties of cement mortar and concrete.
- Investigate the effects of FNS aggregate on hardened mortar and concrete properties such as compressive strength, tensile strength and modulus of elasticity, and evaluate the correlations among the mechanical properties.

- Evaluating the durability related properties, such as volume of permeable voids and resistance to chloride ion penetration, alternate wet-dry cycle and elevated temperature exposures.
- Evaluation of the potential ASR of FNS in cementitious composites by using the accelerated test methods and determination of possible mitigation measures.

1.4 Research approach and thesis organisation

Wide ranges of multidisciplinary approaches were taken in this present study including fracture mechanics, statistics, thermal analysis, microstructure analysis and material science. The thesis structure is outlined below.

In Part I, after the introduction, Chapter 2 focuses on the review and analysis of previous research works related to the topic of this study. Chapter 2 outlines the past study on the use of FNS in concrete including the advantages and limitations.

Part II presents the experimental works conducted to determine the effects of FNS fine aggregate on workability and mechanical properties of cement mortar and concrete. This part consists of two chapters. Chapter 3 presents the fresh and hardened properties of mortar using FNS aggregate, while Chapter 4 describes the fresh and hardened properties of concrete using FNS aggregate. Correlations of the mechanical properties of concrete using FNS aggregate were studied. Finally, leaching test results are also presented in this chapter.

Part III presents the experimental program to assess the durability of mortar and concrete. This part consists of six chapters. Previous studies pointed out that FNS aggregates are susceptible to ASR. Therefore, primary focus was to identify potential ASR and determine the suitable mitigation technique. Chapter 5 evaluates the identification of ASR of FNS aggregates by accelerated mortar bar method (AMBT) by two different

standards AS 1141.60.1 and ASTM C1567. In this chapter, fly ash was used as a mitigation measure of ASR. In Chapter 6, a comparative study was conducted between fly ash and ground granulated blast furnace slag to determine their effectiveness on the mitigation of ASR of FNS aggregate. Durability assessments of concrete specimens against exposures to alternative wet-dry cycles and elevated temperature are presented in Chapters 7 and 8, respectively.

Finally, in Part IV, the conclusions of the study and recommendations for further work are presented in Chapter 9.

1.5 References

- Anastasiou, E., Filikas, K. G., & Stefanidou, M. (2014). Utilization of fine recycled aggregates in concrete with fly ash and steel slag. *Construction and Building Materials*, 50, 154-161.
- Choi, Y. C., & Choi, S. (2015). Alkali–silica reactivity of cementitious materials using ferro-nickel slag fine aggregates produced in different cooling conditions. *Construction and Building Materials*, 99, 279-287.
- Coey, J. M. D., Skumryev, V., & Gallagher, K. (1999). Rare-earth metals: Is gadolinium really ferromagnetic?. *Nature*, 401(6748), 35.
- Dalvi, A. D., Bacon, W. G., & Osborne, R. C. (2004, March). The past and the future of nickel laterites. In *PDAC 2004 International Convention, Trade Show & Investors Exchange*(pp. 1-27). Toronto: The prospectors and Developers Association of Canada.
- Davis, J., Bird, J., Finlayson, B., & Scott, R. (2000). The management of gravel extraction in alluvial rivers: a case study from the Avon River, southeastern Australia. *Physical Geography*, 21(2), 133-154.
- JSCE. (1994). Guidelines for Construction Using Ferronickel Slag Fine Aggregate Concrete. *Concr. Libr. JSCE No. 24*. <http://www.jsce.or.jp>.
- Liu, P. C. (1991). Damage to concrete structures in a marine environment. *Materials and structures*, 24(4), 302-307.
- Maragkos, I., Giannopoulou, I. P., & Papias, D. (2009). Synthesis of ferronickel slag-based geopolymers. *Minerals Engineering*, 22(2), 196-203.
- Mithun, B. M., & Narasimhan, M. C. (2016). Performance of alkali activated slag concrete mixes incorporating copper slag as fine aggregate. *Journal of Cleaner Production*, 112, 837-844.
- Ohno, M. (2017). Green and Durable Geopolymer Composites for Sustainable Civil Infrastructure. *PhD dissertation*, The University of Michigan. <http://hdl.handle.net/2027.42/140947>
- Olonade, K. A., Ajibola, I. K., & Okeke, C. L. (2018). Performance evaluation of concrete made with sands from selected locations in Osun State, Nigeria. *Case Studies in Construction Materials*, 8, 160-171.
- Padmalal, D., Maya, K., Sreebha, S., & Sreeja, R. (2008). Environmental effects of river sand mining: a case from the river catchments of Vembanad lake, Southwest coast of India. *Environmental geology*, 54(4), 879-889.
- Preciso, E., Salemi, E., & Billi, P. (2012). Land use changes, torrent control works and sediment mining: effects on channel morphology and sediment flux, case study of the Reno River (Northern Italy). *Hydrological Processes*, 26(8), 1134-1148.

- Sakoi, Y., Aba, M., Tsukinaga, Y., & Nagataki, S. (2013). Properties of concrete used in ferronickel slag aggregate. In *Proceedings of the 3rd International Conference on Sustainable Construction Materials and Technologies*, Tokyo, Japan.
- Seafriends. (2005). Mining the sea sand. Seafriends Marine Conservation and Education Centre, Goat Island Rd., Leigh, New Zealand.
<http://www.seafriends.org.nz/oceano/seasand.htm>
- Thomas, M. D. A., Fournier, B., Folliard, K. J., & Resendez, Y. A. (2012). *Alkali-Silica Reactivity Surveying and Tracking Guidelines* (No. FHWA-HIF-12-046).
- Valcuende, M., Benito, F., Parra, C., & Miñano, I. (2015). Shrinkage of self-compacting concrete made with blast furnace slag as fine aggregate. *Construction and Building Materials*, 76, 1-9

Every reasonable effort has been made to acknowledge the owners of copyright material. I would be pleased to hear from any copyright owner has been omitted or incorrectly acknowledged.

Chapter 2: USE OF FERRONICKEL SLAG (FNS) IN CONCRETE

The contents presented in this chapter were published in the following paper:

Saha, A. K., Khan, M. N. N., & Sarker, P. K. (2018). Value added utilization of by-product electric furnace ferronickel slag as construction materials: A review. Resources, Conservation and Recycling, 134, 10-24.

This chapter presents a literature review on the use of ferronickel slag in concrete as both partial and full replacement of natural sand and partial replacement of binder. Very limited studies that are available on the use of FNS as a raw material for geopolymer have been included in the review. The previous research findings are presented, analysed and limitations identified.

2.1 Overview

Concrete is the second most consumed material in the world and the demand of concrete is increasing day by day. As a result, about 7.5 billion cubic meters of concrete is produced every year for construction purposes (USGS, 2016). Concrete usage has an annual growth rate of 6% (Ghods et al., 2017). Generally, a significant part of concrete's volume is occupied by fine aggregate, which plays an essential role in the properties of concrete such as workability, strength and durability. River sand is the commonly adopted fine aggregate. However, due to adverse environment effects of river dredging various alternatives to river sand are explored and used in many parts of the world. Some possible alternative fine aggregates are manufactured sand (M Sand), offshore sand, slag sand, bottom ash, copper slag sand and quarry dust (Masterbuilder, 2014).

Similarly, the use of various industrial by-products as a supplementary cementing material (SCM) has attracted keen interest in the construction industry. Among different SCMs, fly ash, blast furnace slag and steel slag are the most popular and have been studied extensively during the last few decades. The application of fly ash and blast furnace slag as SCM can improve the durability properties of concrete significantly by pozzolanic reaction (Achal et al., 2011; Berndt et al., 2009; Lee et al., 2006; Wang et al., 2008a; Wang et al., 2008b; Yeau et al., 2005). However, the binder occupies only a small volume fraction of concrete which is about 12-16%. Besides, grinding of these by-products is energy intensive. Therefore, researchers have been trying to use industrial by-products as aggregate as this needs little or no processing of the raw by-product. It has been reported that the utilization of coal bottom ash, coal fly ash, steel slag, blast furnace slag and plastic wastes as a partial replacement of sand in concrete exhibits satisfactory strength and durability performance. In addition, the application of high density industrial slag as an aggregate improves the strength properties of concrete (Aggarwal et al., 2007; Andrade et al., 2009; Pofale et al., 2010; Yüksel et al., 2007; Ismail et al., 2008). Higher percentages (50%) of sand replacement by steel slag also improved the strength properties of concrete (Qasrawi et al., 2009). Furthermore, production of self-healing concrete using carbonated steel slag aggregate has been reported in literature (Pang et al., 2016). Steel slag aggregate is not only applicable in concrete production but also can be utilized in road construction, wastewater or gas treatment and as a fertiliser in agriculture production (Yi et al., 2012). On the other hand, the application of bottom ash as a partial replacement of sand reduces the strength properties of concrete due to the low density of the bottom ash than sand; however, it improves the fresh properties and the durability properties including permeability, wetting-drying cycles and freezing-thawing resistance of concrete (Aggarwal et al., 2007; Andrade et al., 2009; Yüksel et al., 2007). Similarly, the inclusion of recycled

plastic as fine aggregate reduces the strength of concrete (Ismail et al., 2008). However, the application of fly ash as a partial replacement of sand improves the strength properties of concrete (Pofale et al., 2010).

2.2 Properties of FNS

FNS can be classified into two different classes depending on the cooling method of the molten slag, known as air-cooled slag and water-cooled slag. The air-cooled slag is slowly cooled by the air in an open pit whereas water cooled slag is rapidly cooled by using water as shown in Fig. 2.1 (Choi & Choi, 2015). As seen from Fig. 2.1, air-cooled nickel slag is light grey in colour and brittle in nature. As a result, it can be crushed very easily (Sato et al., 2011). On the other hand, water-cooled FNS is dark in colour, spherical in size with hollow structure and slippery in nature (JMIA, 1991).

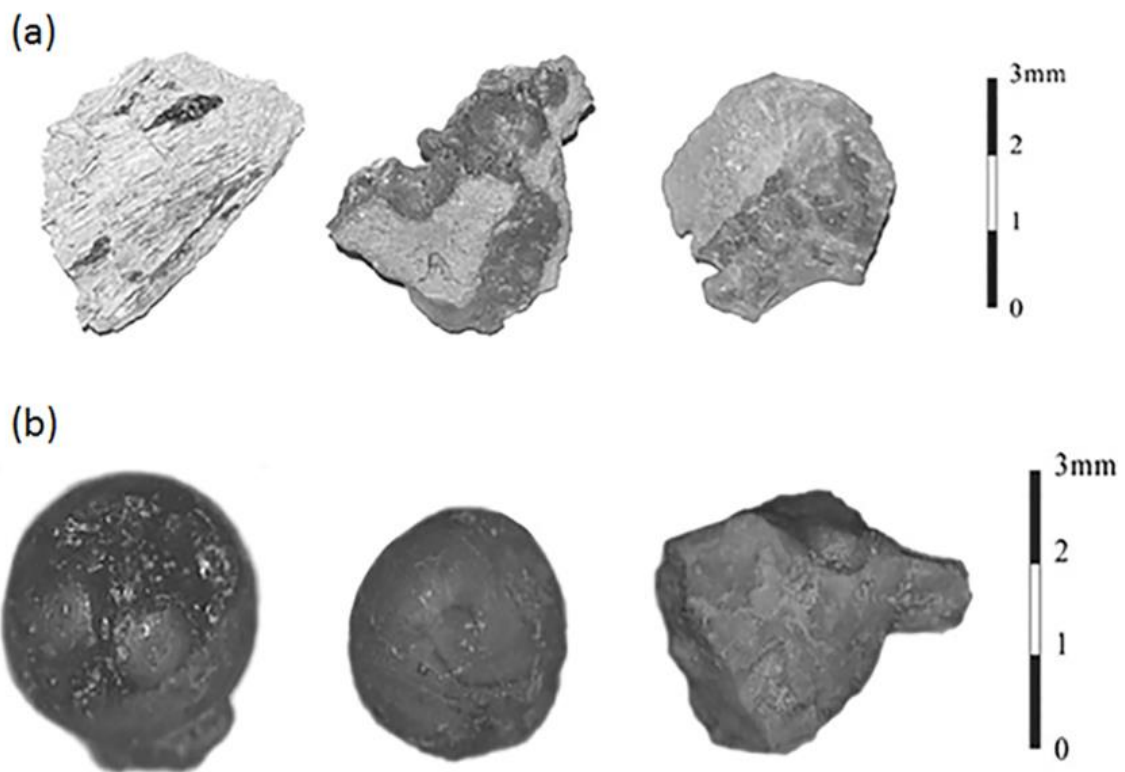


Fig. 2.1 FNS (a) air-cooled and (b) water-cooled (Choi & Choi, 2015)

Table 2.1 Chemical compositions of nickel slag (mass %)

Material	FNS-A (Sato et al., 2011)	FNS-W (Sato et al., 2011)	FNS-W (Komnitsas et al., 2007; 2009; 2013)	FNS-W (Maragkos et al., 2009)	FNS-W (Lemonis et al., 2015)	FNS-A (Choi & Choi, 2015)	FNS-W (Choi & Choi, 2015)	FNS (Fidancevska et al., 2003)
SiO ₂	55.6	52.7	32.74	40.29	41.18	62.80	58.1	19.8
Al ₂ O ₃	-	-	8.32	10.11	5.98	1.95	2.29	12.25
Fe ₂ O ₃	7.57	6.70	43.83	37.69	40.02	7.13	11.10	17.62
MgO	27.8	34.0	2.76	5.43	7.79	24.70	26.50	9.66
SO ₃	0.06	0.04	0.18	-	0.64	0.03	0.04	0.87
CaO	5.18	2.30	3.73	3.65	4.12	2.07	0.29	4.48
Na ₂ O	-	-	-	-	0.09	0.13	0.09	0.33
K ₂ O	-	-	-	-	0.37	0.02	0.06	0.04
Cr ₂ O ₃	-	-	3.07	2.58	2.75	-	-	2.48
NiO	-	-	0.1	0.09	0.13	-	-	0.30
Co ₃ O ₄	-	-	0.02	-	0.02	-	-	0.14
LOI ^a	-	-	-	-	-	0.94	1.24	-
Type of ores	-	-	laterites	laterites	laterites	-	-	-
Source	Japan	Japan	LARCO, Greece	LARCO, Greece	LARCO, Greece	SNNC, South Korea	SNNC, South Korea	-

^a loss of ignition; FNS-A: air-cooled FNS slag; FNS-W: water cooled FNS slag

The chemical compositions of FNS obtained from different sources are presented in Table 2.1. It can be seen that FNS primarily consists of SiO₂, MgO, and Fe₂O₃. This material consists of amorphous silica as well as crystalline minerals such as enstatite, forsterite and dropsied. The chemical compositions of this slag can be different depending on its source, processing and cooling method (Lemonis et al., 2015; Maragkos et al., 2009; Komnitsas et al., 2007). Generally, nickel slag generated from laterite ore contains a high Fe₂O₃ and low MgO whereas, that from garnierite ore contains low Fe₂O₃ and high MgO. The physical properties of FNS are presented in Table 2.2. It can be seen from the table that generally air-cooled FNS shows higher density and higher water absorption than the

water-cooled FNS (Choi & Choi, 2015; Togawa et al., 1996). Therefore, properties of FNS from a new source have to be determined as its properties may vary depending on the source and the processing method.

Table 2.2 Physical Properties of FNS aggregate

Physical properties	FNS-A (Choi & Choi, 2015)	FNS-W (Choi & Choi, 2015)	FNS-A (Sato et al., 2011)	FNS-W (Sato et al., 2011)	FNS-W (Sakoi et al., 2013)	FNS-W (Shoya et al., 1999)	FNS-A (Togawa et al., 1996)	FNS-W (Togawa et al., 1996)
Specific gravity (g/cm ³)	3.11	2.81	2.93	3.08	2.84	2.97	3.02	2.84
Water absorption (%)	1.64	0.71	1.87	0.13	1.98	1.2	2.20	0.73

2.3 Performance of FNS as aggregate in concrete

2.3.1 Fresh properties

2.3.1.1 Workability

Workability is defined as the ease of transportation, placement, compaction and finishing of the concrete mixture. Slump test is the most recognized test to measure the workability of concrete. Workability of concrete primarily depends on water-cement ratio, binder compositions, and aggregates. For example, the concrete mixtures with a constant water-cement ratio, the slump variation depends on the aggregate properties such as gradation, particle size, particle density and angularity. A well-graded aggregate exhibits higher workability than a poorly graded aggregate. Besides, larger particles require less water to saturate the surface. Hence, the workability increases with the increase of aggregate particle size for the same water content. Moreover, workability of concrete reduces with the increment of the angularity and the interlocking friction of aggregate (Santamarina, 2008;

Hu & Wang, 2005). Shoya et al. (1999) found that the workability of concrete reduced marginally with the increase of FNS. The authors conducted both slump flow test and V-funnel flow test to determine the workability of concrete and noticed similar results. The authors described that, due to the poor gradation as well as high angularity of FNS aggregate, it showed higher internal friction between the particles. As a result, it reduced workability of concrete. Moreover, a technical report by Japan Mining Industry Association (JMIA, 1991) indicated that the slump value of FNS aggregate mixed concrete is identical when compared with the conventional aggregate concrete.

2.3.1.2 Bleeding

The accumulation of water on the surface of concrete after compaction and finishing is known as bleeding. Segregation of aggregates is the primary reason behind bleeding of freshly mixed concrete. Usually, high density aggregates exhibit higher bleeding. On the other hand, water has the lowest density among all materials in a concrete mix. As a result, water can easily get separated from the other constituents of a concrete mixture. This phenomenon also depends on other factors such as poor mixing of concrete, excess workability and excessive vibration. FNS aggregate has a higher density than natural sand. Therefore, bleeding of concrete using FNS aggregate is of particular interest. The bleeding properties of concrete using FNS aggregate are shown in Fig. 2.2. According to the bleeding tests of Shoya et al. (1999) as per JIS A 1123 (1997), FNS aggregate concrete showed identical bleeding as compared to conventional aggregate concrete, and the magnitude of bleeding was below $0.003 \text{ (cm}^3\text{/cm}^2\text{)}$. However, Sato et al. (2011) reported that bleeding of FNS aggregate concrete increased with the increase of FNS content in the mixture. The authors suggested that this increase of bleeding was due to the higher unit weight of FNS aggregate than sand. Thus, consolidation of aggregate particles in a freshly mixed concrete led to increased bleeding. In their study, the amount of bleeding for conventional concrete

and 100% FNS concrete were 0.28 and 0.33 (cm^3/cm^2), respectively. Furthermore, Togawa et al. (1996) used furnace slag, silica fume and limestone powder as a SCM in FNS concrete to reduce bleeding.

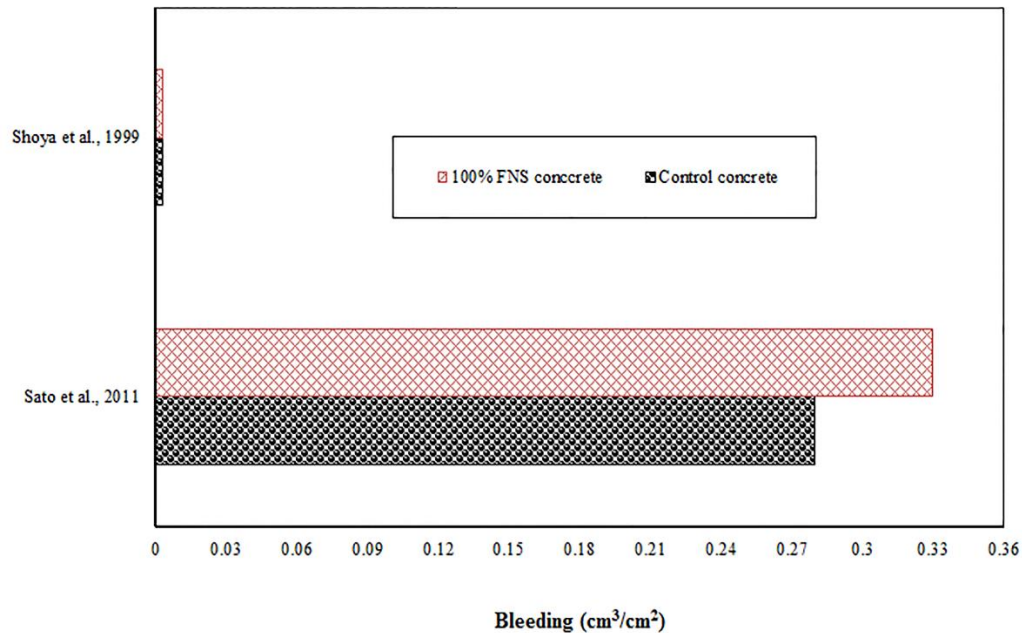


Fig. 2.2 Bleeding of FNS concrete

2.3.2 Hardened properties

2.3.2.1 Compressive strength

Compressive strength is the most commonly used hardened properties of concrete. Although aggregate has a significant role on the strength properties of concrete, it depends primarily on binder composition and water-cement ratio. Togawa et al. (1996) found that compressive strength is slightly increased for up to 50% replacement of sand by FNS; however, there is a reduction in compressive strength at 100% replacement level. After that, Shoya et al. (1999) showed a similar trend of strength of concrete using FNS aggregate. It can be seen that the compressive strength for control, 50% FNS, and 100% FNS concretes were 41.2, 45.7 and 41.7 MPa, respectively. The FNS aggregates used in their study had a higher unit weight, fineness modulus and hardness compared to natural

sand. As a result, it improved the particle packing when used in concrete. Therefore, 50% replacement of sand by FNS aggregates showed better strength performance in concrete, whereas 100% FNS aggregate reduced the compressive strength of concrete due to the poor gradation of slag aggregates. In addition, full replacement of sand by FNS increased the voids ratio due to high fineness modulus of the FNS aggregates. Similarly, Sakoi et al. (2013) reported that 50% FNS aggregate showed higher compressive than the normal concrete. Higher density and better aggregate gradation of FNS aggregates lead to the increase of compressive strength. On the other hand, full replacement of sand by FNS exhibited lower compressive strength than the control concrete due to the larger size and angularity of the FNS, which increased the internal voids.

2.3.2.2 Modulus of elasticity

The modulus of elasticity is a significant property of concrete. This value represents the stiffness and rigidity of concrete material. Modulus of elasticity of concrete is often expressed as a function of its compressive strength. However, modulus of elasticity also depends on the aggregate properties. Sakoi et al. (2013) and Shoya et al. (1999) pointed out that modulus of elasticity of concrete increased with the increase of FNS aggregate content. It can be seen that modulus of elasticity increased from 28 to 32 GPa up to 50% replacement of sand by FNS (Sakoi et al., 2013). The higher modulus of elasticity of concrete is mainly attributed to the presence of the high density FNS aggregates, which improves the density of concrete by increasing the stiffness and rigidity of concrete samples.

2.3.2.3 Flexural and tensile strengths

Generally, concrete is weak in tension. Therefore, the reinforcement came into practice to improve the tensile strength capacity of concrete. Usually, Steel bars in concrete structures carry the majority of the tensile stress. Furthermore, concrete sections without reinforcement can withstand a small amount of tensile stress due to lateral forces and

internal stress. This property depends on the compressive strength of concrete as well as the properties of aggregates. Higher angularity and roughness characteristics of aggregate have a positive effect on tensile strength of concrete due to improved friction and interlocking between the binder matrix and aggregate surface (Molugaram et al., 2014; Wu et al., 2001). At the beginning, Shoya et al. (1999) reported that tensile strength of FNS aggregate concrete is identical to that of conventional concrete.

2.3.3 Durability properties

2.3.3.1 Alkali-silica reaction

Alkali-silica reaction (ASR) is a complex phenomenon in concrete. Although it has been studied extensively during the last few decades, still there is a debate among scientists about its mechanism. Generally, ASR takes place between the reactive silica of aggregates and the alkaline solutions in micro pores of concrete. The primary source of alkali is the binder matrix. The silica present in aggregates in the form of quartz is chemically inert. However, poorly crystalline silica has an affinity to react with alkali and generate amorphous hydrous silica (Swamy 2002; Ichikawa and Miura 2007). In addition, researchers also investigated the percentage of amorphous silica in reactive aggregates from various sources and the corresponding expansions by accelerated mortar bar test (AMBT) and concrete prism test (CPT) (Grattan-Bellew et al., 2010; Shehata and Thomas 2000; Shafaatian et al., 2013; Moser et al., 2010). The authors noticed that there is an inherent relationship between the expansion of the samples and the percentage of amorphous silica in aggregate. This relationship is that expansion increases with the increase of the percentage of amorphous silica in aggregates. However, the relationship may vary due to the variations in aggregate source, aggregate type and test type. Therefore, the percentage of amorphous silica content in aggregate acts as a governing factor in ASR mechanism and sometimes small proportion of amorphous silica in aggregate can cause expansion of concrete and mortar.

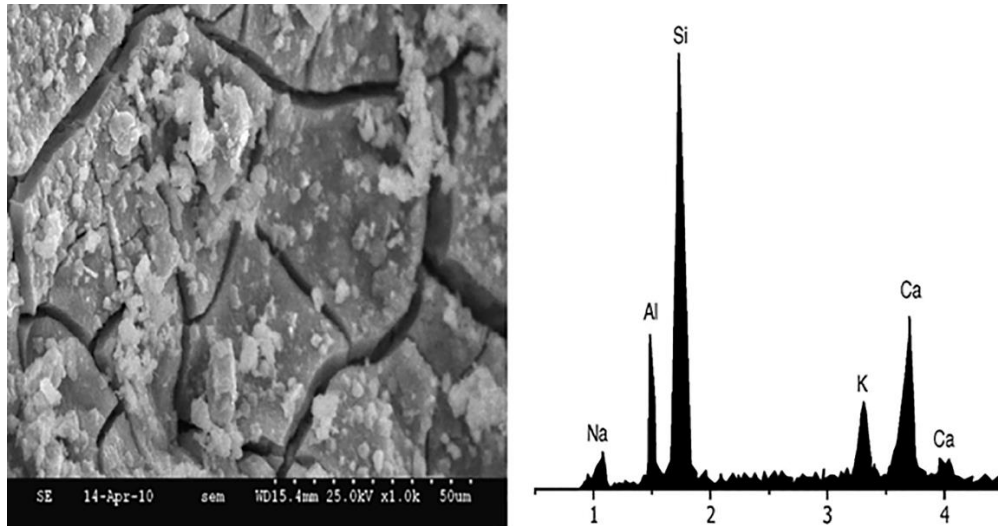


Fig. 2.3 Microstructure of ASR affected FNS specimen (Choi & Choi, 2015)

At first, Tomosawa et al. (1997) studied ASR of concrete using FNS aggregates. The authors concluded that the application of low alkali cement and addition of fly ash or ground granulated blast furnace slag are effective measures to suppress the reactivity of FNS aggregates. Then, Choi & Choi (2015) reported that the water-cooled FNS aggregates showed excessive ASR expansion, whereas air cooled FNS aggregates exhibited small expansion as in control specimens. According to their tests as per ASTM C1260 (2014), the ASR expansion of water-cooled FNS mortar was within a range of 0.6 to 0.8% after 28 days; however, both the reference mortar and air-cooled FNS aggregate mortar showed approximately 0.05% expansion. The authors indicated two primary reasons behind the ASR of water-cooled FNS aggregates. Firstly, the rapid cooling of FNS by water leads to formation of micro cracks on the surface of FNS particles. As a result, the dissolved silica and water can be transported through the cracks. Secondly, the rapid cooling leads to poorly crystalline and non-crystalline silica in FNS aggregates. The microstructure of ASR affected specimens are given in Fig. 2.3 (Choi & Choi, 2015). It can be seen that the aggregate surface is affected by extensive cracking due to the formation of ASR gel and the chemical composition of this gel confirms the presence of high amount of silica,

calcium, alumina and alkali. It is noticeable that the FNS mortar bars with no fly ash showed expansion of approximately 0.8%; however, with the addition of 5, 10, 20, and 30% fly ash as SCM, the expansions were 0.70, 0.50, 0.15 and 0.05%, respectively, as shown in Fig. 2.4 (Choi & Choi, 2015).

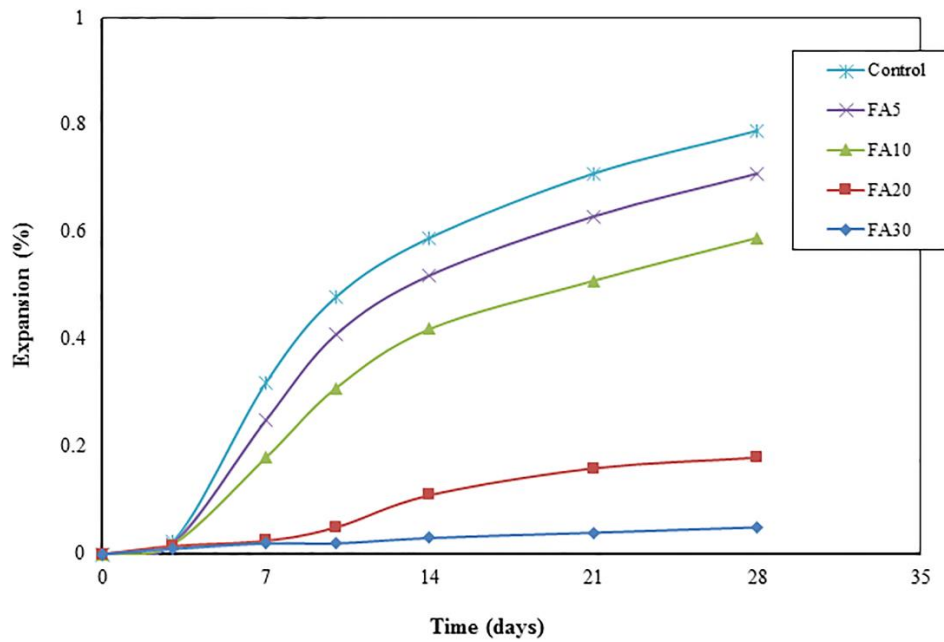


Fig. 2.4 Influence of class F fly ash in FNS samples as an ASR mitigation technique (Choi & Choi, 2015)

Furthermore, 30% replacement of cement by fly ash resulted an identical expansion to the reference mortar bar. Besides, ground granulated blast furnace slag also can reduce the expansion due to ASR, but a large volume of replacement is required. It has been reported that 60% replacement of cement by blast furnace slag kept the expansion below the acceptable limit. The expansions of mortar bars for using 15, 30, 45 and 60% ground granulated blast furnace slag as a SCM were 0.70, 0.55, 0.40 and 0.10%, respectively (Choi & Choi, 2015). The mechanism of fly ash to reduce the ASR is mainly dependent on four factors. Firstly, the inclusion of fly ash can reduce the hydroxyl ion in pore solution (Shehata et al., 1999; Shi, 2004). Secondly, it can minimize the pore size and the thickness

of the transition zone between cement paste and aggregates (Kuroda et al., 2000; Mehata & Monteiro, 2006). Thirdly, it can reduce the aggregate dissolution rate (Shafaatian et al., 2013). Finally, fly ash can reduce the percentage of portlandite from the binder, which acts as a buffer to maintain the pH of pore solution (Hou et al., 2004). The formation of primary ettringite with a high calcium to silica ratio (Ca/Si) due to the hydration of cement and the pozzolanic reaction of fly ash that has the properties of low viscosity and swelling pressure (Vayghan et al., 2016). Therefore, the use of fly ash as an SCM was considered an adequate measure to mitigate the potential ASR of FNS fine aggregate.

2.3.3.2 Freezing and thawing resistance

Resistance to freezing and thawing cycles evaluates the soundness of concrete in exposures to adverse weather conditions. Concrete samples are exposed to the repeated cycles of freezing and thawing in this test. Usually, the samples are exposed to -18 °C for freezing and 4 °C for thawing in a cyclic order within 2 to 5 hours. The freezing and thawing resistance test results are found in various published are presented in Table 2.3. It can be seen that two different kinds of assessments are adopted in determination of the resistance against freeze-thaw exposures, namely dynamic modulus of elasticity and durability factor.

Table 2.3 Freeze and thaw resistance of FNS concrete

FNS (%)	¹ RDME (%) 300 Cycles (Sakoi et al., 2013)	RDME (%) 300 Cycles (Sato et al., 2011)	² DF (%) 300 Cycles (Shoya et al., 1999)
0	85	85	71.6
25	-	82	-
50	82	-	84.7
100	-	80	86.4

¹ Relative Dynamic Modulus of Elasticity; ² Durability Factor

In tests according to JIS A 1148 (2010), Sakoi et al. (2013) found that FNS samples showed almost similar relative dynamic modulus of elasticity after freeze and thaw cycles when compared to the control specimens. On the other hand, Sato et al. (2011) reported a decreasing trend of relative dynamic modulus of elasticity for FNS samples. Besides, Togawa et al. (1996) suggested that the use of limestone powder can improve the durability characteristics of FNS concrete. Shoya et al. (1999) reported that durability factor of FNS concrete increased as compared to control concrete after the freeze and thaw cycles tested as per ASTM C 666 (1992). From Table 2.3, it can be seen that the durability factor was slightly over 70% for the control specimens, whereas the durability factors of specimens containing 50% and 100% FNS were 85% and 87%, respectively. This increase of durability factor was attributed to the higher density and lower fineness modulus of FNS aggregates than natural sand.

2.3.3.3 Drying shrinkage

The loss of capillary water from the hardened concrete mix leads to contraction of concrete, which is known as drying shrinkage. High drying shrinkage can cause internal cracks and warping as well as external deflection in concrete. Generally, drying shrinkage of concrete depends on cement paste volume, water-cement ratio and water absorption of aggregates. The drying shrinkage test results of FNS aggregate concrete are presented in Table 2.4. Shoya et al. (1999) showed that the use of FNS as aggregate in concrete reduced drying shrinkage slightly as compared to the control concrete. In their tests the drying shrinkage for control, 50% FNS and 100% FNS concrete were 510, 450 and 420 micro strains, respectively. The water content of these specimens were 165, 160 and 155 kg/m³, respectively. Therefore, FNS aggregate concrete specimens with the lower water-cement ratio resulted in lower drying shrinkage, as expected. However, Sakoi et al. (2013) found that drying shrinkage of FNS concrete was slightly higher than control specimens. High

water absorption of FNS aggregates resulted in greater drying shrinkage of these samples since the water cement ratio was kept constant for all the mixes. The drying shrinkage ranged between 350 and 400 micro strains in their study under. Nevertheless, drying shrinkage of the specimens containing FNS aggregate was within the range of values usually observed in concrete using natural sand as fine aggregate.

Table 2.4 Drying shrinkage of FNS concrete

FNS (%)	Drying shrinkage ($\times 10^{-5}$ strain)	
	(Sakoi et al., 2013)	(Shoya et al., 1999)
0	35	51
50	40	45
100	-	42

2.3.3.4 Air permeability and carbonation

The air permeability test evaluates the pores in concrete and it gives an indication of the ease of transportation of fluids into concrete. Besides, carbonation is the reaction between CO_2 from the surroundings and Ca(OH)_2 of binder matrix that forms CaCO_3 . Since the carbonation process uses Ca(OH)_2 , it reduces the pH of concrete which may increase the risk of reinforcement corrosion. Shoya et al. (1999) determined air permeability and carbonation of FNS aggregate concrete samples using the method proposed by Nagataki and Ujike (1988). The authors used 490 kPa load-bearing pressure and the water replacement method to determine the amount of air penetrated through the concrete. The authors reported that the air permeability of FNS concrete samples were similar to the control concrete. The coefficient of air permeability ranged between 2.51×10^{-5} and 2.44×10^{-5} m/sec. Furthermore, the carbonation test of FNS concrete gave identical result to that of the control specimen. The neutralised depth of the concrete samples remained between 6.97 and 5.72 mm after 91 days (Shoya et al., 1999).

2.3.4 Applications in pavement constructions

Different types of industrial slag have been utilised in pavement construction as base and sub-base aggregates or as a cementitious material in recent decades. Significant research work has been carried out on the use of electric arc furnace slag (EAF) both as coarse aggregate and fine aggregate in pavement constructions (ASA, 2002; Behnood & Ameri, 2012; Wu et al., 2007; Ziari et al., 2015; Oluwasola et al., 2015; Oluwasola et al., 2015). As a coarse aggregate, this slag exhibits high skid resistance due to high angularity in surface dressing (Pasetto & Baldo 2006). In addition, the application of EAF as a coarse aggregate provides satisfactory results in asphalt in terms of strength, water sensitivity, stability and deformation (Ameri & Behnood, 2012). Furthermore, Marshall Stability and flow are significantly higher in asphalt using EAF coarse aggregate (Ahmedzade & Sengoz, 2009). Besides, the combination of EAF as a coarse aggregate with limestone as a filler provides satisfactory results. Ziari et al. (2015) reported that replacement of fine aggregate by 50% EAF aggregate in hot mix asphalt showed satisfactory performance by the reduction of air voids and improvement of stiffness. The use of this slag as a fine aggregate improves the mechanical properties such as tensile strength and stability of asphalt (Ameri et al., 2013; Behnood & Ameri, 2012). Moreover, resilient modulus of asphalt improved significantly by the use of slag aggregate which is almost twice as compared to traditional asphalt (Hainin et al., 2012; Hainin et al., 2013; Hainin et al., 2014). However, asphalt with EAF as a fine aggregate shows poor performance in water submergence test (Bagampadde et al., 1999). This is may be due to the presence of significant amount of impurities in industrial slag. Therefore, Emery (1984) suggested to remove the impurities such as lime, refractory and wood from industrial slags before its use in asphalt mixtures as aggregate. The physical properties of EAF and FNS aggregates are relatively similar as both type of aggregate possess high density, low water absorption and angular shaped particles

(Bagampadde et al., 1999; Ziari et al., 2015). Some researchers investigated the suitability of the FNS aggregates as a fine aggregate in hot mix asphalt (HMA) (Emery et al., 1984; Wang et al., 2011; Wang & Thompson, 2011; Krayushkina et al., 2012).

Emery (1984) initially adopted nickel slag aggregate as a base material in mining road and found that nickel slag exhibited satisfactory performance in adverse traffic operating conditions. Wang et al. (2011) conducted accelerated laboratory testing by asphalt pavement analyser in order to evaluate the durability of asphalt using slag aggregate. Furthermore, the authors carried out petrographic examination to identify reactive silica and autoclave testing for evaluation of free lime and free magnesia of the FNS aggregates. According to the test results, the authors concluded that nickel slag is mineralogically, physically and environmentally stable and can be adopted as coarse aggregate and fine aggregate in HMA. Similarly, Wang and Thompson (2011) suggested that air cooled FNS can be used as a suitable alternative to traditional aggregates in the base course and HMA. In addition, Krayushkina et al. (2012) showed that FNS is a suitable alternative for HMA and can be used as a base course in a highway construction. However, research works carried out with FNS aggregate in pavement construction is very limited. Therefore, more research is necessary to carry out in the area of pavement constructions.

2.4 Ground FNS as a supplementary binder in concrete

It is well known that production of cement emits a significant amount of CO₂ to the atmosphere. Therefore, researchers have been working since the past few decades on various industrial by-products such as blast furnace slag, fly ash, steel slag, copper slag, sugarcane bagasse ash, ladle furnace slag and basic oxygen furnace slag as SCM during (Das et al., 2007; Shi & Qian, 2000; Loh et al., 2013; Shi et al., 2008; Rodriguez et al., 2009; Carvalho et al., 2017). The utilization of blast furnace slag as a SCM in concrete reduces the heat of hydration and improves the long-term strength and durability properties

(Das et al., 2007). Similarly, fly ash blended concrete exhibits high durability properties including resistance to alkali silica reaction; sulphate and acid attacks (Shi & Qian, 2000). Besides, copper slag, sugarcane bagasse ash, ladle furnace slag, basic oxygen furnace slag can improve the strength and durability of concrete due to the presence of high amorphous silica and low free lime or magnesia (Loh et al., 2013; Shi et al., 2008; Rodriguez et al., 2009; Carvalho et al., 2017). On the other hand, steel slag consists of excessive free lime, which can cause deleterious volume expansion (Shi & Qian, 2000). Thus, industrial waste containing high amorphous silica and low free CaO or MgO can be used as SCM. The chemical properties of FNS, as presented in Table 2.1, shows that it usually contains high silica. However, FNS from some sources have very high amount of MgO, which is over 20%. Excessive amount of free magnesia can cause volumetric instability of concrete.

Mo et al. (2005) pointed out that the presence of high MgO in binder reduces shrinkage-cracking in concrete. This MgO leads to an autogenous expansion in later curing ages, as a result, it can compensate the concrete's contraction due to cold weather and shrinkage (Mo et al., 2005). However, the maximum allowable limit of MgO in a SCM is 15% as per AS 3582.2 (2016). It generates Bruucite ($Mg(OH)_2$) by the hydration of MgO, which is expansive in nature. As a result, it can increase the concrete volume by up to 17% and also lead to loss of strength. Rahman et al. (2017) studied the soundness and the strength properties of FNS blended concrete. The authors found that the strength properties were slightly lower due to reduction of lime content. On the other hand, the soundness test results including Le-Chatelier, autoclave and extended heat curing were within the allowable limit in FNS samples. In addition, X-ray diffraction (XRD) analysis traced the presence of MgO in the form of forsterite as presented in Fig. 2.5. The crystalline structure of forsterite is orthorhombic, which is chemically inert and stable (Klein et al., 1998). Therefore, the MgO present in the form of forsterite does not participate in hydration

reaction to produce expansive $Mg(OH)_2$ (Maghsoudlou et al., 2016; Kosanović et al., 2005). Therefore, FNS samples did not show any significant expansion in soundness tests (Rahman et al., 2017).

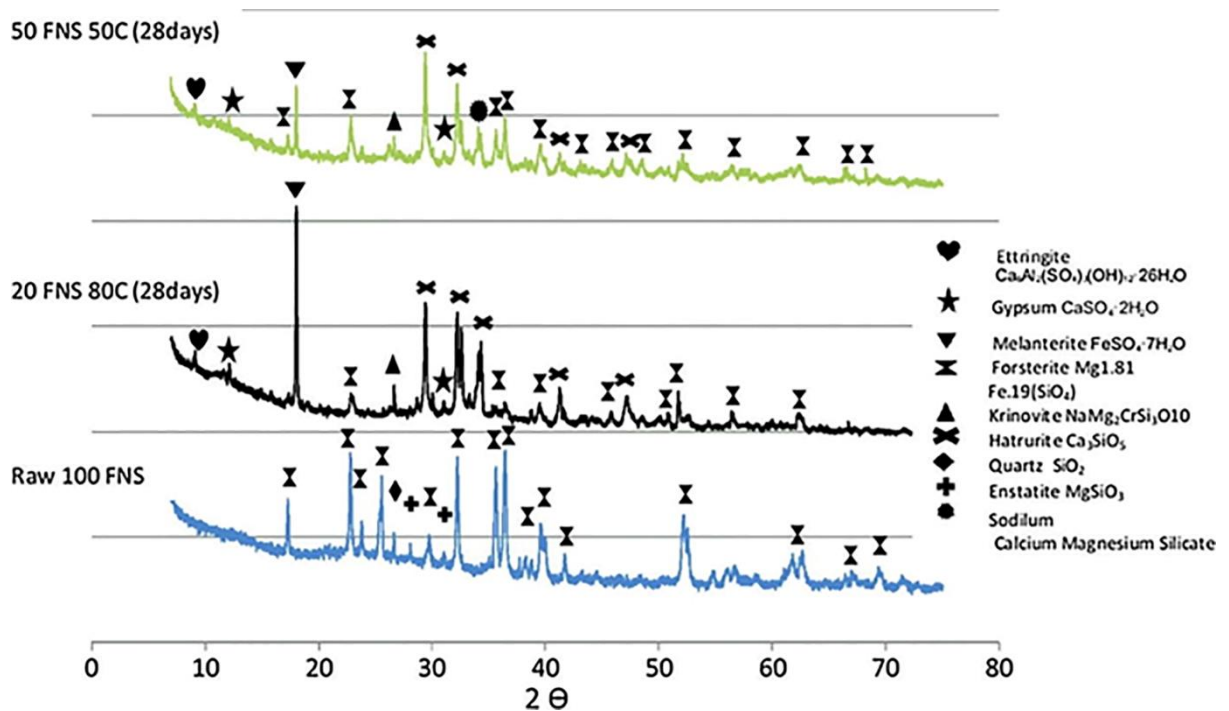


Fig. 2.5 Phase analysis of raw FNS and FNS blended cement pastes (Rahman et al., 2017)

Furthermore, Lemonis et al. (2015) conducted a hydration study on the FNS blended samples and found that the FNS blended samples exhibited a slower rate of hydration than the control samples. Thus, the compressive strength development was slower in FNS mixed concrete than in the conventional cement concrete. However, the amorphous silica present in FNS reacted at the later ages and formed secondary calcium silicate hydrate (C-S-H) gel and improved the density of microstructure. The study also showed that the use of ground FNS as part of the binder similar water demand as for the control mix. Similarly, Katsiotis et al. (2015) concluded that the presence of FNS slowed down the hydration process and the strength development in FNS blended concrete. In addition, the authors reported an increase of compressive strength at later stages of curing due to the effect pozzolanic reaction of FNS. FNS has not been studied extensively by the

scientific community unlike fly ash or blast furnace slag. Therefore, further research is recommended in this area.

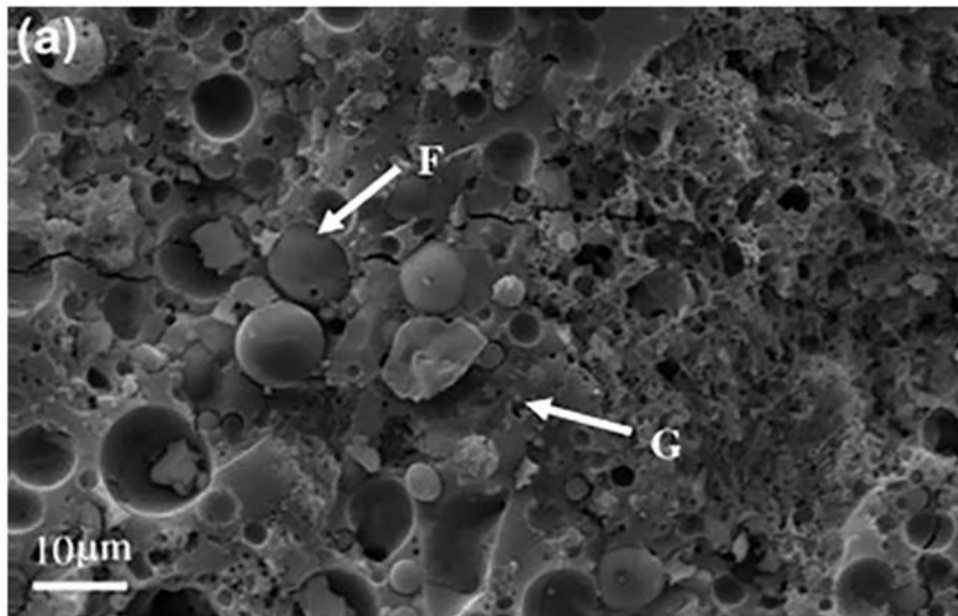
2.5 Use of FNS in geopolymers

Geopolymer is an emerging alternative binder to Portland cement. Significant amount of research has been carried out on the development of geopolymer concrete during the recent time (Hardjito et al., 2005; Hardjito et al., 2004; Geopolymer Institute, 2017; Yang et al., 2014; Zheng et al., 2010; Zhang et al., 2017). Geopolymer is considered as a binder of low carbon footprint since Portland cement is replaced by industrial by-products such as fly ash, metakaolin or slag. In geopolymerisation, an aluminosilicate material such as fly ash, GGBFS or metakaolin is activated by an alkaline solution to generate three-dimensional polymeric chains (Hardjito et al., 2005). It was shown in past works that strength and durability of geopolymer concrete are comparable to those of Portland cement concrete (Hardjito et al., 2004). As a result, geopolymer concrete has been recently used in some industrial applications. One example is the Brisbane West Wellcamp Airport (BWWA) in Australia constructed in 2014 (Geopolymer Institute, 2017).

It is noticeable from the chemical compositions of FNS that it contains substantial amounts of SiO_2 and Al_2O_3 . Thus, it has the potential to replace fly ash partially or entirely in fly ash based geopolymer concrete. Yang et al. (2014) showed that 20% FNS was found to be an optimum quantity as a binder in geopolymer concrete that exhibited the highest strength and lowest shrinkage properties. The authors explained that the FNS contained high SiO_2 and MgO with relatively low Al_2O_3 as compared to fly ash. Consequently, it increased the Si/Al ratio of the geopolymer ingredients and improved compressive strength. The microstructural images of 0% and 20% FNS geopolymer concrete are presented in Fig. 2.6, it can be seen that microstructure of 20% FNS geopolymer specimens were denser as compared to the specimens without FNS. However, a higher dosage of FNS (40% and 60%)

led to the reduction of strength due to lower Si/Al ratio (<2) and presence of large pores. In addition, Zheng et al. (2010) suggested an intermediate Si/Al ratio for the optimum results. In another study by Yang et al. (2014) pointed out that, MgO present in the FNS experienced an elevated temperature extractive metallurgy, thus became inert. As a result, the issue regarding the volume stability in fly ash in geopolymer concrete was not noticeable due to the addition of FNS as a binder.

In another study, Zhang et al. (2017) reported that the use of 20% and 40% FNS in geopolymer improved compressive strength as compared to fly ash based geopolymer. The authors also pointed out that FNS geopolymer has an emission of 0.19-0.23 tonnes of CO₂ per tonne of concrete, which is significantly less than the traditional cement concrete. Furthermore, microstructure analysis revealed formation of Na-Al(Mg)-Si-O-H gel in the FNS based geopolymers. Therefore, the authors concluded that the MgO present in the FNS was not chemically inert since it took part in the geopolymerisation process.



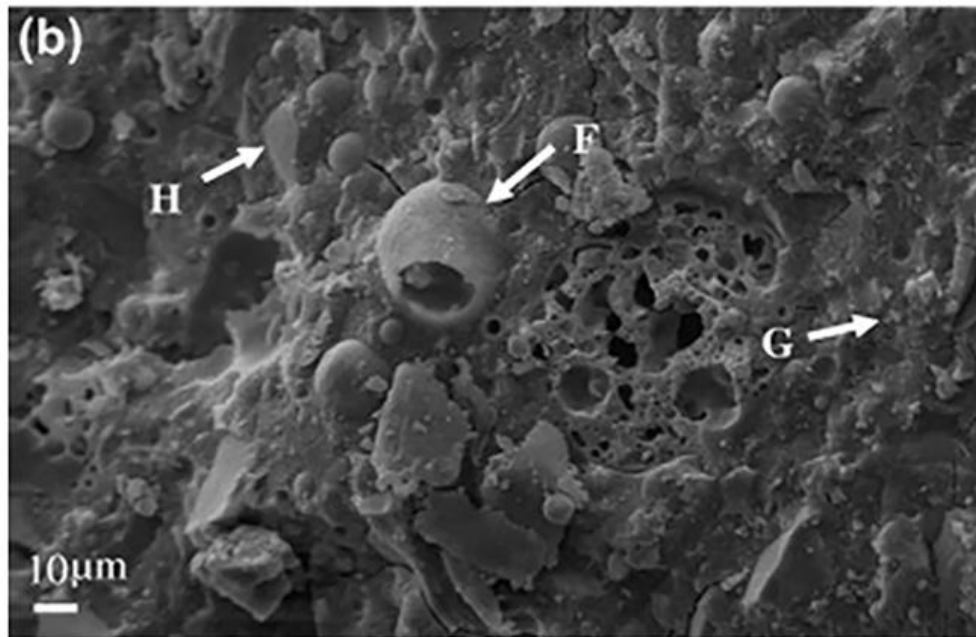


Fig. 2.6 Microstructure of fly ash geopolymer with (a) 0% FNS and (b) 20% FNS. (F-fly ash particles, H-HMNS particles, G-gel phase formed.) (Yang et al., 2014)

Furthermore, according to Maragkos et al. (2009), the characteristics of FNS geopolymer depends on the solid to liquid ratio (S/L). The optimum quantity of S/L and NaOH concentration were 5.6 g/mL and 7M, respectively in their study. This optimum conditions exhibited a significantly high compressive strength of 118 MPa and very low water absorption of about 0.8%. In addition, Komnitsas et al. (2007) investigated the properties of kaolinite based geopolymer with ground FNS blends. The authors found that heating time and the temperature had a negligible effect on the compressive strength, whereas curing period had a prominent effect on strength development. The reaction phases of geopolymer binders were identified by XRD, the results are shown in Fig. 2.7 (2007).

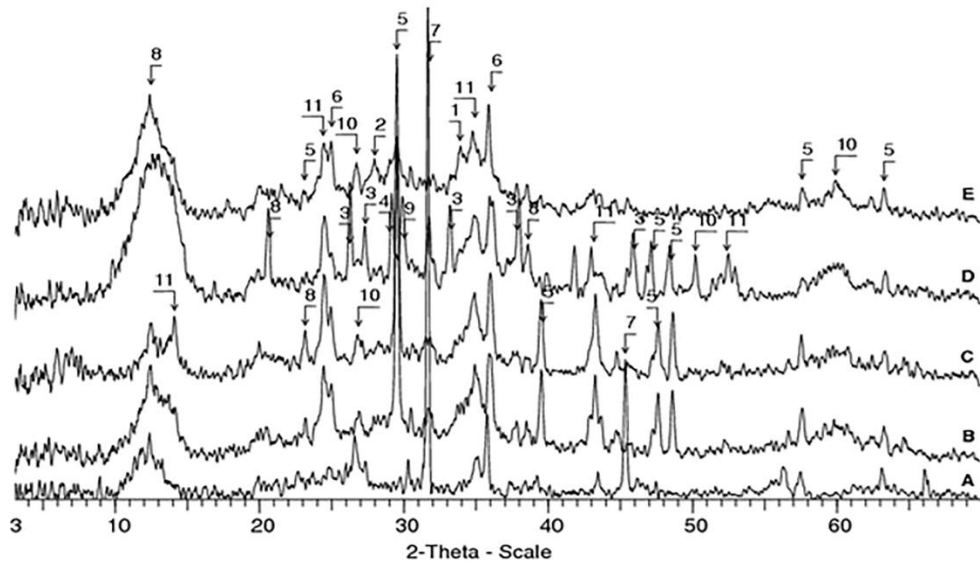


Fig. 2.7 XRD analysis of geopolymers with FNS under various conditions (A: 60 °C–24 h–7 d; B: 60 °C–24 h–28 d; C: 60 °C–48 h–28 d; D: 80 °C–48 h–28 d; 1: Kaolinite, 2: Maghemite, 3: Magnetite, 4: Quartz, 5: Sodalite) (Komnitsas et al., 2007)

The presence of various minerals such as trona, sodalite, thermonatrite and maghemite can be seen in the geopolymer binders. These minerals are primarily composed of Na, Si, Al and O. It is noticeable that there was no sign of MgO in the chemical analysis. Thus MgO present in FNS acted as inert in the chemical reactions. It can be noted that the geopolymer samples showed excellent resistance to freeze-thaw cycles. However, it displayed strength loss in the acidic environment due to the formation of aragonite, akermanite, halite, magnesium calcite and calcite minerals on the surface of the samples. These minerals are formed due to carbonation under acidic environment. Komnitsas et al. (2009) pointed out that the presence of alkali in FNS accelerated the hydration process. The authors confirmed that only Si, Al and O participated in hydration reaction by using Fourier Transform Infrared Spectroscopy (FTIR) analysis. Finally, Komnitsas et al. (2013) also evaluated the effect of NO_3^- or SO_4^{2-} in the geopolymer mixture. According to the experimental results, the presence of these ions reduced strength development due to the consumption of alkali, thus minimized the formation of a gel. Besides, Sakkas et al. (2014)

evaluated the effect of fire exposure on the FNS based geopolymer. The authors found that these geopolymers had a low thermal conductivity and high fire resistance like commercial fire resisting materials. The authors also reported 120 MPa compressive strength, which is in the ultra-high strength concrete category.

From the above discussion, it can be seen that FNS can be a viable supplementary material in fly ash or metakaolin based geopolymer mixtures. However, there is a debate among the researchers about the role of MgO in geopolymerisation. Yang et al. (2014) and Zhang et al. (2017) reported that MgO participated in hydration reaction, whereas Komnitsas et al. (2007, 2009, 2013) argued that magnesium acted as chemically inert in FNS based mixtures. It also depends on the source of the FNS. Therefore, FNS from a new source has to be thoroughly investigated before its application as a geopolymer precursor.

2.6 Environmental effects

Though the utilization of industrial by-products as binder or aggregate in concrete brings several advantages, their effects on the surrounding environment due to possible leaching of heavy metals into the groundwater or soil needs to be investigated (Hillier et al., 1999; Marion et al., 2005; Srivastava et al., 2008). Marion et al. (2005) conducted a comparative study in order to identify the leaching of heavy metal from concrete containing blast furnace slag as SCM and porphyry as manufactured aggregate. The authors found that heavy metals released were negligible and well below the regularity limits as per United States Environmental Protection Agency (USEPA, 2009). Similarly, Li et al. (2012) found that leaching of toxic metals from concrete mixed with municipal solid waste incineration bottom ash were below the recommended limits. Manso et al. (2006) conducted a study on EAF slag where, it was used as both binder as well as aggregate in concrete. The authors observed that the leaching of toxic metals were well below the regularity limits in both cases. However, the leaching of heavy metals from the concrete containing EAF slag as a

binder were higher as compared to concrete with EAF slag aggregates due to higher cloistering effect. Furthermore, Motz and Geiseler (2001) concluded that the leaching of heavy metals from concrete with steel slag aggregate was negligible and environmentally safe for commercial applications. Besides, the application of pozzolanic materials such as fly ash and silica fume can play a vital role to reduce the leaching of manufactured aggregate by stabilizing the toxic chemicals in pore solution (Yousuf et al., 1995).

It can be seen from Table 2.1 that FNS contains some heavy metals such as Cr, Ni and Co. Therefore, it is necessary to assess the leaching properties of FNS as an aggregate or binder. FNS has been used in landfill applications in Korea. Kang et al. (2014) examined the soil from different locations where FNS was used as a landfill material. The authors conducted an investigation to determine the number of heavy metals which can be possibly leached out from FNS. This experimental study revealed that though pH of the soil was higher than silt, leaching of heavy metals were well below the allowable limits recommended by the United States Environmental Protection Agency (USEPA, 2009). Katsiotis et al. (2015) evaluated the leaching phenomena by tank diffusion in FNS blended concrete according to NEN 7375 (2004). The authors reported that the leaching of heavy metals were within the toxicity limits. On the other hand, geopolymer samples were reported as less susceptible to leaching of heavy metals in the surrounding environment due to low porosity. According to Komnitsas et al. (2013), FNS geopolymers encapsulated the heavy metals such as Pb, Cu, Cr and Ni. Therefore, heavy metals could not leach out from the concrete and maintained the structural integrity. In addition, Fidancevska et al. (2007) pointed out that heavy metals in FNS aggregate are chemically inert. Similarly, Demotica et al. (2012) concluded that toxicity of FNS was less than the maximum allowable concentrations recommended by the standard (USEPA, 2009) and FNS is classified as a non-hazardous material. Recently, Huang et al. (2017) stated that leaching toxicity of Cr in

the case of the mortar containing 30% FNS powder is rather low (<0.2 mg/L), which meets the GB 30760 standard (2014). However, Tangahu et al. (2015) found that the concentration of Cr in FNS from reclamation area exceeded the quality standard in toxicity characteristic leaching procedure (TCLP) based on Indonesia's government regulation.

From the above discussion, FNS was generally shown to be an environmentally friendly construction material. Its use as a binder or aggregate in concrete and geopolymer exhibited very low leaching of heavy metals. Therefore, this slag can be used in construction practice without any harmful impact on the environment.

2.7 Limitations and challenges

From the above discussion, it is apparent that FNS is an environmentally friendly construction material and its use will reduce the waste management cost of nickel industries. However, the use of FNS so far has been very limited and is mainly remained in land filling with some use in concrete productions. There is some notable research work carried out using this material as an aggregate in concrete around 1990 and eventually, this material has been added to the Japanese Industrial Standards (JIS) in 1994 (JSCE, 1994). However, Tomosawa et al. (1997) noticed that this slag is alkali-silica reactive and suggested that the use of low alkali cement or blast furnace slag or fly ash as a supplementary binder to prevent the resulting expansion. Consequently, alkali-silica reactivity is a hindrance to the use wide application of FNS as fine aggregate in concrete. On the other hand, the use fly ash is a well-established ASR mitigation technique. It is also noted that published research related to ASR of FNS are insufficient. Choi and Choi (2015) used accelerated mortar bar test to assess the reactivity of this aggregate under aggressive environment. Therefore, there is a scope to evaluate the long-term ASR performance of FNS aggregates in concrete. Shehata and Thomas (2000) used 18 different types of fly ash with reactive siliceous limestone (Spratt) to evaluate the ASR for two years. In their study,

class F fly ash was found to be more effective to mitigate the ASR as compared to class C fly ash. The continuation of their study indicated that 25% or 40% cement replacement by Class F fly ash was effective to mitigate the deleterious ASR expansion after 18 years of field exposure; however, control concrete with reactive aggregate suffered from excessive expansion and cracking (Thomas et al., 2011). The reactivity of different aggregates can be different, which mainly depends on its mineral composition. Therefore, an experimental study to evaluate ASR of concrete containing FNS aggregate with various proportions of class F fly ash needs to be conducted. Such test results will provide concrete manufacturers with detailed knowledge on the mitigation of potential ASR of FNS aggregates in concrete. Although ASTM C1293 (2015) suggests conducting the ASR experiment for a duration of two years, a longer testing period of 5 to 10 years will be highly efficient to identify any slow reactivity phenomena of FNS aggregate combined with fly ash. Besides, an experimental study can be conducted using ground FNS (after grinding as cement substitution) as ASR mitigation technique in FNS aggregate concrete or mortar.

The presence of high percentage of magnesium in FNS is hindering its application as a SCM. The chemical analysis of FNS indicates the presence MgO it is about 30% (Table 2.1). It has been well established that, presence of excessive MgO can lead to deleterious expansion after 2-5 years of curing due to the hydration reaction of MgO (Du, 2005). The maximum allowable limit of MgO is 15% in a binder according to AS 3582.2 standard (2016). However, Rahman et al. (2017) reported that the MgO present in FNS aggregate is in a crystal form known as forsterite, which was not found to take part in reactions in Portland cement systems. Komnitsas et al. (2007, 2009, 2013) also reported the similar findings for FNS based geopolymers. However, Yang et al. (2014) and Zhang et al. (2017) stated that the MgO present in FNS is not chemically inert based on hydration reaction product in geopolymer concrete. Moreover, it can be concluded that the variation in

experimental results between the researchers is due to the different sources and manufacturing process of FNS and the differences in use. Therefore, a detailed investigation is needed in order to understand FNS as a binder from any particular source in order to evaluate the crystal structure of magnesia and its effect on the durability properties of FNS concrete. Besides, 20% replacement of binder by FNS in control concrete or fly ash/metakaolin based geopolymer concrete will keep the MgO content below 10%, which is acceptable as per AS 3582.2 standard (2016). The FNS slag has not been adopted widely due to the lack of extensive research on the durability properties of FNS blended concrete.

Recently, some studies have been conducted on the use of FNS in geopolymers. However, hydration reactions associated with geopolymer are yet to be completely understood, especially the aspects of volume stability (Zuhua et al., 2009; Chanh et al., 2008; Zhang et al., 2009). Moreover, further research is needed to identify the fresh and durability properties of FNS blended cement concrete as well as geopolymer concrete.

2.8 Summary

The following points are summarised from the literature review:

1. The increase of FNS aggregate reduced workability of concrete. Furthermore, bleeding was found to increase slightly in presence of high-density FNS aggregate.
2. The utilization of FNS as up to 50% replacement of natural sand improved the mechanical properties such as compressive strength, modulus of elasticity, tensile strength and flexural strength.
3. The durability properties of FNS concrete such as air permeability and carbonation similar to those of conventional concrete. However, there is a dispute among the researchers about the freeze and thaw resistance of FNS due to the difference in the FNS properties. Moreover, drying shrinkage is higher in FNS concrete.

4. The potential ASR expansion of FNS aggregate is an important aspect that needs to be considered in mix designs. The presence of amorphous silica in water-cooled FNS aggregate may cause ASR expansion. Use of SCMs such as fly ash and blast furnace slag as partial cement replacement can be an effective way to mitigate the potential ASR expansion of FNS fine aggregate.
5. FNS is a suitable alternative to natural aggregates for pavement construction.
6. The MgO present in FNS is in a crystalline structure known as forsterite, which is highly stable in hydration reactions both in OPC concrete and geopolymer concrete.
7. FNS shows satisfactory performance as a binder in both OPC concrete and geopolymer. In fly ash based geopolymer, the use of 20% FNS exhibits higher compressive strength than the reference concrete.
8. There is no negative impact on the environment due to the utilization of FNS in the concrete.
9. Finally, the utilization of FNS as aggregate or supplementary binder could be a good step towards sustainable infrastructure development.

2.9 References

- Achal, V., Pan, X., & Özyurt, N. (2011). Improved strength and durability of fly ash-amended concrete by microbial calcite precipitation. *Ecological Engineering*, 37(4), 554-559.
- Aggarwal, P., Aggarwal, Y., & Gupta, S. M. (2007). Effect of bottom ash as replacement of fine aggregates in concrete. *Asian journal of civil engineering (building and housing)*, 8(1), 49-62.
- Ahmedzade, P., & Sengoz, B. (2009). Evaluation of steel slag coarse aggregate in hot mix asphalt concrete. *Journal of Hazardous Materials*, 165(1-3), 300-305.
- Ameri, M., & Behnood, A. (2012). Laboratory studies to investigate the properties of CIR mixes containing steel slag as a substitute for virgin aggregates. *Construction and Building Materials*, 26(1), 475-480.
- Ameri, M., Hesami, S., & Goli, H. (2013). Laboratory evaluation of warm mix asphalt mixtures containing electric arc furnace (EAF) steel slag. *Construction and Building materials*, 49, 611-617.
- Andrade, L. B., Rocha, J. C., & Cheriaf, M. (2009). Influence of coal bottom ash as fine aggregate on fresh properties of concrete. *Construction and Building Materials*, 23(2), 609-614.
- AS 1012.10. (2014). Determination of Indirect Tensile Strength of Concrete Cylinders ('Brazil' or Splitting Test). Standards Australia, Sydney, Australia.
- AS 1012.17. (1997). Methods of Testing Concrete - Determination of the Static Chord Modulus of Elasticity and Poisson's Ratio of Concrete Specimens. Standards Australia, Sydney, Australia.
- AS 1012.3.1. (2014). Determination of Properties Related to the Consistency of Concrete - Slump Test. Standards Australia, Sydney, Australia.
- AS 3582.2. (2016). Supplementary Cementitious Materials Part 2: Slag-Ground Granulated Blast-Furnace. Standards Australia, Sydney, Australia.
- ASTM C109 / C109M-16a, (2016). Standard Test Method for Compressive Strength of Hydraulic Cement Mortars (Using 2-in. or [50-mm] Cube Specimens). ASTM International, West Conshohocken, PA.
- ASTM C1260, (2014). Standard Test Method for Potential Alkali Reactivity of Aggregates (Mortar-Bar Method). ASTM International, West Conshohocken, PA.
- ASTM C666, (1992). Standard Test Method for Resistance of Concrete to Rapid Freezing and Thawing. ASTM International, West Conshohocken, PA.
- ASTM, C. 1293, (2015) Standard Test Method for Determination of Length Change of Concrete Due to Alkali-Silica Reaction, ASTM International, West Conshohocken, PA.
- Australasian Slag Association (ASA), (2002). A guide to the use of iron and steel slag in roads, Wollongong, NSW.
- Bagampadde, U., Wahhab, H. A. A., & Aiban, S. A. (1999). Optimization of steel slag aggregates for bituminous mixes in Saudi Arabia. *Journal of Materials in Civil Engineering*, 11(1), 30-35.

- Behnood, A., & Ameri, M. (2012). Experimental investigation of stone matrix asphalt mixtures containing steel slag. *Scientia Iranica*, 19(5), 1214-1219.
- Berndt, M. L. (2009). Properties of sustainable concrete containing fly ash, slag and recycled concrete aggregate. *Construction and building materials*, 23(7), 2606-2613.
- Carvalho, S. Z., Vernilli, F., Almeida, B., Demarco, M., & Silva, S. N. (2017). The recycling effect of BOF slag in the portland cement properties. *Resources, Conservation and Recycling*, 127, 216-220.
- Van Chanh, N., Trung, B. D., & Van Tuan, D. (2008, November). Recent research geopolymer concrete. In *The 3rd ACF International Conference-ACF/VCA, Vietnam* (Vol. 18, pp. 235-241).
- Choi, Y. C., & Choi, S. (2015). Alkali-silica reactivity of cementitious materials using ferro-nickel slag fine aggregates produced in different cooling conditions. *Construction and Building Materials*, 99, 279-287.
- Das, B., Prakash, S., Reddy, P. S. R., & Misra, V. N. (2007). An overview of utilization of slag and sludge from steel industries. *Resources, conservation and recycling*, 50(1), 40-57.
- Du, C. (2005). A review of magnesium oxide in concrete. *Concrete international*, 27(12), 45-50.
- Emery, J. (1984). Steel slag utilization in asphalt mixes. In *Proceedings. Canadian Technical Asphalt Association*.
- Fidancevska, E., Mangutova, B., Milosevski, D., Milosevski, M., & Bossert, J. (2003). Obtaining of dense and highly porous ceramic materials from metallurgical slag. *Science of Sintering*, 35(2), 85-91.
- Fidancevska, E., Vassilev, V., Milosevski, M., Parvanov, S., Milosevski, D., & Aljihmani, L. (2007). Composites based on industrial wastes III. production of composites of Fe-Ni slag and waste glass. *Journal of the University of Chemical Technology and Metallurgy*, 42(3), 285-290.
- GB 30760. (2014). Technical specification for coprocessing of solid waste in cement kiln. National Standards of People's Republic of China. <https://www.chinesestandard.net/Default.aspx?PDF-English-ID=GB%2030760-2014>
- Geopolymer institute, (2017). Geopolymer cement and Geopolymer Concrete. <https://www.geopolymer.org/applications/geopolymer-cement/>
- Ghods, P., Alizadeh, R., & Salehi, M. (2017). Electrical methods and systems for concrete testing, United States patent US 9,638,652. <https://www.google.com/patents/US9638652>.
- Grattan-Bellew, P. E., Mitchell, L. D., Margeson, J., & Min, D. (2010). Is alkali-carbonate reaction just a variant of alkali-silica reaction ACR= ASR?. *Cement and Concrete Research*, 40(4), 556-562.
- Hainin, M. R., Rusbintardjo, G., Aziz, M. A. A., Hamim, A., & Yusoff, N. M. (2013). Laboratory evaluation on steel slag as aggregate replacement in stone mastic asphalt mixtures. *Jurnal Teknologi*, 65(2), 13-19.

- Hainin, M. R., Rusbintardjo, G., Hameed, M. A. S., Hassan, N. A., & Yusoff, N. I. M. (2014). Utilisation of steel slag as an aggregate replacement in porous asphalt mixtures. *Jurnal Teknologi (Sciences and Engineering)*, 69(1), 67-73.
- Hainin, M. R., Yusoff, N. I. M., Mohammad Sabri, M. F., Abdul Aziz, M. A., Sahul Hameed, M. A., & Farooq Reshi, W. (2012). Steel slag as an aggregate replacement in Malaysian hot mix asphalt. *ISRN Civil Engineering*, 2012.
- Hardjito, D., Wallah, S. E., Sumajouw, D. M., & Rangan, B. V. (2004). On the development of fly ash-based geopolymer concrete. *Materials Journal*, 101(6), 467-472.
- Hardjito, D., Wallah, S. E., Sumajouw, D. M., & Rangan, B. V. (2005). Fly ash-based geopolymer concrete. *Australian Journal of Structural Engineering*, 6(1), 77-86.
- Hillier, S. R., Sangha, C. M., Plunkett, B. A., & Walden, P. J. (1999). Long-term leaching of toxic trace metals from Portland cement concrete. *Cement and Concrete Research*, 29(4), 515-521.
- Hou, X., Struble, L. J., & Kirkpatrick, R. J. (2004). Formation of ASR gel and the roles of CSH and portlandite. *Cement and Concrete research*, 34(9), 1683-1696.
- Hu, J., & Wang, K. (2005, August). Effects of aggregate on flow properties of mortar. In *Proceeding of the Mid-Continent Transportation Research Symposium* (p. 8).
- Huang, Y., Wang, Q., & Shi, M. (2017). Characteristics and reactivity of ferronickel slag powder. *Construction and Building Materials*, 156, 773-789.
- Ismail, Z. Z., & Al-Hashmi, E. A. (2008). Use of waste plastic in concrete mixture as aggregate replacement. *Waste Management*, 28(11), 2041-2047.
- Ichikawa, T., & Miura, M. (2007). Modified model of alkali-silica reaction. *Cement and Concrete research*, 37(9), 1291-1297.
- JIS A 1123. (1997). Method of test for bleeding of concrete. Japanese Standards Association. <https://infostore.saiglobal.com/store/details.aspx?ProductID=956225>
- JIS A 1148. (2010). Method of test for splitting tensile strength of concrete. Japanese Standards Association. https://webdesk.jsa.or.jp/books/W11M0090/index/?bunsyo_id=JIS%20A%201148:2010
- JMIA. (1991). Research of ferronickel slag fine aggregate for concrete, Japan Mining Industry Association. <http://jglobal.jst.go.jp>.
- JSCE. (1994). Guidelines for Construction Using Ferronickel Slag Fine Aggregate Concrete. Concr. Libr. JSCE No. 24. <http://www.jsce.or.jp>.
- Kang, S. S., Park, K., & Kim, D. (2014). Potential Soil Contamination in Areas Where Ferronickel Slag Is Used for Reclamation Work. *Materials*, 7(10), 7157-7172.
- Katsiotis, N. S., Tsakiridis, P. E., Velissariou, D., Katsiotis, M. S., Alhassan, S. M., & Beazi, M. (2015). Utilization of ferronickel slag as additive in Portland cement: a hydration leaching study. *Waste and Biomass Valorization*, 6(2), 177-189.
- Klein, C., Hurlbut, C.S., & Dana, J.D. (1998). Manual of mineralogy. Twenty first ed. Wiley, New Jersey, United States, pp. 373–375.
- Komnitsas, K., Zaharaki, D., & Bartzas, G. (2013). Effect of sulphate and nitrate anions on heavy metal immobilisation in ferronickel slag geopolymers. *Applied clay science*, 73, 103-109.

- Komnitsas, K., Zaharaki, D., & Perdikatsis, V. (2007). Geopolymerisation of low calcium ferronickel slags. *Journal of Materials Science*, 42(9), 3073-3082.
- Komnitsas, K., Zaharaki, D., & Perdikatsis, V. (2009). Effect of synthesis parameters on the compressive strength of low-calcium ferronickel slag inorganic polymers. *Journal of Hazardous Materials*, 161(2-3), 760-768.
- Kosanović, C., Stubičar, N., Tomašić, N., Bermanec, V., & Stubičar, M. (2005). Synthesis of a forsterite powder by combined ball milling and thermal treatment. *Journal of alloys and compounds*, 389(1-2), 306-309.
- Krayushkina, K., Prentkovskis, O., Bieliatynskiy, A., & Junevičius, R. (2012). Use of steel slags in automobile road construction. *Transport*, 27(2), 129-137.
- Kuroda, M., Watanabe, T., & Terashi, N. (2000). Increase of bond strength at interfacial transition zone by the use of fly ash. *Cement and Concrete Research*, 30(2), 253-258.
- Lee, K. M., Lee, H. K., Lee, S. H., & Kim, G. Y. (2006). Autogenous shrinkage of concrete containing granulated blast-furnace slag. *Cement and Concrete Research*, 36(7), 1279-1285.
- Li, X. G., Lv, Y., Ma, B. G., Chen, Q. B., Yin, X. B., & Jian, S. W. (2012). Utilization of municipal solid waste incineration bottom ash in blended cement. *Journal of Cleaner Production*, 32, 96-100.
- Loh, Y. R., Sujan, D., Rahman, M. E., & Das, C. A. (2013). Sugarcane bagasse—The future composite material: A literature review. *Resources, Conservation and Recycling*, 75, 14-22.
- Maghsoudlou, M. S. A., Ebadzadeh, T., Sharafi, Z., Arabi, M., & Zahabi, K. R. (2016). Synthesis and sintering of nano-sized forsterite prepared by short mechanochemical activation process. *Journal of Alloys and Compounds*, 678, 290-296.
- Manso, J. M., Polanco, J. A., Losanez, M., & Gonzalez, J. J. (2006). Durability of concrete made with EAF slag as aggregate. *Cement and Concrete Composites*, 28(6), 528-534.
- Maragkos, I., Giannopoulou, I. P., & Pnias, D. (2009). Synthesis of ferronickel slag-based geopolymers. *Minerals Engineering*, 22(2), 196-203.
- Marion, A. M., De Laneve, M., & De Grauw, A. (2005). Study of the leaching behaviour of paving concretes: quantification of heavy metal content in leachates issued from tank test using demineralized water. *Cement and Concrete Research*, 35(5), 951-957.
- Masterbuilder, (2014). River Sand Substitutes – An Overview. Masterbuilder, India's premier construction magazine. <https://www.masterbuilder.co.in/river-sand-substitutes-overview/>.
- Mehta, P. K., & Monteiro, P. J. (2006). Microstructure and properties of hardened concrete. *Concrete: Microstructure, properties and materials*, 41-80.
- Mo, L., Deng, M., Tang, M., & Al-Tabbaa, A. (2014). MgO expansive cement and concrete in China: Past, present and future. *Cement and Concrete Research*, 57, 1-12.
- Molugaram, K., Shanker, J. S., & Ramesh, A. (2014). A study on influence of shape of aggregate on strength and quality of concrete for buildings and pavements. In *Advanced materials research* (Vol. 941, pp. 776-779). Trans Tech Publications.

- Motz, H., & Geiseler, J. (2001). Products of steel slags an opportunity to save natural resources. *Waste Management*, 21(3), 285-293.
- Moser, R. D., Jayapalan, A. R., Garas, V. Y., & Kurtis, K. E. (2010). Assessment of binary and ternary blends of metakaolin and Class C fly ash for alkali-silica reaction mitigation in concrete. *Cement and Concrete Research*, 40(12), 1664-1672.
- Nagataki, S., & Ujike, I. (1988). Effect of heating condition on air permeability of concrete at elevated temperature, *Trans. Jap. Concr. Inst.* 10, 147-154. <https://ci.nii.ac.jp/naid/110009743015/en/>
- NEN 7375. (2004). Leaching characteristics determination of the leaching of inorganic components from moulded or monolithic materials with the diffusion test-solid earthy and stony materials, Netherlands Normalisation Institute Standard, Delft. <https://www.iso.org>
- Oluwasola, E. A., Hainin, M. R., & Aziz, M. M. A. (2015). Evaluation of rutting potential and skid resistance of hot mix asphalt incorporating electric arc furnace steel slag and copper mine tailing, *Ind. J. Engg. Mater. Sci.* 22, 550–558.
- Oluwasola, E. A., Hainin, M. R., & Aziz, M. M. A. (2015). Evaluation of asphalt mixtures incorporating electric arc furnace steel slag and copper mine tailings for road construction. *Transportation Geotechnics*, 2, 47-55.
- Pang, B., Zhou, Z., Hou, P., Du, P., Zhang, L., & Xu, H. (2016). Autogenous and engineered healing mechanisms of carbonated steel slag aggregate in concrete. *Construction and Building Materials*, 107, 191-202.
- Pasetto, M., & Baldo, N. (2006). Electric arc furnace steel slags in high performance asphalt mixes: A laboratory characterisation. In *TMS Fall Extraction and Processing Division: Sohn International Symposium*, San Diego.
- Pofale, A. D., & Deo, S. V. (2010). Comparative long term study of concrete mix design procedure for fine aggregate replacement with fly ash by minimum voids method and maximum density method. *KSCE Journal of Civil Engineering*, 14(5), 759-764.
- Qasrawi, H., Shalabi, F., & Asi, I. (2009). Use of low CaO unprocessed steel slag in concrete as fine aggregate. *Construction and Building Materials*, 23(2), 1118-1125.
- Rahman, M. A., Sarker, P. K., Shaikh, F. U. A., & Saha, A. K. (2017). Soundness and compressive strength of Portland cement blended with ground granulated ferronickel slag. *Construction and Building Materials*, 140, 194-202.
- Rodriguez, Á., Manso, J. M., Aragón, Á., & Gonzalez, J. J. (2009). Strength and workability of masonry mortars manufactured with ladle furnace slag. *Resources, conservation and recycling*, 53(11), 645-651.
- Sakkas, K., Nomikos, P., Sofianos, A., & Panias, D. (2014). Utilisation of FeNi-slag for the production of inorganic polymeric materials for construction or for passive fire protection. *Waste and Biomass Valorization*, 5(3), 403-410.
- Sakoi, Y., Aba, M., Tsukinaga, Y., & Nagataki, S. (2013). Properties of concrete used in ferronickel slag aggregate. In *Proceedings of the 3rd International Conference on Sustainable Construction Materials and Technologies*, Tokyo, Japan.
- Santamarina, J.C. (2008). Flow test evaluation. https://smartech.gatech.edu/bitstream/handle/1853/23048/e-20-k79_9124.pdf.

- Sato, T., Watanabe, K., Ota, A., Aba, M., & Sakoi, Y. (2011). Influence of excessive bleeding on frost susceptibility of concrete incorporating ferronickel slag as aggregates. In *36th Conference on Our World in Concrete & Structures*.
- Shafaatian, S. M., Akhavan, A., Maraghechi, H., & Rajabipour, F. (2013). How does fly ash mitigate alkali–silica reaction (ASR) in accelerated mortar bar test (ASTM C1567)? *Cement and Concrete Composites*, *37*, 143-153.
- Shehata, M. H., & Thomas, M. D. (2000). The effect of fly ash composition on the expansion of concrete due to alkali–silica reaction. *Cement and Concrete Research*, *30*(7), 1063-1072.
- Shehata, M. H., Thomas, M. D., & Bleszynski, R. F. (1999). The effects of fly ash composition on the chemistry of pore solution in hydrated cement pastes. *Cement and Concrete Research*, *29*(12), 1915-1920.
- Shi, C. (2004). Effect of mixing proportions of concrete on its electrical conductivity and the rapid chloride permeability test (ASTM C1202 or ASSHTO T277) results. *Cement and Concrete Research*, *34*(3), 537-545.
- Shi, C., Meyer, C., & Behnood, A. (2008). Utilization of copper slag in cement and concrete. *Resources, Conservation and Recycling*, *52*(10), 1115-1120.
- Shi, C., & Qian, J. (2000). High performance cementing materials from industrial slags—a review. *Resources, Conservation and Recycling*, *29*(3), 195-207.
- Shoya, M., Sugita, S., Tsukinaga, Y., Aba, M., & Tokuhasi, K. (1999). Properties of self-compacting concrete with slag fine aggregates. In *Exploiting Wastes in Concrete*, Thomas Telford Publishing.
- Skaf, M., Manso, J. M., Aragón, Á., Fuente-Alonso, J. A., & Ortega-López, V. (2017). EAF slag in asphalt mixes: A brief review of its possible re-use. *Resources, Conservation and Recycling*, *120*, 176-185.
- Srivastava, S., Chaudhary, R., & Khale, D. (2008). Influence of pH, curing time and environmental stress on the immobilization of hazardous waste using activated fly ash. *Journal of hazardous materials*, *153*(3), 1103-1109.
- Swamy, R.N. (1992), Testing for alkali–silica reaction, in: R.N. Swamy (Ed.), *The Alkali–Silica Reaction in Concrete*, Blackie, Glasgow and London, and Van Nostrand-Reinhold, New York, pp. 54–95.
- Tangahu, B. V., Warmadewanthi, I. D. A. A., Saptarini, D., Pudjiastuti, L., Tardan, M. A. M., & Luqman, A. (2015). Ferronickel slag performance from reclamation area in Pomalaa, southeast Sulawesi, Indonesia. *Advances in Chemical Engineering and Science*, *5*(03), 408.
- Thomas, M., Dunster, A., Nixon, P., & Blackwell, B. (2011). Effect of fly ash on the expansion of concrete due to alkali-silica reaction—Exposure site studies. *Cement and Concrete composites*, *33*(3), 359-367.
- Togawa, K., Shoya, M., & Kokubu, K. (1996). Characteristics of bleeding, freeze-thaw resistance and watertightness of concrete with ferro-nickel slag fine aggregates. *Journal of the Society of Materials Science, Japan*, *45*(1), 101-109.
- Tomosawa, F., Nagataki, S., Kajiwara, T., & Yokoyama, M. (1997). Alkali-aggregate Reactivity of Ferronickel-Slag Aggregate Concrete. *ACI Special Publication*, *170*, 1591-1602.

- US EPA. (2009). Hazardous waste characteristics. United States Environmental Protection Agency, Washington, D.C., United States. <https://www.epa.gov/sites/production/files/2016-01/documents/hw-char.pdf/>.
- US-GS. (2009). Mineral Commodity Summaries. United States Geological Survey, Reston, Virginia, United States. <https://minerals.usgs.gov/minerals/pubs/mcs/2009/mcs2009.pdf>
- Vayghan, A. G., Rajabipour, F., & Rosenberger, J. L. (2016). Composition–rheology relationships in alkali–silica reaction gels and the impact on the gel's deleterious behavior. *Cement and Concrete Research*, 83, 45-56.
- Wang, G., & Thompson, R. (2011). Slag use in highway construction-the philosophy and technology of its utilization. *International Journal of Pavement Research and Technology*, 4(2), 97-103.
- Wang, G., Thompson, R., Wang, Y., 2011. Hot-mix asphalt that contains nickel slag aggregate: laboratory evaluation of use in highway construction. *Trans. Res. Record: J. Trans. Res. Board.* 2208, 1-8. <https://doi.org/10.3141/2208-01>
- Wang, G., Thompson, R., & Wang, Y. (2011). Hot-mix asphalt that contains nickel slag aggregate: laboratory evaluation of use in highway construction. *Transportation Research Record: Journal of the Transportation Research Board*, (2208), 1-8.
- Wang, S., Miller, A., Llamazos, E., Fonseca, F., & Baxter, L. (2008). Biomass fly ash in concrete: mixture proportioning and mechanical properties. *Fuel*, 87(3), 365-371.
- Wu, K. R., Chen, B., Yao, W., & Zhang, D. (2001). Effect of coarse aggregate type on mechanical properties of high-performance concrete. *Cement and Concrete Research*, 31(10), 1421-1425.
- Wu, S., Xue, Y., Ye, Q., & Chen, Y. (2007). Utilization of steel slag as aggregates for stone mastic asphalt (SMA) mixtures. *Building and Environment*, 42(7), 2580-2585.
- Yang, T., Yao, X., & Zhang, Z. (2014). Geopolymer prepared with high-magnesium nickel slag: characterization of properties and microstructure. *Construction and Building Materials*, 59, 188-194.
- Yasuaki, M., Hiromichi, T., Yoshio, O., & Kenji, M. (1989). A study on cooling condition and structure of ferronickel slag: cooling condition for prevention of alkali-aggregate reaction. *Shigen-to-Sozai*, 105(14), 1067–1071.
- Yeau, K. Y., & Kim, E. K. (2005). An experimental study on corrosion resistance of concrete with ground granulate blast-furnace slag. *Cement and Concrete Research*, 35(7), 1391-1399.
- Yi, H., Xu, G., Cheng, H., Wang, J., Wan, Y., & Chen, H. (2012). An overview of utilization of steel slag. *Procedia Environmental Sciences*, 16, 791-801.
- Yousuf, M., Mollah, A., Vempati, R. K., Lin, T. C., & Cocke, D. L. (1995). The interfacial chemistry of solidification/stabilization of metals in cement and pozzolanic material systems. *Waste management*, 15(2), 137-148.
- Yüksel, İ., Bilir, T., & Özkan, Ö. (2007). Durability of concrete incorporating non-ground blast furnace slag and bottom ash as fine aggregate. *Building and Environment*, 42(7), 2651-2659.
- Zhang, Z., Zhu, Y., Yang, T., Li, L., Zhu, H., & Wang, H. (2017). Conversion of local industrial wastes into greener cement through geopolymer technology: a case study of high-magnesium nickel slag. *Journal of cleaner production*, 141, 463-471.

- Zhang, Z. H., Yao, X., Zhu, H. J., Hua, S. D., & Chen, Y. (2009). Preparation and mechanical properties of polypropylene fiber reinforced calcined kaolin-fly ash based geopolymer. *Journal of Central South University of Technology*, 16(1), 49-52.
- Zheng, L., Wang, W., & Shi, Y. (2010). The effects of alkaline dosage and Si/Al ratio on the immobilization of heavy metals in municipal solid waste incineration fly ash-based geopolymer. *Chemosphere*, 79(6), 665-671.
- Ziari, H., Nowbakht, S., Rezaei, S., & Mahboob, A. (2015). Laboratory investigation of fatigue characteristics of asphalt mixtures with steel slag aggregates. *Advances in Materials Science and Engineering*, 2015.
- Zuhua, Z., Xiao, Y., Huajun, Z., & Yue, C. (2009). Role of water in the synthesis of calcined kaolin-based geopolymer. *Applied Clay Science*, 43(2), 218-223.

Every reasonable effort has been made to acknowledge the owners of copyright material. I would be pleased to hear from any copyright owner has been omitted or incorrectly acknowledged.

PART II: MECHANICAL PROPERTIES

Chapter 3: WORKABILITY & STRENGTH PROPERTIES OF MORTAR USING FNS AGGREGATE

The contents presented in this chapter were published in the following paper:

Saha, A. K., & Sarker, P. K. (2017). Compressive strength of mortar containing ferronickel slag as replacement of natural sand. Procedia engineering, 171, 689-694.

This chapter evaluates the workability and strength properties of mortar containing different percentages of FNS aggregate. The influence of FNS aggregate on these properties has been evaluated and compared with those of the control mixture and a suitable proportion of FNS aggregate has been suggested for mortar and concrete mixtures.

3.1 Overview

Construction works require a significant amount of earth's natural resources. Sand has been used as a fine aggregate in concrete for decades. The demand for concrete is increasing with the growth in both developed and developing countries. However, our natural resources are limited, and sand is not extensively available in every country. Therefore, use of industrial by-products as aggregate can help solve this scarcity of natural sand and reduce the disposal cost of these by-products. Moreover, the production cost of concrete may also reduce, which will have a positive impact on the economic growth of the society. In search

of suitable alternatives to natural sand, research is being conducted on different types of industrial by-products, for instance, steel slag, blast furnace slag, copper slag and FNS. Aggregates constitute almost 70% to 80% of the volume of concrete. As a result, aggregates affect the fresh and hardened properties of concrete to a great extent. For example, steel slag aggregate was shown suitable for producing high strength concrete (Polanco et al., 2011; Dongxue et al., 1997; Maslehuddin et al., 2003). Furthermore, steel slag aggregate also performed better than the natural aggregate to produce hot mix asphalt concrete (Ahmedzade et al., 2009). However, blast furnace slag as a replacement of fine aggregate showed poor strength performance in concrete (Yüksel et al., 2006) though, ground granulated blast furnace slag and fly ash are usually found effective in improvement of the durability properties (Li & Zhao, 2003; Yüksel et al., 2007). The strength properties of mortar and concrete are influenced by the density, gradation and particle shape of aggregates used in the mix (Al-Negheimish et al., 1997). Granulated FNS showed higher density and lower water absorption compared to natural sand (Sato et al., 2011). The fresh concrete properties were also influenced by ferronickel slag. Concrete bleeding was shown to increase with an increment of ferronickel slag in concrete (Kokubu & Shoya, 1994). Compressive strength was found to increase by the replacement of sand by FNS. However, there is a difference in opinion among the researchers. Sakoi et al. (2013) pointed out that compressive strength remained same regardless the presence of FNS. Using industrial waste in construction works may impose a threat of leaching out of heavy metals and pollute the environment. However, FNS was found to be safe to use in land reclamation works as well as in construction works (Kang et al., 2014).

The properties of ferronickel slag largely depend on the source of ore as well as the smelting process. The slag used in this study was produced by sea water-cooling of the by-product from the smelting of garnierite nickel ore. The aim of the present chapter is to

evaluate the workability and strength of cement mortar containing FNS in different percentages of the fine aggregate. Furthermore, the effects of fly ash on the workability and strength of mortar are evaluated.

3.2 Materials and Methods

Ordinary portland cement (OPC), class F fly ash, FNS and natural sand were used in this study. Density and fineness modulus were determined for both natural sand and FNS. The FNS (2.78 g/cm^3) had a higher density compared to sand (2.16 g/cm^3). Furthermore, the fineness modulus of FNS (4.07) was higher than that of sand (1.95). The FNS particles are angular in shape and coarser than sand in size. The gradations of natural sand, FNS and their combinations in different percentages are plotted in Fig. 3.1. It can be seen that the grain size distribution becomes well-graded when the two aggregates are combined together. The best-graded combination is obtained for 50% replacement of sand by FNS.

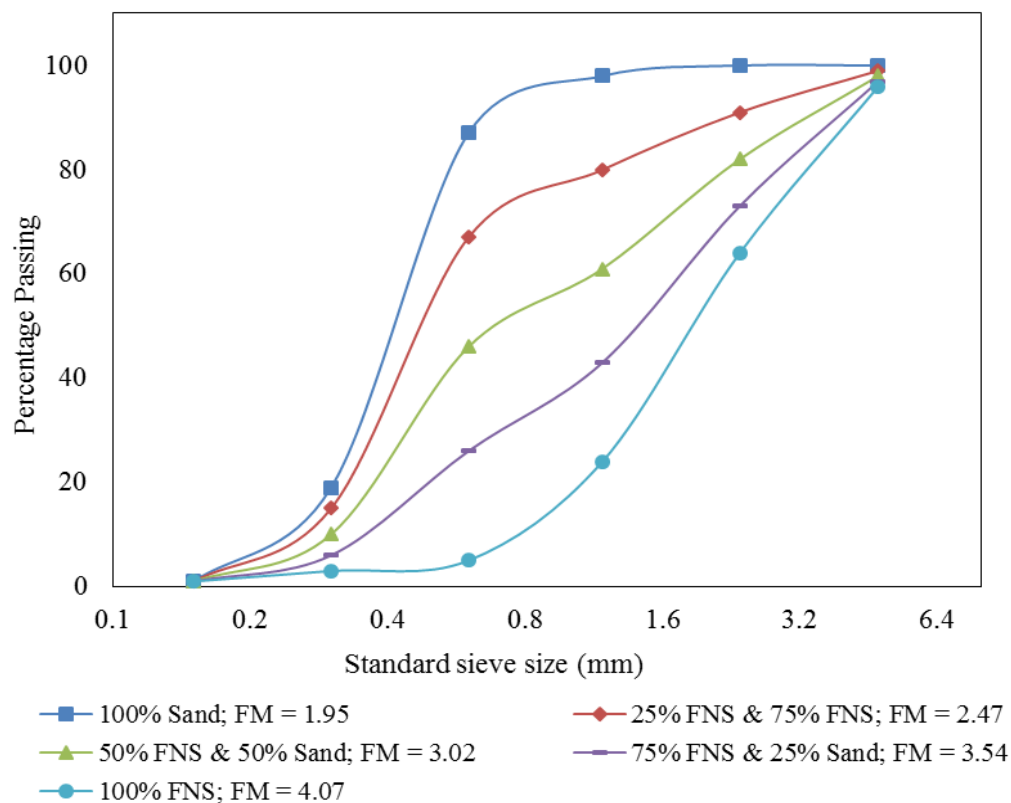


Fig. 3.1 Gradation of fine aggregates

Ten different mixtures were prepared in this study. In Series A, only OPC was used as the binder and sand was replaced in five different proportions (0%, 25%, 50%, 75% and 100%) by FNS. In series B, fly ash was used as 30% replacement of cement. Same combinations of the fine aggregates as in Series A were used in the mixtures of Series B. The water to cement ratio was kept constant at 0.47 for all the mixes. The reason for selecting 30% replacement of OPC with a class F fly ash was that it can reduce the CO₂ emission to a considerable extent (Nath & Sarker, 2013). The mixture proportions are given in Table 3.1.

Table 3.1 Mix proportions of mortar

Series	Sample ID	Binder (kg/m ³)		Fine aggregate (kg/m ³)		W/C
		OPC	FA	Sand	FNS	
A	A1	602	0	1355	0	0.47
	A2	602	0	1015	338	
	A3	602	0	678	678	
	A4	602	0	338	1015	
	A5	602	0	0	1355	
B	B1	421	181	1355	0	
	B2	421	181	1015	338	
	B3	421	181	678	678	
	B4	421	181	338	1015	
	B5	421	181	0	1355	

Flow test was conducted to determine the workability of the freshly mixed mortar. The flow table with the mortar was dropped 25 times in 15 seconds after removing the mould. The percentage increase of the final diameter of the spread after the drops to the original diameter is used to describe the flow of mortars. Fig. 3.2 shows the flow value measurements of the mortar mixes. Mortar cubes (50 mm) were cast for compressive strength tests. The samples were left in the mould for one day and then stripped from the

moulds. The samples were then cured by immersion in a lime saturated water tank. Compressive strengths of mortar were determined at 3, 7, 28 and 56 days after casting.

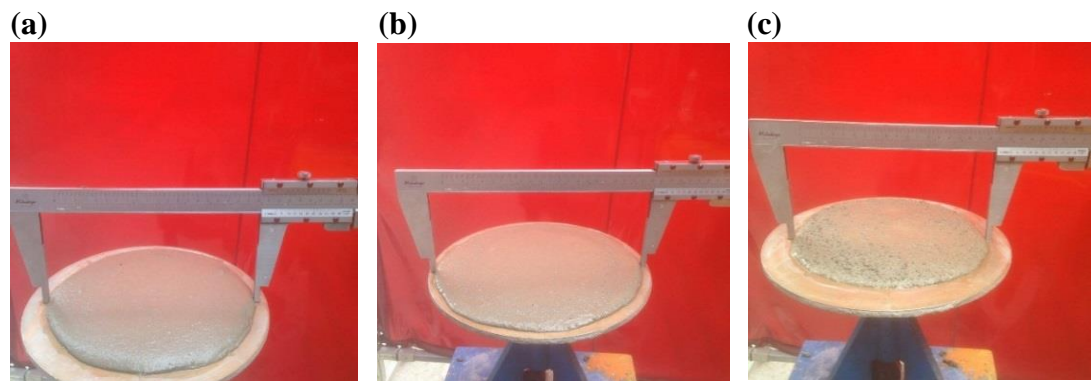


Fig. 3.2 Flow test (a) 100% sand; (b) 50% FNS and 50% sand (c) 100% FNS

3.3 Results and Discussion

3.3.1 Workability of mortar

Flow value was used to express the workability of mortar mixes. Fig. 3.3 shows the plot of flow values against the FNS contents. It can be seen that the flow of mortar increased with the increase of FNS till 50% sand replacement. However, the flow declined for replacement of sand by FNS beyond 50%. Since FNS particles are coarser than sand particles, less water is required to wet the FNS particles (Santamarina, 2008). Moreover, Workability of mortar largely depends on the gradation of fine aggregates in the mix (Hu & Wang, 2005). Since 50% sand replacement resulted in a well-graded aggregate combination, this showed the highest flow of mortar. The flow declined by FNS content of more than 50% because of the increase of angular particles in the mixture. Furthermore, fly ash has a positive effect on the workability of a mix. It can be seen that the fly ash blended mixes exhibited higher flow value than the OPC-only mixes. This is because of the well-known ball bearing effect of fly ash particles.

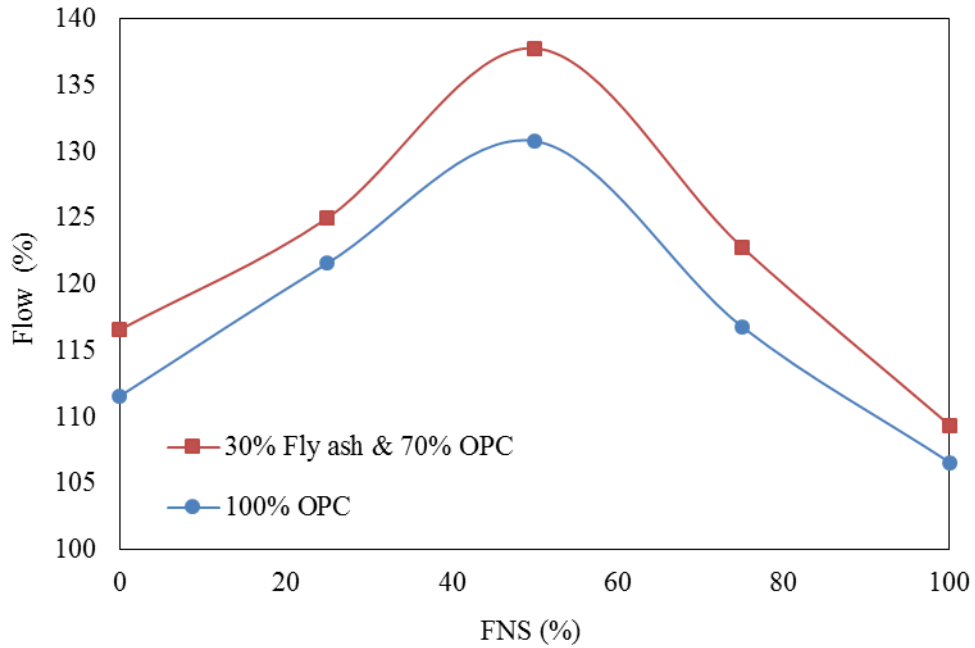


Fig. 3.3 Flow of mortar mixes

3.3.2 Compressive strength

The samples were dried in air before testing for compressive strength. The compressive strength results for series A are given in Fig. 3.4. It can be observed from the figure that compressive strength increased with the increase of FNS content up to 50% replacement level and then it declined with further increase of FNS. The similar phenomenon was observed at the ages of 3, 7, 28 and 56 days. The maximum 28-day compressive strength of 57 MPa was achieved for 50% FNS (Mix A3). The 28-day compressive strength of the samples with no FNS was 38 MPa. Therefore, 50% FNS resulted in about 50% increase of the 28-day compressive strength. Moreover, the compressive strength of samples containing 100% FNS (Mix A5) aggregate is 44 MPa, which was higher than that of the control sample.

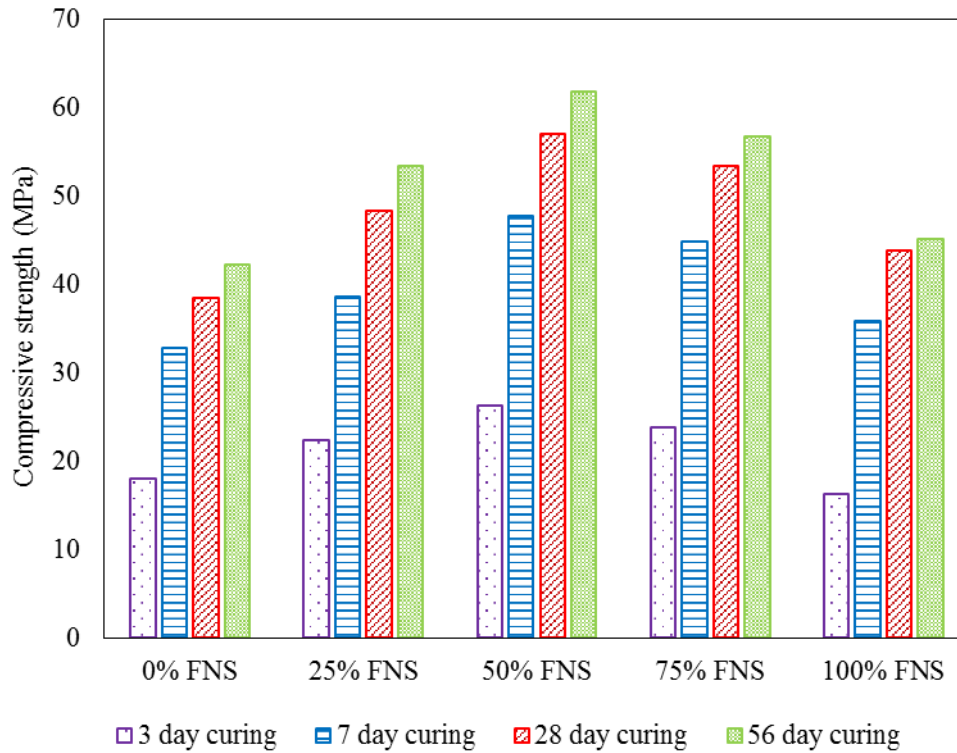


Fig. 3.4 Compressive strength of the mixtures with 100% OPC (Series A)

The compressive strength results of the mixtures containing 30% fly ash as cement replacement are presented in Fig. 3.5. It can be seen that compressive strength increased with the increase of FNS content up to 50% and then declined with further increase of FNS. The similar trend is observed at 3, 7, 28 and 56 days of age. Maximum 28-day compressive strength was 35 MPa for 50% FNS content. As expected, the compressive strength of the specimens of this series was less than the corresponding mixtures of series A because of the use of 30% fly ash as cement replacement. Fig. 3.6 exhibits the effect of 30% fly ash on the strength development of the mixtures containing 50% FNS. It can be seen that the strength development is slowed down by fly ash from the early ages. However, the difference between the strengths at early ages is reduced by the pozzolanic reaction of fly ash with the increase of age.

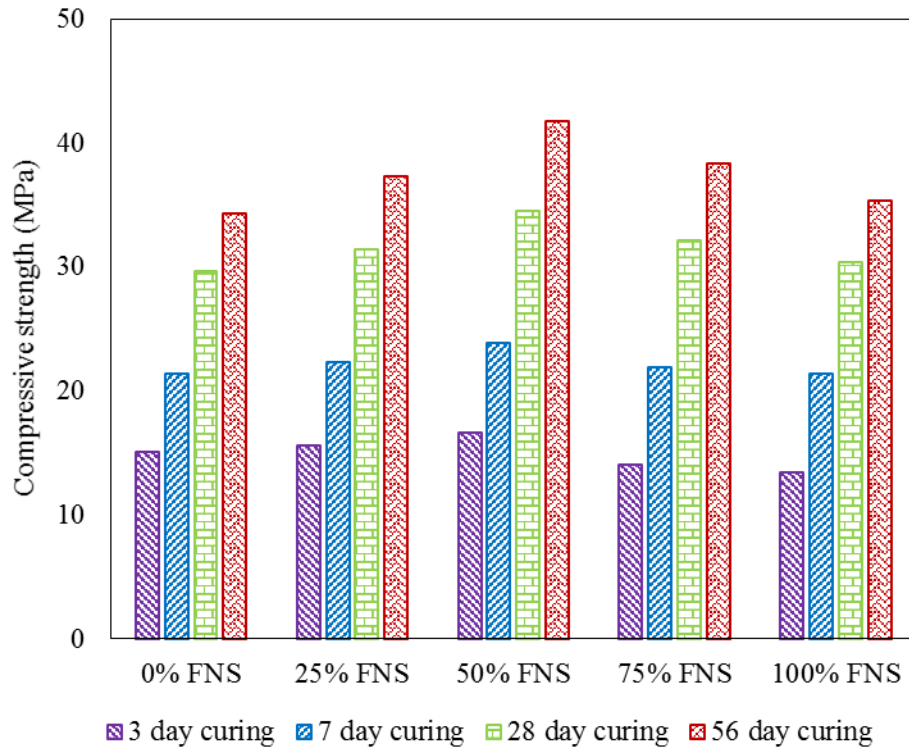


Fig. 3.5 Compressive strength of the mixtures with 30% fly ash and 70% OPC (series B)

From the above discussion, it is observed that FNS can improve the compressive strength considerably for up to 50% replacement of sand. This is attributed to the particle packing effect of the well-graded aggregates for 50% replacement of sand by the FNS.

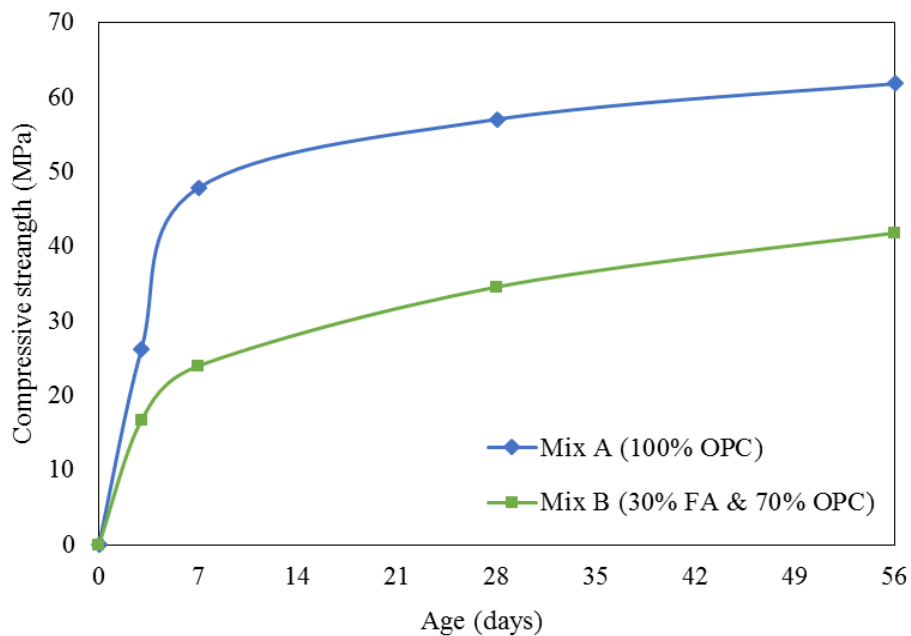


Fig. 3.6 Effect of fly ash on compressive strength development (50% FNS as aggregate).

3.4 Summary

The effect of FNS aggregates on the properties of mortar samples were analysed by experimental work and following conclusions are drawn from the study:

1. The workability and compressive strength of cement mortars containing different percentages of FNS as replacement of natural sand were evaluated. The results show that the optimum level of sand replacement by FNS is 50% for maximizing the compressive strength of mortar. This is because of the best particle packing was achieved by the well-graded aggregates at this combination.
2. Furthermore, 50% FNS also resulted in improved workability of mortar as determined by the flow test. The increase of flow by FNS is attributed to its relatively larger size compared to natural sand that reduced the water demand.
3. Use of a class F fly ash as 30% replacement of cement improved workability of mortar by the ball bearing effect. Fly ash decreased compressive strength of the mortars with and without FNS at both early and late ages up to 56 days.

4.5 References

- Ahmedzade, P., & Sengoz, B. (2009). Evaluation of steel slag coarse aggregate in hot mix asphalt concrete. *Journal of Hazardous Materials*, 165(1-3), 300-305.
- Al-Negheimish, A. I., Al-Sugair, F. H., & Al-Zaid, R. Z. (1997). Utilization of local steel making slag in concrete. *J King Saud Univ Eng Sci*, 9(1), 39-55.
- Dongxue, L., Xinhua, F., Xuequan, W., & Mingshu, T. (1997). Durability study of steel slag cement. *Cement and Concrete Research*, 27(7), 983-987.
- Güneysi, E., & Gesoğlu, M. (2008). A study on durability properties of high-performance concretes incorporating high replacement levels of slag. *Materials and Structures*, 41(3), 479-493.
- Hu, J., & Wang, K. (2005, August). Effects of aggregate on flow properties of mortar. In *Proceeding of the Mid-Continent Transportation Research Symposium* (p. 8).
- Kang, S. S., Park, K., & Kim, D. (2014). Potential Soil Contamination in Areas Where Ferronickel Slag Is Used for Reclamation Work. *Materials*, 7(10), 7157-7172.
- Kokubu, K., & Shoya, M. (1994). Guidelines for construction using Ferronickel slag fine aggregate concrete, Concrete library of JSCE No. 24.
- Li, G., & Zhao, X. (2003). Properties of concrete incorporating fly ash and ground granulated blast-furnace slag. *Cement and Concrete Composites*, 25(3), 293-299.
- Maslehuddin, M., Sharif, A. M., Shameem, M., Ibrahim, M., & Barry, M. S. (2003). Comparison of properties of steel slag and crushed limestone aggregate concretes. *Construction and building materials*, 17(2), 105-112.
- Nath, P., & Sarker, P. K. (2013). Effect of mixture proportions on the drying shrinkage and permeation properties of high strength concrete containing class F fly ash. *KSCE Journal of Civil Engineering*, 17(6), 1437-1445.
- Polanco, J. A., Manso, J. M., Setién, J., & González, J. J. (2011). Strength and Durability of Concrete Made with Electric Steelmaking Slag. *ACI Materials Journal*, 108(2).
- Rahman, M. A., Sarker, P., & Shaikh, F. (2015). Fresh and Early-Age Properties of Cement Pastes and Mortars Blended with Nickel Slag. In *Construction Innovations, Research into Practice*. Concrete Institute of Australia.
- Sato, T., Watanabe, K., Ota, A., Aba, M., & Sakoi, Y. (2011). Influence of excessive bleeding on frost susceptibility of concrete incorporating ferronickel slag as aggregates. In *36th Conference on Our World in Concrete & Structures*.
- Sakoi, Y., Aba, M., Tsukinaga, Y., & Nagataki, S. (2013). Properties of concrete used in ferronickel slag aggregate. In *Proceedings of the 3rd International Conference on Sustainable Construction Materials and Technologies, Tokyo, Japan* (pp. 1-6).

- Santamarina, J. C. (2008). Flow test evaluation. https://smartech.gatech.edu/bitstream/handle/1853/23048/e-20-k79_9124.pdf (accessed on 05/04/2016)
- Yüksel, I., Özkan, Ö., & Bilir, T. (2006). Use of granulated blast-furnace slag in concrete as fine aggregate. *ACI Materials Journal*, 103(3), 203.
- Yüksel, İ., Bilir, T., & Özkan, Ö. (2007). Durability of concrete incorporating non-ground blast furnace slag and bottom ash as fine aggregate. *Building and Environment*, 42(7), 2651-2659.

Every reasonable effort has been made to acknowledge the owners of copyright material. I would be pleased to hear from any copyright owner has been omitted or incorrectly acknowledged.

Chapter 4: MECHANICAL PROPERTIES AND LEACHING STUDY OF CONCRETE USING FNS AGGREGATE

The contents presented in this chapter were published in the following paper:

Saha, A. K., & Sarker, P. K. (2017). Sustainable use of ferronickel slag fine aggregate and fly ash in structural concrete: mechanical properties and leaching study. Journal of Cleaner Production, 162, 438-448.

This chapter evaluates the mechanical properties of concrete and the leaching characteristics of concrete samples containing different proportions of FNS aggregate. The fresh concrete properties such as workability and hardened concrete properties such as compressive strength, tensile strength and modulus of elasticity were determined. The experimental data were analysed and co-relations between the strength properties were evaluated. Finally, the environmental impact of using FNS aggregate in concrete was assessed by leaching results of the test specimens.

4.1 Overview

Different types of industrial by-products were studied in the past few decades in order to find suitable alternatives of natural sand in concrete. Blast furnace slag, steel slag, copper slag, foundry slag and ferronickel slag are the most common types of by-product slags that can be used as fine aggregate in concrete. Rashad et al. (2016) showed that the use of blast furnace slag as a replacement of natural sand improved the compressive strength of mortar. The slag used in their study had a similar specific gravity but higher water absorption as

compared to natural sand. The increase of compressive strength was attributed to the improved particle packing by the fine slag particles. Tiwari et al. (2016) reported the properties of concrete using steel slag fine aggregate of higher fineness modulus and specific gravity as compared to natural sand. It was pointed out that while partial replacements of sand by steel slag improved the strength, the full replacement of sand reduced strength of concrete. Mithun and Narasimhan (2016) reported that concrete containing copper slag exhibited similar compressive strength, flexural strength and splitting tensile strength as compared those of the reference concrete. Ladomerský et al. (2016) demonstrated that partial substitution of natural sand by a foundry slag exhibited similar workability as well as strength properties in a concrete mixture. However, this aggregate exhibited poor performance of concrete in frost resistance.

It can be observed from the literature review that utilization of ferronickel slags from different sources were attempted in different applications. Some of the reported results are shown to be conflicting because the materials were produced from ores of different sources and by different methods. For instance, the FNS aggregates produced in Japan used slow cooling in the pit by natural air, whereas other producers used fast cooling by water. This study was conducted on the evaluation of a proprietary ferronickel slag obtained from the smelting of garnierite ores found in New Caledonia. The ore is smelted at 1500 °C to 1600 °C, and the by-product molten slag is granulated by sea water cooling. Thus, this particular slag is different from those used in the other studies since they were produced from different ores and used different smelting temperatures and cooling methods. About 12 tonnes of the slag is produced as a by-product in the production of one tonne of ferronickel alloy and a deposit of about 25 million tonnes of this slag is currently accumulated in the premises in spite of its broad uses by local construction industries for decades.



Fig. 4.1 Concrete breakwaters using ferronickel slag aggregates as 30% replacement of natural sand

Fig. 4.1 shows an example of the use of this FNS aggregate as a partial replacement of natural sand in the construction of concrete blocks in New Caledonia. These concrete blocks are in service for 20 years and protecting the land from sea waves without any sign of visible degradation in spite of the exposure to a harsh environment. Therefore, utilisation of this available by-product has potential to significantly improve sustainability of concrete production by reducing the use of virgin materials. However, a comprehensive study is necessary in order to understand the properties of concrete using the FNS aggregate. The workability of fresh concrete, mechanical properties of hardened concrete and leaching of heavy metals from the concrete using FNS as fine aggregate and fly ash as a supplementary cementing material are evaluated in this study. Thus, this chapter presents a study on concrete utilising two industrial by-products evaluating the engineering properties and any possible toxicity effect by leaching.

4.2 Experimental Work

4.2.1 Materials

Commercially available ordinary Portland cement (OPC) was used as the principal binder. A class F fly ash was used as a partial replacement of OPC. Natural sand, ferronickel slag

(FNS) and their combinations were used as the fine aggregate in concrete mixtures. The coarse aggregate was granite with a maximum size of 20 mm. The chemical compositions of the cement, fly ash and FNS, as determined by X-ray Florescence (XRF), are given in Table 4.1. The cement used was general purpose cement and the fly ash was of low-calcium class F-type containing 76% silica. It can be observed from the table that the FNS mainly consists of silicon, magnesium and iron.

Table 4.1 Chemical compositions and loss on ignition (LOI) of OPC, FNS & fly ash (mass %)

Chemical composition	OPC	FNS	Fly ash
SiO ₂	20.29	53.29	76.34
Al ₂ O ₃	5.48	2.67	14.72
Fe ₂ O ₃	2.85	11.9	3.69
MgO	1.24	31.6	0.54
SO ₃	2.49	-	0.11
CaO	63.11	0.42	0.60
Na ₂ O	0.29	0.11	0.19
K ₂ O	0.45	-	0.96
Cr ₂ O ₃	0.02	1.08	-
P ₂ O ₅	0.17	-	0.10
SrO	0.05	-	-
TiO ₂	0.27	-	0.61
Mn ₂ O ₃	0.08	-	0.07
ZnO	0.04	-	-
NiO	-	0.1	-
Co ₃ O ₄	-	0.01	-
LOI ^a	3.39	-	0.53

^a loss on ignition

The physical appearances of FNS aggregate, natural sand and coarse aggregate are shown in Fig. 4.2. It can be seen that FNS consisted of angular particles of varying sizes, and the natural sand consisted of round particles of relatively smaller size. The physical properties of the natural sand, FNS and coarse aggregates used in this study are given in Table 4.2. It can be seen that the particle density of FNS is 22% higher than that of natural sand. The water absorption of FNS is slightly higher than that of natural sand. The properties of FNS are within the allowable limits according to the Australian Standard AS

2758.1 (2014). The particle size distributions of the natural sand, FNS and their combinations were presented in chapter 3.

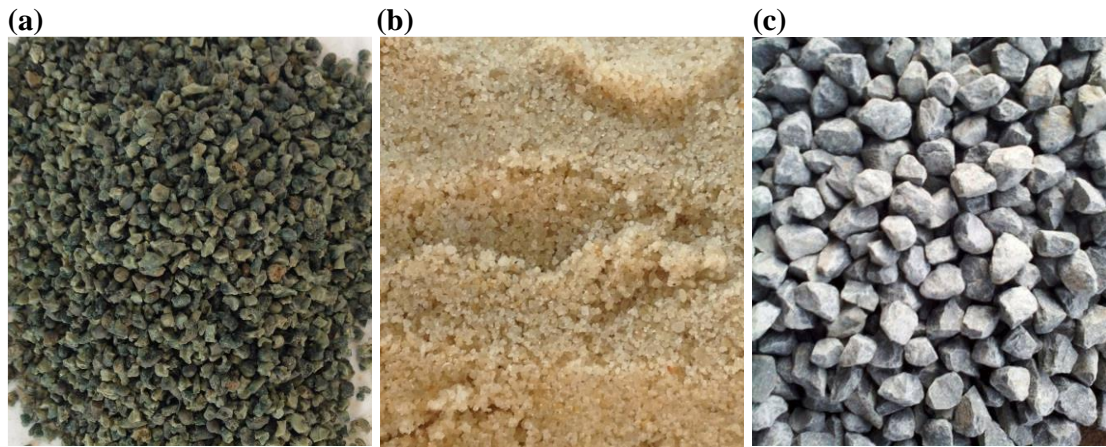


Fig. 4.2 (a) FNS aggregate; (b) sand and (c) coarse aggregate

Table 4.2 Physical properties of aggregates

Property	Sand	FNS	Coarse aggregate
SSD density (kg/m^3)	2160	2780	2710
Apparent particle density (kg/m^3)	2320	2850	2730
Fineness modulus	1.95	4.07	7.6
Water absorption (%)	0.35	0.42	0.48

4.2.2 Mixture proportions and test methods

The mix proportions of the concrete mixtures are given in Table 4.3. FNS aggregate was used to replace 50% and 100% volume of the natural sand. The water to cementitious materials ratio and the proportion of coarse aggregate were kept constant in all the mixtures. The concrete mix design was conducted by absolute volume method as recommended by the American Concrete Institute (ACI). A 28-day target compressive strength of 50 MPa was used for the control mix without fly ash and containing 100% natural sand. The binder content was 390 kg/m^3 and the water to binder ratio was 0.33. These parameters were used to achieve early-age compressive strengths suitable for most practical applications even

after partially replacing cement by a class the F fly ash (Nath and Sarker, 2011). A naphthalene based superplasticizer conforming to ASTM C 494 (2016) as a “class A” admixture was used in the mixtures. The binder was 100% OPC for three mixtures and 30% fly ash was used as a cement replacement for the other three mixtures. The mixtures are designated by PC-FNS and FA-FNS for no fly ash and 30% fly ash, respectively. The number with the mixture designation represents the percentage of FNS as a replacement of natural sand.

Table 4.3 Mix proportions

Mix ID	Binder (kg/m ³)		Fine aggregate (kg/m ³)		Coarse aggregate (kg/m ³)	Water (kg/m ³)	Superplastic iser (kg/m ³)
	OPC	Fly ash	Sand	FNS			
PC-FNS0	390	0	710	0	1194	129	4
PC-FNS50	390	0	355	435	1194	129	4
PC-FNS100	390	0	0	870	1194	129	4
FA-FNS0	273	117	710	0	1194	129	4
FA-FNS50	273	117	355	435	1194	129	4
FA-FNS100	273	117	0	870	1194	129	4

The aggregates were prepared to saturated surface-dry (SSD) condition before mixing of concrete. The binder and the aggregates were dry-mixed together in a pan mixer first and then the water and plasticizer were added. The ingredients were then wet-mixed until a homogeneous mixture was obtained. The freshly mixed concrete was used to conduct slump test as a measure of workability and then the specimens were cast for determination of the hardened properties of concrete. The test specimens were demoulded one day after casting and then they were cured in water at 23 °C for 28 days. Three identical specimens were tested and the mean value of the results was reported.

The slump test and air content test of fresh concrete was carried out in accordance with the Australian Standard AS 1012.3.1 (2014) and ASTM C231 (2017), respectively.

Compressive strengths of the specimens were determined at the ages of 7 days, 28 days and 56 days in accordance with the Australian Standard AS 1012.9 (2014) using 100 mm × 200 mm cylinder specimens. The samples were loaded at a rate of 20 MPa/min until failure.

The tensile strength of concrete is an important property that is used to determine the load at which a concrete member may crack. The splitting tensile strength test was conducted according to the Australian Standard AS 1012.10 (2014) using 150 mm × 300 mm cylinder specimens. The specimen was loaded at a rate of 1.5 MPa/min indirect tensile stress until failure. The failure load was recorded and the splitting tensile strength was calculated by Eq. (1).

$$f_{sp} = \frac{2,000 P}{\pi L D} \quad (1)$$

Where, f_{sp} is the indirect tensile strength, (MPa); P is the maximum applied force (kN); L is the height (300 mm) and D is the diameter (150 mm) of cylinder.

Flexural strength of concrete was tested according to the Australian Standard AS 1012.11 (2000) using 400 mm long specimens with a cross-section of 100 mm × 100 mm. The test was conducted in a universal testing machine with a loading rate of 1.0 MPa/min until failure. The force was applied to the specimens through a frame containing two supporting rollers and two loading rollers. The maximum load was recorded and the flexural strength was calculated by Eq. (2).

$$f_{cf} = \frac{PL(1,000)}{bd^2} \quad (2)$$

Whereas, f_{cf} = flexural strength (MPa); P = maximum applied load (kN); L= span length (mm); b = width of specimen (mm); d = depth of specimen (mm).

The modulus of elasticity of concrete was measured according to Australian Standard AS 1012.17 (1997) using 100 mm × 100 mm cylinder specimens. The specimen was loaded at a rate of 15 MPa/min by a UTM and the vertical and horizontal deflections

were measured by linear variable differential transformers (LVDT). The stress-strain curve was plotted and modulus of elasticity was calculated from the slope of the graph.

The leaching of heavy metals from hardened concrete specimens containing FNS fine aggregate was determined by the tank leaching test method as per NEN 7345 (1995) standard recommended by the Netherlands Normalisation Institute. This test was chosen because it is recognised as the best representation of the possible leaching from concrete by diffusion in actual environmental exposures (Scott et al., 2005). Concrete cylinders of 100 mm diameter and 200 mm height were used for this test. The specimens were immersed in a closed tank of water and the heavy metals released from the specimens were determined. The water to concrete sample volume ratio (w/s) was five. The leachates were changed after 8 hours and 1, 2, 4, 9, 16, 36 and 64 days. The total dissolved metals in the leachates of 64 days were evaluated by inductively coupled plasma atomic emission spectroscopy (ICPAES).

4.3 Results and Discussion

4.3.1 Workability & Air content

Slump test results of the concrete mixtures are plotted in Fig. 4.3. The slump values of the mixtures containing 100% natural sand, 50% FNS and 100% FNS were 130 mm, 145 mm and 115 mm, respectively.

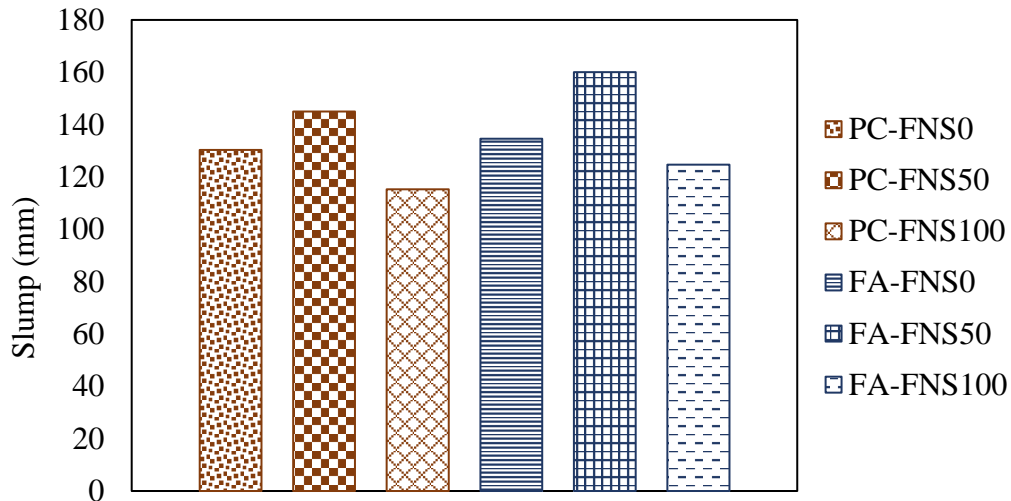


Fig. 4.3 Slump of concrete with different percentages of FNS aggregate

Therefore, the slump of the mixtures without fly ash varied in the range of 115 mm to 145 mm. The effect of aggregates on the workability of concrete usually depends on the particle shape and the size distribution. The surface area of aggregates decreases with the increase of particle size and thus, less water is required to wet the aggregates. Therefore, about 12% increase in slump shown by the concrete containing 50% FNS is attributed to the decrease of surface area since the FNS has a higher fineness modulus as compared to natural sand, as shown in Table 4.2. On the other hand, about 9% decrease in slump was observed by the use of 100% FNS as compared to the mix containing 100% natural sand. This is attributed to the angular shape of the FNS aggregates as compared to the round shape of natural sand. The large increase of the angular shaped particles and higher surface roughness decreased the workability of the mixture with 100% FNS. The slump values of the mixtures containing 30% fly ash as cement replacement were 135 mm, 160 mm and 125 mm for 100% sand, 50% FNS and 100% FNS respectively. The slumps of these mixtures were higher as compared to those of the mixtures with no fly ash. The well-known ball bearing effect of the spherical shaped fly ash particles increased the workability of these mixtures. As shown in Fig. 4.3, the effect of FNS on workability of the mixtures

containing fly ash is similar to that shown by the mixtures without fly ash. The trend of the effect of FNS aggregate on workability of concrete was similar to that in mortar mixtures presented in the previous chapter. No segregation or excessive bleeding was observed during the process of mixing, compaction and finishing of the concrete containing FNS aggregates.

The air contents of the freshly mixed concretes were determined and the test results are plotted with respect to the percentage of FNS content in the mixture in Fig. 4.4. According to the graph, with the increment of FNS percentage the air content of freshly mixed concrete gradually increased. Air contents of the mixtures PC-FNS0, PC-FNS50 and PC-FNS100 were 1.8%, 2.2% and 3.1%, respectively. A similar trend was observed in the mixtures containing fly ash. The air contents of mixes FA-FNS0, FA-FNS50 and FA-FNS100 were 1.6%, 2.1% and 2.8%, respectively. The increase of air content is attributed to the increase of entrapped air in concrete with the increase of FNS particles which are angular in shape. Furthermore, inclusion of 30% fly ash resulted in marginally lower air contents. This is attributed to the spherical particle shape of fly ash that resulted in a better particle packing and flow of the mixture with a lower air content.

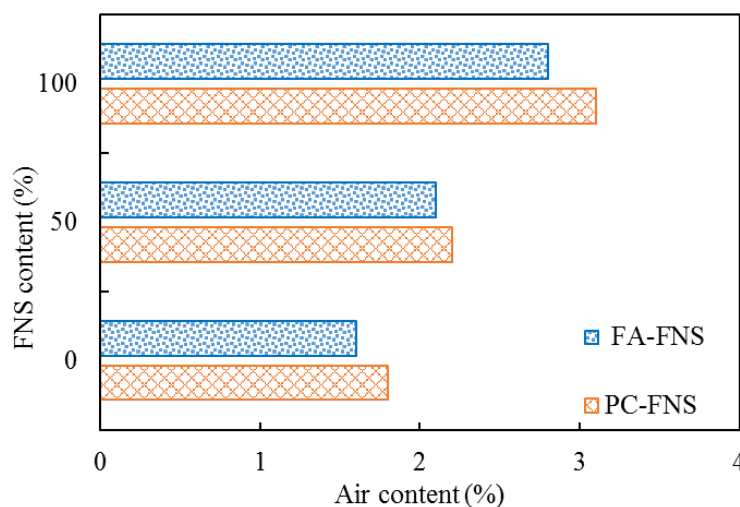


Fig. 4.4 Air content of concrete with different percentages of FNS aggregate

4.3.2 Compressive strength

The typical concrete cylinders after compressive strength test are shown in Fig. 4.5. It can be seen from the broken cylinders that the FNS fine aggregates were uniformly distributed without any segregation.



Fig. 4.5 Samples after compressive strength test (left: PC-FNS0, middle: PC-FNS50
right: PC-FNS100)

The colour of the fractured surface became darker with the increase of FNS aggregates due to the dark blue colour of FNS. The failure pattern of the specimens containing FNS aggregates was similar to that of the specimens with natural sand. The mean compressive strength results of the mixtures at different ages are plotted in Fig. 4.6. The 28-day compressive strengths of the mixtures without fly ash were 61 MPa, 66 MPa and 45 MPa for 100% sand, 50% FNS and 100% FNS, respectively. Therefore, compressive strength increased by 8% for 50% FNS and then decreased by 26% for the use of 100% FNS. The increase of compressive strength for 50% FNS and then decrease for 100% FNS by similar percentages are also observed at the ages of 7 days and 56 days. The 7-day and 56-day compressive strengths of the concrete mix with 50% FNS as sand replacement were 56 MPa and 70 MPa, respectively.

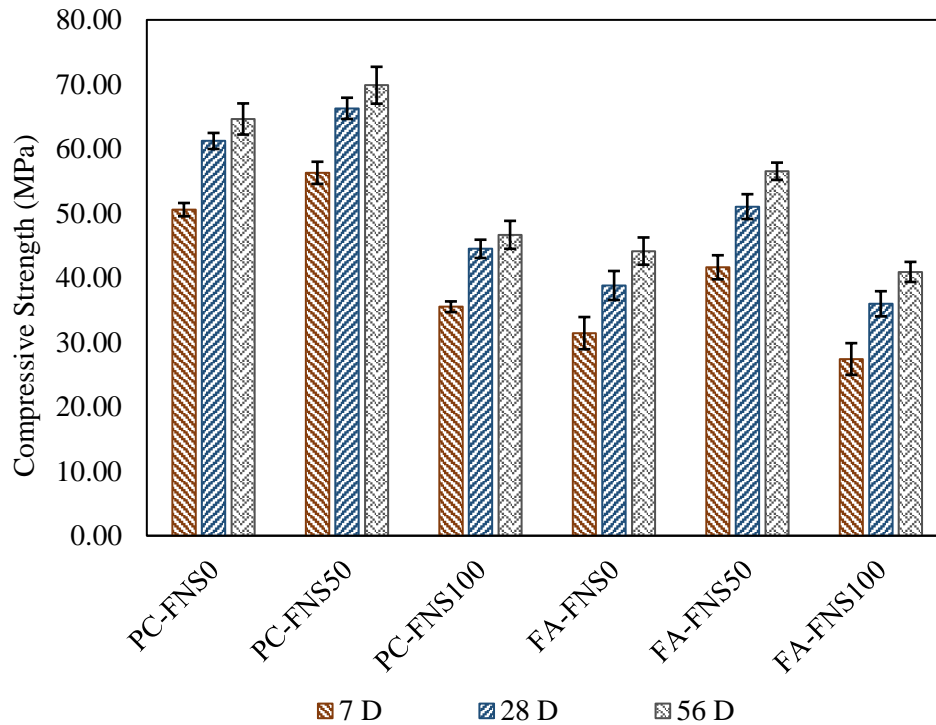


Fig. 4.6 Mean compressive strengths (Error bars at one standard deviation)

The strength increase for 50% FNS and then a larger decrease for 100% FNS can be explained by the particles size distribution of the aggregates. Replacement of sand by 50% FNS provided a well-graded aggregate with fineness modulus of 3.01 as compared to 1.95 for the reference concrete and 4.07 for the concrete with 100% FNS. As shown by the particle size distributions, the natural sand has less coarse particles and the FNS has less fine particles. Thus, the combined fine aggregate with 50% from each type has improved particle packing. Additionally, FNS particles are angular which increased the interlocking bond with the binder matrix. Furthermore, the density of FNS aggregates are significantly higher compared to sand thus inclusion of this aggregate improved the load bearing capacity of concrete. Finally, the increment of slump was also a crucial factor for this strength increment of FNS concrete compared to control specimens. Since the 100% FNS has more coarse particles with very low fines, it has a higher void content that has resulted in a significant drop in compressive strength. The full replacement of sand by FNS

aggregate increased the voids content of concrete due to relatively low fine particles that resulted in a decline of compressive strength. Similar phenomenon of FNS aggregate was also observed by Shoya et al. (1999). A full replacement of sand by FNS has also resulted in lower compressive strength of cement mortar as compared to control mixtures.

A general decrease of the compressive strength can be observed in Fig. 4.6 by the use of 30% fly ash as a cement replacement. This is consistent with the reduction of strength usually observed by the use of class F fly ash as a cement replacement when the water to binder ratio is kept constant (Nath and Sarker, 2013). The 28-day compressive strength of the mixture containing 50% FNS decreased from 66 MPa to 51 MPa by the use of 30% fly ash as cement replacement. This is a reduction by 23%, which can be expected since the fly ash has very low calcium content (0.6%). The 28-day compressive strengths of the mixtures with 30% fly ash were 39 MPa, 51 MPa and 36 MPa for 100% sand, 50% FNS and 100% FNS, respectively. Thus, the strength increases for 50% FNS was 30% and strength decrease for 100% FNS was 8% in this series. The percentages of strength increase by 50% FNS and strength decrease by 100% FNS were similar at 7 days and 56 days. The trend of the effect of FNS on compressive strength in this series is similar to that in the series without fly ash. However, the percentage of strength increase by 50% FNS is higher and strength decrease by 100% FNS is lower in the mixtures with fly ash than in the mixtures without fly ash. The strength enhancement of the fly ash in these mixtures is attributed to the better particle packing effect of the fly ash particles which are finer than the cement particles.

Overall, the trend of the effect of FNS aggregate on compressive strength of concrete was similar to that in the mortar mixtures presented in previous chapter.

4.3.3 Splitting tensile strength

The mean values of the 28-day splitting tensile strength of concrete are given in Table 4.4. The results are also plotted in Fig. 4.7 with error bars at one standard deviation. From the illustration, it can be seen that the splitting tensile strength of the mixtures without fly ash (PC-FNS series) varied from 3.94 MPa to 4.33 MPa. The tensile strength for 100% sand, 50% FNS and 100% FNS were 4.33, 4.73 and 3.94 MPa, respectively.

Table 4.4 Mechanical properties of concrete at the age of 28 days

Mix ID	Density (kg/m ³)	Compressive (MPa)	Split. Tensile (MPa)	Flexural (MPa)	MoE ^a (GPa)
PC-FNS0	2444	61.22	4.33	6.09	41.96
PC-FNS50	2514	66.28	4.73	6.86	44.69
PC-FNS100	2491	44.49	3.94	5.74	38.44
FA-FNS0	2470	38.80	3.84	5.25	36.19
FA-FNS50	2510	51.04	4.44	6.23	39.10
FA-FNS100	2489	35.97	3.66	4.96	32.81

^a Modulus of elasticity

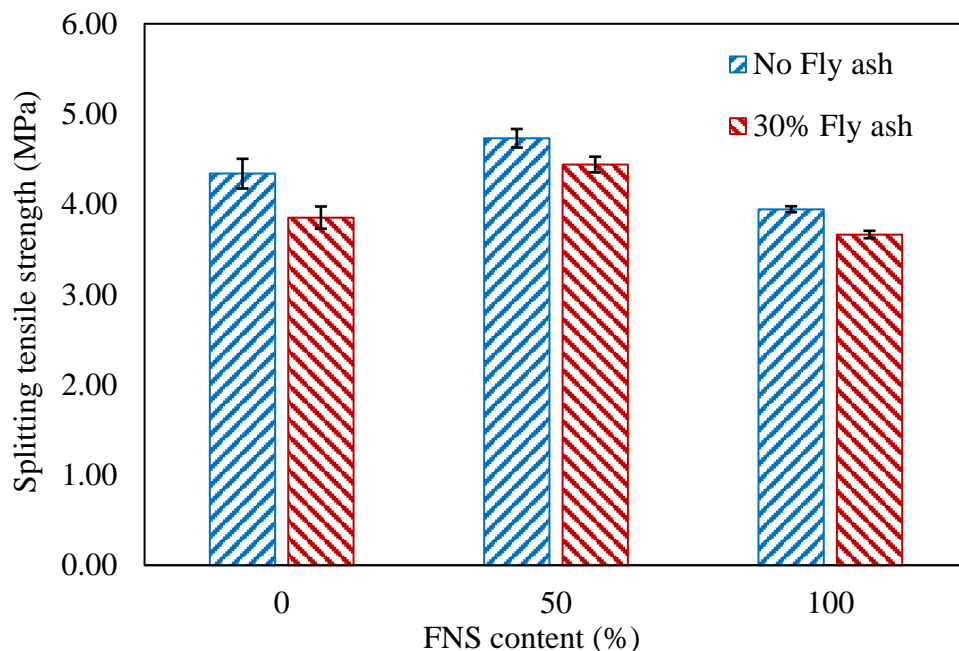


Fig. 4.7 Mean splitting tensile strengths (Error bars at one standard deviation)

The splitting tensile strength increased by 9% as compared to the control specimen due to the replacement of sand by 50% FNS aggregate. However, tensile strength reduced

by 10% as compared to the control mixture due to the full replacement of sand by FNS aggregate. The trend is similar to the trend of compressive strength development of concrete due to the sand replacement by FNS. It is noticeable that the 100% FNS samples showed a 26% reduction in compressive strength, but only 10% reduction in splitting tensile strength. The less reduction of tensile strength by the FNS is attributed to the angular shape of the particles that provided higher resistance to splitting by better interlocking of the fine aggregates angular shape and rough surfaces. As shown in Fig. 4.8, the splitting plane of the specimen with 100% FNS was more tortuous than that of the specimen with 100% sand. The increase of tortuosity of the splitting plane is attributed to the better interlocking of the angular FNS particles.

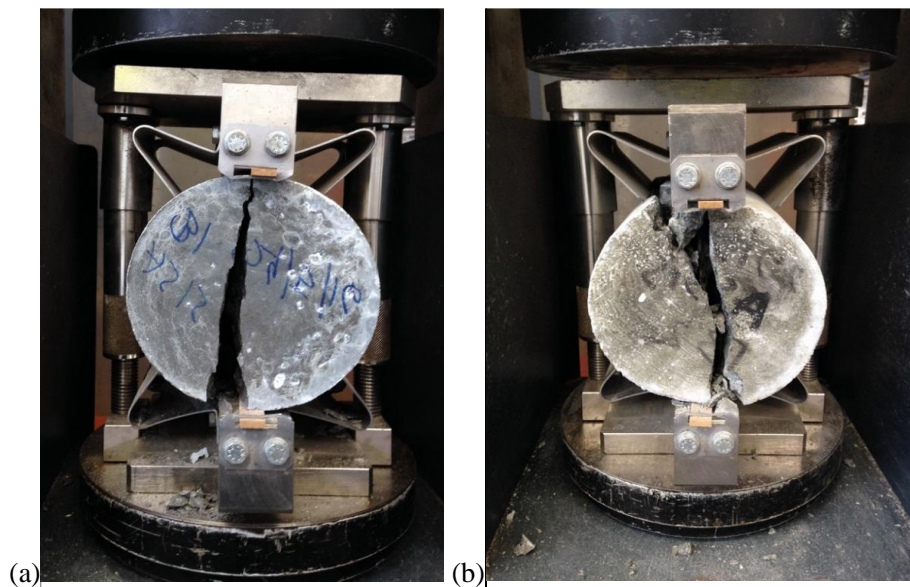


Fig. 4.8 Cracking pattern after splitting tensile strength test; (a) 100% sand (b) 100% FNS

As shown in Fig. 4.7, the inclusion of 30% fly ash in the binder reduced splitting tensile strength as compared to the mixtures without fly ash. For instance, the splitting tensile strength samples of 50% FNS decreased from 4.73 MPa to 4.44 MPa by the use of 30% fly ash as cement replacement. The reduction is about 6.5% which is anticipated because of the 23% strength reduction in a compressive strength test. The splitting tensile

strength of the mixtures with 30% fly ash varied within a range of 3.66 to 4.44 MPa. The splitting tensile strength for 100% sand, 50% FNS and 100% FNS was 3.85, 4.44 and 3.66 MPa, respectively. Thus, splitting tensile strength increased by about 15% for 50% FNS as compared to the control mixture. On the other hand, splitting tensile strength reduced by 5% for the 100% FNS samples as compared to the control sample because of the lack of fine particles.

4.3.4 Flexural strength

The 28-day flexural strength results are given in Table 9.4 and plotted in Fig. 4.9. The flexural strength of concrete without fly ash varied between 5.74 MPa and 6.86 MPa.

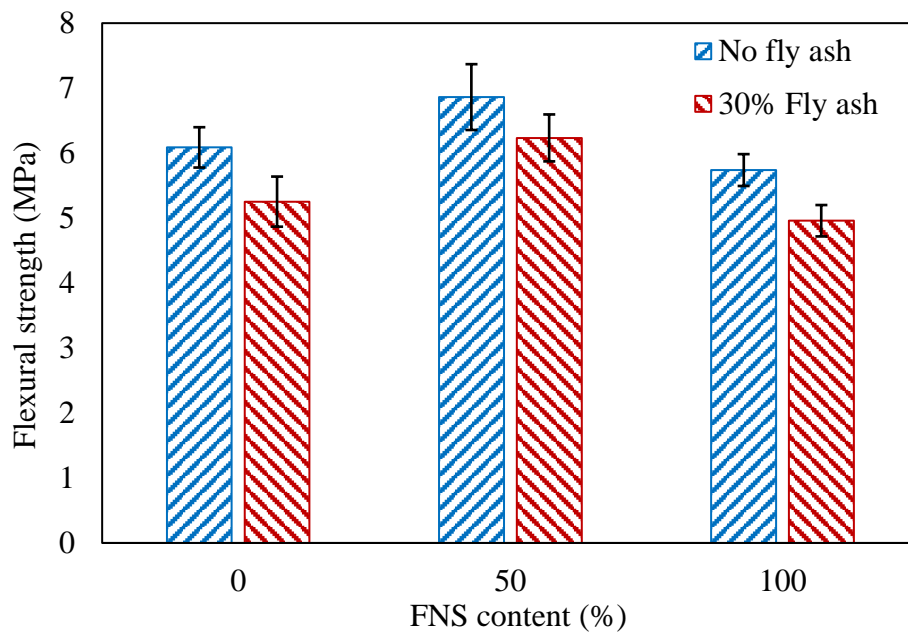


Fig. 4.9 Mean flexural strengths of concrete (Error bars at one standard deviation)

Flexural strength of the specimens with 100% sand, 50% FNS and 100% FNS were 6.09, 6.86 and 5.74 MPa, respectively. Flexural strength increased by about 12% for the use of 50% FNS as sand replacement. On the other hand, flexural strength decreased by about 5% for 100% FNS samples as compared to the control specimens. The flexural strength followed a similar trend as the splitting tensile strength. It can be pointed out the

angularity of FNS aggregate also improved the flexural strength, 100% FNS samples showed a 26% reduction in compressive strength, but only 5% reduction in flexural strength. As discussed earlier, the angular shape of the FNS particles improved the interlocking between the particles and as a result, showed better higher flexural strengths. The flexural strength of the specimens of 50% FNS decreased from 6.86 MPa to 6.23 MPa by the use of 30% fly ash in the binder. The reduction of flexural strength is less than 10% as compared to 23% reduction in compressive strength. The samples containing 100% sand, 50% FNS and 100% FNS showed flexural strengths of 5.25, 6.23 and 4.96 MPa respectively. Thus, flexural strength increased by about 18% for the samples having 50% FNS as compared to the control samples. On the other hand, flexural strength decreased by about 6% in the samples containing 100% FNS as compared to the control samples.

4.3.5 Modulus of elasticity

The modulus of elasticity results are given in Table 4.4 and plotted as bar diagrams in Fig. 4.10. It can be seen that modulus of elasticity was within a range of 38.44 GPa to 46.69 GPa for the samples with no fly ash. The modulus of elasticity were 41.96, 46.69 and 38.44 GPa for the mixtures with 100% sand 50% FNS and 100% FNS, respectively. The modulus of elasticity increased by about 11% by the use of 50% FNS as a sand replacement. On the other hand, it decreased by about 8% for 100% FNS. Modulus of elasticity of concrete is a complex phenomenon as the material is heterogeneous. It also depends on the concrete density and the aggregate properties in addition to the compressive strength of concrete. The density of the hardened concrete for each mix is presented in Table 4.4. It can be seen that the density was highest for the mixture with 50% FNS and 50% natural sand. This is because of the continuous grading of the fine aggregates resulted by this combination of natural sand and FNS, as shown in Fig. 4.2. Thus, the lowest void content and highest density for this combination of the fine aggregates resulted in the highest elastic

modulus. On the other hand, the concrete containing 100% FNS exhibited slightly lower density than that containing 50% FNS due to the lack of fine particles. There was an increase in the void content in the concrete containing 100% FNS that has resulted in decrease of density and compressive strength, eventually reducing the elastic modulus.

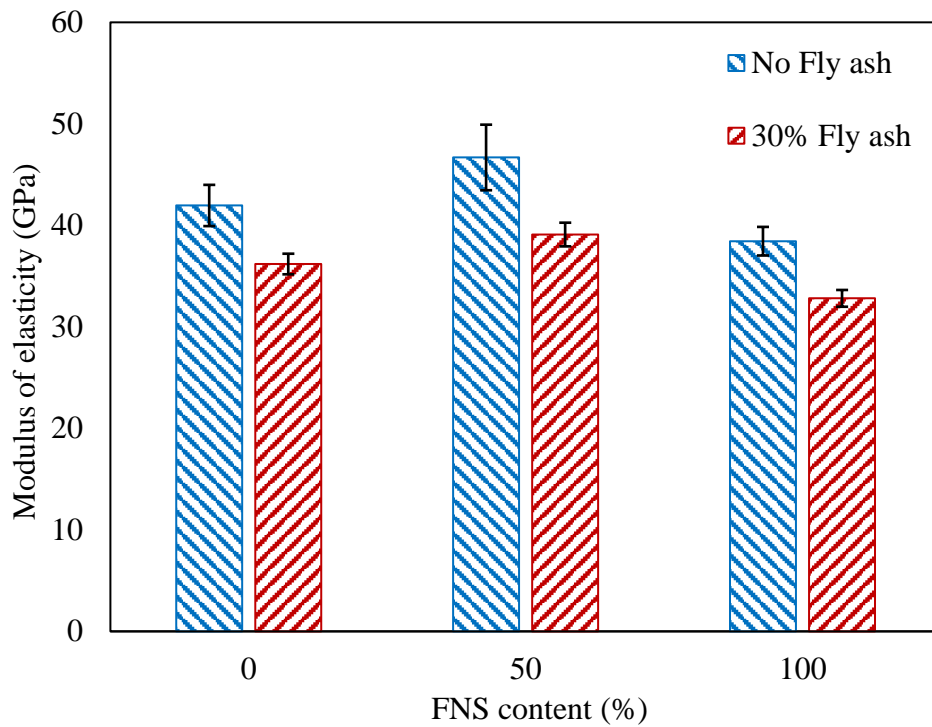


Fig. 4.10 Mean modulus of elasticity (Error bars at one standard deviation)

Generally, a reduction in the elastic modulus was observed by the inclusion of 30% fly ash as cement replacement. The samples with 50% FNS showed a decrease of the modulus of elasticity from 47 GPa to 39 GPa by the use of 30% fly ash in the binder which is about 16% decrease of the modulus of elasticity. The modulus of elasticity values were 36 GPa, 39 GPa and 33 GPa for the samples having 100% sand, 50% FNS and 100% FNS aggregate respectively.

Therefore, the combined effect of fly ash and FNS was an initial reduction of compressive strength due to cement replacement, then an increase of strength by the use of 50% FNS with sand and then a decline of compressive strength by the use of 100% FNS as

fine aggregate. The combined use of fly ash helped improve the particle packing of the mixtures containing high percentage of FNS that had relatively less fine particles. Similar trend of the combined effect of fly ash and FNS was also shown by the tensile strength, flexural strength and elastic modulus properties of concrete.

4.3.6 Leaching characteristics of hardened concrete

Leaching test results of the specimens containing 100% FNS aggregate with 100% OPC binder, 50% FNS aggregate with 30% fly ash as cement replacement and 100% FNS with 30% fly ash are presented in Table 4.5. The pH values of the leachates from specimens of 100% FNS with 100% OPC, 50% FNS with 30% fly ash and 100% FNS with 30% fly ash were 10.8, 8.1 and 8.9, respectively.

Table 4.5 Total dissolved metals in the leachates of concrete containing FNS aggregate and regulatory limits

Total dissolved metal	Concentration of heavy metals in leachate (mg/L)			Regulatory level by US EPA (mg/L)	Cumulative release of heavy metals from concrete cylinders (mg/m ²)			Stable non-reactive hazardous waste limit values (mg/m ²)
	PC-FNS100	FA-FNS50	FA-FNS100		PC-FNS100	FA-FNS50	FA-FNS100	
As	0.011	0.009	0.01	5.0	0.2918	0.2387	0.2653	1.3
Cd	0.0063	0.0064	0.0069	1.0	0.1671	0.1698	0.1830	0.20
Co	0.0017	0.0011	0.0014	NG	0.0451	0.0292	0.0371	NG
Cr	0.0021	0.0014	0.0016	5.0	0.0557	0.0371	0.0424	5
Cu	0.011	0.0095	0.014	NG	0.2918	0.2520	0.3714	45
Fe	0.006	0.003	0.005	NG	0.1592	0.0796	0.1326	NG
Hg	0.0012	0.001	0.0014	0.2	0.0318	0.0265	0.0371	0.1
Ni	0.019	0.015	0.018	NG	0.5040	0.3979	0.4775	6
Pb	0.0011	0.001	0.001	5.0	0.0292	0.0265	0.0265	6
Zn	0.0056	0.0051	0.0059	NG	0.1485	0.1353	0.1565	30

*NG: No guideline

The leachates of the specimens of FA-FNS series were less because of the alkali binding capacity of fly ash that reduced the alkali diffusion from concrete. The amount of

a leaching metal was calculated per unit volume of the leachate (mg/L) and per unit surface area of the concrete specimen (mg/m²), as given in Table 4.5. Generally, it can be seen from the table that very small amounts of various metals were leached out from the concrete specimens. Therefore, the metals were effectively locked against excessive leaching from the concrete specimens containing 50% and 100% FNS fine aggregate with or without fly ash as a partial cement replacement. Low level of leaching of metals was also reported from raw ferronickel slag produced from laterite ore in the Philippines (Demotica et al., 2012). Similarly, the leaching of heavy metals were low as compared to regulatory limits when 20% cement was replaced by ground ferronickel slag produced from limonitic laterites in Greece (Katsiotis et al., 2015).

The limits on the leaching of heavy metals (mg/L) recommended by the United States Environmental Protection Agency (US EPA, 2009) in the characterisation of hazardous wastes are given in Table 4.5 for comparison with the values determined in the tests. The concentration of heavy metals exceeding the allowable limits are designated as toxic and are not allowed for use as landfills. It can be seen from the table that the amounts of metals such as Arsenic (As), Cadmium (Cd), Chromium (Cr), Mercury (Hg) and Lead (Pb) leached out of the all the specimens were much less than the limits recommended by the US EPA (2009). Therefore, the FNS is considered non-toxic and categorised as non-hazardous in terms of these metals. In addition, the landfill waste acceptance criteria for the leachability of monolithic wastes used by the UK Environment Agency (2005) are also given in Table 4.5 for comparison. These regulatory limits are expressed in terms of the amount of metals leached out per unit surface area of the specimen (mg/m²). The concentration of metals in the leachate below the given limit is identified as chemically stable and non-reactive. It can be seen that the amount of metals such as As, Cd, Cr, Copper (Cu), Hg, Nickel (Ni), Pb and Zink (Zn) are far below the regulatory limits of the UK

Environment Agency. Thus the concrete specimens are categorised as stable and non-reactive in terms of these metals. Therefore, the leaching of heavy metals from the concrete specimens containing up to 100% FNS aggregate was far below the regulatory limits and the ferronickel slag is considered environmentally compatible when used as fine aggregate in concrete production.

4.4 Correlation of the mechanical properties with compressive strength

A correlation can be usually observed between the mechanical properties such as splitting tensile strength, flexural strength and modulus of elasticity with the compressive strength of concrete using natural sand as the fine aggregate. Thus, various concrete design standards have recommended equations in terms of compressive strength to predict the tensile strength, flexural strength and modulus of elasticity. It can be seen from Table 4.6 that the ratios of splitting tensile strength to compressive strength are 0.07 and 0.10 for the mixtures using 100% natural sand. On the other hand, the corresponding ratios for the mixtures with 50% or 100% FNS replacing natural sand are also in the range of 0.07 to 0.10. Therefore, it can be said that the correlation between splitting tensile strength and compressive strength of concrete using natural sand is same as that of concrete using FNS aggregate.

Table 4.6 Relationship between the mechanical properties and compressive strength

Mix ID	Split/ Comp.	Split. tensile (MPa)		Flexural/ Comp.	Flexural	Modulus of	
		AS 3600	ACI 318		(MPa)	elasticity (GPa)	
					AS 3600	AS 3600	ACI 318
PC-FNS0	0.07	3.64	4.00	0.10	6.06	35.05	36.77
PC-FNS50	0.07	3.79	4.18	0.10	6.32	35.90	38.26
PC-FNS100	0.09	3.07	3.36	0.13	5.11	31.96	31.35
FA-FNS0	0.10	2.85	3.10	0.14	4.75	30.78	29.28
FA-FNS50	0.09	3.30	3.62	0.12	5.50	33.23	33.58
FA-FNS100	0.10	2.73	2.97	0.14	4.55	30.16	28.19

Since the splitting tensile strength and compressive strength follows a definite correlation, the splitting tensile strength is generally estimated by simple relationships recommended by the design standards. The splitting tensile strength is expressed in terms of compressive strength in these equations and multiplied by different coefficients. The Australian Standard AS 3600 (2009) recommends Eq. (3) for concrete at 28 days of standard curing.

$$f'_{ct} = 0.36\sqrt{f'_c} \quad (3)$$

Whereas f'_{ct} and f'_c are the characteristic uniaxial tensile and compressive strengths of concrete respectively. The mean uniaxial tensile strength (f_{ctm}) is obtained by multiplying the characteristic tensile strength by 1.4. The uniaxial tensile strength is taken as 0.9 times the splitting tensile strength ($f_{ct.sp}$). The relationships between the characteristic strength and the mean compressive strength for concretes of different grade are given in the standard. For 25-65 MPa grade concrete, the mean in situ compressive strength is given by Eq. (4). The mean in situ compressive strength (f_{cmi}) can be calculated by multiplying the cylinder compressive strength (f_{cm}) by 0.9.

$$f_{cmi} = f'_c + 3 \text{ (MPa)} \quad (4)$$

The ACI Code 318 (2008) provides an approximate relationship between the mean splitting tensile strength and the characteristic compressive strength, which is given by Eq. (5). The relationships between the characteristic and mean compressive strengths are given by Eqs. (6) to (8).

$$f_{ct.sp} = 0.56\sqrt{f'_c} \quad (5)$$

$$f_{cm} = f'_c + 7.0 \text{ (MPa)} \quad \text{for } f'_c < 21 \text{ MPa} \quad (6)$$

$$f_{cm} = f'_c + 8.3 \text{ (MPa)} \quad \text{for } 21 < f'_c \leq 35 \text{ MPa} \quad (7)$$

$$f_{cm} = 1.1f'_c + 5 \text{ (MPa)} \quad \text{for } f'_c > 35 \text{ MPa} \quad (8)$$

The ACI Code and the Australian Standard were used to calculate the splitting tensile strengths of the concretes. The ratio between the experimental value and the calculated value are shown in Table 4.7.

Table 4.7 Ratio of the experimental to calculated mechanical properties

Mix ID	Split tensile strength		Flexural strength	Modulus of elasticity	
	AS 3600	ACI 318	AS 3600	AS 3600	ACI 318
PC-FNS0	1.19	1.08	1.00	1.20	1.14
PC-FNS50	1.25	1.13	1.09	1.24	1.17
PC-FNS100	1.28	1.17	1.12	1.20	1.23
FA-FNS0	1.35	1.24	1.11	1.18	1.24
FA-FNS50	1.34	1.23	1.13	1.18	1.16
FA-FNS100	1.34	1.23	1.09	1.09	1.16

The experimental and calculated splitting tensile strengths are also plotted in Fig. 4.11. It can be seen that the ratio of the experimental splitting tensile strength of the concretes containing FNS aggregate to that calculated by the Australian Standard varied between 1.25 and 1.34. The corresponding ratios for the two mixes with 100% natural sand were 1.19 and 1.35. Therefore, the equation of AS 3600 predicted the splitting tensile strength of the concrete containing FNS aggregate conservatively and with the similar accuracy for concretes using natural sand. Similarly, the ACI 318 Code equation also predicted the splitting tensile strength of the concretes containing FNS aggregates conservatively. As can be seen from Fig. 4.11, the predictions by the AS 3600 equation is more conservative than the ACI 318 equation.

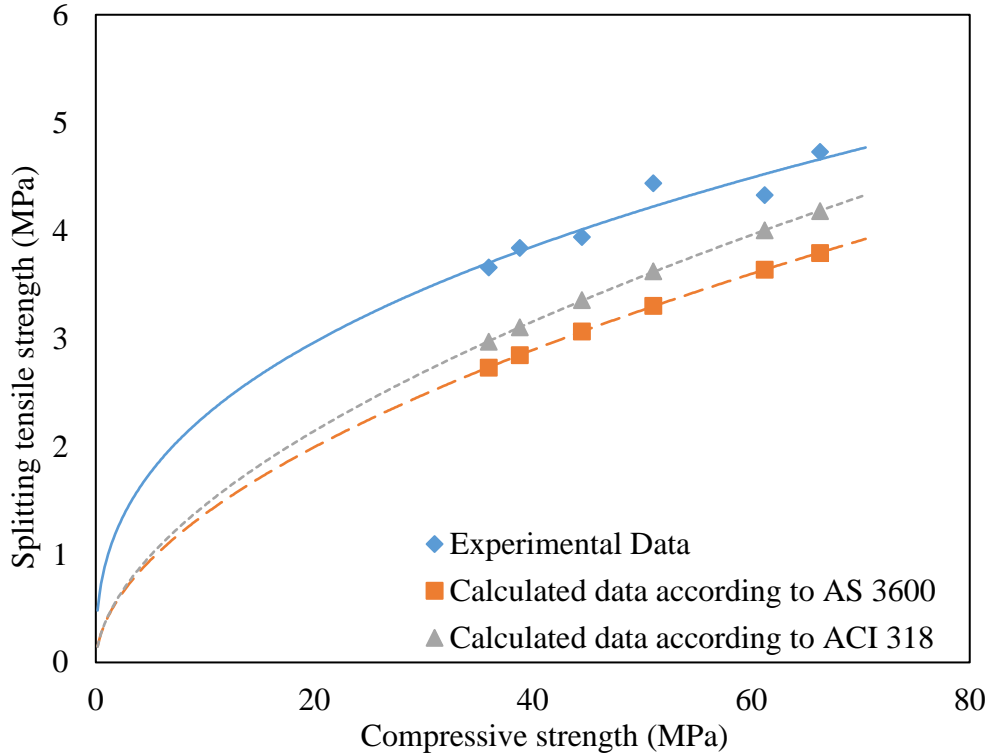


Fig. 4.11 Relationship between splitting tensile strength and compressive strength

The relationship between the flexural strength and the compressive strength of concrete is discussed in this section. It can be observed from Table 4.6 that the ratio of the experimental flexural strength to compressive strength for the specimens with FNS aggregate concretes varied in the range of 0.10 to 0.14 and those for the samples with 100% natural sand were in the range of 0.10 to 0.14. Therefore, the same correlation for concrete containing FNS aggregate is same as that of the concrete containing a natural sand fine aggregate. The Australian standard AS 3600 recommends Eq. (9) to calculate the flexural strength of concrete. The mean flexural strength is obtained by multiplying the characteristic value (f_{ctf}') by 1.4.

$$f_{ctf}' = 0.36\sqrt{f_c'} \quad (9)$$

The ratio of the experimental to calculated flexural strength by the AS 3600 are presented in Table 4.7. The experimental and calculated flexural strengths are also plotted in Fig.

4.12. The ratio varied between 1.0 and 1.13. As seen from Fig. 4.12, the predictions by the AS 3600 are conservative and similar for concretes with FNS and natural sand.

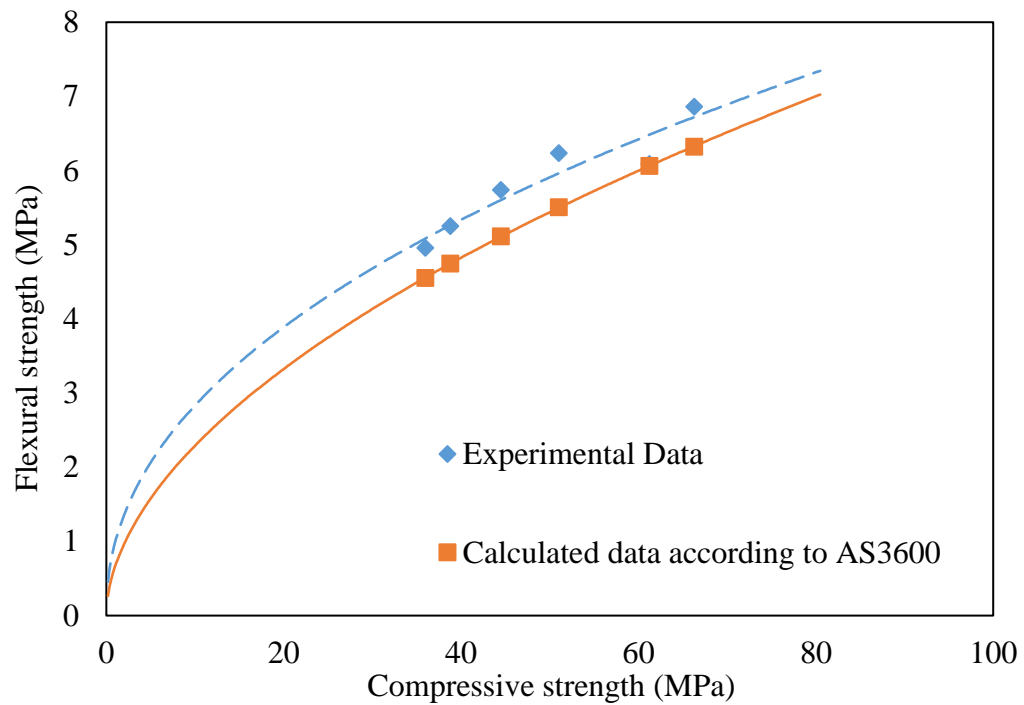


Fig. 4.12 Relationship between flexural strength and compressive strength.

This section presents the relation between the modulus of elasticity and the compressive strength of concrete. The Australian Standard AS 3600 recommends the Eqs. (10) - (11) to predict the modulus of elasticity from the compressive strength and density of concrete.

$$E_c = (p^{1.5}) \times (0.043f_{cmi}^{0.50}) \text{ (MPa)} \quad f_{cmi} \leq 40 \text{ MPa} \quad (10)$$

$$E_c = (p^{1.5}) \times (0.024f_{cmi}^{0.50} + 0.12) \text{ (MPa)} \quad f_{cmi} > 40 \text{ MPa} \quad (11)$$

where, p is the density of concrete (kg/m^3).

ACI 318 recommends the Eq. (12) to calculate the modulus of elasticity.

$$E_c = 4.70f_{cm}^{0.50} \text{ (GPa)} \quad (12)$$

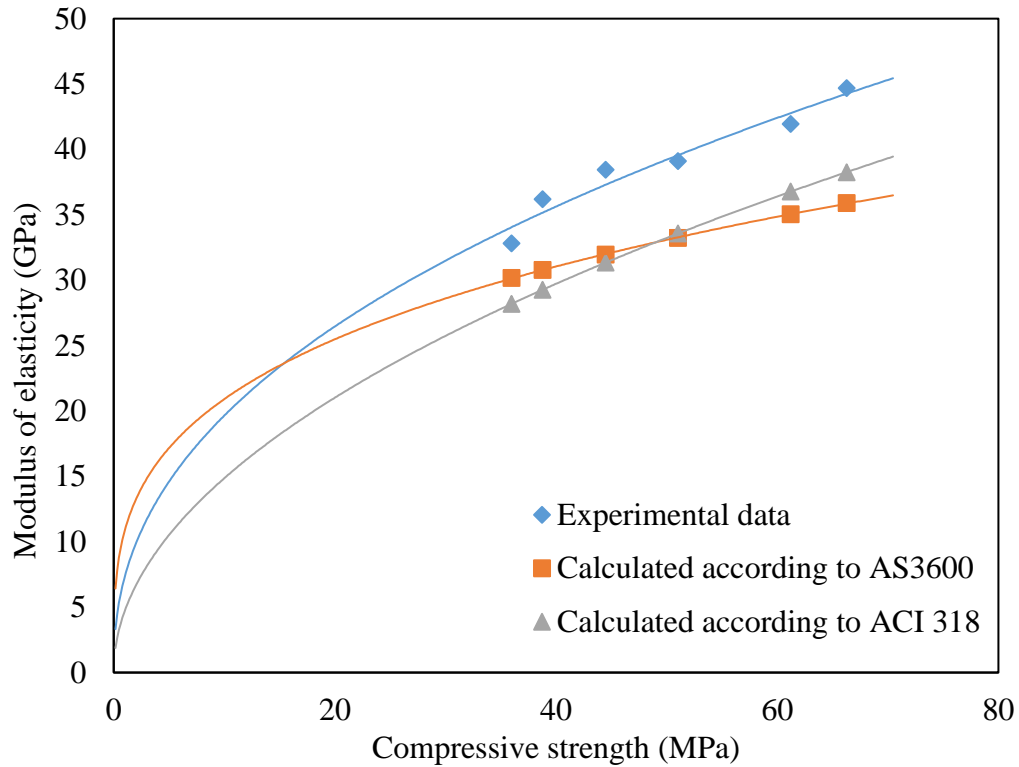


Fig. 4.13 Relationship between compressive strength and Modulus of elasticity

The modulus of elasticity of the concrete samples was calculated using the AS 3600 and ACI 318 equations. The calculated values are shown in Table 4.6 and plotted in Fig. 4.13. The ratios of the experimental to calculated flexural strengths are given in Table 4.7. It can be seen that the ratio of the test to the calculated modulus of elasticity by the AS 3600 varied between 1.09 and 1.24 for the samples with FNS aggregate. The corresponding ratios for the samples with 100% natural sand were between 1.18 and 1.20. Similarly, the test to prediction ratios by the ACI 318 equations varied between 1.16 and 1.24 for the samples with FNS aggregate. The ratios were between 1.14 and 1.23 for the samples with 100% natural sand. Therefore, the equations of both the methods predicted the modulus of elasticity with similar accuracies for concretes made with FNS aggregate and natural sand. As seen in Fig. 4.13, both the standards predicted the modulus of elasticity values conservatively for concretes using FNS as a replacement of natural sand and fly ash as a replacement of cement.

4.5 Summary

Ferronickel slag fine aggregate was used as a replacement of natural sand by 50% and 100%, and fly ash was used as 30% replacement of Portland cement in concrete mixtures. The effect of FNS aggregate on the properties of concrete was evaluated by experimental work and the following conclusions are drawn from the study:

1. The combination of 50% FNS with 50% natural sand improved the grading of fine aggregate and provided a well graded aggregate. The use of 50% FNS slightly increased the workability of concrete due to the improvement of grading of the combined fine aggregate. However, workability then decreased for the use of 100% FNS due to the angular shape of all the fine aggregate particles.
1. The highest compressive strength was obtained for the FNS50 mixtures in both the concrete groups. The 28-day compressive strengths of concretes with 50% FNS aggregate were 66 MPa and 51 MPa for no fly ash and 30% fly ash, respectively. The trends of compressive strength development up to 56 days were similar for both types of fine aggregates. The maximum strength development occurred for 50% FNS because this combination achieved best particle packing and interlocking properties. In addition, concrete with this mix combination exhibited higher slump and density compared to control concrete. Furthermore, the effect of FNS in the compressive strength of mortar was more prominent because mortar does not contain coarse aggregate. As a result, FNS aggregates generally occupy a much greater volume in mortar as compared to concrete mixture, where coarse aggregate is used along with fine aggregates.
2. The 28-day splitting tensile strength of the concrete containing 50% or 100% FNS aggregate varied between 7% and 10% of the corresponding compressive strength.

Similarly, the 28-day flexural strengths of the concrete specimens with FNS aggregate varied between 10% and 14% of the corresponding compressive strengths. Thus, the correlations of tensile and flexural strengths with the compressive strength of concrete using FNS aggregate up to 100% is same as that for concrete using 100% natural sand. The modulus of elasticity of the concrete specimens containing FNS aggregate was similar to those of concrete specimens containing natural sand.

3. The equations of design standards for conventional concrete such as Australian Standard and ACI Code can be used for conservative predictions of the splitting tensile strength, flexural strength and elastic modulus of concrete using FNS fine aggregate.
4. Leaching of heavy metals from the hardened concrete specimens incorporating 50% or 100% FNS fine aggregate were far below the limits recommended by regulatory authorities such as the US EPA and the UK Environment Agency. Therefore, FNS can be considered environmentally compatible for using as a fine aggregate in concrete.
5. Considering good mechanical and leaching properties, the use of FNS as a partial replacement of natural sand together with fly ash as a partial replacement of cement can be considered as a promising alternative to produce green concrete for structural applications.

4.6 References

- ACI Committee, American Concrete Institute, & International Organization for Standardization, 318. (2008). Building code requirements for structural concrete and commentary, American Concrete Institute.
- ASTM C 494. (2016). Standard Specification for Chemical Admixtures for Concrete. Available at: www.compass.astm.org (Accessed on 14 April, 2017).
- ASTM C 231. (2017). Standard Test Method for Air Content of Freshly Mixed Concrete by the Pressure Method. Available at: www.compass.astm.org (Accessed on 14 April, 2018).
- AS 1012.17. (1997). Methods of testing concrete - Determination of the static chord modulus of elasticity and Poisson's ratio of concrete specimens. Available at: www.siaglobal.com (Accessed on 14 May, 2015).
- AS 1012.11. (2000). Methods of testing concrete - Determination of the modulus of rupture. Available at: www.siaglobal.com (Accessed on 14 May, 2015).
- AS 3600. (2009). Concrete structures. Available at: www.siaglobal.com (Accessed on 14 May, 2015).
- AS 2758.1 (2014). Aggregates and rock for engineering purposes. Available at: www.siaglobal.com (Accessed on 12 May, 2015).
- AS 1012.3.1. (2014). Determination of properties related to the consistency of concrete - Slump test. Available at: www.siaglobal.com (Accessed on 14 May, 2015).
- AS 1012.10. (2014). Determination of indirect tensile strength of concrete cylinders ('Brazil' or splitting test). Available at: www.siaglobal.com (Accessed on 14 May, 2015).
- AS 1012.9. (2014). Methods of testing concrete - Compressive strength tests-Concrete, mortar and grout specimens. Available at: www.siaglobal.com (Accessed on 14 May, 2015).
- Demotica, J. S., Amparado Jr, R. F., Malaluan, R. M., & Demayo, C. G. (2012). Characterization and leaching assessment of ferronickel slag from a smelting plant in Iligan City, Philippines. *International Journal of Environmental Science and Development*, 3(5), 470.
- Katsiotis, N. S., Tsakiridis, P. E., Velissariou, D., Katsiotis, M. S., Alhassan, S. M., & Beazi, M. (2015). Utilization of Ferronickel Slag as Additive in Portland Cement: A Hydration Leaching Study. *Waste and Biomass Valorization*, 6(2), 177-189.
- Ladomerský, J., Janotka, I., Hroncová, E., & Najdená, I. (2016). One-year properties of concrete with partial substitution of natural aggregate by cupola foundry slag. *Journal of Cleaner Production*, 131, 739-746.
- Mithun, B. M., & Narasimhan, M. C. (2016). Performance of alkali activated slag concrete mixes incorporating copper slag as fine aggregate. *Journal of Cleaner Production*, 112, 837-844.
- Nath, P., & Sarker, P. (2011). Effect of fly ash on the durability properties of high strength concrete. *Procedia Engineering*, 14, 1149-1156.

- Nath, P., & Sarker, P. K. (2013). Effect of mixture proportions on the drying shrinkage and permeation properties of high strength concrete containing class F fly ash. *KSCE Journal of Civil Engineering*, 17(6), 1437-1445.
- Nederlands Normalisatie Instituut (NEN), 7345. (1995). Leaching Characteristics of Solid Earthy And Stony Building And Waste Materials - Leaching Tests - Determination of the Leaching of Inorganic Components from Buildings and Monolithic Waste Materials With The Diffusion Test. Available at: www.sia-global.com (Accessed on 15 May, 2015).
- Rashad, A. M., Sadek, D. M., & Hassan, H. A. (2016). An investigation on blast-furnace slag as fine aggregate in alkali-activated slag mortars subjected to elevated temperatures. *Journal of Cleaner Production*, 112, 1086-1096.
- Scott, J., Beydoun, D., Amal, R., Low, G., & Cattle, J. (2005). Landfill management, leachate generation, and leach testing of solid wastes in Australia and overseas. *Critical Reviews in Environmental Science and Technology*, 35(3), 239-332.
- Shoya, M., Sugita, S., Tsukinaga, Y., Aba, M., & Tokuhasi, K. (1999). Properties of self-compacting concrete with slag fine aggregates. *Exploiting Wastes in Concrete*, 121-130. Thomas Telford Publishing.
- Tiwari, A., Singh, S., & Nagar, R. (2016). Feasibility assessment for partial replacement of fine aggregate to attain cleaner production perspective in concrete: A review. *Journal of Cleaner Production*, 135, 490-507.
- Tomosawa, F., Nagataki, S., Kajiwara, T., & Yokoyama, M. (1997). Alkali-aggregate Reactivity of Ferronickel-Slag Aggregate Concrete. *ACI Special Publication*, 170, 1591-1602.
- United Kingdom Environment Agency. (2005). Guidance on sampling and testing of wastes to meet landfill waste acceptance procedures. Available at: www.environment-agency.gov.uk/static/documents/Business/sampling_and_testing_1069398.pdf (Accessed on 15 May 2015).
- United States Environmental Protection Agency (US EPA). 2009. Hazardous Waste Characteristics. Available at: www.epa.gov/sites/production/files/2016-01/documents/hw-char.pdf (Accessed on 15 May 2015).

Every reasonable effort has been made to acknowledge the owners of copyright material. I would be pleased to hear from any copyright owner has been omitted or incorrectly acknowledged.

PART III: DURABILITY PROPERTIES

Chapter 5: POTENTIAL ALKALI SILICA REACTION OF FNS AGGREGATE

The contents presented in this chapter were published in the following paper:

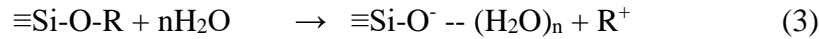
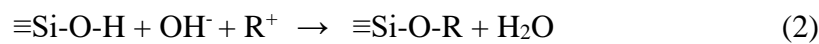
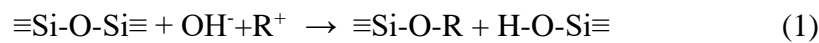
Saha, A. K., & Sarker, P. K. (2018). Potential alkali silica reaction expansion mitigation of ferronickel slag aggregate by fly ash. Structural Concrete, 19(5), 1376-1386.

This chapter investigates the potential alkali silica reaction (ASR) of ferronickel slag (FNS) aggregate. Class F fly ash was used as a possible ASR mitigation in accelerated mortar bar test (AMBT) specimens containing 50% FNS.

5.1 Overview

Alkali silica reaction (ASR) is an important durability issue of concrete produced using reactive aggregates. The reaction of reactive siliceous aggregate with the alkali present in binder leads to formation of an expansive gel and imparts swelling pressure that may cause cracking and strength loss of concrete structures (Giebson et al., 2017; Wiedmann et al., 2017). Stanton (1940) first identified this deleterious expansion in concrete. Extensive research has been carried out since then on the mitigation of this durability issue. There are different kinds of reactive aggregate that can be found in nature or as industrial by-products, such as cristobalite, opaline silica, volcanic glasses, cryptocrystalline quartz, strained quartz, chalcedony and spratt (Berra et al., 1991; Na et al., 2016). The chemical reactions

that take place in ASR can be expressed by Eqs. 1-3 (Glasser, 1992; Ichikawa & Miura, 2007). It can be seen that at the initial stage of ASR, the alkali ion (R^+) from pore solution reacts with the silica ($\equiv Si-O-Si \equiv$) and generates alkali silicate ($Si-O-R$) gel and silicic acid ($Si-OH$). Then, the silicic acid again reacts with the alkali and generates more alkali silicate. At the final stage, this gel absorbs water from the pore solution and expands in volume. The volume expansion imparts swelling pressure to the surrounding concrete. The presence of calcium ion (Ca^{2+}) plays an important role in ASR. It acts as a buffer to maintain alkalinity of the pore solution (Chatterji, 1979). Dron and Brivot (1993) observed that calcium ion reacts with the alkali-silicate gel at the final stage of ASR and produces alkali-calcium-silicate-hydrate ($R-C-S-H$).



In order to mitigate the ASR expansion, different types of supplementary cementing material (SCM) has been studied extensively over the past decades. SCMs can bind the free alkali and reduce alkalinity of the pore solution that is required for ASR to take place (Matos & Sousa-Coutinho, 2016; Thomas, 2011). Therefore, the use of fly ash and ground granulated blast furnace slag (GGBFS) has been found to reduce ASR expansion (Thomas, 1996). The chemical composition of an SCM can significantly influence its effectiveness to reduce ASR. It was observed that high alkali and high calcium fly ash (class C fly ash) are less effective in mitigation of ASR expansion as compared to low alkali and low calcium fly ash (Shehata et al., 1999; Shehata & Thomas, 2002). However, Turk et al. (2017) argued that the use of a class F fly ash up to 30% as an SCM was not enough to

reduce the ASR of reactive aggregates found in Turkey. Therefore, the type and dosage of an SCM can significantly affect the ASR of reactive aggregates.

Due to low grade of nickel ores found in the earth, a significant amount of slag is produced as by-product in the production process of ferronickel alloy. FNS aggregate consists of high density and low absorption particles that makes it a suitable alternative to natural sand in concrete. Chemical analysis showed that FNS contains a high amount of magnesium. When used in the form of ground fine powder, the hydration reaction of magnesium oxide may lead to formation of brucite and cause expansion over a period of time (Du, 2005). However, it was found that the magnesium of this FNS is bound in a crystalline structure known as forsterite, which is chemically stable and does not take part in hydration reaction (Rahman et al., 2017). Previous chapters showed that the use of FNS fine aggregate as 50% replacement of natural sand resulted in well grading of aggregate and maximum compressive strength with good workability of mortar and concrete. Therefore, this aggregate combination has been used to study the effect of different percentages of fly ash on the ASR of FNS aggregate. Fly ash was used as partial replacement of cement from 10% to 30% and its effectiveness to mitigate ASR has been investigated using accelerated mortar bar tests. Microstructural studies by scanning electron microscopy (SEM) and energy-dispersive X-ray spectroscopy (EDS), and TGA were carried out in order to understand the effect of fly ash percentage on ASR.

5.2 Experimental Work

5.2.1 Materials

The binders used in this study were commercially available ordinary Portland cement (OPC) and a class F fly ash. The FNS fine aggregate was a by-product of the smelting of

garnierite nickel ore which is granulated by seawater cooling and then rain-washed on stockpiles. The type of OPC was general-purpose cement.

5.2.2 Mixture proportions and test methods

The mortar mix proportions are given in Table 5.1. The control mix consisted of 100% cement as the binder and is designated by OPC100. The other three mixes contained 10%, 20% or 30% fly ash, and are designated by FA10, FA20 and FA30, respectively. The ASR expansions of FNS aggregate with different percentages of fly ash were determined by accelerated mortar bar tests (AMBT) in accordance with the Australian standard (AS 1141.60.1, 2014). Though the standard suggests a test period of 21 days, it was extended up to 64 days in order to evaluate any slow reactivity associated with the FNS. Mortar mixtures were prepared with a water to binder ratio of 0.47 and aggregate to binder ratio of 2.25, in accordance with the test standard.

Table 5.1 Mortar mixture proportions

Mix ID	Binder (kg/m ³)		Fine aggregate (kg/m ³)		W/C
	OPC	FA	Sand	FNS	
OPC100	602	-	678	678	0.47
FA10	541.8	60.2	678	678	
FA20	481.6	120.4	678	678	
FA30	421	181	678	678	

Fifty mm cube specimens were cast for compressive strength and porosity tests. The specimens were demoulded at 24 hours after casting and cured in lime-saturated water. Compressive strengths were tested at 7, 28 and 56 days of age. Porosity was determined by measuring the volume of permeable voids according to the ASTM standard (ASTM C642). After 28 days of curing, the specimens were oven dried at 110 °C for a period of 3 days to reach the mass equilibrium and then submerged in water for 48 hours. The saturated surface

dry (SSD) weight of the sample was then determined. Porosity was calculated by using these mass values of the specimen. The AMBT specimens consisted of 25×25×275 mm mortar bars with studs inserted at the ends. The specimens were cured in hot water bath at 80 °C for 24 hours after demoulding and the initial length reading was taken using a length comparator. The specimens were then kept in 1M sodium hydroxide bath at 80 °C for 64 days and the length measurements were conducted at time intervals given in the AS 1141.60.1 standard. Furthermore, cube specimens were subjected to the same exposure condition and compressive strengths were determined at 7, 28 and 56 days to evaluate the effect of AMBT exposure on compressive strength.

Thermogravimetric analyses (TGA) were carried out on hardened cement pastes containing no fly ash (OPC 100), 10% fly ash (FA10), 20% fly ash (FA20) and 30% fly ash (FA30). The water-binder ratio was kept constant at 0.47 to make it consistent with the mortar mixes used for AMBT. This test was carried out in order to understand the effect of fly ash percentage on Portlandite content of the products produced in AMBT.

Microstructural investigation was carried out by scanning electron microscope (SEM) in order to evaluate the effect of fly ash on the ASR of FNS aggregate. Imaging was conducted after 21 days of exposure to the AMBT condition. The AMBT specimens were cut with a saw and representative samples were carbon coated for SEM image. The images were taken using a combination of secondary electron (SE) and backscattered electron (BSE) at an accelerating voltage of 15 kV. A combination of SE and BSE was adopted in order to observe the topography and identify different elements of the microstructure. Energy-dispersive X-ray spectroscopy (EDS) of selected points on the image was conducted in order to identify the reaction products.

5.3 Results

5.3.1 Compressive strength

An average compressive strength was determined from three identical specimens and the results are presented in Table 5.2. It can be seen that compressive strength gradually decreased with the increase of fly ash. The control mixture exhibited high early strength of 48 MPa at 7 days that gradually decreased to 37 MPa, 32 MPa and 24 MPa for 10%, 20% and 30% fly ash, respectively. These are 78%, 64% and 50% of the 7-day strength of the control mixture. However, the pozzolanic reaction of fly ash enhanced strength development of the specimens at later ages. At 56 days of age, compressive strengths of the mortars FA10, FA20 and FA30 were 92%, 78% and 67% of the strength of control mixture, respectively. The fly ash contained high silica and low calcium that reduced the rate of hydration and strength at the early age. However, the presence of high silica content participated in pozzolanic reaction and formation of a secondary C-S-H gel that resulted in continued strength development beyond 28 days of age.

Table 5.2 Compressive strength of mortars containing 50% FNS fine aggregate

Mix ID	Compressive strength (MPa)		
	7 Days	28 Days	56 Days
OPC100	48	57	62
FA10	37	48	57
FA20	31	39	49
FA30	24	35	47

5.3.2 Porosity

Volume of permeable voids (VPV) test was carried out in order to determine the total porosity of hardened mortar specimens. Porosity of a specimen depends on the air voids, gel pores, capillary pores and micro cracks (Andrews-Phaedonos, 1996). The changes in VPV of mortar specimens with the increase of fly ash are plotted in Fig. 5.1. It can be seen

that porosity gradually decreased with the increase of fly ash. VPV of the control samples was 17.97% that decreased to 17.50%, 15.24% and 14.40% with the inclusion of 10%, 20% and 30% fly ash, respectively. Therefore, porosity decreased by 3%, 16% and 20% with the use of 10%, 20% and 30% fly ash, respectively. The reduction of porosity by the inclusion of fly ash is attributed to the densification of microstructure by pozzolanic reaction product and filling effect of the unreacted fly ash particles.

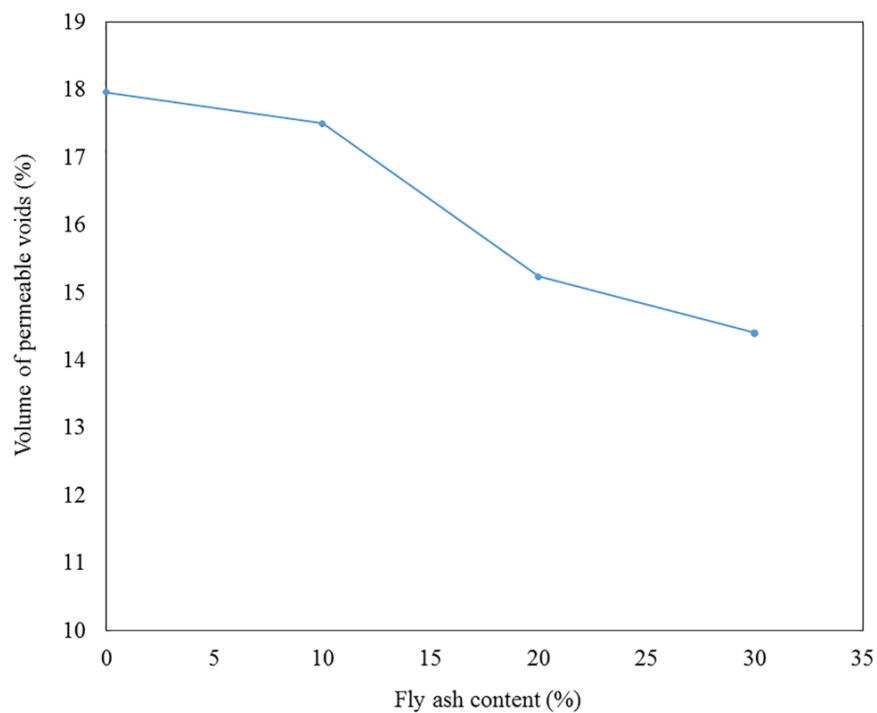


Fig. 5.1 Volume of permeable voids of mortar with respect to fly ash percentage

5.3.3 AMBT results

Accelerated mortar bar test is a quick and effective method to identify the reactivity of aggregates. According to the Australian Standard AS 1141.60.1 (2014), mortar bar expansions below 0.1% at the end of 21 days of the test are classified as nonreactive. When the 10-day expansion is below 0.1% and the 21-day expansion is between 0.1% and 0.3%, it is classified as slowly reactive. The 21-day expansion above 0.3% is classified as reactive. The accelerated mortar bar test (AMBT) is a part of different international standards such

as, RILEM AAR-2 (Nixon & Sims, 2016) and ASTM C1567 (2013). According to both these standards, expansion below 0.1% after 16 days of testing is classified as non-reactive and above 0.1% is classified as reactive.

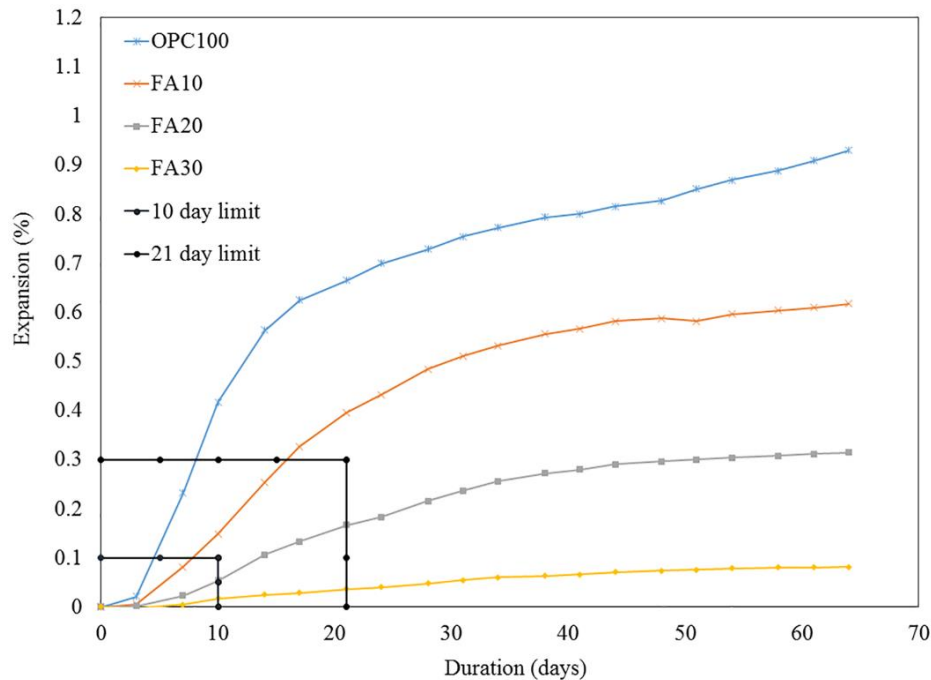


Fig. 5.2 ASR expansion of mortar bars containing different percentages of fly ash

Expansions of the mortar bars containing 50% FNS aggregate and 50% sand with different proportions of fly ash are plotted in Fig. 5.2. It can be seen that mix OPC100 experienced a significant expansion that was 0.930% at the end of 64 days of testing. It is also noticeable that expansion of the OPC100 specimens exceeded the 21-day limit of AS 1141.60.1. At the end of 21 days exposure, the expansion was 0.664%, which is more than twice the allowable limit. The use of 10% fly ash as cement replacement reduced expansion by 34% as compared to the control samples after 64 days of exposure. However, the expansion was above the allowable limit and it was in “reactive” category according to AS 1141.60.1. At the end of 21 days of exposure, the expansion of FA10 specimens was 0.392%. Furthermore, the 16-day expansions of OPC100 and FA10 was 0.624% and 0.326%, respectively. These values exceed the allowable limit of RILEM AAR-2 and

ASTM C1567 standards. Therefore, both these mixes are classified as reactive in accordance with the limits of all three standards.

Expansion decreased by 66% as compared to that of the control specimens by the use of 20% fly ash in the binder. At the end of 10 and 21 days of exposure, the expansions were 0.056% and 0.167%, respectively, which is in “slowly reactive” category according to the Australian standard. The 16-day expansion of these samples was 0.131%, which is in the reactive category according to RILEM AAR-2 and ASTM C1567. Further increase of fly ash to 30% reduced expansion by 91% as compared to the expansion of the control specimens. The expansions after 10 and 21 days of exposure were 0.017% and 0.036%, respectively. According to AS 1141.60.1, these expansions are categorised as “non-reactive”. The 16-day expansion of this sample was 0.028%, which is in the non-reactive category according to RILEM AAR-2 and ASTM C1567.

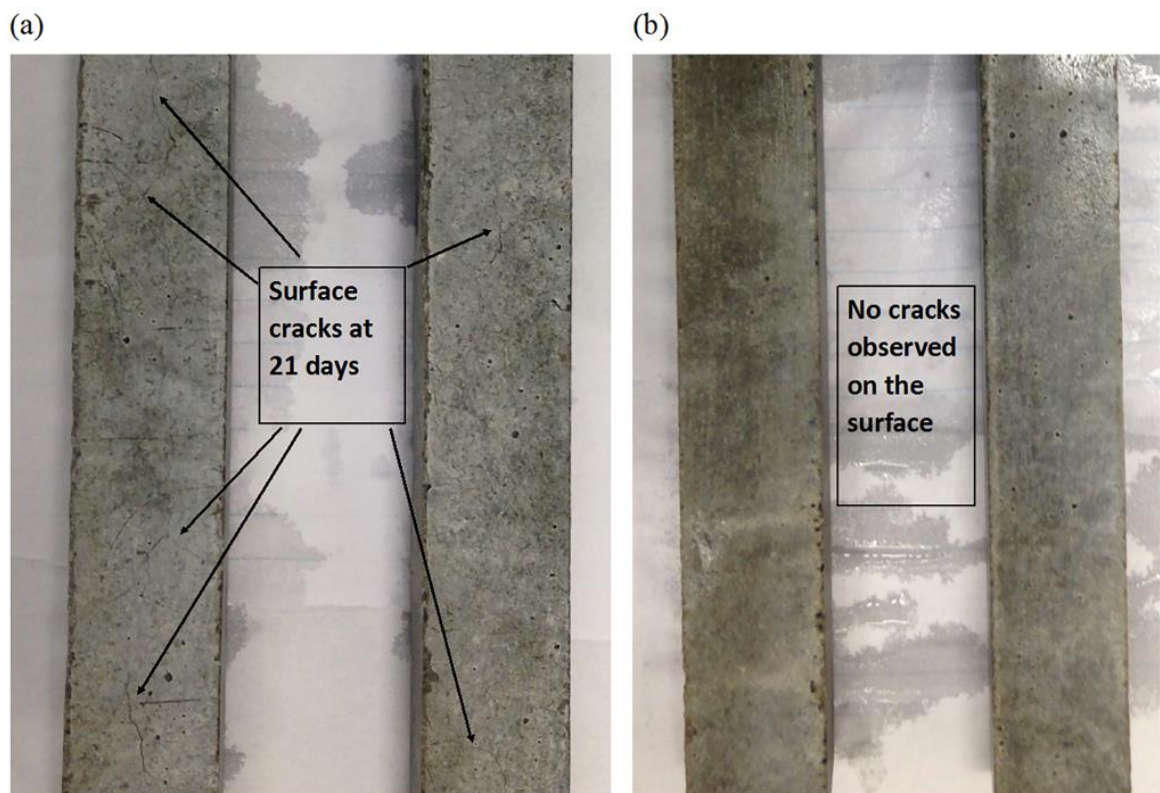


Fig. 5.3 Visual inspection of AMBT samples after 21 days exposure

Photographs of the specimens at the end of 21 days of testing are presented in Fig. 5.3. It can be seen that the specimens of mixtures OPC100 and FA10 experienced some visible cracks on the surface. This is consistent with the 10 and 21-day expansions that classified both the mixtures as “reactive. However, the number of cracks in specimens of FA10 were significantly less than in those in the specimens of OPC100. The specimens of FA20, which were classified as “slowly reactive” by the 10 and 21-day expansions, did not exhibit any surficial crack in the visual inspections. Also, the specimens of FA30, which were classified as “non-reactive”, did not show any cracking on the surface. Therefore, the use of 30% class F fly ash as a SCM is considered adequate for mitigation of the expansion associated with 50% FNS as fine aggregate.

5.3.4 Effect of AMBT exposure on compressive strength

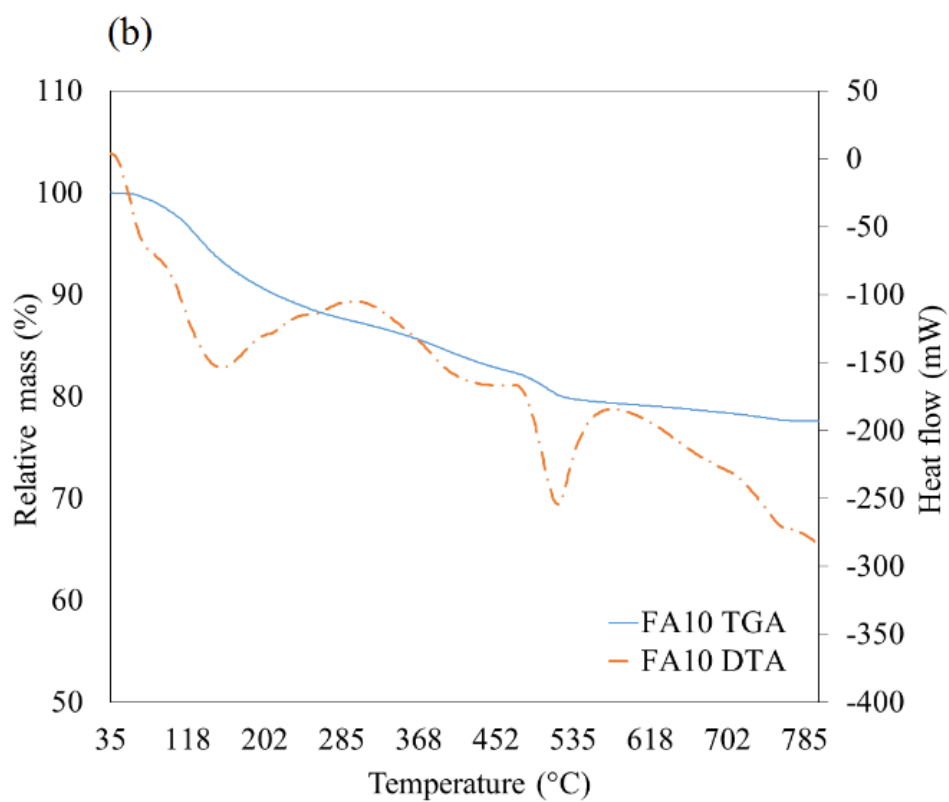
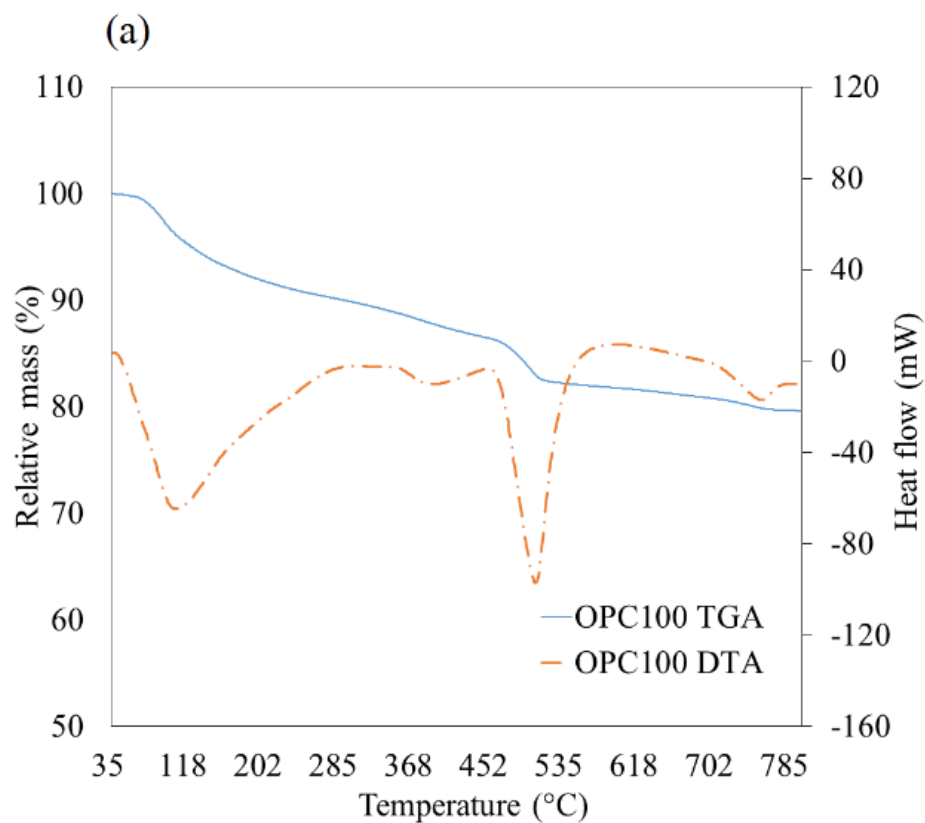
Compressive strengths of mortar cubes were determined after exposure to the AMBT test condition and the results are given in Table 5.3. It can be seen that the OPC100 and FA10 samples suffered 31% and 28% strength loss after 56 days of exposure, respectively. On the other hand, the FA20 samples suffered a relatively low strength loss of 16%. The aggressive exposure of 1M NaOH at 80 °C resulted in the expansion and cracking of the OPC100 and FA10 samples, which were reflected by the significant strength losses. However, FA30 specimens exhibited strength gain rather than strength loss in the AMBT exposure. This is because 30% fly ash significantly reduced ASR of the FNS aggregates, which is consistent with no cracking upon visual observations. In addition, the high-temperature exposure accelerated the pozzolanic reaction of fly ash. Thus, there was a relative strength improvement of 9% after 56 days of the exposure period.

Table 5.3 Effect of AMBT exposure on compressive strength of mortar samples

Mix ID	Compressive strength (MPa)			Change of strength (%)		
	7 Days	28 Days	56 Days	7 day	28 day	56 Days
OPC100	43	41	43	-10	-28	-31
FA10	34	37	41	-8	-23	-28
FA20	30	34	43	-3	-13	-12
FA30	25	38	51	4	9	9

5.3.5 Thermogravimetric analysis

The TGA results are presented in Figs. 5.4(a)-(d). The diagrams show the changes in mass of the specimen subjected to a progressive temperature increase. The DTA graph shows three endothermic peaks. The initial peak was observed at 110 °C for OPC100, which is due to evaporation of the weakly bound water in calcium silicate hydrate (C-S-H), and ettringite (Aly et al., 2012; Chappex & Scrivener, 2012). However, for the specimens containing fly ash, the initial peak was observed at around 150 °C. Thus, a comparison was made among the C-S-H contents of the specimens by measuring the mass losses in a temperature range of 45 °C to 150 °C. Thus, the C-S-H contents of specimens OPC100, FA10, FA20 and FA30 were found to be 6.42%, 6.37%, 5.23% and 4.98%, respectively. The calcium oxide contents of specimens containing fly ash decreased due to the replacement of OPC by fly ash. Thus, less C-S-H gel was formed in the fly ash blended cement pastes, which also explains the low compressive strength of the fly ash mortar samples as compared to OPC100. The second peak was observed in the vicinity of 500 °C, which is due to the decomposition of portlandite (CH) (Esteves, 2011; Frías & Cabrera, 2001).



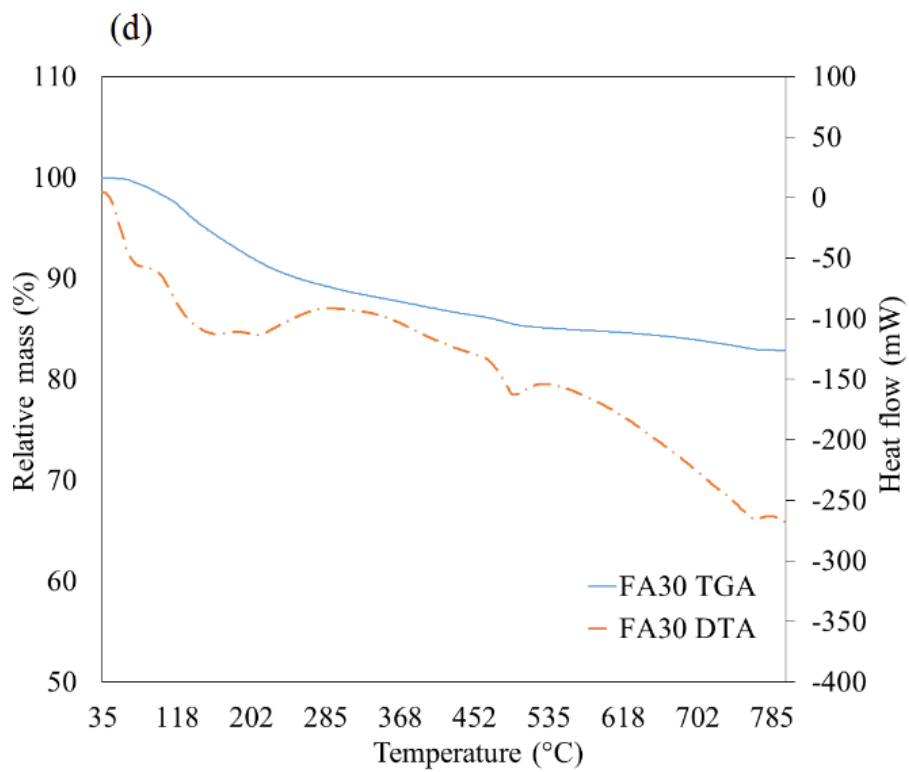
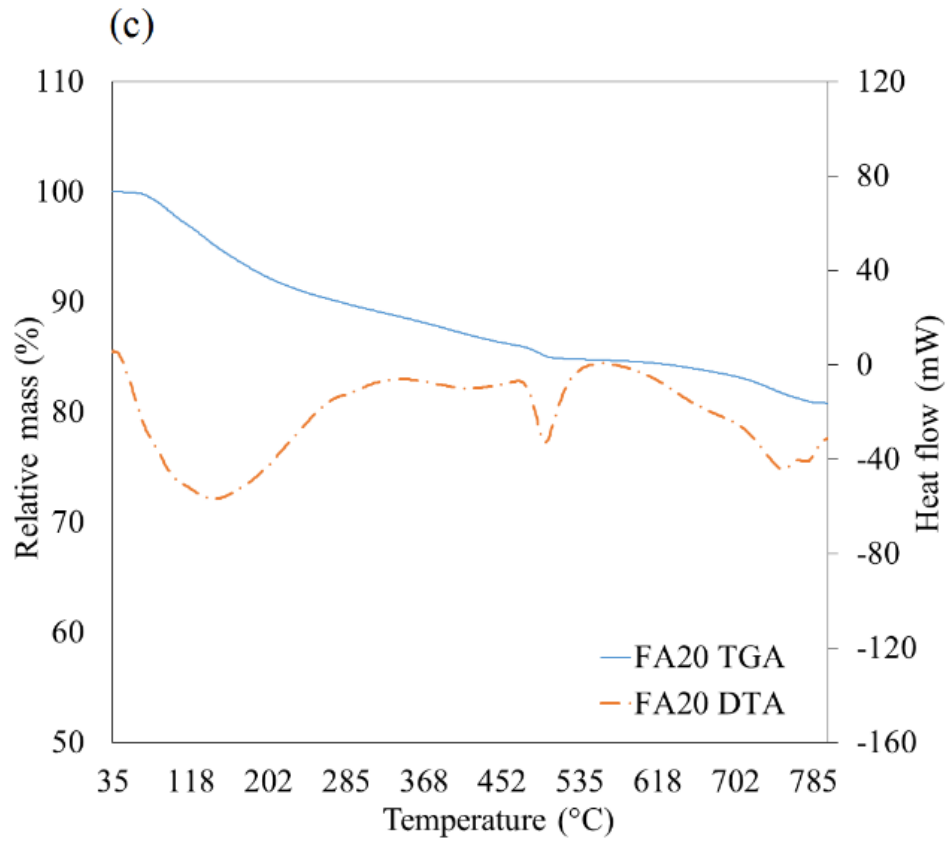


Fig. 5.4 Thermogravimetric mass changes of paste samples exposed to AMBT condition

Therefore, a comparison is made to determine the portlandite content by measuring the mass loss at a temperature range of 450 °C to 550 °C. The CH content was 4.25%, 3.27%, 1.58% and 1.36% for the paste samples of OPC100, FA10, FA20 and FA30, respectively. Thus, cement replacement by fly ash reduced the CH content due to its pozzolanic reaction that eventually reduced the ASR of FNS aggregate. The third peak was observed in the vicinity of 760 °C, which occurred due to the decomposition of calcium carbonate and release of carbon dioxide (Vedalakshmi et al., 2003; Shui et al., 2010).

5.3.6 Microstructure analysis by SEM and EDS

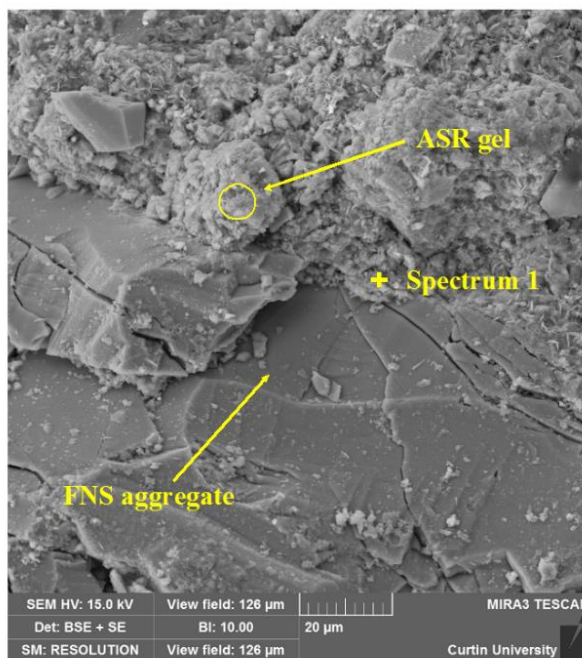
Fig. 5.5(a) shows the microstructure of the sample OPC100. The specimen showed an expansion of 0.66%. Several micro cracks around the aggregate, as well as some cracks across the aggregate can be seen in this SEM image. The presence of ASR gels of fibrous morphology can be noticeable on the aggregate surface, in the cracks of aggregates and in pores of the binder matrix. Similar morphologies of ASR products have been well documented in the literature (Beglarigale & Yazici, 2013; Yazici, 2012). These cracks in aggregates are associated to the aggregate dissolution due to the alkali attack from the binder matrix. ASR gel filled the cracks, absorbed moisture from the surroundings and expanded to increase the crack width. The cracks developed around the slag aggregate and extended to the aggregate cross-section, and therefore caused expansion and cracking of the specimens. The EDS analysis of ASR gel of OPC100 is given in Fig. 5.5(b). It can be seen that the ASR gel consists of silicon, calcium, sodium and potassium. The presence of magnesium is noticeable due to the magnesium content of FNS aggregate.

Fig. 5.5(c) shows an image of the sample of FA10. Formation of cracks due to ASR gel in the FNS aggregate surface can be seen in this figure. In addition, these gels also accumulated in the cracks of the aggregates and induced swelling pressure. The generation of small cracks filled with ASR gel are also noticeable in the cross-section of the

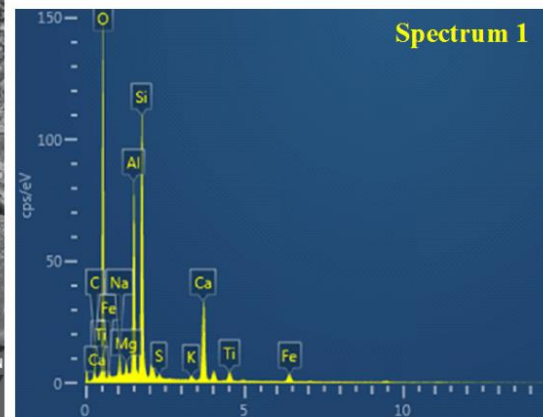
aggregates. The chemical analysis of the gels in the cracks, as presented in Fig. 5.5(d), shows the presence of silicon, calcium, aluminium, sodium, potassium and magnesium. The presence of aluminium is due to the use of fly ash. However, the number of cracks and crack width in this specimen are less than those in OPC100.

The microstructural image of the sample containing 20% fly ash as SCM is presented in Fig. 5.5(e). It is noticeable that the aggregates suffered minor disintegration due to alkali attack. Very thin cracks can be observed at the interface of FNS aggregate and binder matrix, which indicates significantly less ASR in the FA20 specimen as compared to the OPC100 and FA10 specimens. Also, no cracks were observed in the aggregate.

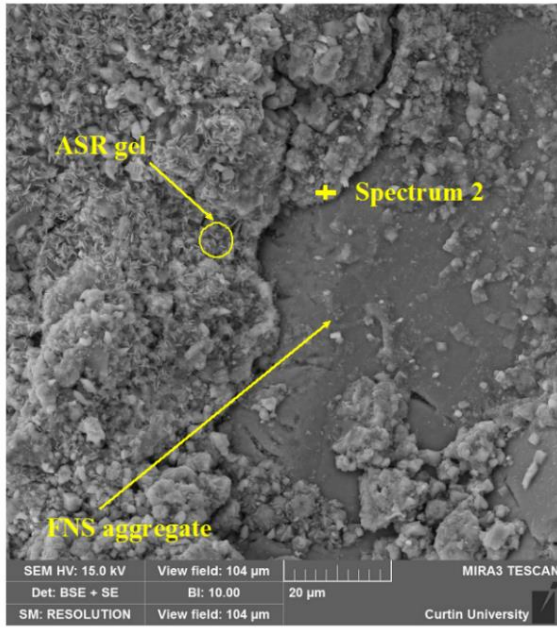
(a)



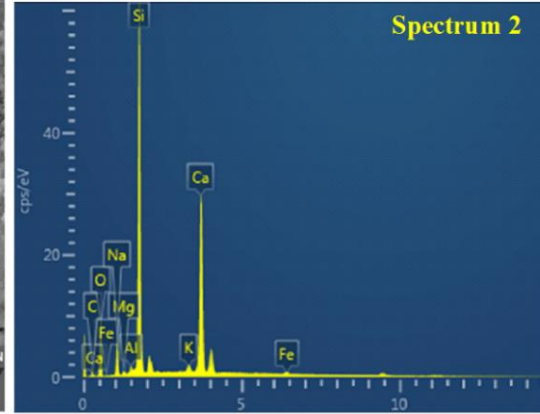
(b)



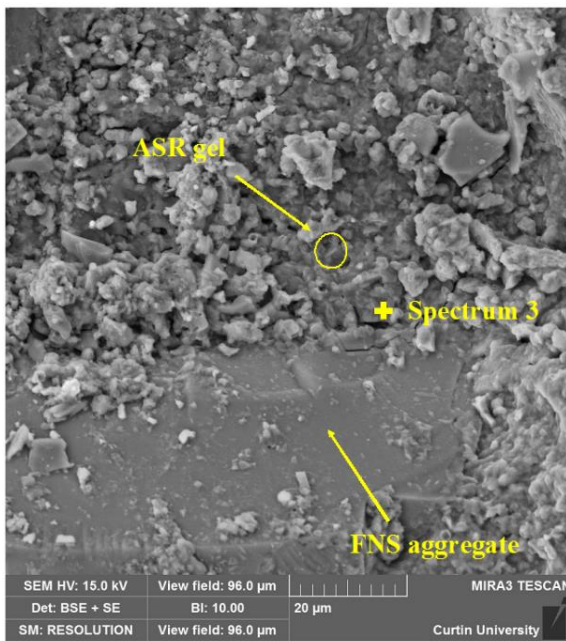
(c)



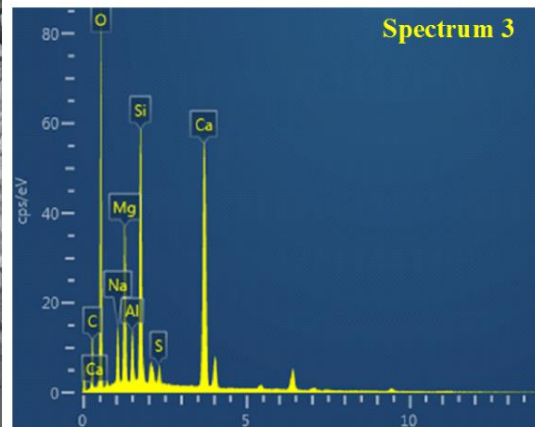
(d)



(e)



(f)



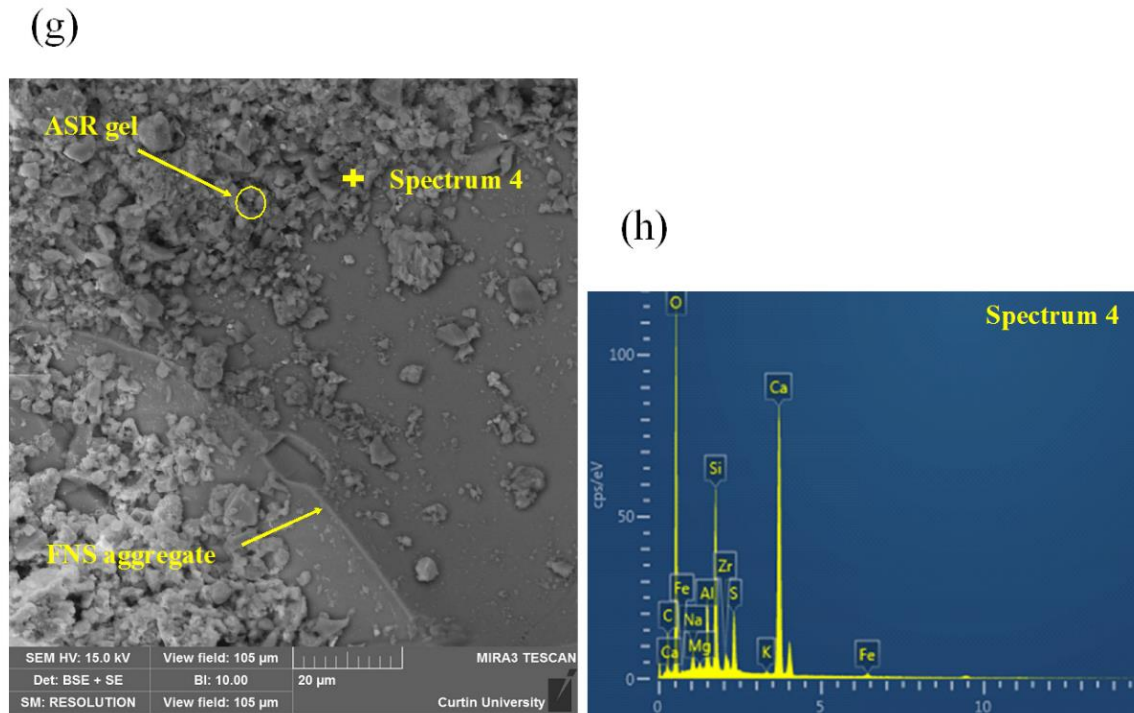


Fig. 5.5 SEM and EDS of specimens after 21 days of NaOH exposure

EDS in the cracks, as given in Fig. 5.5(f), shows that the gel consisted of high calcium/silicon ratio as compared to those of OPC100 and FA10. This phenomenon of high calcium/silicon ratio in ASR gel was attributed due to the presence of fly ash, which reduces the aggregate dissolution thus minimize the silica content from the ASR gel. The ASR gel with high Ca/Si ratio has a low swelling pressure. Therefore, this ASR gel caused less cracking in the microstructure of the specimen. Gholizadeh-Vayghan & Rajabipour (2017) synthesised ASR gels consisting of different Ca/Si ratios and found that ASR gel with high Ca/Si had a low swelling pressure that can be dispersed in the microstructure. On the other hand, ASR gel with low Ca/Si has the affinity to absorb moisture and provide swelling pressure to the surrounding environment.

The SEM image of samples with 30% fly ash (FA30) is given in Fig. 5.5(g). It can be seen that the aggregate surface exhibits a firm bonding with the binder matrix. No cracking was observed on the aggregate, which indicates that the FNS aggregate in FA30

specimens had very minor dissolution. Furthermore, negligible amounts of ASR gels were observed on the aggregate surface. EDS analysis of the ASR gel on aggregate surface point out the gels consisting of high Ca/Si ratio. Therefore, due to the high Ca/Si ratio, the ASR gel did not impart swelling pressure to cause cracking.

5.4 Discussion

It is evident from the presented test results that expansion of the mortar specimens decreased with the increase of fly ash, and 30% fly ash was found to reduce the expansion below the 10-day and 21-day AMBT limits of the Australian Standard. The effectiveness of fly ash to reduce the ASR expansion is attributed to different reasons. First, the alkalinity of pore solution is reduced by fly ash. The fly ash contained very low amount of calcium oxide, which is only 0.6% by mass. Thus, the total alkalinity of the binder decreased with the increase of fly ash as cement replacement. The increase of the low-calcium fly ash as cement replacement reduced the amount of Portlandite generated by the hydration of cement. The subsequent pozzolanic reaction of fly ash further consumed Portlandite. The presented TGA results confirmed the reduction of Portlandite by fly ash. Therefore, fly ash as a SCM reduced the overall alkalinity of pore solution that reduced the ASR of FNS aggregate.

Secondly, fly ash helped by reducing the permeability of the binder matrix. The presented VPV test results show that porosity decreased with the increase of fly ash. The densification of the binder matrix by fly ash resulted in an increase of strength at a higher rate with the increase of age as compared to the control mix. Therefore, the internal voids are filled by the secondary C-S-H gel produced by fly ash (Ghrici et al., 2007). The accelerated mortar bar test exposure involves immersion of the specimen in an alkaline solution. The reduction of permeability by fly ash helped reduce ingress of alkaline solution from outside of the sample. This helped to reduce the ASR of FNS in the AMBT condition.

Finally, fly ash also helped with the ASR gel modification. Fly ash is found to react with the alkali silicate gel and change the gel properties. The EDS analysis was carried out to determine the Ca/Si ratio of products for all four samples and the values were 1.78, 2.18, 2.46 and 2.63 for OPC100, FA10, FA20 and FA30, respectively. Thus, the Ca/Si ratio of the ASR gel gradually increased with the increase of fly ash. Therefore, the modified ASR gel generated low swelling pressure that did not cause severe internal cracking on the aggregate surface. As a result, specimens containing 20% and 30% fly ash did not exhibit any cracking on the aggregate surface even after an extended period of the accelerated mortar bar test.

5.5 Summary

The effect of fly ash on ASR expansion of by-product FNS fine aggregate was studied by accelerated mortar bar tests. The fine aggregate of the mortar bar specimens consisted of 50% FNS and 50% natural sand. A class F fly ash was used as 10%, 20% and 30% replacement of cement. The following conclusions are drawn from the study:

1. Expansion of mortar bar specimens decreased with the increase of fly ash in the accelerated test condition. According to the 10-day and 20-day expansion limits of the Australian Standard, the mortar bar specimens were classified as reactive, slowly reactive and non-reactive for the fly ash contents of 10%, 20% and 30%, respectively.
2. Surface cracks were observed in the specimens using no fly ash and 10% fly ash. There was no surface cracks in the specimens using 20% and 30% fly ash.
3. The volume of permeable voids decreased from 18% to 14% by the use of 30% fly ash which shows densification of the binder matrix by pozzolanic reaction of fly ash.

4. The TGA results showed that Portlandite content of paste samples exposed to AMBT condition decreased from 4.25% to 1.36% by the use of 30% fly ash.
5. The Ca/Si ratio of the ASR product increased from 1.78 to 2.63 by the use of 30% fly ash. This shows a modification of the ASR product by fly ash.
6. Overall, fly ash reduced the ASR expansion of FNS aggregates by reduction of the alkalinity of pore solution, densification of the binder matrix by pozzolanic reaction and modification of the ASR gel to cause less swelling pressure and cracking.
7. Therefore, the use of FNS aggregate and fly ash can be considered as a feasible option for production of technically sound and environmentally friendly concrete.

5.6 References

- Aly, M., Hashmi, M. S. J., Olabi, A. G., Messeiry, M., Abadir, E. F., & Hussain, A. I. (2012). Effect of colloidal nano-silica on the mechanical and physical behaviour of waste-glass cement mortar. *Materials & Design*, 33, 127-135. doi:10.1016/j.matdes.2011.07.008
- Andrews-Phaedonos, F. (1996). Establishing the durability performance of structural concrete. VicRoads, Melbourne, Australia, 79.
- AS 1141.60.1 (2014). Method for Sampling and Testing Aggregates, Potential Alkali Silica Reactivity – Accelerated Mortar Bar Method. Standards Australia, Sydney, Australia.
- ASTM C642 (2006). Standard test method for density, absorption, and voids in hardened concrete. West Conshohocken, Pennsylvania, United States.
- ASTM C1567 (2013). Standard Test Method for Determining the Potential Alkali-Silica Reactivity of Combinations of Cementitious Materials and Aggregate (Accelerated Mortar-Bar Method). West Conshohocken, Pennsylvania, United States.
- Berra, M., Mangialardi, T., Paolini, A. E., & Turriziani, R. (1991). Critical evaluation of accelerated test methods for detecting the alkali-reactivity of aggregates. *Advances in Cement Research*, 4(13), 29-37.
- Beglarigale, A., & Yazici, H. (2013). Mitigation of detrimental effects of alkali-silica reaction in cement-based composites by combination of steel microfibers and ground-granulated blast-furnace slag. *Journal of Materials in Civil Engineering*, 26(12), 04014091.
- Chatterji, S. (1979). The role of Ca (OH)₂ in the breakdown of Portland cement concrete due to alkali-silica reaction. *Cement and concrete research*, 9(2), 185-188.
- Chappex, T., & Scrivener, K. (2012). Alkali fixation of C–S–H in blended cement pastes and its relation to alkali silica reaction. *Cement and Concrete Research*, 42(8), 1049-1054.
- Dron, R., & Brivot, F. (1993). Thermodynamic and kinetic approach to the alkali-silica reaction. Part 2: Experiment. *Cement and Concrete Research*, 23(1), 93-103.
- Du, C. (2005). A review of magnesium oxide in concrete. *Concrete international*, 27(12), 45-50.
- Esteves, L. P. (2011). On the hydration of water-entrained cement–silica systems: combined SEM, XRD and thermal analysis in cement pastes. *Thermochimica Acta*, 518(1), 27-35.
- Frías, M., & Cabrera, J. (2001). Influence of MK on the reaction kinetics in MK/lime and MK-blended cement systems at 20 C. *Cement and concrete research*, 31(4), 519-527.
- Gholizadeh-Vayghan, A., & Rajabipour, F. (2017). The influence of alkali–silica reaction (ASR) gel composition on its hydrophilic properties and free swelling in contact with water vapor. *Cement and Concrete Research*, 94, 49-58.
- Ghrici, M., Kenai, S., & Said-Mansour, M. (2007). Mechanical properties and durability of mortar and concrete containing natural pozzolana and limestone blended cements. *Cement and Concrete Composites*, 29(7), 542-549.

- Giebson, C., Volland, K., Ludwig, H. M., & Meng, B. (2017). Alkali-silica reaction performance testing of concrete considering external alkalis and preexisting microcracks. *Structural Concrete*, 18(4), 528-538.
- Glasser FP (1992) Chemistry of the alkali aggregate reaction. In: R.N. Swamy (ed) *The Alkali-Silica Reaction in Concrete*, Blackie, Glasgow and London, and Van Nostrand-Reinhold, New York, pp 30-53
- Ichikawa, T., & Miura, M. (2007). Modified model of alkali-silica reaction. *Cement and Concrete research*, 37(9), 1291-1297.
- Matos, A. M., & Sousa-Coutinho, J. (2016). ASR and sulphate performance of mortar containing industrial waste. *Structural Concrete*, 17(1), 84-95. doi:10.1002/suco.201400095
- Na, O., Xi, Y., Ou, E., & Saouma, V. E. (2016). The effects of alkali-silica reaction on the mechanical properties of concretes with three different types of reactive aggregate. *Structural Concrete*, 17(1), 74-83.
- Nixon, P. J., & Sims, I. (2016). RILEM Recommended Test Method: AAR-2—Detection of Potential Alkali-Reactivity—Accelerated Mortar-Bar Test Method for Aggregates. In: Nixon P., Sims I. (eds) *RILEM Recommendations for the Prevention of Damage by Alkali-Aggregate Reactions in New Concrete Structures*. RILEM State-of-the-Art Reports, vol 17. Springer, Dordrecht.
- Rahman, M. A., Sarker, P. K., Shaikh, F. U. A., & Saha, A. K. (2017). Soundness and compressive strength of Portland cement blended with ground granulated ferronickel slag. *Construction and Building Materials*, 140, 194-202.
- Shehata, M. H., Thomas, M. D., & Bleszynski, R. F. (1999). The effects of fly ash composition on the chemistry of pore solution in hydrated cement pastes. *Cement and Concrete Research*, 29(12), 1915-1920.
- Shehata, M. H., & Thomas, M. D. (2002). Use of ternary blends containing silica fume and fly ash to suppress expansion due to alkali-silica reaction in concrete. *Cement and Concrete Research*, 32(3), 341-349.
- Shui, Z. H., Zhang, R., Chen, W., & Xuan, D. X. (2010). Effects of mineral admixtures on the thermal expansion properties of hardened cement paste. *Construction and Building Materials*, 24(9), 1761-1767.
- Stanton, T.E. (1940). Expansion of concrete through reaction between cement and aggregate. *Proc Am Soc Civil Eng*, 66(10), 1781-811.
- Thomas, M. (2011). The effect of supplementary cementing materials on alkali-silica reaction: A review. *Cement and Concrete Research*, 41(12), 1224-1231.
- Thomas, M. D. A. (1996). *Review of the effect of fly ash and slag on alkali-aggregate reaction in concrete*. Building Research Establishment Report, BR314, Construction Research Communications, Watford, UK, 1996.
- Turk, K., Kina, C., & Bagdiken, M. (2017). Use of binary and ternary cementitious blends of F-Class fly-ash and limestone powder to mitigate alkali-silica reaction risk. *Construction and Building Materials*, 151, 422-427.
- Vedalakshmi, R., Raj, A. S., Srinivasan, S., & Babu, K. G. (2003). Quantification of hydrated cement products of blended cements in low and medium strength concrete using TG and DTA technique. *Thermochimica Acta*, 407(1), 49-60.

- Wiedmann, A., Weise, F., Kotan, E., Müller, H. S., & Meng, B. (2017). Effects of fatigue loading and alkali–silica reaction on the mechanical behavior of pavement concrete. *Structural Concrete*, 18(4), 539-549.
- Yazici, H. (2012). The effect of steel micro-fibers on ASR expansion and mechanical properties of mortars. *Construction and Building Materials*, 30, 607-615.

Every reasonable effort has been made to acknowledge the owners of copyright material. I would be pleased to hear from any copyright owner has been omitted or incorrectly acknowledged.

Chapter 6: USE OF FLY ASH AND BLAST FURNACE SLAG TO MITIGATE POTENTIAL ASR OF FNS AGGREGATE

The contents presented in this chapter were published in the following paper:

Saha, A. K., & Sarker, P. K. (2016). Expansion due to alkali-silica reaction of ferronickel slag fine aggregate in OPC and blended cement mortars. Construction and Building Materials, 123, 135-142.

This chapter evaluates the effectiveness of ground granulated blast furnace slag (GGBFS) to mitigate alkali silica reaction (ASR) of ferronickel slag (FNS) aggregates. In addition, a comparative study was conducted with GGBFS, fly ash and ordinary Portland cement (OPC) samples. Accelerated mortar bar test (AMBT) method was carried out to determine the alkali silica reactivity. Microstructure analysis was carried out to understand the ASR test results.

6.1 Overview

Stanton (1942) identified that concrete structure can suffer from deleterious expansion due to ASR. Cole et al. (1981) reported surface cracking and expansion of old dams in Australia suffering from ASR. The mechanism of ASR is complicated and there are differences in opinions among researchers. According to Lee (2005), the reactive silica in aggregate is depolymerised in a highly alkaline condition. Hydrolysis of the silica takes place in the presence of sodium and potassium hydroxides and an alkali silicate gel is formed. This gel absorbs a large quantity of water from the surroundings resulting in an expansion of its

volume. This expansion of the alkali-silica gel may cause micro cracking inside the aggregate as well as at the interface between aggregate and cement paste (Ponce & Batic, 2006). Usually, aggregates with amorphous structure, lattice defects and large surface area are more susceptible to ASR expansion (Poole, 1992). The crystalline structure of silica is stable and the amorphous silica is considered to be reactive (Lukschová et al., 2009). The presence of calcium is also regarded as an important factor in ASR expansion. The calcium content of the binder has a significant influence on the expansion due to ASR. The ASR expansion increases with the rise of calcium content in the binder (Carrasquillo & Farbiarz, 1989). Chatterji (1979) showed that the expansion could be reduced by leaching out of the Ca(OH)_2 from concrete. It was also observed that the reactive silica did not cause any harmful expansion if there was no calcium available in the binder (Bleszynski & Thomas 1998). The presence of a higher percentage of calcite was also found to cause greater expansion of concrete (García-Lodeiro et al., 2007). Since ASR is a slow process, accelerated tests of mortar or concrete specimens are usually conducted to assess the alkali reactivity of an aggregate. Such accelerated tests are recommended in testing Standards and Codes. Besides, Carse and Dux (1990) showed a correlation between the accelerated ASR test results and the actual ASR in concrete structures.

Use of supplementary cementitious materials (SCM) such as fly ash, blast-furnace slag and silica fume is usually considered as a mitigating measure against the ASR expansion of concrete. However, the effectiveness of an SCM in reducing the ASR depends on the type and dosage of the SCM, and the type of the reactive aggregate. The effectiveness of an SCM depends on its alkali content, with higher alkali content exhibiting higher expansion (Duchesne & Bérubé, 1994). Shehata and Thomas (2000), and Shafaatian et al. (2013) showed that expansion of mortar specimens containing reactive aggregates was reduced by the use of fly ash as a partial replacement of cement. Fly ash can

significantly reduce the alkalinity of pore solution resulting in a reduction of the ASR (Nixon et al., 1986). The use of reactive aggregates in powder form with the binder can also reduce ASR as the powder acts as a pozzolan and reduces the alkalinity of the pore solution (Moisson et al., 2004). Although ASR is being studied for the past few decades, the exact chemical reactions that cause the expansion and cracking of concrete remains in shadow.

Accelerated ASR tests were conducted on mortar specimens containing different percentages of FNS as a replacement of natural sand. Fly ash and GGBFS were used as partial replacements of cement and their effectiveness on the ASR expansion were studied. Microstructural analysis using scanning electron micrographs (SEM) and energy-dispersive X-ray spectroscopy (EDS) was performed to obtain an insight into the ASR products and the resulting expansions observed for the mortar mixtures containing different percentages of the FNS and SCMs.

8.2 Experimental Work

6.2.1 Materials

The materials used in this study were FNS aggregate, ordinary Portland cement (OPC), class F fly ash and GGBFS. This particular FNS is extracted by pyro-metallurgy from garnierite ore and cooled by seawater. Petrographic analysis of the FNS showed the existence of glass containing amorphous and cryptocrystalline silica that might cause ASR when used as aggregate in cement composites. Therefore, a study on the potential ASR expansion of the aggregate is essential for its development as an alternative fine aggregate for concrete.

6.2.2 Mixture proportions and test methods

Petrography and expansion tests are two most common tests used for identification of the alkali reactivity of aggregates. However, petrography test has the limitation of its efficiency in identifying the fine-grained reactive silica (Godart et al., 2013). Accelerated mortar bar test (AMBT) was performed in this study, as it has been well accepted as a quick and efficient test to determine the alkali reactivity of fine aggregates. Since the aggregate's slow reactivity might not come into reaction within a short period of 21 days, the test can be continued for a longer period of time (Thomas et al., 2006). Therefore, the test was extended up to 64 days in this study. The tests were conducted in accordance with the AS 1141.60.1 (2014) Standard. The mortar bars were cast from mixtures with a water to binder ratio of 0.47 and binder to fine aggregate ratio of 1:2.25, as recommended in the Standard. The test specimens were made from mortar mixtures with FNS replacing natural sand by 25%, 50%, 75% and 100%. Fly ash and GGFS were used as replacements of cement by 30% in order to study their effectiveness on mitigation of the ASR of FNS. A 30% cement replacement was selected as this percentage is considered to give a substantial reduction in the CO₂ emission with a reasonable reduction in the strength of concrete (Nath & Sarker, 2013). The mixture proportions of the mortars are given in Table 6.1. The binder of the mixtures of Series A was 100% OPC and those of Series B and C had 30% fly ash and 30% GGBFS, respectively.

Mortar bar specimens of 25 × 25 × 285 mm were cast with gage studs inserted at the ends to measure the length change of the specimen. The specimens were cured at room temperature for 24 hours and then they were submerged in a water bath at 80 °C for one day, after which the initial measurement of the length was taken. Then, the samples were submerged in a bath of 1 mol/L NaOH solution. The first measurement of the change in length was conducted after three days of immersion using a digital length comparator with

an accuracy of 0.001 mm. The measurements were then continued at three days of intervals.

A mortar bar specimen and measurement of its length change are shown in Fig. 6.1.

Measurements were taken within 10 seconds of removing samples from the solution.

Table 6.1 Mixture proportions of mortars

Mix ID	Binder (kg/m ³)			Fine aggregate (kg/m ³)		W/C
	OPC	FA	GGBFS	Sand	FNS	
A1	602	-	-	1355	0	0.47
A2	602	-	-	1015	338	
A3	602	-	-	678	678	
A4	602	-	-	338	1015	
A5	602	-	-	0	1355	
B1	421	181	-	1355	0	
B2	421	181	-	1015	338	
B3	421	181	-	678	678	
B4	421	181	-	338	1015	
B5	421	181	-	0	1355	
C1	421	-	181	1355	0	
C2	421	-	181	1015	338	
C3	421	-	181	678	678	
C4	421	-	181	338	1015	
C5	421	-	181	0	1355	



Fig. 6.1 Length measurement of a mortar bar specimen

6.3 Results and Discussion

6.3.1 Mortar bar expansion

The changes in the expansion of the mortar bars with increasing immersion period for the mixtures of 100% OPC (Series A) are shown in Fig. 6.2. It can be seen that the expansion is relatively small in the specimen with 100% natural sand. However, expansion increased significantly with the inclusion of FNS in the mixture. The high expansion of the specimens is attributed to the presence of amorphous silica in the FNS. Petrographic examination showed that the FNS contained 44% amorphous and cryptocrystalline silica structures. Since the amorphous silica is reactive with the free alkali present in the binder matrix, the FNS showed high expansion due to the alkali-silica reaction. There was substantial increase of expansion in the specimens with 25% and 50% FNS. Expansion increased at relatively smaller rates with further increases in the percentage of FNS. Expansion of the specimens with 100% natural sand increased gradually over the period of immersion. On the other hand, expansion of the specimens with 25% to 100% FNS increased at a high rate until 14 days and then continued to increase at slower rates until 64 days. The expansions after 64 days of immersion were 0.21%, 0.55%, 0.93%, 1.06% and 1.09% for the FNS contents of 0%, 25%, 50%, 75% and 100%, respectively. Thus, it can be seen that there are only small increases in the 64-day expansions by the increase in FNS above 50% up to 100%. This trend is similar for the earlier periods of immersion.

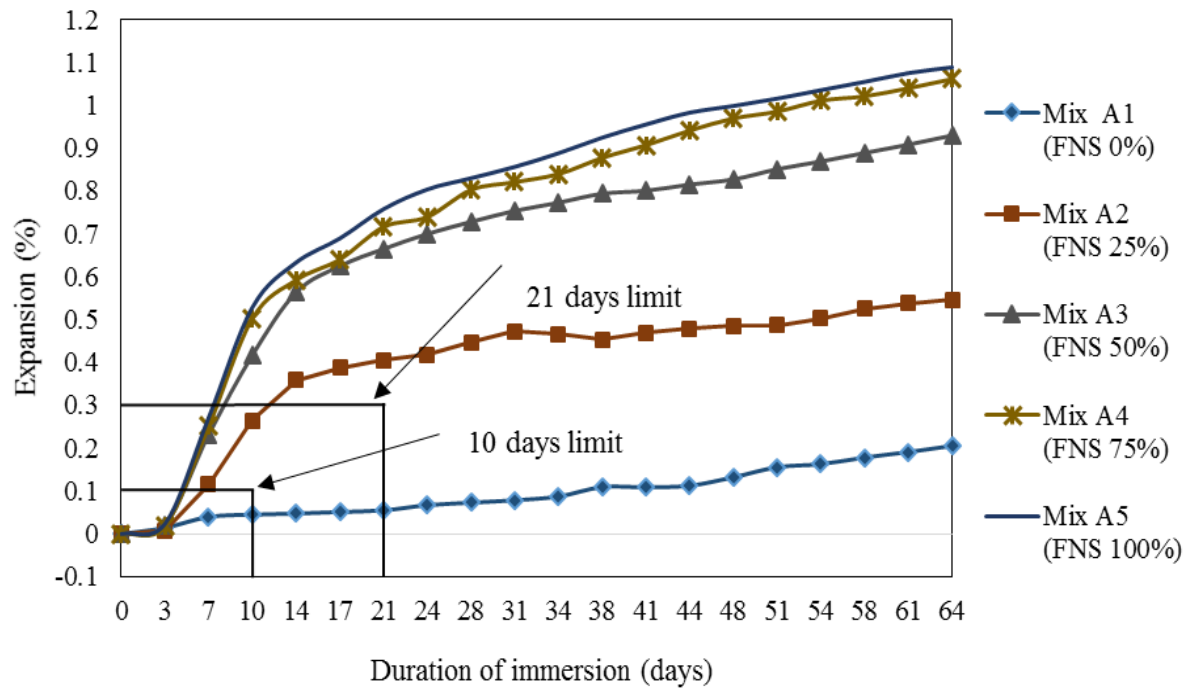


Fig. 6.2 ASR expansions of the mixtures of 100% OPC (Series A)

Table 6.2 Limits of AMBT expansion for reactivity classification as per AS1141.60.1

Mean mortar bar expansion (E), %		Aggregate reactivity classification
Duration in 1M NaOH at 80 °C		
10 days	21 days	
—	$E < 0.10$	Non-reactive
$E < 0.10$	$0.10 \leq E < 0.30$	Slowly reactive
$E \geq 0.10$	—	Reactive
—	$0.30 \leq E$	Reactive

The reactivity classification according to the Australian Standard AS 1141.60.1 is reproduced in Table 6.2 in order to compare with the AMBT results for different mixtures obtained in this study. According to this table, an aggregate should be classified as reactive if the expansion exceeds 0.30% within 21 days of immersion. Appropriate measures are required to reduce the expansion if reactive aggregates are to be used in concrete. The expansions of all the fifteen mixtures of this study after 21 days of immersion are collected

in Table 6.3. Each mixture classified as reactive (R) or non-reactive (NR) by using the limits given in Table 6.2 are shown in Table 6.3. As shown in Fig. 6.2, the 14-day expansion of the specimens containing no FNS (Mix A1) is 0.05%, which is much smaller than the 0.3% limit set by the Standard. Therefore, the natural sand is classified as non-reactive. On the other hand, the 14-day expansions of the specimens containing 25% to 100% FNS are higher than the 0.3% limit. Therefore, the FNS is classified as a reactive aggregate in accordance with AS 1141.60.1. According to the Australian Standard AS 2758.1 (2014), some ASR mitigating measure is required for this FNS if it is to be used as an aggregate for concrete. Therefore, 30% fly ash and 30% GGBFS were used as SCMs, and their effects on the expansions of the mixtures containing 25% to 100% FNS were studied.

Table 6.3 Expansion of mortar bars after 21 days in 1M NaOH solution at 80 °C

Binder Composition	Percentage of FNS as fine aggregate (%)				
	0	25	50	75	100
100% OPC (Series A)	0.06	0.40	0.66	0.72	0.76
reactive classification	NR ^a	R ^b	R	R	R
30% Fly ash + 70% OPC (Series B)	0.02	0.03	0.05	0.05	0.06
reactive classification	NR	NR	NR	NR	NR
30% GGBFS + 70% OPC (Series C)	0.04	0.34	0.63	0.69	0.72
reactive classification	NR	R	R	R	R

^a non reactive, ^b reactive

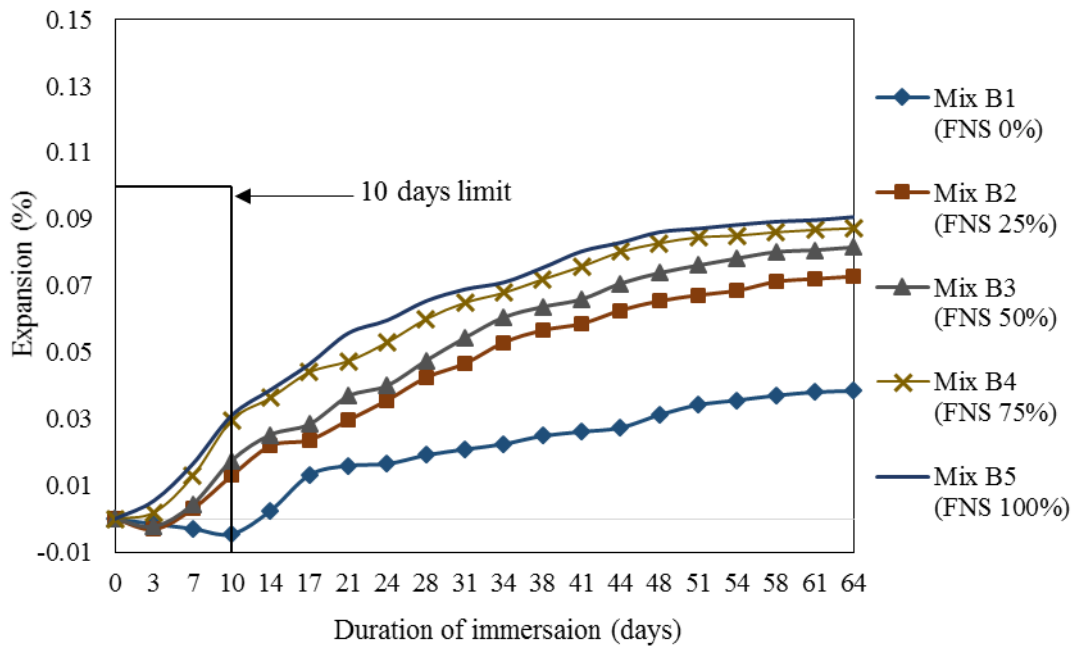


Fig. 6.3 ASR expansions of the mixtures of 70% OPC and 30% fly ash (Series B)

The expansion results of the mixtures with 30% fly ash replacing cement (Series B) are presented in Fig. 6.3. Slight initial shrinkage was observed in the specimens of 0 to 50% FNS. This is attributed to the initial autogenous shrinkage and low expansion by the use of fly ash replacing 30% cement. It can be seen that the expansions of the mixtures containing 30% fly ash are much lower than the values for the mixtures of 100% OPC. For example, the maximum 64-day expansion in this series is 0.09% for the mixture with 100% FNS. This value is much smaller than the expansion (1.09%) for the mixture with 100% FNS and 100% OPC. This shows that 30% fly ash as cement replacement has significantly reduced the expansion due to ASR in the mortar specimens containing 25% to 100% FNS. While the expansions of all the mixtures are seen to increase with increasing duration of immersion, the rates of increase are seen to be negligibly small after immersion for 64 days. As shown in Table 6.3, the expansions varied between 0.02% and 0.06% for 0% to 100% FNS. These values are much smaller than the 0.3% limit of the Australian Standard. Therefore, the replacement of cement by 30% class F fly ash can be considered as an

effective ASR mitigating measure for concrete using FNS up to 100% replacement of natural sand.

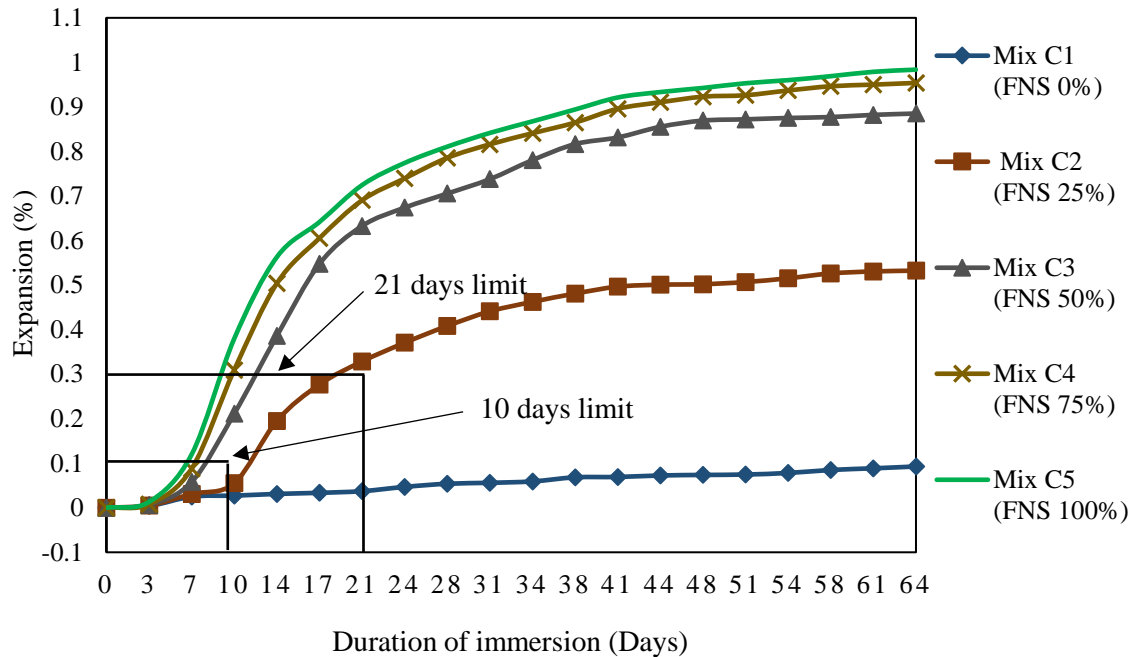


Fig. 6.4 ASR expansions of the mixtures of 70% OPC and 30% GGBFS (Series C)

The expansions of the specimens containing 30% GGBFS as cement replacement (Series C) are shown in Fig. 6.4. It can be observed that the expansions of the specimens of this series are higher than those using fly ash as cement replacement. The higher expansions of these mixtures are attributed to the higher CaO content of GGBFS (41%) as compared to that of fly ash (0.6%). The higher CaO increased the total alkali content of the binder as compared to the mixtures with fly ash. Thus, the expansions due to ASR are higher in the mixtures with GGBFS than those of the mixtures with fly ash. The specimens with FNS continued to expand for immersions beyond 21 days, and the expansion became almost stable after 64 days of immersion. The 64-day expansion varied from 0.53% to 0.98% for the FNS content varying between 25% and 100%. Similar to the mixtures of other two series, there has been very small increase in the expansion for the increase in the percentage of FNS beyond 50%.

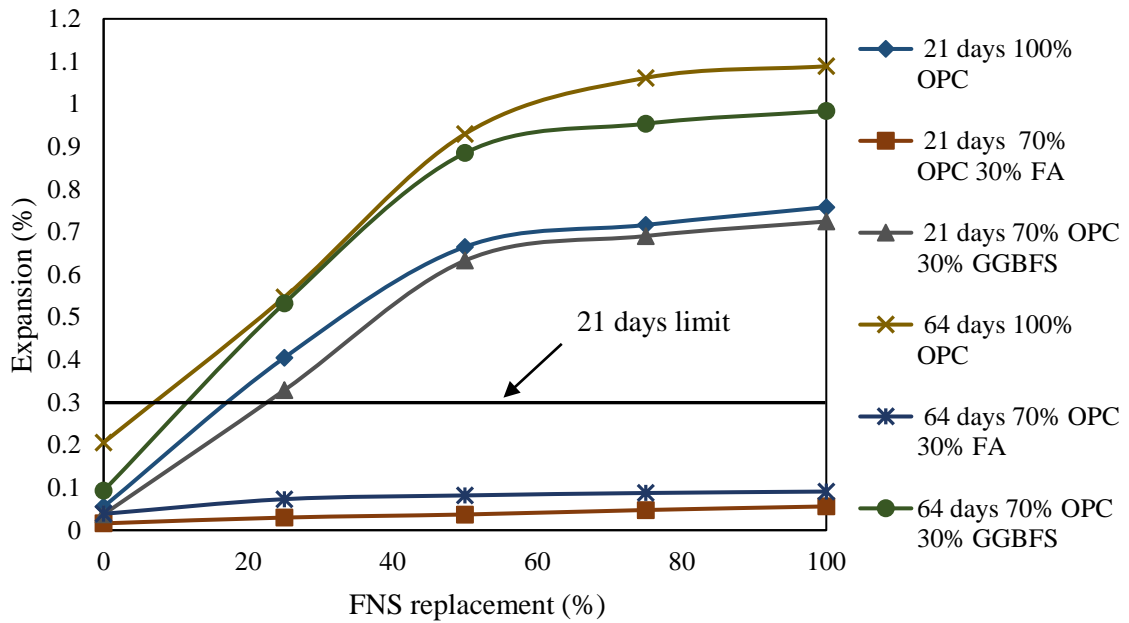


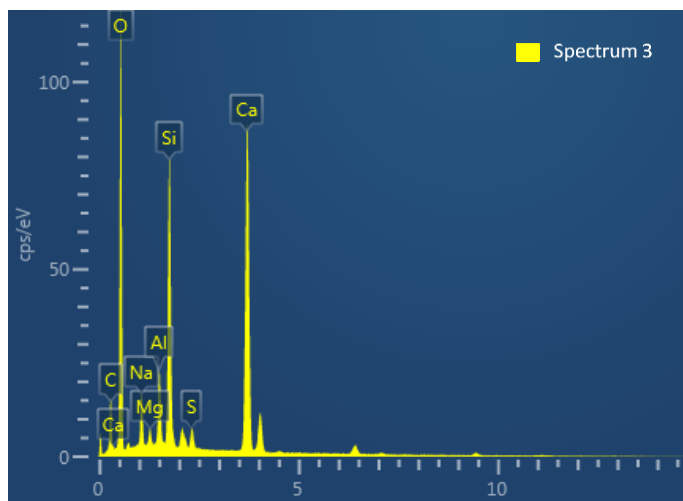
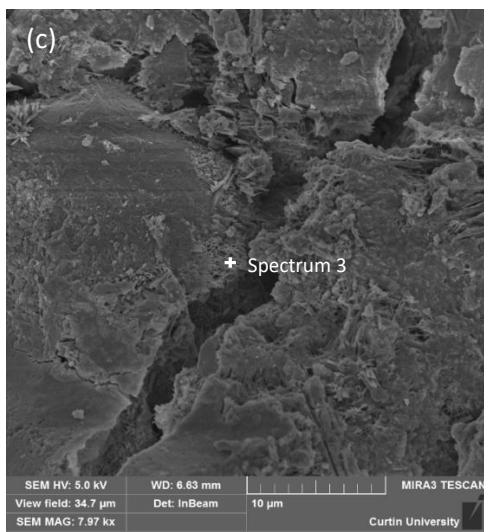
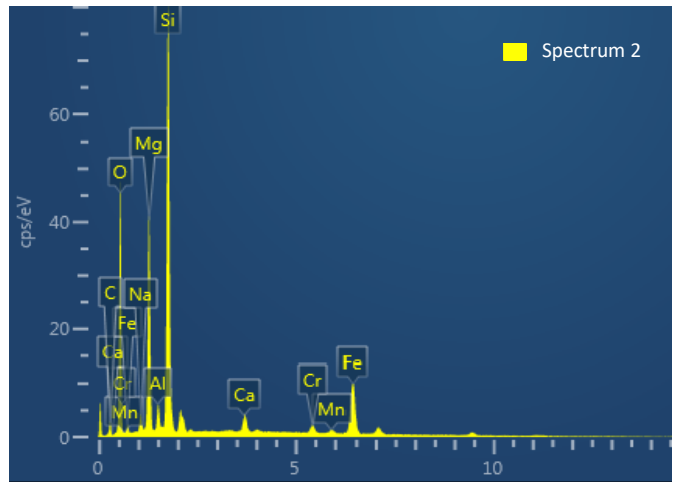
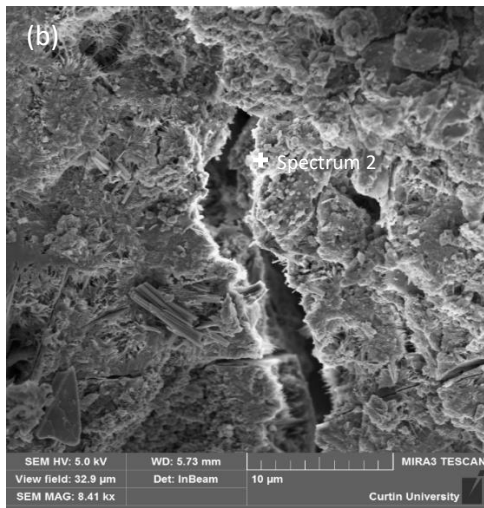
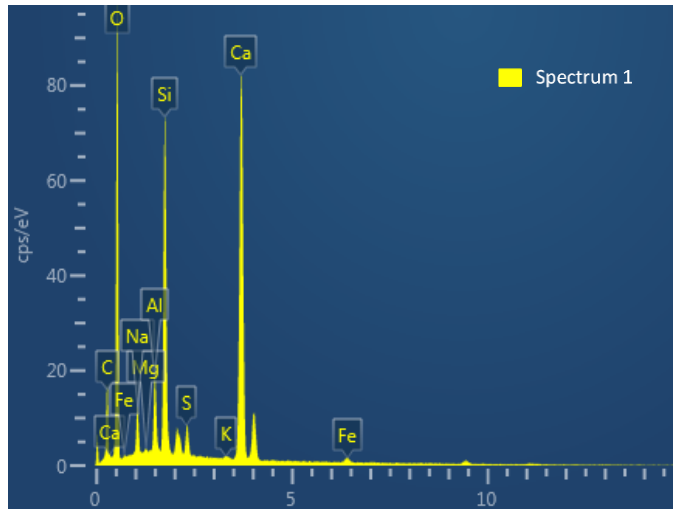
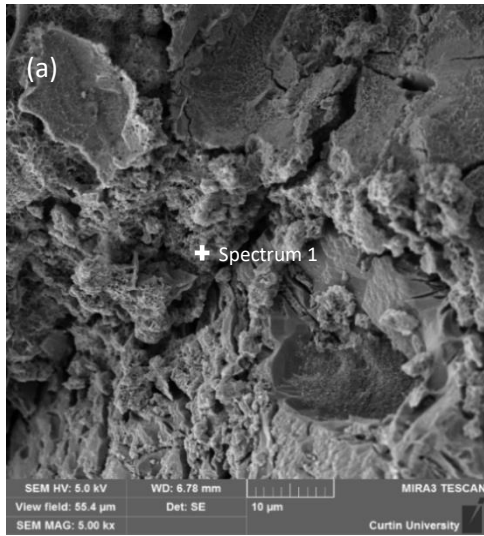
Fig. 6.5 Variation of expansion with the percentage of FNS

Expansions of the specimens after 21 and 64 days of immersion are plotted against the percentage of FNS as replacement of natural sand in Fig. 6.5. The 0.3% limit on the expansion after 21 days of immersion is also shown in this figure. It can be seen from the figure that the expansions of the specimen containing 30% fly ash are below this limit for the mixtures up to 100% FNS. Expansion of the specimen with 25% FNS and 30% GGBFS just exceeded the limit of the Australian Standard marginally and further increased with the increase of the percentage of FNS. However, the increase in expansion for the specimens of 75% and 100% FNS were very small as compared to that with 50% FNS. This trend is similar to the mixtures with 100% OPC, 30% fly ash and 30% GGBFS. The increase in the expansion for the FNS content beyond 50% is very small because there is less free alkali available for reaction with the additional FNS aggregates. Therefore, it can be concluded that 30% fly ash effectively reduced the expansion below the limit of the Australian Standard when FNS was used as a replacement of natural sand by up to 100%. However, the reduction of expansion by 30% GGBFS as cement replacement for FNS content of 25% and above was not enough to meet the limit of the Australian Standard.

From the above discussion, it is quite clear that, the effectiveness to mitigate alkali silica reaction (ASR) by supplementary cementitious materials (SCM) primarily depends on their chemical composition. It has been well established that, SCM with high silica content found to be more effective to mitigate ASR (Shehata & Thomas, 2000). In the present study ground granulated blast furnace slag (GGBFS) consist of only 32.4% silica content whereas fly ash contained 76.3% silica. Due to the low silica content, application of 30% GGBFS was unable to mitigate ASR expansion of FNS particles. Similar results were also reported by (Choi & Choi, 2015) where 30% replacement of cement by GGBFS was unable to mitigate ASR of FNS aggregate. The study also showed that a high replacement percentage of GGBFS such as 50%, to mitigate ASR. However, such high replacement percentage resulted a low early strength compared to traditional concrete. Thus, fly ash is more efficient compared to GGBFS to mitigate ASR for FNS particles.

6.3.2 Microstructural investigation by SEM and EDS

The specimens containing 100% FNS aggregates from the 3 series of mixtures were selected to study the microstructure of the reaction product by using SEM photographs and corresponding EDS data. The microstructures of the specimens containing 100% natural sand were also investigated to compare with those containing FNS aggregate. Fig. 6.6 presents the SEM images and the corresponding EDS data for the mixtures A1, A5, B1, B5, C1 and C5. Generally, foil-like crystals, rosette-like accumulation and hexagonal acicular crystals are the most frequent types of ASR products found in SEM imaging (Santon, 1942). Some of these distinct features can be observed in the SEM images of the specimens containing FNS aggregates, especially those using 100% OPC, and 30% GGBFS and 70% OPC.



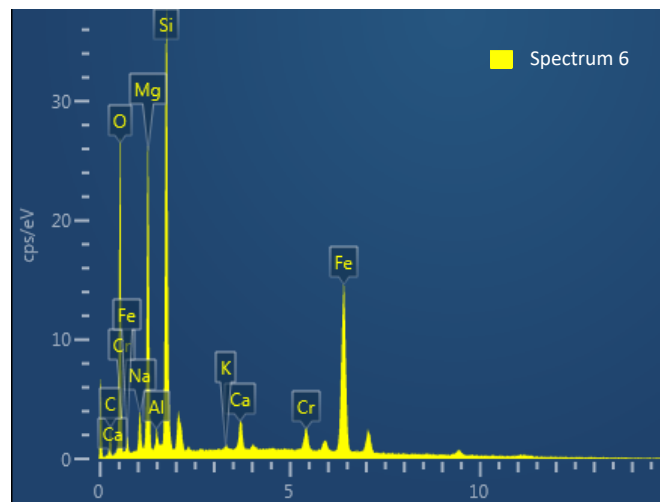
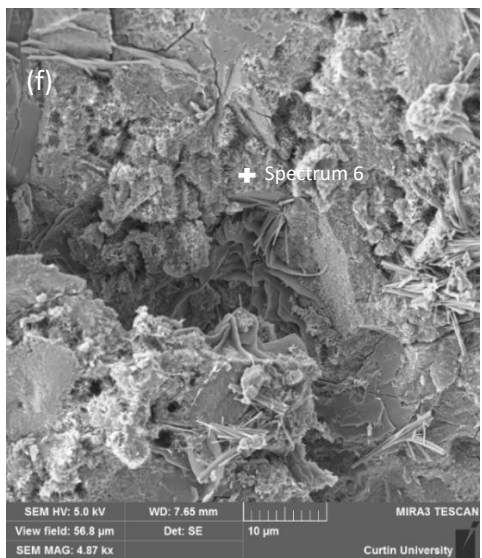
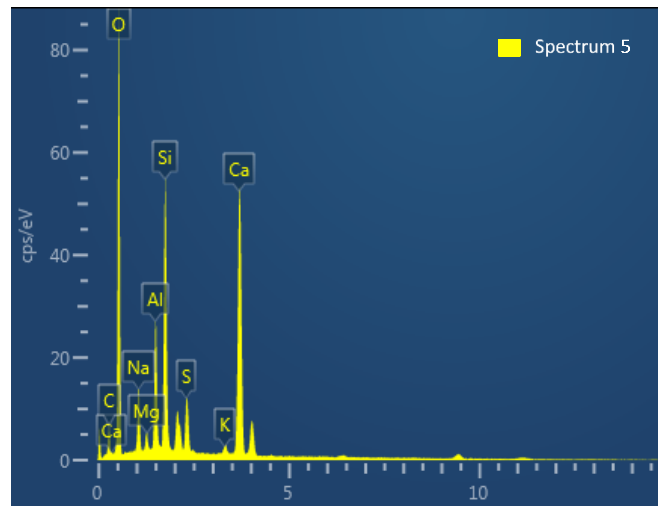
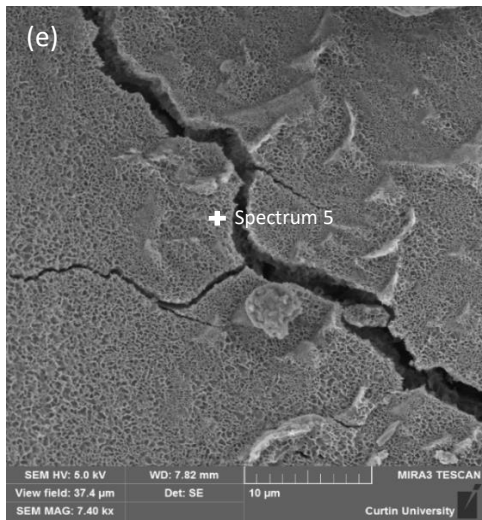
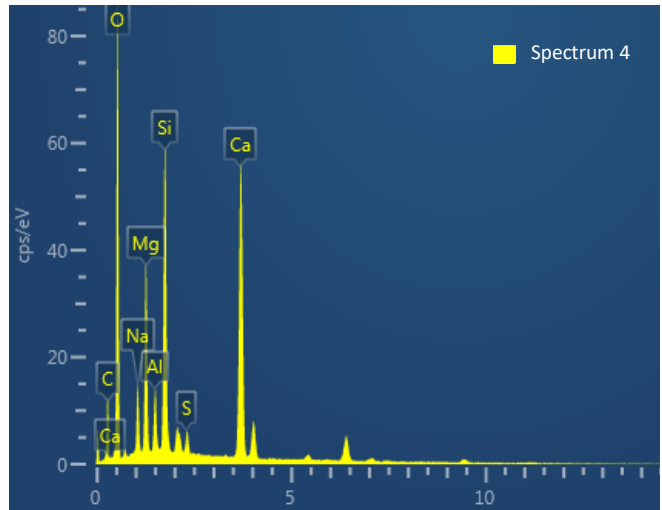
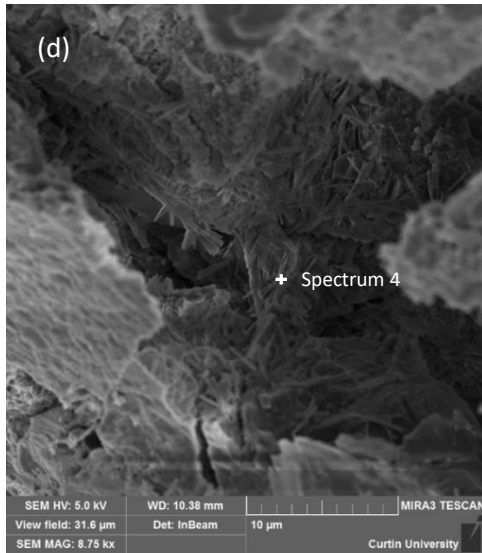


Fig. 6.6 SEM and EDS data of, (a) Mix A1; (b) Mix A5; (c) Mix B1; (d) Mix B5; (e) Mix C1 and (f) Mix C5

The SEM images of the samples containing FNS with 100% OPC (Fig. 6.6b), and 70% OPC and 30% GGBFS (Fig. 6.6f) exhibited formation of foil-like crystals and rosette-like accumulation on the aggregate surface and in the micro-cracks. The EDS data of the product in these specimens show that they have high silica content. As a result, they have low Ca/Si ratios as compared to the other specimens. The Ca/Si ratio of the specimens with 100% OPC (A5) and 30% GGBFS (C5) are 1.64 and 1.85 respectively. On the other hand, specimens of the mixtures A1, B1, B5 and C1 have Ca/Si ratios of 2.33, 2.57, 2.59 and 2.44, respectively. The lower Ca/Si ratios of specimens A5 and C5 indicate that the silica of the FNS aggregates reacted with alkaline pore solution to make the ratio lower. Since there was no FNS aggregate in the mixtures A1, B1 and C1, there was no contribution of silica from the aggregates to the reaction product. Thus, the Ca/Si ratios of these samples were high. Since the specimen B5 contained 30% fly ash as cement replacement, there was less Portlandite available for the FNS aggregate to react with. For this reason, the Ca/Si ratio was high for this specimen. Thus, ASR expansion of the specimens using 30% fly ash as supplementary cementitious material was low even though FNS was used as 100% fine aggregate in these specimens.

6.4 Summary

The reactivity of a proprietary ferronickel slag aggregate in cement mortar was studied by using the accelerated mortar bar test. The test consisted of periodic measurement of the length change of mortar specimens while immersed in 1M NaOH solution at 80 °C. Following conclusion are drawn from the study:

1. The FNS aggregate was classified as reactive according to the Australian Standard AS 1141.60.1. Uses of class F fly ash and GGBFS as supplementary cementitious materials were investigated as the ASR mitigating measure of the FNS.

2. It was found from the AMBT results that 30% fly ash reduced the 21-day expansion of mortar bars containing up to 100% FNS to below 0.3% limit set by the Australian Standard.
3. Expansions of the other specimens containing OPC alone or with 30% GGBFS in the binder and FNS content of 25% or more were above this limit. Expansions of these specimens increased significantly for continued immersion up to 64 days. Expansions of the specimens with 30% fly ash and up to 100% FNS remained below 0.3% for 64 days of immersion.
4. The SEM photographs and EDS data showed the presence of ASR products on surface of FNS aggregates in the specimens except those using 30% fly ash.
5. Thus, 30% fly ash as a supplementary cementitious material was found as an effective measure for mitigating the ASR expansion of the ferronickel slag aggregate up to 100% replacement of natural sand.

6.5 References

- AS 2758.1 (2014). Aggregates and rock for engineering purposes. Available at: www.sia-global.com (Accessed on 12 May, 2015).
- AS 1141.60.1 (2014). Method for sampling and testing aggregates, Potential alkali silica reactivity - Accelerated mortar bar method. Available at: www.sia-global.com (Accessed on 12 May, 2015).
- Bleszynski, R. F., & Thomas, M. D. (1998). Microstructural studies of alkali-silica reaction in fly ash concrete immersed in alkaline solutions. *Advanced Cement Based Materials*, 7(2), 66-78.
- Carrasquillo, R. L., & Farbiarz, J. (1989). *Alkali-aggregate reaction in concrete containing fly ash: Final report* (No. FHWA/TX-90+ 450-3F).
- Carse, A., & Dux, P. F. (1990). Development of an accelerated test on concrete prisms to determine their potential for Alkali-Silica reaction. *Cement and Concrete Research*, 20(6), 869-874.
- Chatterji, S. (1979). The role of Ca (OH) 2 in the breakdown of portland cement concrete due to alkali-silica reaction. *Cement and concrete research*, 9(2), 185-188.
- Cole, W. F., Lancucki, C. J., & Sandy, M. J. (1981). Products formed in an aged concrete. *Cement and Concrete Research*, 11(3), 443-454.
- Y.C. Choi, S. Choi, Alkali-silica reactivity of cementitious materials using ferro-nickel slag fine aggregates produced in different cooling conditions. *Construction and Building Materials*, 99, (2015) 279-287.
- Duchesne, J., & Bérubé, M. A. (1994). The effectiveness of supplementary cementing materials in suppressing expansion due to ASR: another look at the reaction mechanisms part 2: pore solution chemistry. *Cement and Concrete Research*, 24(2), 221-230.
- García-Lodeiro, I., Palomo, A., & Fernández-Jiménez, A. (2007). Alkali-aggregate reaction in activated fly ash systems. *Cement and Concrete Research*, 37(2), 175-183.
- Godart, B., de Rooij, M. R., & Wood, J. G. (2013). *Guide to Diagnosis and Appraisal of AAR Damage to Concrete in Structures*. Springer Verlag.
- Shafaatian, S. M., Akhavan, A., Maraghechi, H., & Rajabipour, F. (2013). How does fly ash mitigate alkali-silica reaction (ASR) in accelerated mortar bar test (ASTM C1567)?. *Cement and Concrete Composites*, 37, 143-153.
- Shehata, M. H., & Thomas, M. D. (2000). The effect of fly ash composition on the expansion of concrete due to alkali-silica reaction. *Cement and Concrete Research*, 30(7), 1063-1072.
- Lee, N. (2005). Alkali-Silica Reactivity in Concrete. *New Zealand: Branz Ltd*.
- Lukschová, Š., Příkryl, R., & Pertold, Z. (2009). Petrographic identification of alkali-silica reactive aggregates in concrete from 20th century bridges. *Construction and building materials*, 23(2), 734-741.
- Moisson, M., Cyr, M., Ringot, E., & Carles-Gibergues, A. (2004). Efficiency of reactive aggregate powder in controlling the expansion of concrete affected by alkali-silica

- reaction (ASR). In *12th International Conference on AAR in concrete, Beijing, China* (pp. 617-624).
- Nath, P., & Sarker, P. K. (2013). Effect of mixture proportions on the drying shrinkage and permeation properties of high strength concrete containing class F fly ash. *KSCE Journal of Civil Engineering*, 17(6), 1437-1445.
- Nixon, P. J., Page, C. L., Bollinghaus, R., & Canham, I. (1986). The effect of a PFA with a high total alkali content on pore solution composition and alkali silica reaction. *Magazine of Concrete Research*, 38(134), 30-35.
- Ponce, J. M., & Batic, O. R. (2006). Different manifestations of the alkali-silica reaction in concrete according to the reaction kinetics of the reactive aggregate. *Cement and Concrete Research*, 36(6), 1148-1156.
- Poole, A. B. (1992). Introduction to alkali-aggregate reaction in concrete. *The Alkali-Silica Reaction in Concrete, Blackie, Glasgow and London, and Van Nostrand-Reinhold, New York*, 1-29.
- Stanton, T. E. (1942). Expansion of concrete through reaction between cement and aggregate. *Transactions of The American Society of Civil Engineers*, 107(1), 54-84.
- Thomas, M., Fournier, B., Folliard, K., Ideker, J., & Shehata, M. (2006). Test methods for evaluating preventive measures for controlling expansion due to alkali-silica reaction in concrete. *Cement and Concrete Research*, 36(10), 1842-1856.

Every reasonable effort has been made to acknowledge the owners of copyright material. I would be pleased to hear from any copyright owner has been omitted or incorrectly acknowledged.

Chapter 7: RESISTANCE OF CONCRETE USING FNS AGGREGATE TO ALTERNATE WET-DRY CYCLES

The contents presented in this chapter were published in the following paper:

Saha, A. K., & Sarker, P. K. (2017). Durability characteristics of concrete using ferronickel slag fine aggregate and fly ash. Magazine of Concrete Research, 70(17), 865–874.

The present chapter evaluates the durability characteristics of concrete using FNS aggregate as full and partial replacement of sand. The durability was assessed by measuring porosity, sorptivity, permeable voids, and effect of wet-dry cycles. The test results of concrete using FNS aggregate were compared with those of control specimens. The effect of supplementary cementitious material in FNS aggregate concrete was also investigated. Finally, microstructure analyses were conducted to explain the test results.

7.1 Overview

Use of industrial by-products as supplementary cementitious material or aggregate can improve the sustainability of concrete production by conservation of natural resources and reduction of CO₂ emission. For this reason, utilisation of various by-products in concrete is receiving increased interests in the recent time. Recycled concrete aggregate, steel slag, blast furnace slag, coal bottom ash and foundry slag are some common by-products used as replacement of natural aggregates. It is important to understand the effect of a by-product material on the durability of concrete in order to use it in construction of structures.

Few studies are available in literature on durability properties such as drying shrinkage, freeze-thaw resistance, carbonation, permeability and alkali silica reaction of FNS aggregate concrete. Sato et al. (2011) reported reduced freeze-thaw resistance of concrete due to bleeding caused by FNS aggregates. Similarly, Togawa et al. (1996) reported reduced durability factor in freezing and thawing cycles with the use of air or water cooled FNS aggregates. The authors suggested that the use of supplementary cementing materials such as blast furnace slag, silica fume and limestone powder could improve the freeze-thaw resistance of concrete. Sakoi et al. (2013) reported that freeze-thaw resistance of FNS aggregate concrete was identical to that of natural aggregate concrete. Tomosawa et al. (1997) pointed out the potential ASR expansion of FNS aggregate. However, they demonstrated that the use of low-alkali cement and supplementary cementing material such as fly ash and blast furnace slag could reduce the ASR expansion. Apparently, not every type of FNS aggregate is alkali-silica reactive. Rapid cooling of the slag may contain amorphous silica that may cause the ASR expansion. On the other hand, slowly cooled FNS contains crystalline silica which is more stable and does not exhibit expansion due to ASR (Choi and Choi, 2015). On the other hand, FNS aggregates did not show any notable impact on drying shrinkage, carbonation and permeability properties of concrete (Sakoi et al, 2013; Shoya et al, 1999).

It was found that some important durability-related properties such as porosity, sorptivity, chloride permeability and resistance to wet-dry cycles of FNS aggregate concrete were not studied in the past. The resistance against wet-dry cycles is an important aspect for durability of concrete. Previous studies showed that electric arc furnace (EAF) slag concrete exhibited a strength loss of about 30% due to the exposure to alternate wet-dry cycles (Manso et al, 2006; Pellegrino and Gaddo, 2009). Other studies (Andrade et al, 2009; Yüksel et al, 2007; Kadam and Patil, 2015) showed that concrete containing

manufactured aggregates such as coal bottom ash (CBA) and blast furnace slag (BFS) exhibited higher sorptivity as compared to the natural aggregate concrete. However, use of fly ash as a supplementary cementing material was shown to reduce the sorptivity of concrete by pozzolanic reaction (Soutsos et al, 2017; Dragaš et al, 2016). Chloride permeability of concrete was also affected by the use of manufactured aggregate. The use of high volume CBA was shown to increase chloride permeability of concrete (Kou and Poon, 2009; Ghafoori and Bucholc, 1996). Supplementary cementing material such as fly ash also showed improvement of chloride permeability of concrete (Silva et al, 2017). These studies show that it is important to evaluate the durability characteristics of concrete when an industrial by-product is considered for use as a replacement of natural aggregate. Therefore, this chapter focused on the durability-related properties of FNS aggregate concrete.

This chapter presents the volume of permeable voids, sorptivity, chloride permeability and the resistance against wet-dry cycles of concrete containing FNS aggregate with or without fly ash as a partial cement replacement. Investigations of porosity and microstructures were conducted by scanning electron microscopy (SEM) and energy-dispersive X-ray spectroscopy (EDS) in order to gain insight into the effects of FNS and fly ash on the properties of concrete.

7.2 Experimental Work

7.2.1 Materials

Commercially available Portland cement (PC) was used as the primary binder and class F fly ash was used as a supplementary cementing material. Natural silica sand and FNS were used as fine aggregates and crushed granite with a maximum size of 20 mm was used as coarse aggregate. The flow test was conducted for the sand, ferronickel slag and their

combination using a sand flow cone. The results are given in Table 7.1. It can be seen that the flow time for 100% natural sand was 17.20 sec, which increased to 26.20 sec by the inclusion of 50% FNS in the fine aggregate. On the other hand, 100% FNS fine aggregate did not flow at all. The angular shape, larger size and rough surface of the FNS particles as compared to smaller, round and smooth sand particles reduced flow time of the fine aggregate and eventually to no flow for 100% FNS.

Table 7.1 Flow time of the fine aggregates

Sample specification	Time to flow (seconds)
100% sand	17.2
50% FNS and 50% sand	26.2
100% FNS	Did not flow

7.2.2 Mixture proportions and test methods

The concrete mix design was conducted by the absolute volume method and the mixture proportions are shown in Table 7.2. FNS fine aggregate was used as 50% and 100% volume replacement of natural sand. FNS of 50% in the concrete mixture was selected since this proportion resulted in maximum compressive strength with good flow ability of the mortar mixture. Water to binder ratio was kept constant at 0.33 for all the mixtures. The aggregates were prepared to saturated surface dry condition before mixing of the concrete. A naphthalene based superplasticizer was used to improve the workability of the mixtures. For one group of mixes, 100% PC was used as the binder and for the other group, 30% fly ash was used as a cement replacement. Fly ash was adopted as a supplementary cementing material due to its favorable ASR mitigation mechanism. The mixes are designated by PC-FNS and FA-FNS for without fly ash and with 30% fly ash, respectively. The number at the end of mix ID represents the percentage of sand replacement by FNS. Standard slump

test was carried out in order to determine the workability of the fresh concrete mixtures. The concrete was then placed into 100 mm × 200 mm cylindrical moulds and compacted using a vibrating table. The test specimens were demoulded at 24 hours after casting and then cured in limewater at 23 °C for 28 days. The mean values of the reported results were obtained from the test results of three identical specimens.

Table 7.2 Concrete mix proportions

Mix ID	Binder (kg/m ³)		Fine aggregate (kg/m ³)		Water (kg/m ³)	Coarse aggregate (kg/m ³)	Superplasticizer (kg/m ³)
	Cement	Fly ash	Sand	FNS			
PC-FNS0	390	0	710	0	129	1194	4
PC-FNS50	390	0	355	435	129	1194	4
PC-FNS100	390	0	0	870	129	1194	4
FA-FNS0	273	117	710	0	129	1194	4
FA-FNS50	273	117	355	435	129	1194	4
FA-FNS100	273	117	0	870	129	1194	4

Cylinder compressive strengths were determined in accordance with the Australian Standard, AS 1012.9 (2014). The porosity of concrete specimens was determined by the volume of permeable voids (VPV) test in accordance with the ASTM C642 (2006) Standard. The test measures the porosity of concrete by absorption of water. Fifty mm thick discs were cut from the concrete cylinders after curing for 28 days. The mass of the test sample was recorded after oven drying at 110 °C for a period of 24 hours. The saturated surface dry weight was then recorded after immersion of the sample in water for 48 hours. Finally, the samples were boiled in water for five hours and weighed after cooling down to room temperature. The volume of the permeable voids was calculated from this recorded weight.

Sorptivity test was conducted to evaluate the capillary suction of concrete as per ASTM C1585 (2013). After the 28 days of the curing period, the concrete cylinders were cut into 50 mm thick discs. The samples were oven dried to achieve a constant weight before beginning the sorption by keeping only the bottom surface in contact with water. The sides of the specimen were sealed by duct tape and the top surface by a plastic sheet. As a result, water movement was allowed only from the bottom surface. The mass increments were measured for a period of 9 days with the designated time intervals suggested in the standard. The sorptivity coefficient was measured from the slope of the plot of absorption against the square root of time.

The rapid chloride permeability test (RCPT) was conducted in accordance with the ASTM C1202 (2012). Though RCPT may give high variability of results and may not be considered as a direct measure of durability, it is used as an indication of chloride ingress in concrete. Concrete cylinders were cut to 50 mm thick discs after 28 days of curing and kept in a vacuum desiccator for 3 hours at a pressure of 50 mm Hg following by 18 hours of immersion in water. The saturated samples were then subjected to a direct current of 60V for a duration of 6 hours keeping one side of the specimen in contact with 3% NaCl solution and the other side in contact with 0.3 M NaOH solution. During the test period, the total charge passing through the specimens in coulombs was recorded.

In order to evaluate the resistance of concrete to wet-dry cycles, the samples were exposed to cycles of alternate immersion in water and drying at 110 °C temperature. This exposure condition was considered in order to evaluate the effects of adverse environmental conditions on concrete over the age. The wet-dry cycles exposure started after initial curing of the samples for 28 days. The samples were kept in an oven at 110 °C for 8 hours, after which they were immersed in water at 23 °C for 15 hours to complete one cycle of drying and wetting. After 28 cycles of alternate wetting and drying, the changes in compressive

strength and mass of the specimens were measured. In order to understand the effect of wet-dry cycles, microstructural observations were conducted by using scanning electron microscopy (SEM) and energy-dispersive X-ray spectroscopy (EDS).

7.3 Results and Discussion

7.3.1 Volume of permeable voids

The volume of permeable voids (VPV) (Vicroads, 2007) test is used to determine the total porosity of concrete that is consisted of capillary pores, gel pores, air voids and microcracks. Thus, the VPV indicates the ease of penetration of fluids in to concrete from the surroundings. The changes of VPV of concrete with the percentage of FNS content are plotted in Fig. 7.1.

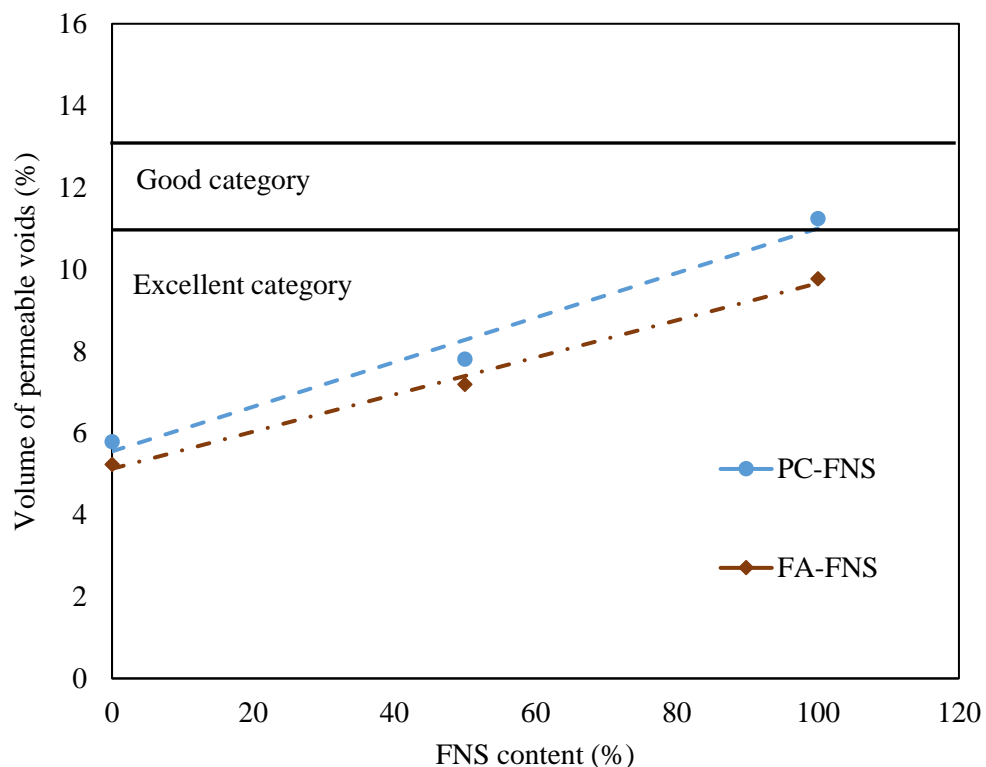


Fig. 7.1 Variation of the volume of permeable voids with FNS content in concrete

It can be seen that the porosity of the samples gradually increased with the increase of FNS aggregate for both the binder groups, with and without fly ash. The VPV values of

the concrete specimens without fly ash in the binder were 5.79%, 7.80% and 11.23% for 0%, 50% and 100% FNS content, respectively. The increase of porosity is attributed to the increase of voids in concrete due to the larger size and angular shape of the FNS particles. The durability classifications according to the VPV value of concrete by VicRoads (2007) are also shown in Fig. 7.1. As shown in the figure, concretes with a VPV value below 11% is classified as “excellent” and those between 11% and 13% are classified as “good”. Thus, the mixtures containing 0% and 50% FNS are classified as “excellent” while the mixture containing 100% FNS is marginally classified as “good” concrete in terms of the VPV. It can be seen from Fig. 7.1 that the VPV of concrete generally decreased by the use of fly ash as a cement replacement for both types of aggregate. The trend of the change of VPV with the increase of FNS aggregate was similar for the concretes with or without fly ash. The VPV values were 5.23%, 7.18% and 9.76% for 0%, 50% and 100% FNS content, respectively, in the concrete containing 30% fly ash as cement replacement. The reduction of porosity by the inclusion of fly ash is attributed due to its higher fineness than cement and its pozzolanic reaction. The reduction of permeability by the addition of fly ash has been well documented in previous studies (Bijen, 1996; Shehata et al, 1999). As shown in Fig. 7.1, the concrete specimens containing 30% fly ash and up to 100% FNS are classified as “excellent” according to the VPV values.

7.3.2 Sorptivity coefficient

The sorptivity coefficients of the samples of both binder groups are plotted in Fig. 7.2. The sorptivity coefficients of the concrete specimens without fly ash were 0.085 mm/min^{1/2}, 0.153 mm/min^{1/2} and 0.219 mm/min^{1/2} for 0%, 50% and 100% FNS, respectively. It is noticeable that the sorptivity value of concrete with 100% FNS aggregate exceeded the allowable limit of 0.21 mm/min^{1/2} suggested by the Cement Concrete & Aggregates Australia (CCAA, 2009). The higher sorptivity coefficient was due to the higher internal

voids associated with the addition of FNS aggregates. The larger size and higher angularity of the FNS particles increased the internal voids that eventually increased the absorption of concrete.

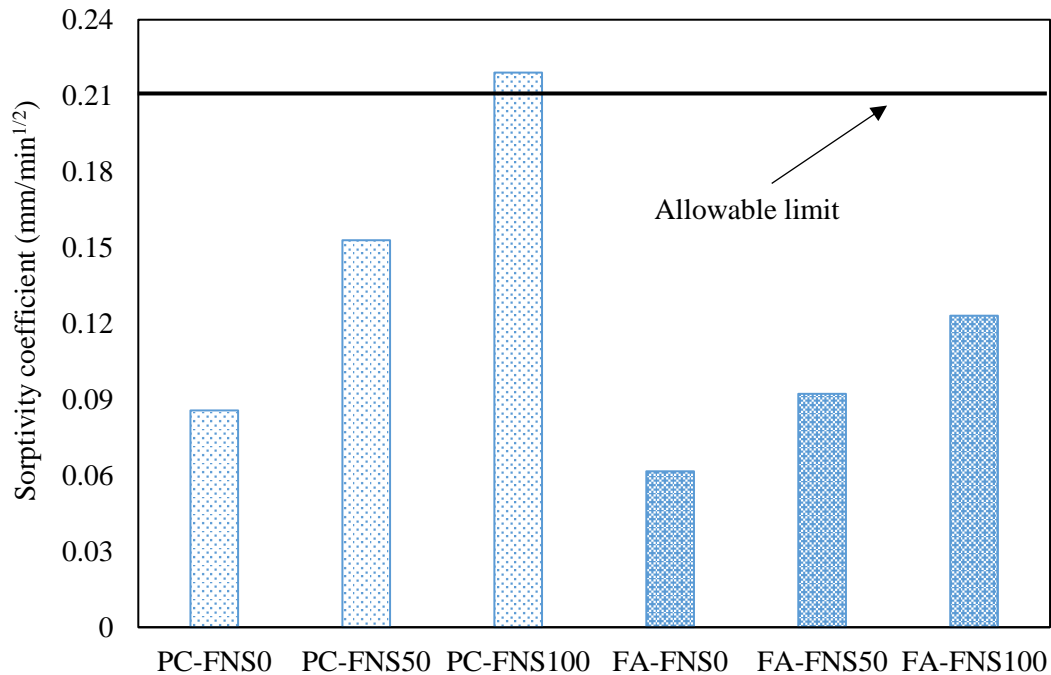


Fig. 7.2 Variation of sorptivity with FNS content

The sorptivity coefficients of the specimens using 30% fly ash were 0.061 mm/min^{1/2}, 0.092 mm/min^{1/2} and 0.123 mm/min^{1/2} for 0%, 50% and 100% FNS, respectively. Thus, sorptivity was significantly reduced by the use of fly ash. The sorptivity values of the specimens of this group are well below the allowable limit of 0.21 mm/min^{1/2} suggested by the Cement Concrete & Aggregates Australia. There are two primary reasons contributing to the reduction of sorptivity of the fly ash concrete. First, fly ash contains a high volume of amorphous silica (Saha and Sarker, 2016) which reduced the capillary pores by the products of pozzolanic reaction with portlandite. Secondly, fly ash particles are generally finer than cement particles (Kuroda et al, 2000) that reduced the interconnecting voids by acting as nucleation sites and the pore filling effect.

7.3.3 Chloride permeability

Chloride permeability of the concrete samples was determined by rapid chloride permeability test (RCPT). The test is based on the principle that the total charge passing through a concrete sample is an indicator of the chloride ion penetration. This test is relatively quick and gives reliable data to compare the chloride permeability values for different specimens. The total charge passed through the concrete samples of two binder groups are presented in Fig. 7.3.

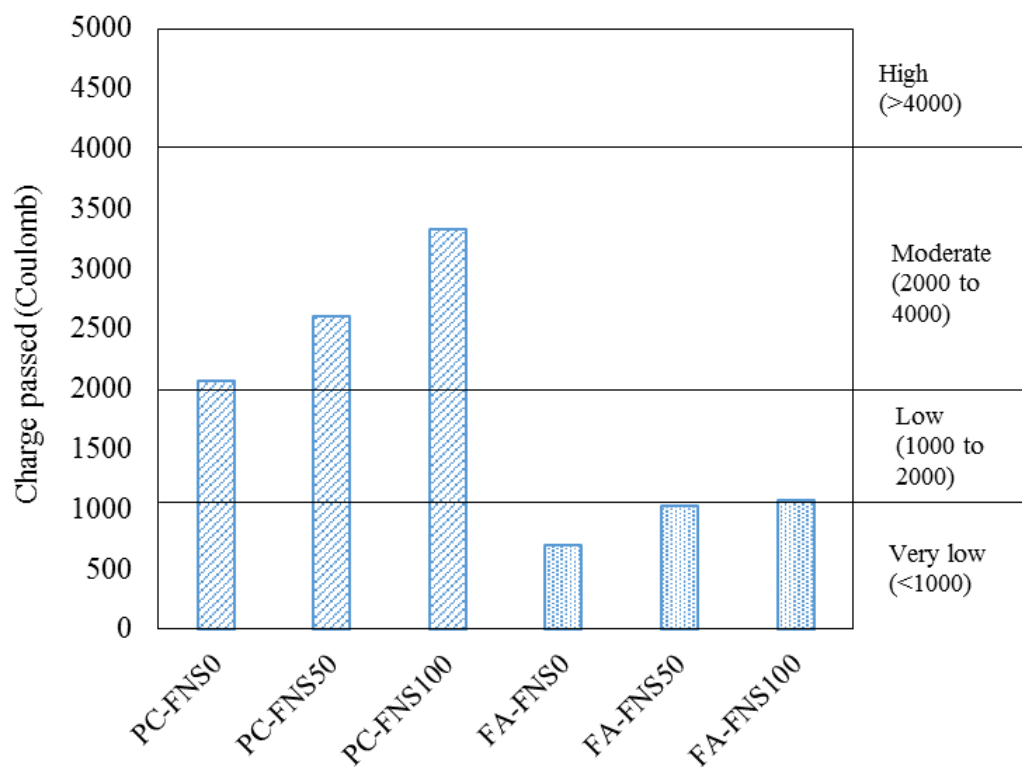


Fig. 7.3 Charged passed during rapid chloride permeability test

The ASTM C 1202 (ASTM, 2012) classifications of concrete from “very low” to “high” values of charge passed are also shown in this figure. It can be seen that the charge passed through the samples with no fly ash (PC-FNS) was within a range of 2066 to 3335 coulombs. The value of charge increased gradually with the increase of the percentage of FNS aggregate. Chloride permeability of the specimens of series PC-FNS has been

classified as “moderate level” by the ASTM C1202 (ASTM, 2012) Standard. FNS aggregates increased the permeable voids in concrete as discussed in previous two sections which is the primary reason for increase of chloride permeability with the increase of FNS aggregates.

On the other hand, the concrete specimens with 30% fly ash in the binder exhibited lower chloride penetration for all the three fine aggregates. The charge passed through the samples were 698 coulombs, 1030 coulombs and 1074 coulombs for 0%, 50% and 100% FNS, respectively. Thus, the specimens are classified as “very low” chloride permeability for 100% natural sand and “low” for using 50% and 100% FNS aggregate. It was shown that fly ash reduced the pore size (Kuroda et al, 2000) by reducing the thickness of the interfacial transition zone between the binder matrix and aggregates. Furthermore, fly ash also reduces the hydroxyl ion (Shehata et al, 1999) in the pore solution of concrete thus reducing the charge passed through the concrete. Over all, while the use of FNS aggregate increased the pore volume, fly ash helped reducing the porosity and the alkalinity of the pore solution to reduce the chloride permeability of concrete.

Additionally, the compressive strength results for concrete with 50% FNS aggregate exhibit a contradictory findings in chloride permeability and capillary absorption. The compressive strength increment of concrete due to the addition of FNS aggregates were primarily due to two reasons. First, the high density of FNS aggregates. Second, high lateral friction and interlocking properties of FNS particles due to surface roughness and aggregate angularity. However, angularity and inconsistent shape of FNS particles created higher internal pores in concrete compared to traditional concrete with only sand aggregate which is primarily rounded and resulted low interconnecting voids. As a result, samples with 50% FNS aggregates exhibited higher strength compared to

traditional concrete even though exhibited marginally higher volume of the permeable voids, chloride permeability and capillary absorption.

7.3.4 Effect of wet-dry cycles

7.3.4.1 Strength and mass variations due to wet-dry cycles

The concrete samples were exposed to alternate wetting and drying for 28 cycles and each cycle consisted of 8 hours of oven drying at 110 °C following by 15 hours of immersion in water at room temperature. The samples were visually observed before and after the wet-dry exposures. The specimens of mixture PC-FNS100 are shown in Fig. 7.4 as the typical appearance of the specimens after the wet-dry cycles. No visible crack or damage was observed in the specimens after 28 cycles of the wet-dry conditions. However, there was a thin layer of whitish substance over the surface of the samples. This surface deposition is attributed to slow migration of the hydrated product from inside the concrete by the alternate wetting and drying conditions.



Fig. 7.4 Physical appearance of PC-FNS100 samples after wet dry cycles

The compressive strengths of the specimens after the cycles of wet-dry exposures are presented in Fig. 7.5. The figure also shows the compressive strength of corresponding mixtures at 58 days of age without exposure to wet-dry cycles. The strength reduction of the specimens is considered due to the minor internal damages in microstructural level by the alternate expansions and contractions because of the alternate changes of temperature

between 110 °C and 23 °C. Besides, the moisture movement and drying shrinkage due to the variation of humidity condition are also considered to play a role in the strength reduction of concrete.

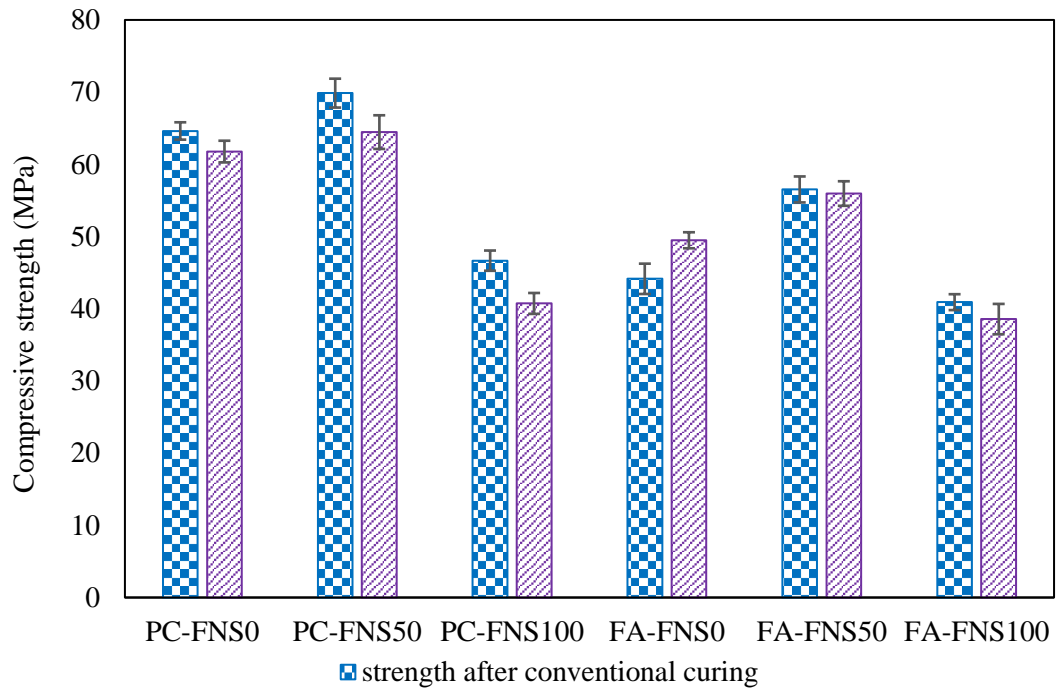


Fig. 7.5 Compressive strengths comparison due to wet-dry cycles exposure

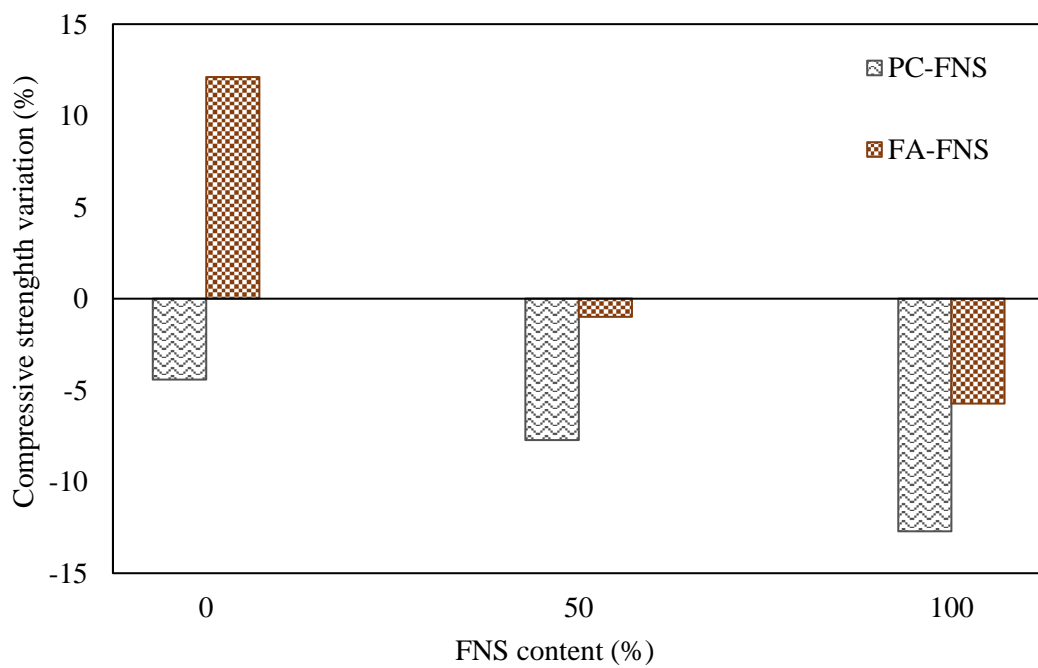


Fig. 7.6 Percentage of strength change by the wet-dry cycles

The percentages of changes in compressive strength after the wet-dry cycles are presented in Fig. 7.6. It is noticeable that, the specimens without fly ash (PC-FNS0) exhibited a strength loss of 4.42 % after the exposures to wet-dry cycles. The strength loss gradually increased for the PC-FNS specimens with the increment of FNS content in concrete. The strength loss was 7.73% and 12.71% for 50% and 100% FNS content, respectively. Manso et al. (2006) and Pellegrino and Gaddo (2009) used similar wet-dry conditions for concrete using steel slag aggregates and reported a strength loss of about 30%. Therefore, FNS aggregate used in this study showed comparatively less strength loss than the steel slag aggregate concrete. The use of FNS aggregates increased permeability and absorption of concrete. Thus, it is possible to have higher water penetration during the wetting cycles that may result in an increased vapour pressure in the specimens containing FNS aggregate during the drying cycle. Therefore, there are three primary reasons for the strength reduction of concrete caused by the internal damages due to wet-dry cycles. Firstly, the simultaneous wetting and drying at elevated temperature caused sudden thermal expansion and contraction. Secondly, water vapour pressure during the drying cycle; and thirdly, the leaching out of some hydrated product. The combined effect of these aspects is considered to cause strength losses of the specimens.

As shown in Fig. 7.5, the concrete specimens with 30% fly ash as cement replacement showed relatively less strength loss after the wet-dry cycles. The compressive strength of samples containing 100% natural sand and 30% fly ash was increased by 12% after the wet-dry cycles. There were 1% and 6% strength losses in the samples with 50% and 100% FNS aggregate respectively. The increment of compressive strength is attributed to the pozzolanic reaction of fly ash. The alternate wetting and drying cycles at elevated temperature accelerated the pozzolanic reaction of fly ash, which caused the less strength loss for the concrete containing FNS aggregate. Furthermore, the effect of water vapour

depends on the porosity and water absorption of the samples. The inclusion of fly ash increase the density of paste matrix and reduce the concrete porosity and absorption, which has been discussed in earlier sections. As a result, compressive strength of the samples with 30% fly ash and 50% FNS aggregate suffered only marginal strength loss (1%), whereas samples with 100% PC as the binder and 50% FNS aggregate suffered a strength loss about 8%.

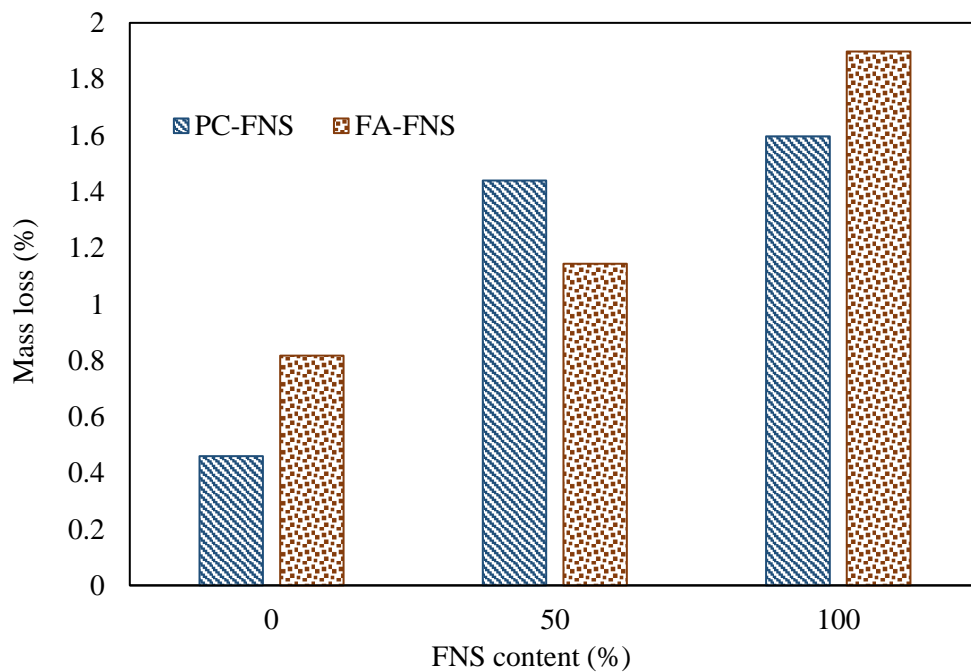
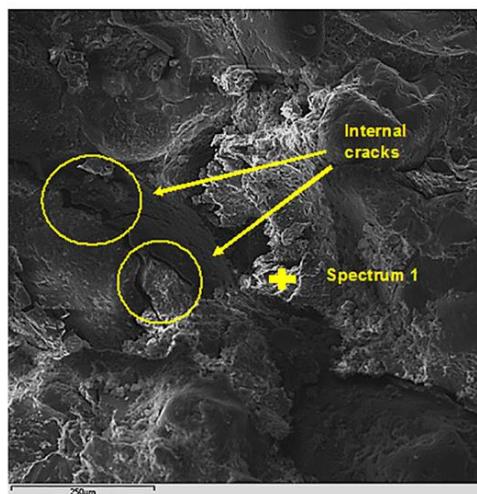


Fig. 7.7 Mass loss due to wet dry cycle exposure

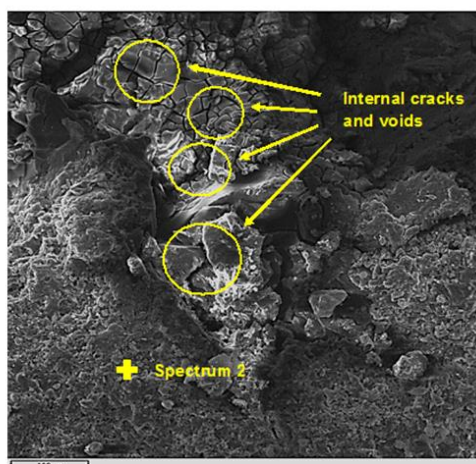
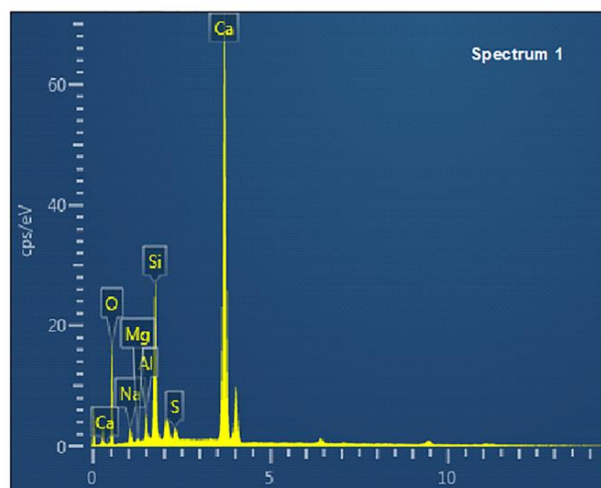
The mass losses of the concrete specimens due to wet-dry cycles are presented in Fig. 7.7. It can be seen that weight loss increased with the increase of FNS content for both the binder types. The weight loss was within a range of 0.45% to 1.89%. The weight loss was almost doubled for a particular binder group due to the inclusion of 100% FNS aggregate as compared to that with 100% natural sand. The trend of the mass loss is similar to the strength loss for both the binder groups. The reasons for mass changes by the wet-dry cycles are considered to be the same as those for the strength changes, as discussed above.

7.3.4.2 Microstructural observation after wet–dry cycles

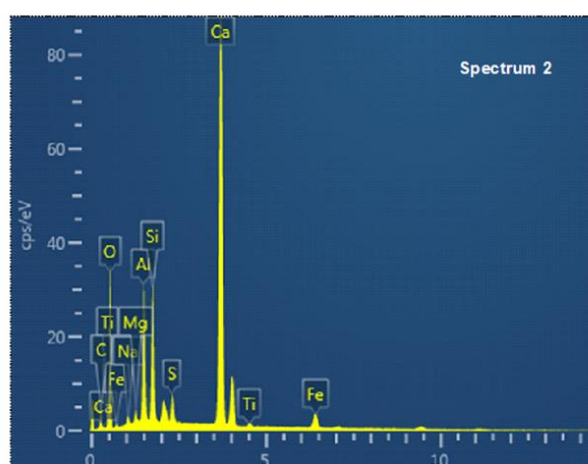
The SEM images and EDS of the concrete microstructures after the wet-dry cycles are used to understand of the effects of FNS and fly ash. The SEM image of the specimen containing 100% natural sand and no fly ash (PC-FNS0) is presented in Fig. 7.8 (a). It can be seen that there were development of internal cracks due to the aggressive wet dry cycle exposures. The EDS of the reaction product is presented in spectrum 1. It can be seen that the hydrated product had a high intensity of Ca and low intensity of Si. This is because the binder did not undergo any pozzolanic reaction since there was no fly ash in this specimen.



(a) PC-FNS0



(b) PC-FNS100



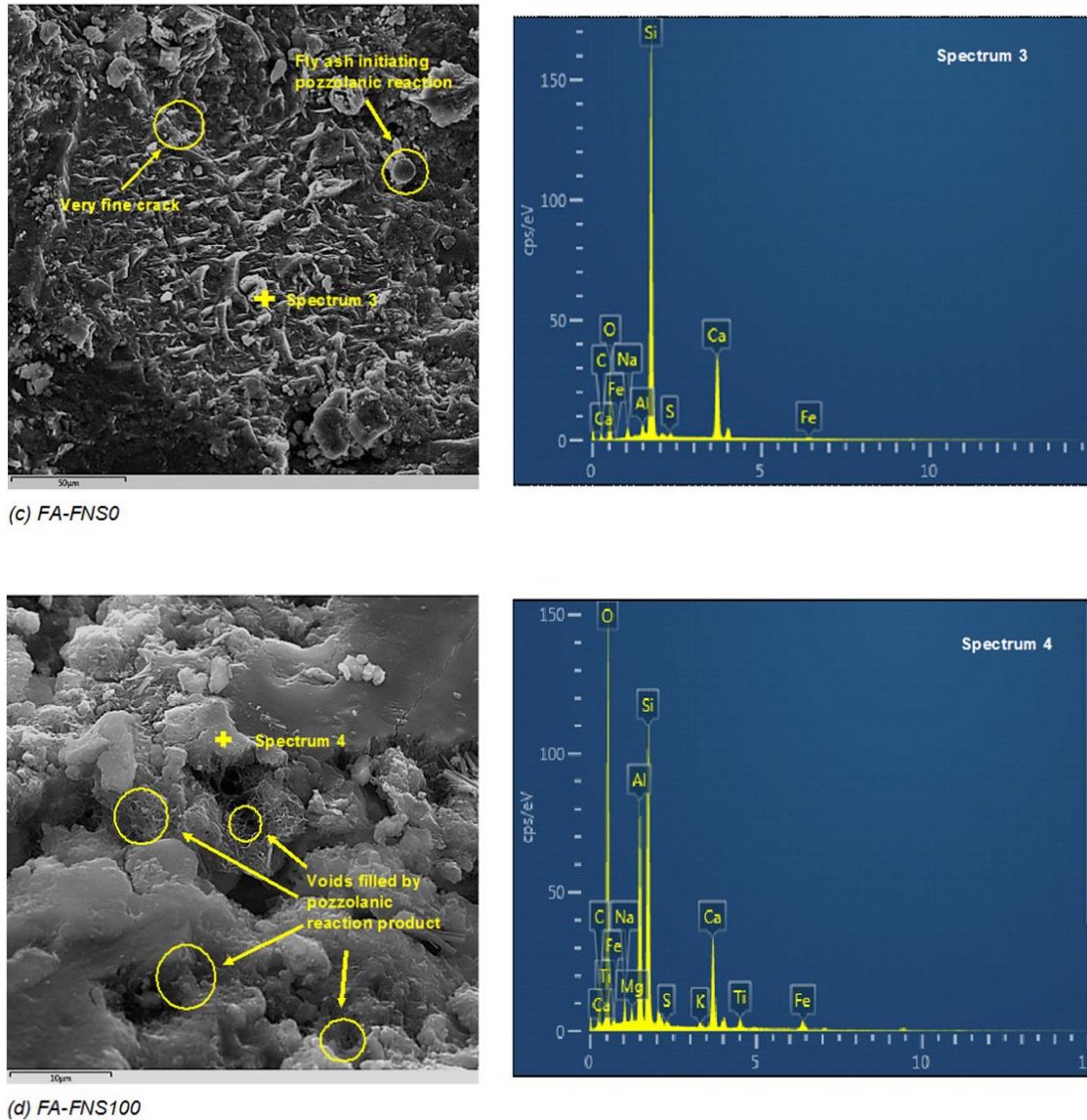


Fig. 7.8 SEM and EDS data of the samples after wet-dry cycles

The SEM image of the specimen with 100% PC as the binder and 100% FNS aggregate (PC-FNS100) is presented in Fig. 7.8 (b). The presence of cracks can be seen at the interface of aggregate and binder in this microstructure. The corresponding EDS (spectrum 2) shows a Ca-rich phase that is similar to the EDS (spectrum 1) of specimen PC-FNS0. The SEM image of the specimen with 30% fly ash and no FNS is presented in Fig. 7.8 (c). It can be seen that the hydrated product consisted of a dense structure, some fly ash particles underwent the pozzolanic reaction and some others were initiating the

process. Additionally, a fine line of crack can be seen in the image, which is significantly thinner as compared to those observed in the SEM image of specimen PC-FNS0. The EDS data in spectrum 3 confirms the pozzolanic reaction of fly ash showing a product of higher intensity of silica and low intensity of calcium. Thus, the wet-dry cycles accelerated pozzolanic reaction of the amorphous silica of fly ash producing a silica-rich hydrated product, commonly known as calcium-silica-hydrate gel. Fig. 7.8 (d) presents the microstructure of the specimen with 30% fly ash and 100% FNS aggregate. Contribution of the pozzolanic reaction product of fly ash to fill up the pores can be seen in this image. This contributed to increase the density of the binder matrix and improve the bond between the aggregate and binder. Thus, the use of fly ash helped reduce the strength loss of FNS aggregate concrete after the wet dry cycles, as shown in Fig. 7.6.

7.4 Summary

By-product FNS was used as fine aggregate to replace 50% and 100% natural sand, and a class F fly ash was used as 30% replacement of cement in concrete. Durability characteristics of the concrete specimens were studied by evaluating the volume of permeable voids (VPV), sorptivity, chloride permeability and resistance to wet-dry cycles exposure. Following conclusions are drawn from this experimental investigation:

1. Generally, VPV was found to increase with the increase of FNS aggregates replacing natural sand. Chloride permeability and capillary absorption of concrete were also found to increase with the increase of sand replacement by FNS aggregate. These increases are attributed to the increase of porosity by the relatively large size and angular shape of the FNS particles. FNS particles are angular in shape even though they create a better bond with the binder matrix, which caused the strength improvement of 50% FNS concrete but the presence of internal voids in

the aggregates as well as high angularity of the FNS particles creates internal voids, which was also reflected in the air content test results.

2. The increase of FNS content also showed higher strength and mass losses due to the exposure to alternate wet-dry cycles. However, the pozzolanic reaction of fly ash reduced the permeable voids, as evidenced by the SEM images and EDS data. Thus, the chloride permeability and capillary water absorption were also reduced by fly ash.
3. The concrete samples with fly ash also suffered from lower strength reduction after the wet-dry cycles as compared to the samples without fly ash. Compressive strength of the samples with 50% FNS and 30% fly ash remained almost unchanged after exposure to the wet-dry cycles.
4. The sorptivity coefficient of this mix was well below the recommended value of $0.21 \text{ mm/min}^{1/2}$ and the rapid chloride permeability was classified as low. Consequently, the durability performance of the concrete containing 50% FNS fine aggregate and 30% fly ash is considered equivalent to that of the concrete using 100% natural sand and 100% cement.
5. Therefore, combined use of FNS fine aggregate and fly ash is a promising option for environmentally friendly and durable concrete.

7.5 References

- Andrade, L. B., Rocha, J. C., & Cheriaf, M. (2009). Influence of coal bottom ash as fine aggregate on fresh properties of concrete. *Construction and Building Materials*, 23(2), 609-614.
- ASTM, C. 1202. (2006). Standard test method for electrical indication of concrete's ability to resist chloride ion penetration, *Philadelphia, PA: Annual Book of ASTM Standards*.
- ASTM, C. 1585. (2004). Standard Test Method for Measurement of Rate of Absorption of Water by Hydraulic-Cement Concretes. American Society of Testing Materials, *Philadelphia, PA: Annual Book of ASTM Standards*.
- ASTM, C. 642. (2006). Standard test method for density, absorption, and voids in hardened concrete. American Society of Testing Materials, *Philadelphia, PA: Annual Book of ASTM Standards*.
- AS, 2758.1. (1998). Aggregates and rock for engineering purposes – concrete aggregates. *Standards Australia Limited, Sydney, NSW, Australia*.
- AS, 1012.9. (2014). Methods of testing concrete Compressive strength tests - Concrete, mortar and grout specimens. *Standards Australia Limited, Sydney, NSW, Australia*.
- Bijen, J. (1996). Benefits of slag and fly ash. *Construction and building materials*, 10(5), 309-314.
- CCAA. (2009). Chloride resistance of concrete, *Cement Concrete & Aggregates Australia, Mascot, NSW, Australia*.
- Choi, Y. C., & Choi, S. (2015). Alkali–silica reactivity of cementitious materials using ferro-nickel slag fine aggregates produced in different cooling conditions. *Construction and Building Materials*, 99, 279-287.
- Dragaš, J., Ignjatović, I., Tošić, N., & Marinković, S. (2016). Mechanical and time-dependent properties of high-volume fly ash concrete for structural use. *Magazine of Concrete Research*, 68(12), 632-645.
- Ghafoori, N., & Bucholc, J. (1996). Investigation of lignite-based bottom ash for structural concrete. *Journal of Materials in Civil Engineering*, 8(3), 128-137.
- Kadam, M. P., & Patil, Y. D. (2015). Effect of sieved coal bottom ash as a sand replacement on the properties of cement concrete. *Magazine of Concrete Research*, 67(5), 227-234.
- Kou, S. C., & Poon, C. S. (2009). Properties of concrete prepared with crushed fine stone, furnace bottom ash and fine recycled aggregate as fine aggregates. *Construction and Building Materials*, 23(8), 2877-2886.
- Kuroda, M., Watanabe, T., & Terashi, N. (2000). Increase of bond strength at interfacial transition zone by the use of fly ash. *Cement and Concrete Research*, 30(2), 253-258.
- Manso, J. M., Polanco, J. A., Losanez, M., & Gonzalez, J. J. (2006). Durability of concrete made with EAF slag as aggregate. *Cement and Concrete Composites*, 28(6), 528-534.

- Pellegrino, C., & Gaddo, V. (2009). Mechanical and durability characteristics of concrete containing EAF slag as aggregate. *Cement and Concrete Composites*, 31(9), 663-671.
- Sakoi, Y., Aba, M., Tsukinaga, Y., & Nagataki, S. (2013). Properties of concrete used in ferronickel slag aggregate. In *Proceedings of the 3rd International Conference on Sustainable Construction Materials and Technologies*, Tokyo, Japan.
- Sato, T., Watanabe, K., Ota, A., Aba, M., & Sakoi, Y. (2011). Influence of excessive bleeding on frost susceptibility of concrete incorporating ferronickel slag as aggregates. In *36th Conference on Our World in Concrete & Structures*.
- Shoya, M., Sugita, S., Tsukinaga, Y., Aba, M., & Tokuhasi, K. (1999). Properties of self-compacting concrete with slag fine aggregates. In *Exploiting Wastes in Concrete* (pp. 121-130). Thomas Telford Publishing.
- Shehata, M. H., Thomas, M. D., & Bleszynski, R. F. (1999). The effects of fly ash composition on the chemistry of pore solution in hydrated cement pastes. *Cement and Concrete Research*, 29(12), 1915-1920.
- Silva, A., Neves, R., & de Brito, J. (2017). Statistical modelling of the influential factors on chloride penetration in concrete. *Magazine of Concrete Research*, 69(5), 255-270.
- Soutsos, M., Hatzitheodorou, A., Kanavaris, F., & Kwasny, J. (2017). Effect of temperature on the strength development of mortar mixes with GGBS and fly ash. *Magazine of Concrete Research*, 69(15), 787-801.
- Togawa, K., Shoya, M., & Kokubu, K. (1996). Characteristics of bleeding, freeze-thaw resistance and watertightness of concrete with ferro-nickel slag fine aggregates. *Journal of the Society of Materials Science, Japan*, 45(1), 101-109.
- Tomosawa, F., Nagataki, S., Kajiwara, T., & Yokoyama, M. (1997). Alkali-aggregate Reactivity of Ferronickel-Slag Aggregate Concrete. *ACI Special Publication*, 170, 1591-1602.
- Vicroads, 89. (2007) Test methods for the assessment of durability of concrete. *Roads Corporation of Victoria*, Victoria, Australia.
- Yüksel, İ., Bilir, T., & Özkan, Ö. (2007). Durability of concrete incorporating non-ground blast furnace slag and bottom ash as fine aggregate. *Building and Environment*, 42(7), 2651-2659.

Every reasonable effort has been made to acknowledge the owners of copyright material. I would be pleased to hear from any copyright owner has been omitted or incorrectly acknowledged.

Chapter 8: EFFECT OF ELEVATED TEMPERATURES ON CONCRETE INCORPORATING FNS AGGREGATE

The contents presented in this chapter were published in the following paper:

Saha, A. K., Sarker, P. K., & Majhi, S. Effect of elevated temperatures on concrete incorporating ferronickel slag as fine aggregate. Fire and Materials, 43(1), 8-21.

This chapter evaluates the elevated temperature exposure effect on concrete containing FNS aggregate. The experimental program was conducted by measuring the temperature increment in concrete core following by mass loss during the elevated temperature exposure. Later a non-destructive testing by ultrasonic pulse velocity (UPV) was conducted to evaluate the internal damage. Finally, strength loss due to high temperature exposure was determined. The test results of FNS concrete were compared with those of the control samples and a relationship between compressive strength loss and UPV was established.

8.1 Overview

Concrete is usually known to have high resistance against elevated temperature. However, there can be a significant loss of strength due to cracking and spalling of concrete when it is exposed to high temperatures for a prolonged period of time. Accidental fire remains a potential risk for structures that may cause massive property damage as well as loss of lives. Therefore, assessment of residual strength of concrete after high temperature exposure is of utmost importance. The residual strength properties of concrete after elevated

temperature exposure have been studied for decades. Malhotra (1956) showed that a concrete mix containing higher aggregate to cement ratio exhibited higher residual strength than a mix with the lower aggregate to cement ratio, with no effect of water to cement ratio on residual strength. On the other hand, Yang et al. (2009) pointed out that the highest exposure temperature and the exposure time are considered as the most influencing factors affecting the residual properties of concrete. Sarshar & Khoury (1993) showed that the concrete mix proportions have no effect on the residual strength of the samples exposed beyond 600 °C. It has been well recognised that the rate of heating plays a significant role on the residual strength. Accelerated heating can cause significant strength reduction of concrete. However, residual strength of concrete exposed to a temperature higher than 600 °C was shown to be not influenced by the rate of heating (Mohamedbhai, 1986). Besides, the cooling method has a significant impact on the residual strength and water-cooling imparts a thermal shock to the concrete resulting in a greater strength loss than air cooling (Luo et al., 2000). At high temperature exposures, the binder in concrete undergoes chemical reactions and lose the capacity to hold aggregates together. At the initial stage of heating, the free water is evaporated from concrete. As a result, shrinkage cracks are formed on the surface and numerous internal voids are created due to escape of the moisture. These voids and cracks cause a notable strength reduction of concrete. When the temperature reaches 530 °C, portlandite (CH) is decomposed and transformed into calcium oxide (CaO) and water (H₂O). Calcium silicate hydrate (CSH) is decomposed at temperatures beyond 600 °C. These changes of the hydrated products lead to a major strength loss of concrete (Yüzer et al., 2004; Kodur, 2014).

High strength concrete (HSC) usually suffers higher strength loss with explosive cracks after heat exposures as compared to normal strength concrete (NSC) (Chan et al., 2000; Li et al., 2004). This is because HSC is made with densely packed particles and low

water-cement ratio. As a result, it creates a dense microstructure, which inhibits the escape of moisture during the high-temperature exposure. Therefore, high vapour pressure leads to the formation of cracks and spalling in concrete. Different kinds of fibres have been used in concrete to improve its fire resistance properties. Steel and synthetic fibres are most commonly used in concrete. Fibres with low melting point, such as polyvinyl alcohol (PVA) fibres are found to be more effective in reducing spalling than the high melting point fibres, such as steel or carbon fibre (Chen & Liu, 2004; Soleimanzadeh, 2013; Ibrahim et al., 2012). This is because the fibres with low melting point melt and reduce the vapour pressure inside concrete by making way for escape of the vapour generated by heat.

The use of fly ash has been found advantageous to improve the residual strength of concrete. According to Ibrahim et al. (2012) at high-temperature, fly ash and calcium silicate undergo a chemical reaction that produces new silicate compounds. Therefore, concrete containing fly ash exhibited higher residual strength as compared to concrete with no fly ash. Xiao & Falkner (2006) showed the effectiveness of blast furnace slag in improving the residual strength of concrete. It was shown that the use of supplementary cementing material not only prevents the strength reduction at high temperature but also improves in some cases. Poon et al. (2003) showed the use of metakaolin as a partial replacement of cement improved compressive strength up to 400 °C as compared to the control concrete of same strength grade. Similarly, Papayianni & Valliasis (2005) observed strength improvement and better stability of fly ash concrete between 200 and 400 °C. In addition, Li et al. (2012) reported strength improvement of the ternary blended concrete containing fly ash and silica fume up to 400 °C. The low temperature exposures such as 200 °C to 400 °C for a prolonged period promotes the hydration of supplementary cementing materials (SCM) such as fly ash and metakaolin. As a result, the amorphous silica present in the SCM reacts with portlandite and enhance compressive strength.

However, when the temperature reaches around 600 °C the portlandite decomposes, and the effect of supplementary cementing material diminishes. The samples exposed to 800 °C showed similar residual strength regardless of the use of fly ash (Tanyildizi & Coskun, 2008).

The properties of aggregate can have a significant effect on the thermal properties of concrete since aggregates make about 70% to 80% volume of concrete. Kodur & Sultan (2003) pointed out that aggregate characteristics played an influential role in fire resistance of concrete. The fire resistance of concrete was measured in terms of thermal expansion, mass loss, specific heat and thermal conductivity. It was found that concrete using carbonated aggregate exhibited higher fire resistance as compared to that using siliceous aggregate. Kong & Sanjayan (2010) showed that gradation and thermal conductivity of aggregate have significant effects on the residual strength of concrete samples exposed to high temperatures. The experimental results showed that concrete with finer aggregate had higher strength loss as compared to that with coarser aggregates. In addition, thermal incompatibility between binder matrix and aggregate leads to notable strength loss. Similarly, Pan et al. (2012) pointed out that concrete using 10 mm aggregates suffered from explosive spalling, whereas that using 14 mm aggregates showed lower spalling when subjected to identical high temperature exposure. It is argued that the larger size aggregate creates longer fracture process zone that makes concrete less susceptible to spalling.

Furthermore, Zhang et al. (2000) pointed out that concrete made with light-weight aggregate does not undergo severe strength loss up to 600 °C as compared to concrete made with normal-weight aggregate. On the contrary, Noumowe et al. (2009) observed that light-weight aggregate concrete suffered significant spalling at 430 °C, due to high thermal gradient and low permeability of the samples. Besides, the chemical composition of aggregates has a major role in concrete exposed to high temperature. According to Husem

(2006), concrete made with limestone aggregates suffered higher strength loss as compared to the concrete with siliceous aggregates. However, difference of opinion also persists. Kodur et al. (2003) holds the view that concrete with dolomite aggregates exhibit high fire resistance as compared to concrete made with siliceous aggregate. The carbonate aggregate consists of significantly higher specific heat as compared to siliceous aggregates, which lead to the decomposition of dolomite ($\text{CaMg}(\text{CO}_3)_2$) of carbonate aggregate and prevents the spalling of concrete. Therefore, the type of aggregate plays an important role on the response of concrete when exposed to high temperature.

Ultrasonic pulse velocity (UPV) is a useful non-destructive technique that can be used to investigate the existence of defects in structures. This method has been found effective to quantify structural damages due to alkali-silica reaction, high-temperature exposure and corrosion of steel reinforcement. UPV through concrete was found to decrease with the increase of voids by high temperature exposures (Sukontasukkul et al., 2010). Yang et al. (2009) showed that UPV could be used to determine the actual temperature at which the specimens were exposed to during the fire exposure. The relative mass loss is another factor that can be used to evaluate the properties of a material after exposure to high temperatures. With the increment in temperature, the mass loss is increased, and residual strength is decreased (Poon et al., 2003).

Construction of infrastructures requires an enormous amount of natural sand since fine aggregate occupies about 30% to 35% of the volume of concrete. In order to reduce the excessive consumption of natural sand, different industrial by-products have been studied during the past decades. Therefore, increased utilization of FNS as fine aggregate has the potential to improve the sustainability of concrete production by reducing the use of natural sand. However, it is necessary to evaluate the effect of FNS on fire endurance properties of concrete in order to understand its behaviour as a construction material. In

this chapter, the residual properties of concrete containing FNS aggregate after fire exposure have been evaluated by changes in compressive strength, mass, ultrasonic pulse velocity and microstructural observation of scanning electron microscopic (SEM) images.

8.2 Experimental Work

8.2.1 Materials

Commercially available ordinary Portland cement (OPC) was used as the primary binder, and low calcium fly ash, classified as Class F was used as a supplementary cementing material. Ferronickel slag sourced from SLN, New Caledonia and natural sand were used as a fine aggregate and granite was used as a coarse aggregate. The physical and chemical properties of the materials has been discussed in previous chapters.

8.2.2 Mixture proportions and test methods

The concrete mix proportions used in this study are given in Table 8.1. Concrete mix design was conducted using the absolute volume method. FNS aggregate was used to replace 50% and 100% volume of sand. The water-binder ratio was kept constant for all the mixes. A naphthalene based superplasticizer was used to improve workability of concrete. The binder was 100% OPC for three mixtures and 30% OPC was replaced by fly ash in the other three mixtures. The cement replacement was done by weight percentage in order to keep the water-cement ratio consistent throughout the mixes. Fly ash was used to mitigate the potential alkali-silica reaction of FNS. The mixtures are designated by PC-FNS and FA-FNS for no fly ash and 30% fly ash, respectively. The number with the mix designation represents the percentage of FNS as a replacement of natural sand. Concrete cylinders of 100 mm diameter and 200 mm height were cast for the tests. The samples were cured in lime water for a period of 28 days. The mass of the sample was recorded after drying in ambient condition for one day. The samples were exposed to 50% relative humidity and 23

°C. This method was consistently used for all the samples of this study. The water content of the samples were 1.8%, 2.1%, 2.4%, 1.7%, 2.2% and 2.4% for the specimens of PC-FNS0, PC-FNS50, PC-FNS100, FA-FNS0, FA-FNS50, FA-FNS100, respectively.

Table 8.1 Concrete mix proportions

Mix ID	Binder (kg/m ³)		Fine aggregate (kg/m ³)		Coarse aggregate (kg/m ³)	Water (kg/m ³)	Superplasticizer (kg/m ³)
	OPC	Fly ash	Sand	FNS			
PC-FNS0	390	0	710	0	1194	129	4
PC-FNS50	390	0	355	435	1194	129	4
PC-FNS100	390	0	0	870	1194	129	4
FA-FNS0	273	117	710	0	1194	129	4
FA-FNS50	273	117	355	435	1194	129	4
FA-FNS100	273	117	0	870	1194	129	4

It can be seen that the moisture content slightly increased with the increment of FNS aggregates because FNS aggregates had a higher water absorption compared to sand. Afterwards, density of the concrete specimens was measured. The densities of the concrete samples were 2469, 2523, 2545, 2463, 2511 and 2537 kg/m³ for mixtures of PC-FNS0, PC-FNS50, PC-FNS100, FA-FNS0, FA-FNS50 and FA-FNS100, respectively. It can be seen that there was an increase in density of the concrete containing 50% FNS and 50% sand combination. This is attributed to the better particle packing of the fine aggregates.

Three identical concrete specimens were individually tested for each test and an average of the test results is reported. The samples were then tested to determine the compressive strength and ultrasonic pulse velocity (UPV). The other samples were exposed to the high-temperature exposure. An electric arc furnace was used to heat the samples at a rate of 5 °C per minute. The samples were heated in four different peak temperatures such as 200, 400, 600 and 800 °C. While heating, the changes of temperature in the furnace and

at the core of the specimen were recorded by using thermocouples and a data logger. The furnace temperature variations with time are shown in Fig. 8.1. After reaching the desired temperature, it was kept steady for a period of two hours. The samples were then cooled down slowly by keeping the samples inside the kiln with the door open. The samples were then cooled down to room temperature by keeping them inside kiln for 12 hours with the door open. Afterwards, the mass, compressive strength and UPV were determined for each sample when they reached the room temperature. Compressive strength was conducted by rubber capping the samples and at a loading rate of 0.33 MPa/sec.

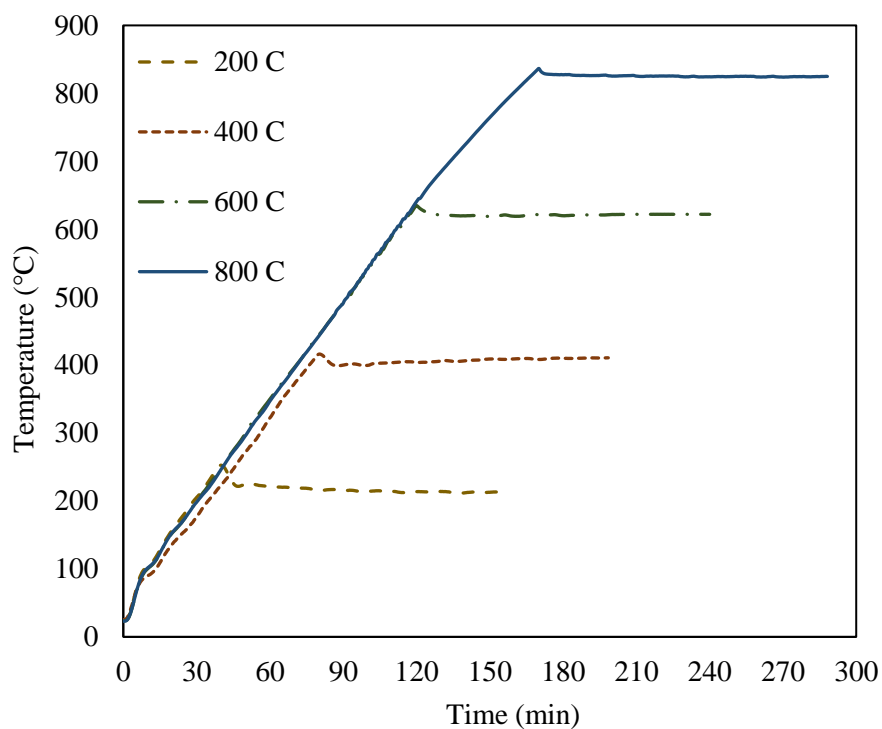


Fig. 8.1 Temperature variation with time inside the furnace

The UPV test setup included transmitting and receiving transducers, which were capable of generating and receiving 50 kHz ultrasonic pulses. The concrete samples were placed between the transducers and silicone gel was used as coupling agent between the surface of concrete and the transducers in order to prevent the signal loss from the sample's surface. Pair of piezoelectric transducers (PZT) of 50 kHz central frequency were used to

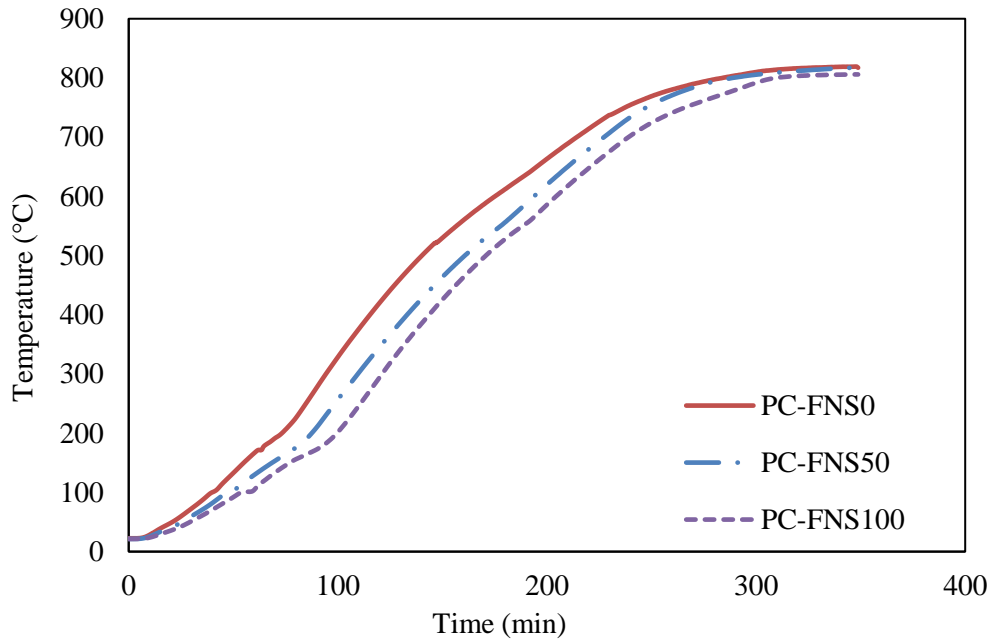
generate the compressional wave through transmission mode. A DPR 300 model pulser-receiver system was used as a source for excitation for the PZT transducers. The ultrasonic data was digitized using a Pico Scope 6 version 6.4.64.0 type modular oscilloscope. The pulse velocity was then calculated by recording the time required for the pulse to travel through the specimen.

In order to conduct the microstructural observation, the specimens were cut in to small cubes of 10 mm after the heat exposure and the surface was polished. Afterwards, they were mounted in stubs with a carbon tape and carbon coating was applied before imaging. The SEM images were taken by a field emission electron microscope at a constant voltage of 10 kV.

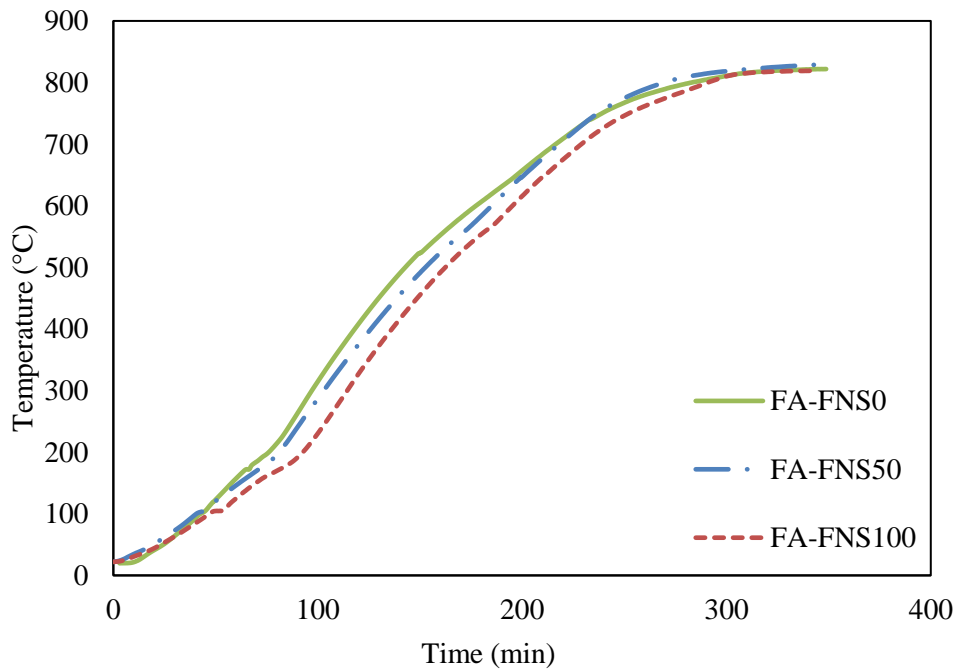
8.3 Results and Discussion

8.3.1 Core temperature of concrete

The variations of temperature with time at the core of the concrete cylinders exposed to 800 °C are presented in Figs. 8.2a and 8.2b. It can be seen from Fig. 8.2a that the rate of temperature rise in the specimen PC-FNS0 was higher as compared to the specimens PC-FNS50 and PC-FNS100. It can be noted that all the specimens were exposed to an identical heating regime in the furnace. The core temperature of the control concrete reached the peak earlier as compared to the specimens PC-FNS50 and PC-FNS100. Thus, the rate of heat flow in the concrete containing 100% natural sand was higher than those containing FNS aggregate.



a. 100% OPC as the binder.



b. 30% fly ash and 70% OPC as the binder.

Fig. 8.2 Variation of core temperature with time

The specimens containing 30% fly ash showed similar trend, as shown in Fig. 8.2b. The rate of heat flow in the specimens slightly decreased with the increase of FNS aggregate in the mixes with or without fly ash. The possible reason for the decrease of heat

flow with increase of FNS aggregate is the presence of the air voids in the larger FNS particles.

8.3.2 Mass loss of concrete after elevated temperature exposure

The mass loss of the specimens due to elevated temperature exposure was determined by measuring the mass of the samples before and after the exposure to heat. The mass loss values of the samples are shown in Fig. 8.3. It can be seen that mass of the specimens decreased at a high rate up to 400 °C and then it decreased at a smaller rate. The mass loss of the specimens varied between 4% and 6% for the exposure of 400 °C. This mass loss is considered to be due to evaporation of free water in concrete. The mass loss of concrete samples at 400 °C varied from 4.9% to 5.7% for the samples with 100% OPC. On the other hand, for the specimens with 30% fly ash, the mass loss varied in the range of 4.3% to 5.1%. Thus, it is noticeable that the fly ash concrete samples showed slightly less mass loss as compared to the samples with 100% OPC. Besides, mass loss slightly increased with the addition of FNS aggregate for specimens with or without fly ash. A gradual mass reduction was observed at the temperature range of 400 °C to 600 °C. The Ca(OH)_2 is decomposed to CaO and H_2O at this temperature range and the mass loss occurred due to evaporation of the water produced in the decomposition of Ca(OH)_2 . Beyond 600 °C, the rate of mass loss further decreased for all the types of specimens.

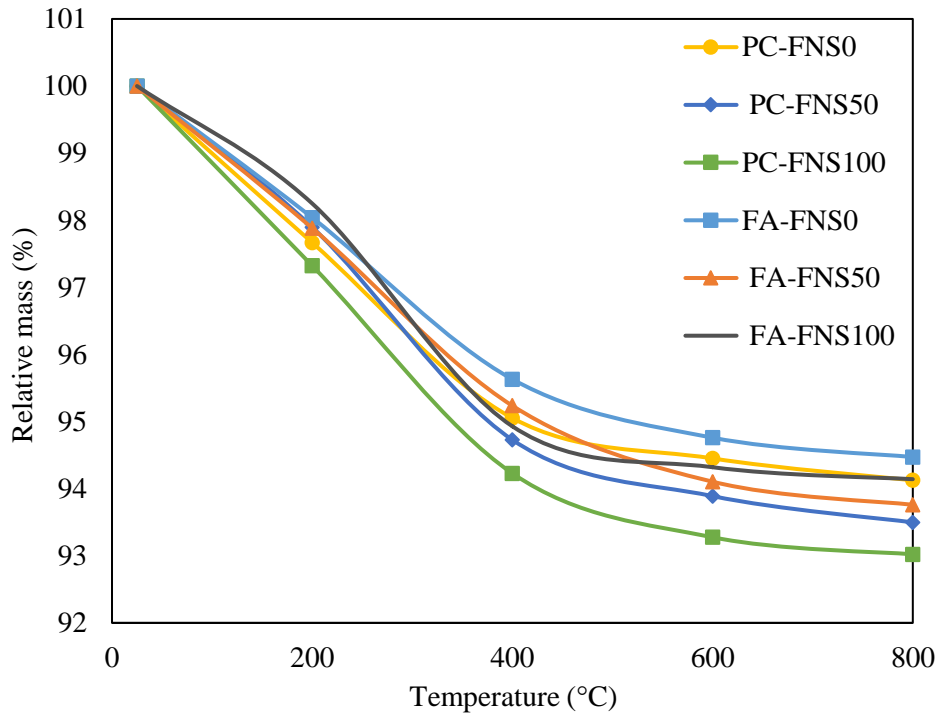


Fig. 8.3 Mass loss of concrete due to fire exposure

This consecutive mass loss was associated with the decomposition of calcium silicate hydrate (C-S-H). After exposure to 800 °C, the mass loss was within a range of 5.8% to 6.9% for 100% OPC as the binder and within a range of 5.5% to 6.2% for the specimens with 30% fly ash in the binder. Besides, the specimens containing FNS showed slightly higher mass loss for both type of binders. This may be attributed to the slightly higher water absorption of the FNS aggregates than natural sand.

8.3.3 Strength of concrete after heat exposure

The typical appearance of the fly ash concrete samples with 50% nickel slag (FA-FNS50) after exposures to 200 °C to 800 °C are shown in Fig. 8.4. It can be seen that there was no visual cracks in the specimens after 200 °C temperature. However, cracks started to appear at the surface from 400 °C. The cracks increased in number and width with the increase of temperature. Significant amount of cracks can be noticeable in the cylinder after exposure

to 800 °C. However, no spalling or explosive cracking was observed in any specimen. Similar surface cracks were observed in the specimens of other the mixtures.



a. After 200 °C.



b. After 400 °C.



c. After 600 °C.



d. After 800 °C.

Fig. 8.4 Specimens of mixture FA-FNS50 after different temperature exposures

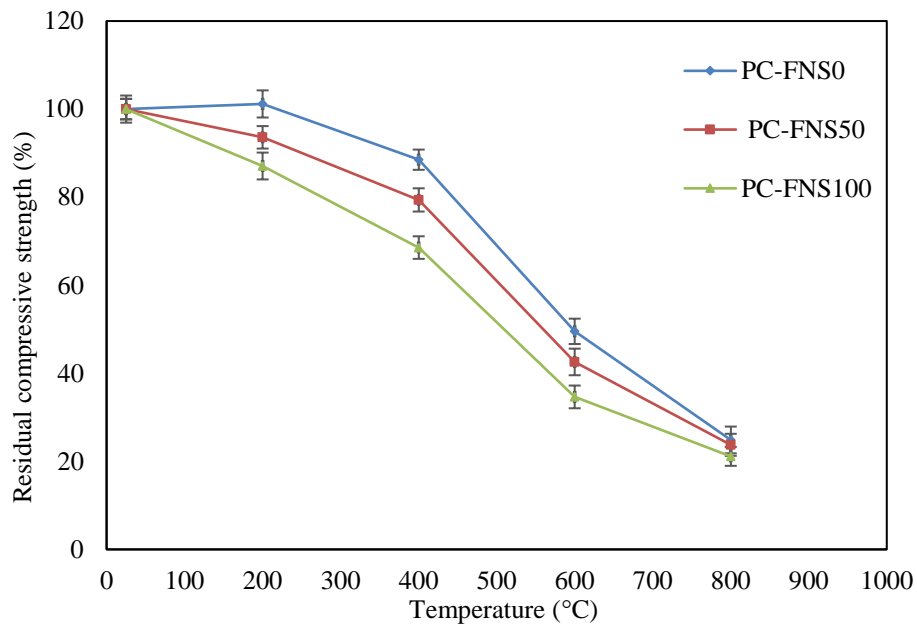
The mean compressive strengths of the concrete cylinders after exposure to high temperature are given in Table 8.2. The variations of residual strength after exposure to different temperatures are presented in Fig. 8.5. It is noticeable that the compressive strength of fly ash concrete without FNS aggregate increased gradually up to 400 °C. On the other hand, the samples with 100% OPC exhibited steady decline of the residual strength.

Table 8.2 Compressive strength and residual strength percentage after fire exposure

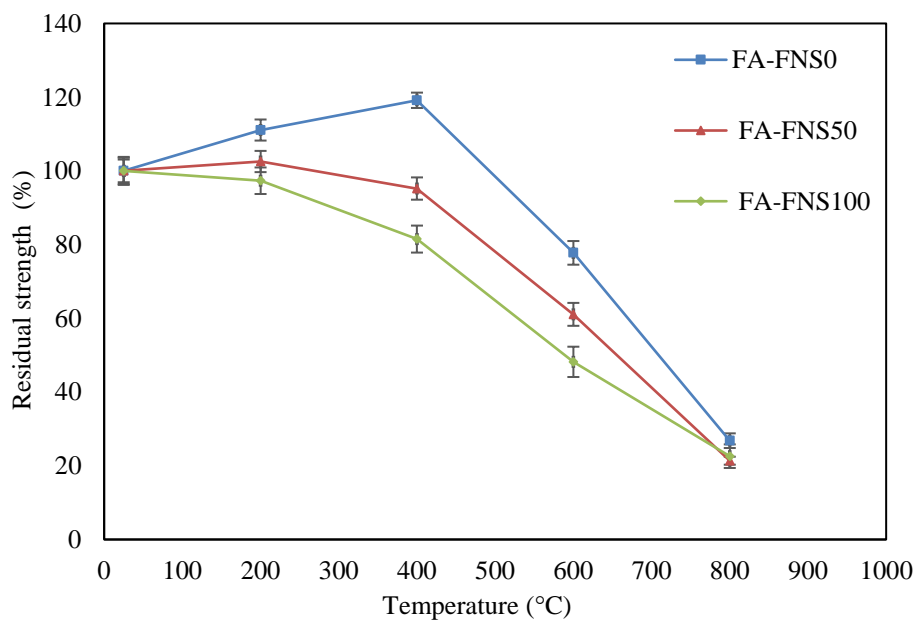
Tem p. (°C)	PC-FNS series (no fly ash)						FA-FNS series (30% fly ash)					
	Compressive strength (MPa)			Residual strength (%)			Compressive strength (MPa)			Residual strength (%)		
	PC-FN S0	PC-FNS 50	PC-FNS 100	PC-FNS 0	PC-FN S50	PC-FNS 100	FA-FNS 0	FA-FNS5 0	FA-FNS 100	FA-FNS 0	FA-FNS 50	FA-FNS 100
25	61	66	44	-	-	-	39	51	36	-	-	-
200	62	62	39	101	94	87	43	52	35	111	103	97
400	54	53	31	89	79	69	46	49	29	119	95	82
600	30	28	15	50	43	35	30	31	17	78	61	48
800	15	16	9	25	24	21	10	11	8	27	21	23

After 400 °C, the residual strength for mixtures FA-FNS0 and PC-FNS0 were 119% and 89%, respectively. Besides, with the addition of FNS aggregates, there was a gradual decrease of residual strength for concretes with or without fly ash. However, the use of fly ash was found to reduce strength loss of the FNS concretes. Residual strengths of the specimens with 100% OPC after exposure to 400 °C were 79% and 69% for the use of 50% and 100% FNS, respectively. The corresponding residual strengths were 95% and 82% for using 50% and 100% FNS, respectively, when there was 30% fly ash in the binder. Therefore, at this temperature, fly ash was found to increase the residual strengths of concrete containing FNS or natural sand. During this stage of heat exposure, primarily the free water available in concrete escapes from the samples, which was discussed in the previous section. The low-temperature exposure promoted the pozzolanic reaction of fly

ash. As a result, the fly ash concrete samples exhibited strength increase due to pozzolanic reaction.



a. 100% OPC as binder.



b. 30% fly ash and 70% OPC as binder.

Fig. 8.5 Residual strength after exposure to different temperatures

It can be seen from the Fig. 8.5 that there was a rapid strength reduction from 400 °C to 600 °C temperature exposure for both PC-FNS and FA-FNS concrete specimens. A

similar trend of strength reduction was observed due to the inclusion of FNS aggregates. The concrete specimens with 100% OPC yielded residual strengths of 50%, 43% and 35% for 0%, 50% and 100% FNS content, respectively. On the other hand, the specimens with 30% fly ash exhibited 78%, 61% and 48% residual strengths for 0%, 50% and 100% FNS aggregate, respectively. Therefore, at this temperature range of heating, the fly ash concrete specimens showed higher percentages of residual strength as compared to the 100% OPC concrete specimens. From 600 °C to 800 °C temperature range, the rate of strength reduction of the 100% OPC specimens reduced slightly, whereas, for the fly ash concrete specimens, the rate of strength reduction was same as in the previous stage of heating. After exposure to 800 °C, the residual strength of the 100% OPC concrete specimens were 25%, 24% and 21% for 0%, 50% and 100% FNS content, respectively. On the other hand, for the fly ash concrete specimens, the residual strengths were 27%, 21% and 23% for 0%, 50% and 100% FNS content, respectively. It can be seen that, at this stage of heating there was no significant difference in the residual strengths due to the use of FNS aggregates. Furthermore, fly ash had no noticeable effect at this stage of heating. This is because the C-S-H is decomposed at 800 °C temperature. As a result, the additional C-S-H produced by the pozzolanic reaction of fly ash was decomposed. Thus, the residual compressive strength at 800 °C was almost identical for all the concrete mixtures.

It can be seen from the above discussion that mass loss does not correlate with residual strengths at different temperature exposures. There was a sharp mass loss for all concrete specimens up to 400 °C, but the compressive strength increased in the fly ash concrete and slightly declined in the 100% OPC specimens. Besides, in the temperature range of 400 °C to 600 °C, the rate of mass loss was steady, but compressive strength exhibited a sharp reduction due to chemical changes in the binder with or without fly ash.

8.3.4 Ultrasonic pulse velocity after elevated temperature exposure

The mean ultrasonic pulse velocities of three identical cylinder specimens from each mix were determined before and after the elevated temperature exposure. As an example, Fig. 8.6 shows the waveforms of specimen FA-FNS50 after exposures to 200 to 800 °C.

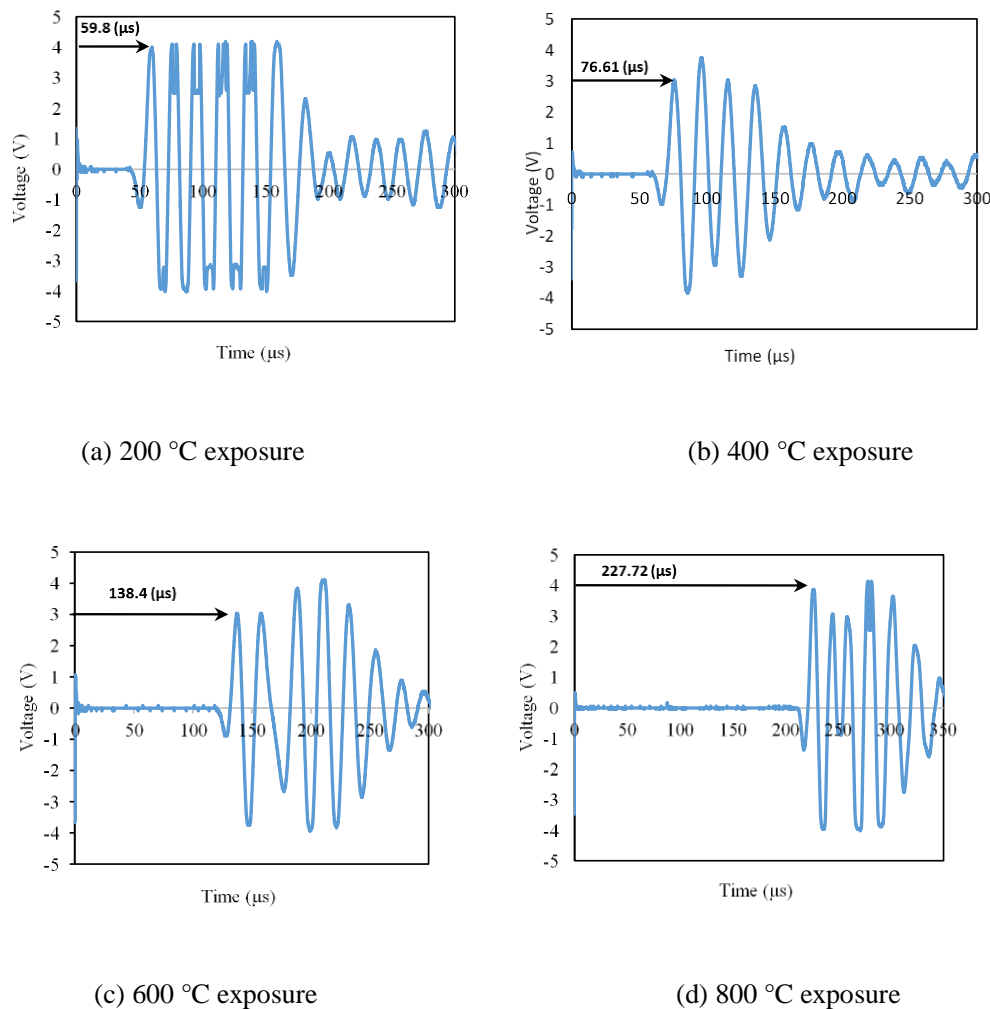


Fig. 8.6 Ultrasonic waveform of FA-FNS50 after different stages of fire exposure

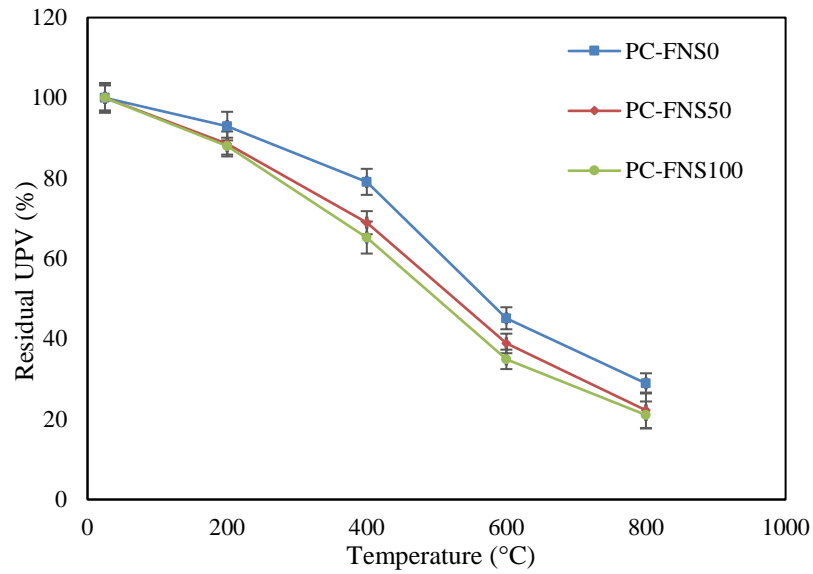
It can be seen that the travelling time of pulse to the receiving transducer increased gradually from 59.8 μs for 200 °C exposure to 227.7 μs for 800 °C exposure. The increase of travel time of the pulse is attributed to increase of cracks in the specimens with increase of exposure temperature, as shown in Fig. 8.4. The UPV for specimen was determined from the travel time of the pulse. The mean values of the UPV obtained from three identical

specimens are reported in Table 8.3. It can be seen that the average UPV values of the fly ash concrete specimens before elevated temperatures exposure were higher than those of the 100% OPC specimens.

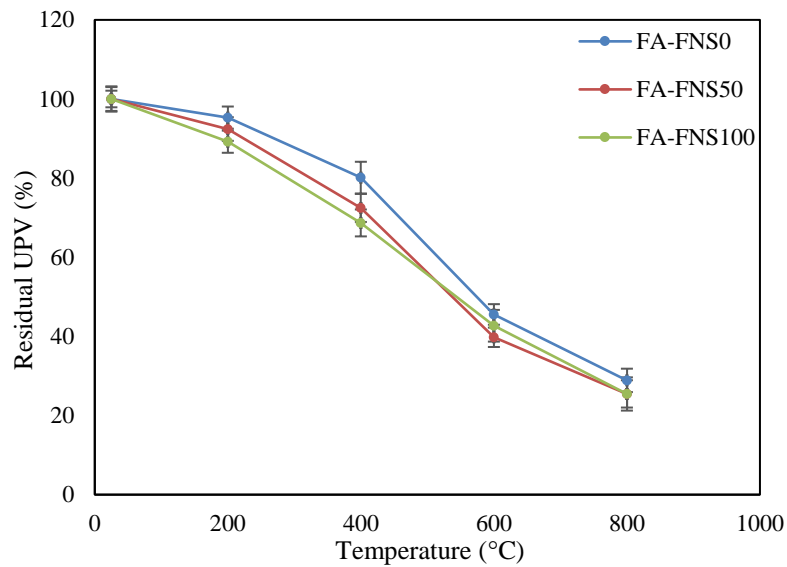
Table 8.3 UPV results after high-temperature exposure

Tem P. (°C)	PC-FNS series (no fly ash)						FA-FNS series (30% fly ash)					
	UPV (km/sec)			Residual UPV (%)			UPV (km/sec)			Residual UPV (%)		
	PC- FN S0	PC- FNS 50	PC- FNS 100	PC- FN S0	PC- FNS 50	PC- FNS 100	FA- FN S0	FA- FNS 50	FA- FNS 100	FA- FN S0	FA- FNS 50	FA- FNS 100
25	3.80	3.79	3.54	-	-	-	3.90	3.85	3.57	-	-	-
200	3.53	3.36	3.12	93	89	88	3.71	3.56	3.19	95	92	89
400	3.00	2.61	2.31	79	69	65	3.12	2.79	2.45	80	72	69
600	1.71	1.47	1.24	45	39	35	1.78	1.53	1.53	46	40	43
800	1.10	0.84	0.75	29	22	21	1.13	0.98	0.91	29	25	25

This phenomenon is attributed to the less amount of voids in the fly ash concrete than the 100% OPC concrete since fly ash is finer than the OPC. It can be noticed that the UPV value of the concrete specimens decreased with the increase of FNS aggregate. This indicates the presence of higher internal voids in concrete contributed by the voids of the FNS aggregates. It is also noticeable that the UPV values for all the mixes reduced gradually with the increment of temperature. The percentage residual UPV of the specimens are shown in Fig. 8.7. It can be seen that the residual UPV gradually decreased with the increase of exposure temperature up to 400 °C. Between 400 °C and 600 °C, the residual UPV decreased at higher rates in both OPC and fly ash concrete specimens. At this stage, the bond between the aggregate and binder became weaker because of dehydration of the binder increasing the voids content and hence rapid reduction of the percentage residual UPV.



a. 100% OPC as binder.



b. 30% fly ash and 70% OPC as binder.

Fig. 8.7 Residual UPV of samples after fire exposure

The chemical change in the binder by decomposition of portlandite created internal voids. At higher temperatures between 600 °C and 800 °C, a gradual reduction of residual UPV was observed. After 800 °C temperature exposure, the UPV values of the 100% OPC concrete samples were within a range of 1.1 km/sec to 0.7 km/sec. The UPVs for the fly ash concrete specimens were in a range of 1.1 km/sec to 0.9 km/sec at the same temperature

range. Thus, it is apparent from the comparisons that residual UPVs were in good correlation with residual compressive strengths of the concrete specimens.

8.3.5 Relationship between compressive strength and UPV

This section evaluates the relationship between residual compressive strength and UPV after high temperature exposure of the specimens. The experimental compressive strength versus UPV after temperature exposure are plotted in Fig. 8.8, which shows a general decrease of compressive strength with the decrease of UPV. Yang et al. (2009) proposed a linear relationship between the residual strength ratio and residual UPV ratio, as given by Equation 1.

$$Y = 1.03015 X_{UPV} - 0.06344 \quad (1)$$

where, Y and X_{UPV} are the residual strength ratio and residual UPV ratio, respectively.

Equation 1 was proposed based on the results 100 mm × 200 mm concrete cylinders with temperature exposures up to 600 °C. The trend line of the residual strengths predicted by Equation 1 is plotted in Fig. 8.8.

It can be seen that this equation can be used to estimate the residual strength ratio of concrete, however, it requires the UPV values both before and after the temperature exposure. An expression of the actual residual strength in terms of UPV only after temperature exposure would be more convenient for strength assessment of concrete after elevated temperature exposure. One such expression was proposed by Awal & Shehu (2015), as given in Equation 2.

$$Y_{RCS} = 0.0098 X_{RUPV} - 1.6118 \quad (2)$$

where, Y_{RCS} is the residual compressive strength in MPa and X_{RUPV} is the residual ultrasonic pulse velocity in m/s.

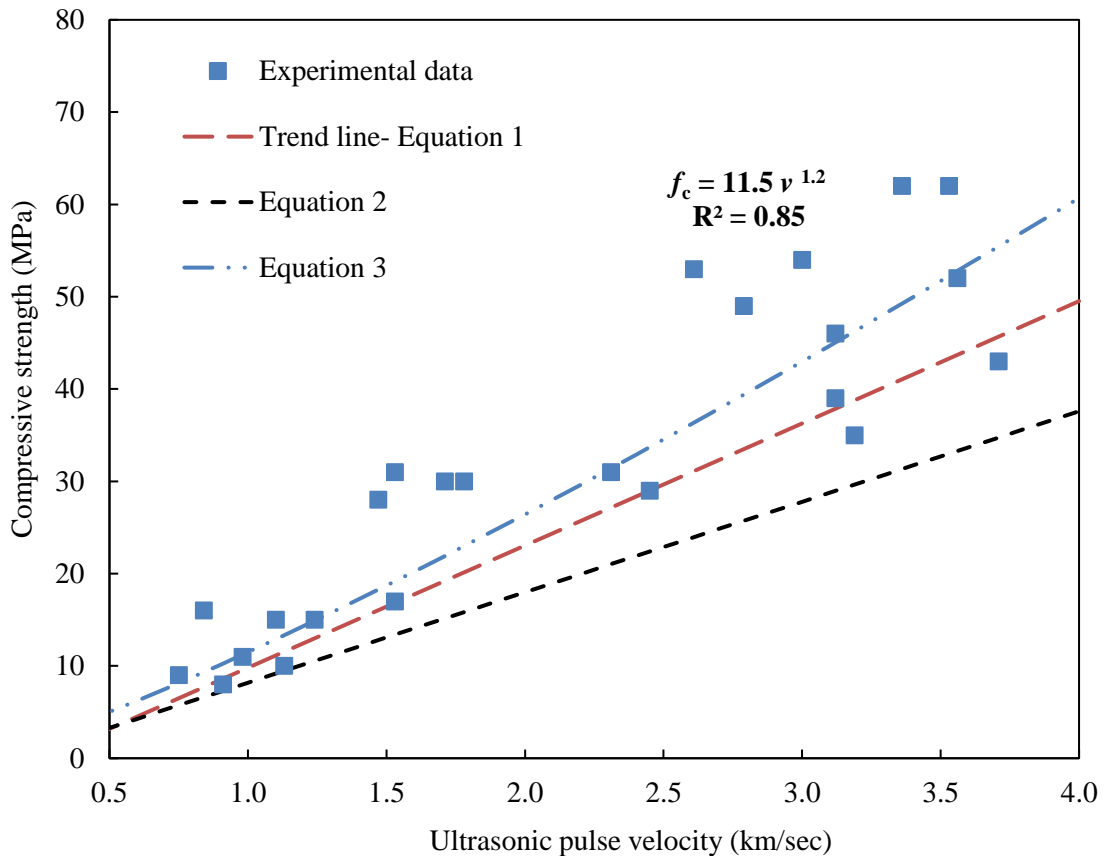


Fig. 8.8 Relationship between residual compressive strength and UPV

Equation 2 was proposed based on the results of 100 mm cube concrete specimens with temperature exposures up to 800 °C. The residual strengths of the test specimens of this study predicted by this equation are plotted in Fig. 8.8. It can be seen that this equation underestimates the residual strengths with a mean test to predicted strength ratio of 1.66. Therefore, Equation 3 was obtained from a power regression analysis of the experimental data. The coefficient of determination of this equation is 0.85. The mean value of the test to predicted residual strengths by this equation is 1.12 with a coefficient of variation of 25%.

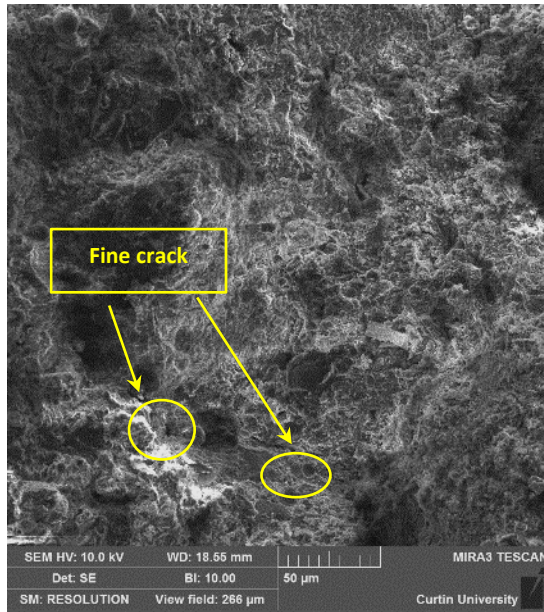
$$f_c = 11.5 (v)^{1.2} \quad (3)$$

where, f_c and v are the residual compressive strength in MPa and ultrasonic pulse velocity of concrete in MPa exposure to elevated temperature.

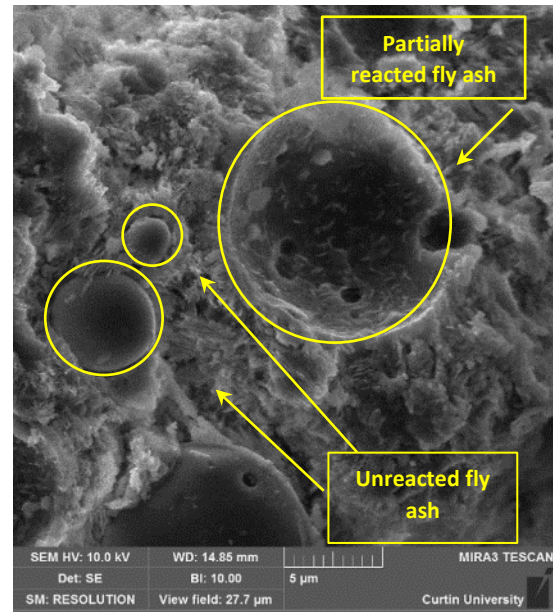
It is noticeable from Fig. 8.8 that, there is a reasonably good correlation between the compressive strength and ultrasonic pulse velocity. It can be observed that the experimental data are closer to the regression line given by Equation 3 for relatively low residual compressive strengths. The scatter of the experimental data with respect to the predicted values by Equation 3 are observed to increase for residual strengths above 30 MPa. This indicates relatively higher accuracy of the equation for higher temperature exposures such as 600 °C to 800 °C, as compared to the results of lower temperature exposures such as 200 °C to 400 °C. At low temperature regimes, the voids are generated due to evaporation of free water from concrete. Though evaporation of free water does not lead to severe strength loss, the existence of the voids is reflected by the reduction of UPV. On the other hand, more discontinuity of the concrete mass is developed by formation of cracks at the exposures of 400 °C to 800 °C, resulting in higher strength losses. For this reason, the UPV results showed better correlations with the residual strengths after higher temperature exposures. Thus, this non-destructive technique of ultra-sonic pulse velocity can be adopted to estimate the residual compressive strengths of concrete incorporating ferronickel slag aggregate after exposures to elevated temperature of up to 800 °C.

8.3.6 Microstructural observation

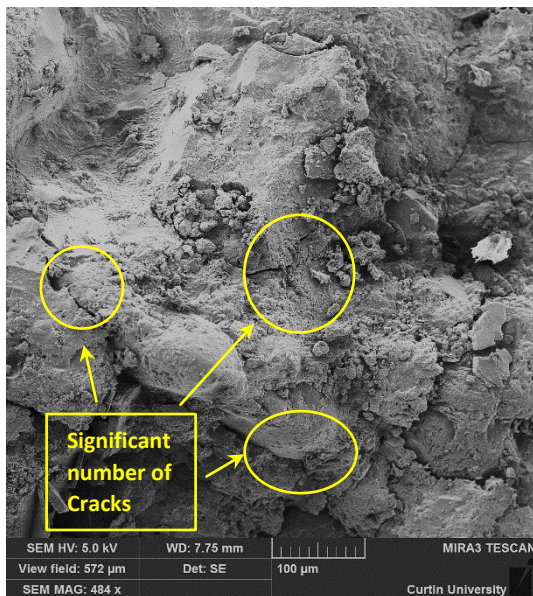
In order to understand the strength increment of the fly ash samples without FNS aggregates (FA-FNS0), scanning electron microscopic (SEM) image was taken after the exposure of 400 °C. The SEM images are shown in Fig. 8.9.



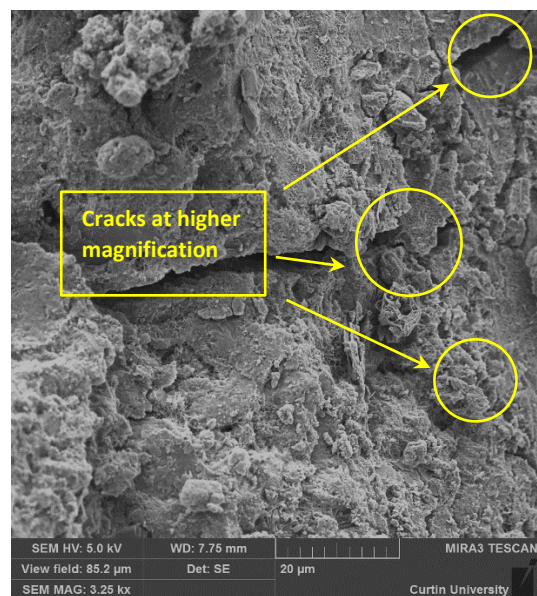
a. FA-FNS0 (500x magnification).



b. FA-FNS0 (5000x magnification).



c. PC-FNS0 (500x magnification).



d. PC-FNS0 (5000x magnification).

Fig. 8.9 SEM images of samples after 400 °C temperature exposure

It can be seen from Fig. 8.9a, which has a magnification of 500x, and even at this low magnification, the binder matrix looks very compact with very few fine cracks. In order to take a closer observation on the surface of the samples, Fig. 8.9b was taken at a 5000x magnification concentrating at the centre of the earlier image. In this figure, both reacted and unreacted fly ash particles can be noticeable. This image also points out that the surface

of reacted fly ash particles firmly adhered with the surrounding paste, whereas the unreacted fly ash particles exhibited some void space between the particle's surface and the surrounding paste. Thus, 2 hours exposure at 400 °C promoted pozzolanic reaction of fly ash and created a dense binder matrix. As a result, the fly ash concrete specimens showed a strength increment. The SEM image of the samples without fly ash (PC-FNS0) is shown in Fig. 8.9c. This image was taken at a field of view of 572 micrometres. A significant number of cracks on the binder matrix can be observed in this specimen. The image was taken at higher magnification given in the Fig. 8.9d with a field of view of 85.2 micrometres. Formation of cracks in the binder matrix due to the heat exposure can be seen in this image. Thus, after the exposure of 400 °C temperature, strength of the specimens reduced as the evaporation of water created voids and internal cracks.

8.4 Summary

The effect of high temperature exposure ranging from 200 to 800 °C on concrete specimens incorporating ferronickel slag fine aggregate and fly ash were studied by determination of mass loss, residual strength and ultrasonic pulse velocity. The following conclusions are drawn from the experimental results:

1. Inclusion of 50% FNS with natural sand increased compressive strength of concrete. The mass loss of concrete varied between 5.5% and 7% after exposure to 800 °C. The concrete cylinders containing up to 100% FNS aggregate showed no spalling with similar cracking patterns of the concrete made using 100 % natural sand. For exposures up to 600 °C, the residual strengths of concretes containing 50% FNS were 94%, 79% and 43% for 200 °C, 400 °C and 600 °C exposures, respectively. These are 7% to 10% smaller than the concrete made with 100% natural sand.

2. The use of 30% fly ash as cement replacement showed improvement of residual compressive strengths of all the mixtures for exposure up to 600 °C. The residual strengths of the concrete made with 30% fly ash and 50% FNS were 102%, 95% and 61% for exposures to 200 °C, 400 °C and 600 °C, respectively. SEM images confirmed the effectiveness of fly ash to improve the residual compressive strength by pozzolanic reaction at low-temperature exposures. The residual strengths of all the concrete specimens exposed to 800 °C varied in a small range of 21% to 26%. This is due to the severe cracks in all the specimens at this temperature irrespective of mixture ingredients.
3. Residual compressive strengths of the specimens after exposure to various temperatures correlated well with the respective UPVs. An equation has been found from exponential regression analysis that can be used to predict the residual strength from UPV with a reasonable accuracy. Therefore, UPV can be used as a non-destructive test to estimate the damage and residual strength of concrete incorporating FNS aggregate and fly ash.

8.5 References

- Awal, A. A., & Shehu, I. A. (2015). Performance evaluation of concrete containing high volume palm oil fuel ash exposed to elevated temperature. *Construction and Building Materials*, 76, 214-220.
- Chan, Y. N., Luo, X., & Sun, W. (2000). Compressive strength and pore structure of high-performance concrete after exposure to high temperature up to 800 C. *Cement and Concrete Research*, 30(2), 247-251.
- Chen, B., & Liu, J. (2004). Residual strength of hybrid-fiber-reinforced high-strength concrete after exposure to high temperatures. *Cement and Concrete Research*, 34(6), 1065-1069.
- Husem, M. (2006). The effects of high temperature on compressive and flexural strengths of ordinary and high-performance concrete. *Fire Safety Journal*, 41(2), 155-163.
- Ibrahim, R. K., Hamid, R., & Taha, M. R. (2012). Fire resistance of high-volume fly ash mortars with nanosilica addition. *Construction and Building Materials*, 36, 779-786.
- Kodur, V. (2014). Properties of concrete at elevated temperatures. *ISRN Civil engineering*, 2014.
- Kodur, V. K. R., & Sultan, M. A. (2003). Effect of temperature on thermal properties of high-strength concrete. *Journal of materials in civil engineering*, 15(2), 101-107.
- Kodur, V. K. R., Cheng, F. P., Wang, T. C., & Sultan, M. A. (2003). Effect of strength and fiber reinforcement on fire resistance of high-strength concrete columns. *Journal of Structural Engineering*, 129(2), 253-259.
- Kong, D. L., & Sanjayan, J. G. (2010). Effect of elevated temperatures on geopolymers paste, mortar and concrete. *Cement and concrete research*, 40(2), 334-339.
- Li, M., Qian, C., & Sun, W. (2004). Mechanical properties of high-strength concrete after fire. *Cement and concrete research*, 34(6), 1001-1005.
- Li, Z., Xu, J., & Bai, E. (2012). Static and dynamic mechanical properties of concrete after high temperature exposure. *Materials Science and Engineering: A*, 544, 27-32.
- Luo, X., Sun, W., & Chan, S. Y. N. (2000). Effect of heating and cooling regimes on residual strength and microstructure of normal strength and high-performance concrete. *Cement and Concrete Research*, 30(3), 379-383.
- Malhotra, H. L. (1956). The effect of temperature on the compressive strength of concrete. *Magazine of concrete research*, 8(23), 85-94.
- Mohamedbhai, G. T. G. (1986). Effect of exposure time and rates of heating and cooling on residual strength of heated concrete. *Magazine of Concrete Research*, 38(136), 151-158.
- Noumowe, A. N., Siddique, R., & Debicki, G. (2009). Permeability of high-performance concrete subjected to elevated temperature (600 C). *Construction and Building Materials*, 23(5), 1855-1861.
- Papayianni, I., & Valliasis, T. (2005). Heat deformations of fly ash concrete. *Cement and Concrete Composites*, 27(2), 249-254.

- Pan, Z., Sanjayan, J. G., & Kong, D. L. (2012). Effect of aggregate size on spalling of geopolymer and Portland cement concretes subjected to elevated temperatures. *Construction and Building Materials*, 36, 365-372.
- Poon, C. S., Azhar, S., Anson, M., & Wong, Y. L. (2003). Performance of metakaolin concrete at elevated temperatures. *Cement and Concrete Composites*, 25(1), 83-89.
- Sarshar, R., & Khoury, G. A. (1993). Material and environmental factors influencing the compressive strength of unsealed cement paste and concrete at high temperatures. *Magazine of concrete research*, 45(162), 51-61.
- Şahmaran, M., Özbay, E., Yücel, H. E., Lachemi, M., & Li, V. C. (2011). Effect of fly ash and PVA fiber on microstructural damage and residual properties of engineered cementitious composites exposed to high temperatures. *Journal of Materials in Civil Engineering*, 23(12), 1735-1745.
- Soleimanzadeh, S., & Mydin, M. O. (2012). Influence of high temperatures on flexural strength of foamed concrete containing fly ash and polypropylene fiber. *International Journal of Engineering-Transactions B: Applications*, 26(2), 117-126.
- Sukontasukkul, P., Pomchiengpin, W., & Songpiriyakij, S. (2010). Post-crack (or post-peak) flexural response and toughness of fiber reinforced concrete after exposure to high temperature. *Construction and Building Materials*, 24(10), 1967-1974.
- Tanyildizi, H., & Coskun, A. (2008). The effect of high temperature on compressive strength and splitting tensile strength of structural lightweight concrete containing fly ash. *Construction and Building Materials*, 22(11), 2269-2275.
- Xiao, J., & Falkner, H. (2006). On residual strength of high-performance concrete with and without polypropylene fibres at elevated temperatures. *Fire safety journal*, 41(2), 115-121.
- Yang, H., Lin, Y., Hsiao, C., & Liu, J. Y. (2009). Evaluating residual compressive strength of concrete at elevated temperatures using ultrasonic pulse velocity. *Fire Safety Journal*, 44(1), 121-130.
- Yüzer, N., Aköz, F., & Öztürk, L. D. (2004). Compressive strength–color change relation in mortars at high temperature. *Cement and Concrete Research*, 34(10), 1803-1807.
- Zhang, B., Bicanic, N., Pearce, C. J., & Balabanic, G. (2000). Residual fracture properties of normal-and high-strength concrete subject to elevated temperatures. *Magazine of Concrete Research*, 52(2), 123-136.

Every reasonable effort has been made to acknowledge the owners of copyright material. I would be pleased to hear from any copyright owner has been omitted or incorrectly acknowledged.

PART IV: CONCLUSIONS AND RECOMMENDATIONS

CHAPTER 9: CONCLUDING REMARKS

The primary focus of this research was to evaluate the effects of using water-cooled FNS by-product obtained from smelting of garnierite nickel ore as fine aggregate in cement mortar and concrete. FNS fine aggregate was used as 25%, 50%, 75% and 100% replacement of natural sand in mortar and concrete mixtures. Three supplementary cementitious materials such as class F fly ash, GGBFS and ground FNS (GFNS) were used as partial cement replacements in combination with different percentages of FNS fine aggregate. Experimental work was conducted in the laboratory in order to determine the effects of FNS on workability, mechanical properties and durability of mortar and concrete. The main conclusions from the experimental results are presented in this chapter. Some recommendations are also made for future study.

9.1 Research impacts

(a) Optimum percentage of FNS fine aggregate in mortar and concrete

Maximum compressive strengths of mortar and concrete mixtures were observed at 50% replacement of natural sand by FNS. There was no negative effect of FNS aggregate up to 50% on the workability of freshly mixed mortar and concrete. The durability related properties such as volume of permeable voids, sorptivity and chloride permeability showed marginally increasing trends with the increase of FNS aggregate. However, the values of these properties remained in the ranges of those recommended for good concrete. Leaching of heavy metals from concrete containing FNS aggregate were far below the limits recommended in different standards. Therefore, the use of FNS aggregate as 50%

replacement of natural sand is considered as optimum in terms of mechanical properties and durability of concrete.

(b) Potential alkali silica reactivity (ASR) of FNS aggregate

The potential ASR of FNS aggregate was investigated by the accelerated mortar bar test. It was found that the expansions of mortar bars using 25% or more FNS aggregate exceeded the allowable limits recommended for the respective test methods when no SCM was used in the binder. The high expansion of specimens observed in the tests is attributed to the amorphous silica present in FNS. However, it is interesting to note that no cracks or ASR product was found in the concrete blocks containing 30% FNS aggregate with no SCM in binder and used as breakwater structures exposed to sea waves for 20 years (Fig. 4.1).

(c) Mitigation of potential ASR of FNS aggregate

The expansion results of accelerated mortar bar test confirmed that 30% cement replacement by class F fly ash or GFNS could successfully mitigate the potential ASR of FNS aggregate. It was confirmed by TGA that the consumption of portlandite by pozzolanic reaction of fly ash and GFNS reduced the ASR of FNS aggregate.

9.2 Main research findings

The main research findings are summarised below.

(a) Workability, mechanical properties and leaching behaviour:

1. Sand replacement by FNS showed increase of the flow of freshly mixed mortar with the increase of FNS content up to 50%. Similarly, a trend of marginal increase of slump was observed in the concrete mixtures containing FNS up to 50%. The increase of workability by FNS is attributed to its larger size than natural sand particles that reduced water demand and improvement of the grading of fine aggregate by FNS. However, workability decreased for FNS contents of 75% and

100% of fine aggregate due to the increase of voids content and angularity of fine aggregate. Furthermore, air content of fresh concrete gradually increased with the increment of FNS aggregate in the mixture. Air contents of the concrete mixtures using 30% fly ash were 1.6%, 2.1% and 2.8% for no FNS, 50% FNS and 100% FNS, respectively. The increase of air content is attributed to the angularity of FNS aggregate that caused entrapped air in the mixture.

2. Compressive strengths of cement mortar and concrete specimens showed maximum values at 50% sand replacement by FNS for the mixtures with or without using fly ash as cement replacement. This is attributed to the improved particle packing and interlocking of aggregates due to the angular shape and rough surface texture of FNS.
3. The 28-day splitting tensile strength of the concrete containing 50% or 100% FNS aggregate varied from 7% to 10% of the corresponding compressive strength. Similarly, the 28-day flexural strengths of the concrete specimens with FNS aggregate varied between 10% and 14% of the corresponding compressive strengths. Thus, the correlations of tensile and flexural strengths with compressive strength of concrete using FNS aggregate up to 100% is same as that for concrete using 100% natural sand. The modulus of elasticity of the concrete specimens containing FNS aggregate was similar to those of concrete specimens containing 100% natural sand.
4. The equations of design standards for conventional concrete such as Australian Standard and ACI Code can be used for conservative predictions of the splitting tensile strength, flexural strength and elastic modulus of concrete using FNS fine aggregate with or without fly ash as a partial cement replacement.

5. Leaching of heavy metals from the hardened concrete specimens incorporating 50% or 100% FNS fine aggregate were far below the limits recommended by regulatory authorities such as the US EPA and the UK Environment Agency. Therefore, FNS can be considered environmentally compatible for use as a fine aggregate in concrete.

(b) Durability of mortar and concrete containing FNS aggregate:

1. Accelerated mortar bar test (AMBT) was conducted in accordance with the Australian Standard (AS 1141.60.1). The expansions of mortar bar specimens decreased with the increase of fly ash in the accelerated test condition. According to the 10-day and 20-day expansion limits of the Australian Standard, the mortar bar specimens were classified as reactive, slowly reactive and non-reactive for the fly ash contents of 0% or 10%, 20% and 30%, respectively. In the accelerated test condition, some surface cracks were observed in the specimens using no fly ash and 10% fly ash. No surface crack was seen in the specimens using 20% and 30% fly ash. The TGA results showed that Portlandite content of paste samples exposed to AMBT condition decreased by the use of 30% fly ash. Also, Ca/Si ratio of the reaction product increased from 1.78 to 2.63 by the use of 30% fly ash. This shows a modification of the reaction product by fly ash. Thus, fly ash reduced the ASR expansion of FNS aggregates in AMBT by reduction of the alkalinity of pore solution, densification of the binder matrix and modification of the product to cause less swelling pressure and cracking. On the other hand, expansions of the specimens containing 30% GGBFS in the binder and FNS content of 25% or more were above the limit of the Australian Standard.
2. While FNS with 100% OPC was found potentially reactive in the above accelerated ASR tests, it is interesting to note that no crack or ASR product was found in the

concrete blocks containing 30% FNS aggregate and no SCM in the binder that have been in use as breakwater structures exposed to sea waves for 20 years (Fig. 4.1). This shows the need for continued long-term study of the ASR aspect of FNS aggregate in concrete under real field conditions.

3. In concrete samples, volume of permeable voids (VPV) was found to increase with the increase of FNS aggregate replacing natural sand. This is attributed to the increment of porosity by the relatively large size, angular shape and presence of internal voids in the FNS particles. However, the pozzolanic reaction of fly ash reduced the permeable voids, as evidenced by the SEM images and EDS data. Thus, the chloride permeability and sorptivity were also reduced by fly ash. The concrete samples with fly ash also suffered from lower strength reduction after the alternate wet-dry cycles as compared to the samples without fly ash. The compressive strength of the samples with 50% FNS and 30% fly ash remained almost unchanged after exposure to the wet-dry cycles. The sorptivity coefficient of this mix was well below the recommended value of $0.21 \text{ mm/min}^{1/2}$ and the rapid chloride permeability was classified as low. Consequently, the durability performance of the concrete containing 50% FNS fine aggregate and 30% fly ash is considered equivalent to that of the concrete using 100% natural sand and 100% cement.
4. The mass loss of concrete varied between 5.5% and 7% after exposure to 800 °C. The concrete cylinders containing up to 100% FNS aggregate showed no spalling with similar cracking patterns of the concrete made using 100 % natural sand. For exposures up to 600 °C, the residual strengths of concrete containing 50% FNS were 94%, 79% and 43% for 200 °C, 400 °C and 600 °C exposures, respectively. These are 7% to 10% smaller than the concrete made with 100% natural sand.

5. The use of 30% fly ash as cement replacement showed improvement of residual compressive strengths of all the mixtures for exposure up to 600 °C. The residual strengths of the concrete made with 30% fly ash and 50% FNS were 102%, 95% and 61% for exposures to 200 °C, 400 °C and 600 °C, respectively. SEM images confirmed the effectiveness of fly ash to improve the residual compressive strength by pozzolanic reaction at low-temperature exposures. The residual strengths of all the concrete specimens exposed to 800 °C varied in a small range of 21% to 26%. This is due to the severe cracks in all the specimens at this temperature irrespective of mixture ingredients.
6. Residual compressive strengths of the specimens after exposure to various temperatures correlated well with the respective ultrasonic pulse velocities (UPV). An equation has been found from exponential regression analysis that can be used to predict the residual strength from UPV with reasonable accuracy. Therefore, UPV can be used as a non-destructive test to estimate the damage and residual strength of concrete incorporating FNS aggregate and fly ash.

9.3 Recommendations for future study

- a) Long term monitoring of concrete with FNS aggregates and different proportions of SCM in different real field exposures would be beneficial to generate useful performance data.
- b) The ASR mitigation phenomena of other SCMs such as silica fume and metakaolin can be evaluated for concrete using FNS aggregate.
- c) Use of FNS in geopolymer concrete and its properties can be evaluated for its further applications to the production of green concrete.

APPENDICES

APPENDIX A: Images of Experiments



Fig. A.1 Slump test of concrete

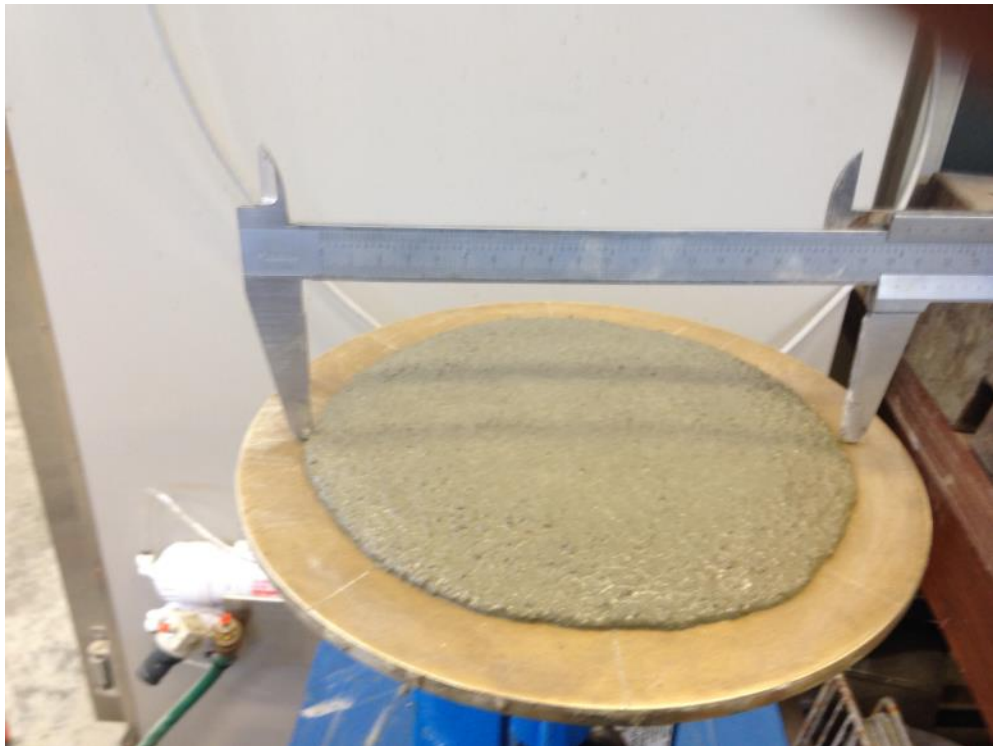


Fig. A.2 Flow test of mortar



Fig. A.3 Compressive strength test of concrete

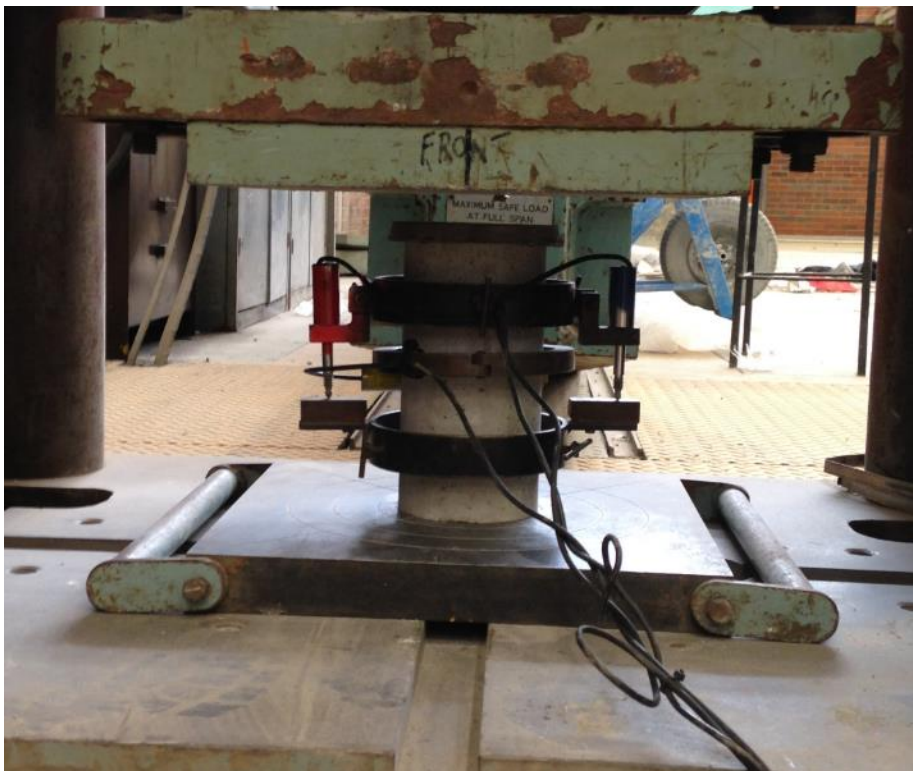


Fig. A.4 Modulus of elasticity test of concrete



Fig. A.5 Splitting tensile strength test of concrete



Fig. A.6 Flexure strength test of concrete



Fig. A.7 Concrete cylinders cutting for RCPT and sorptivity tests

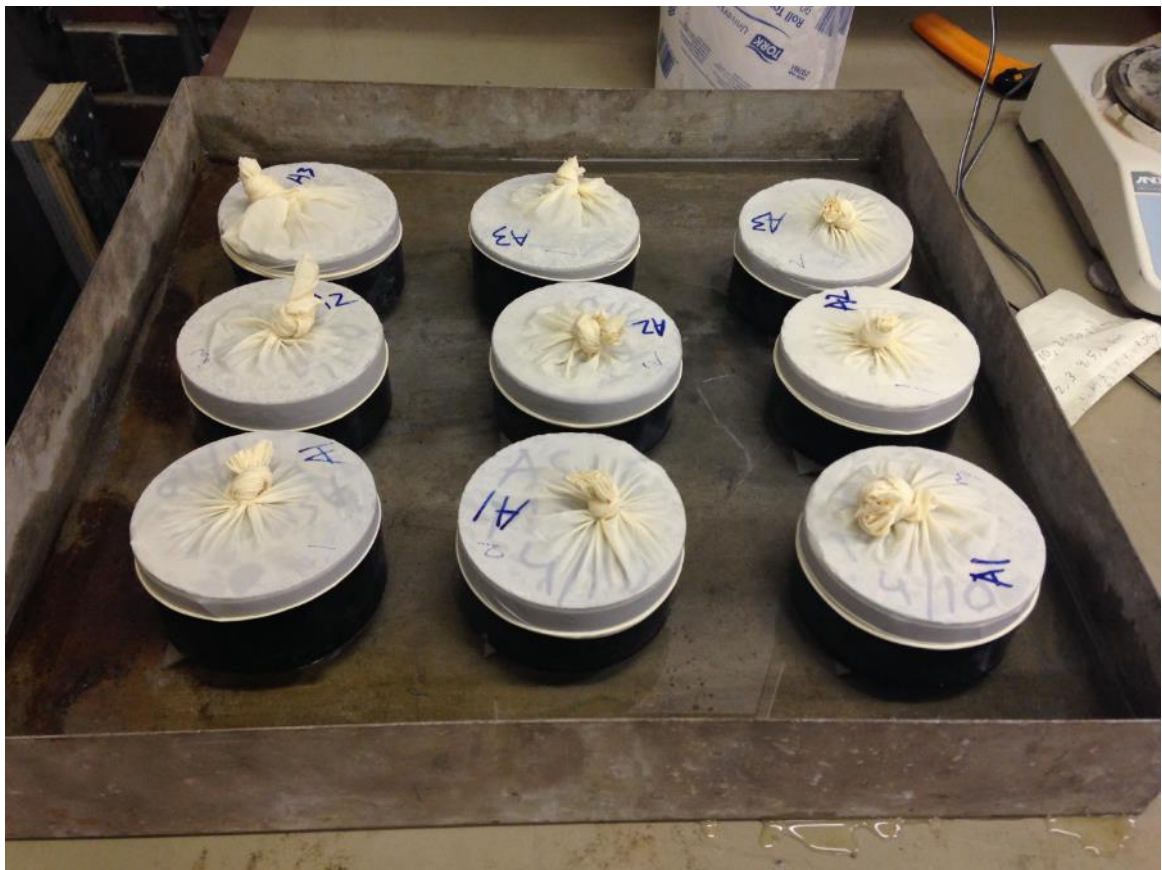


Fig. A.8 Sorptivity test of concrete



Fig. A.9 ASR expansion measurement by length comparator



Fig. A.10 Elevated temperature exposure test

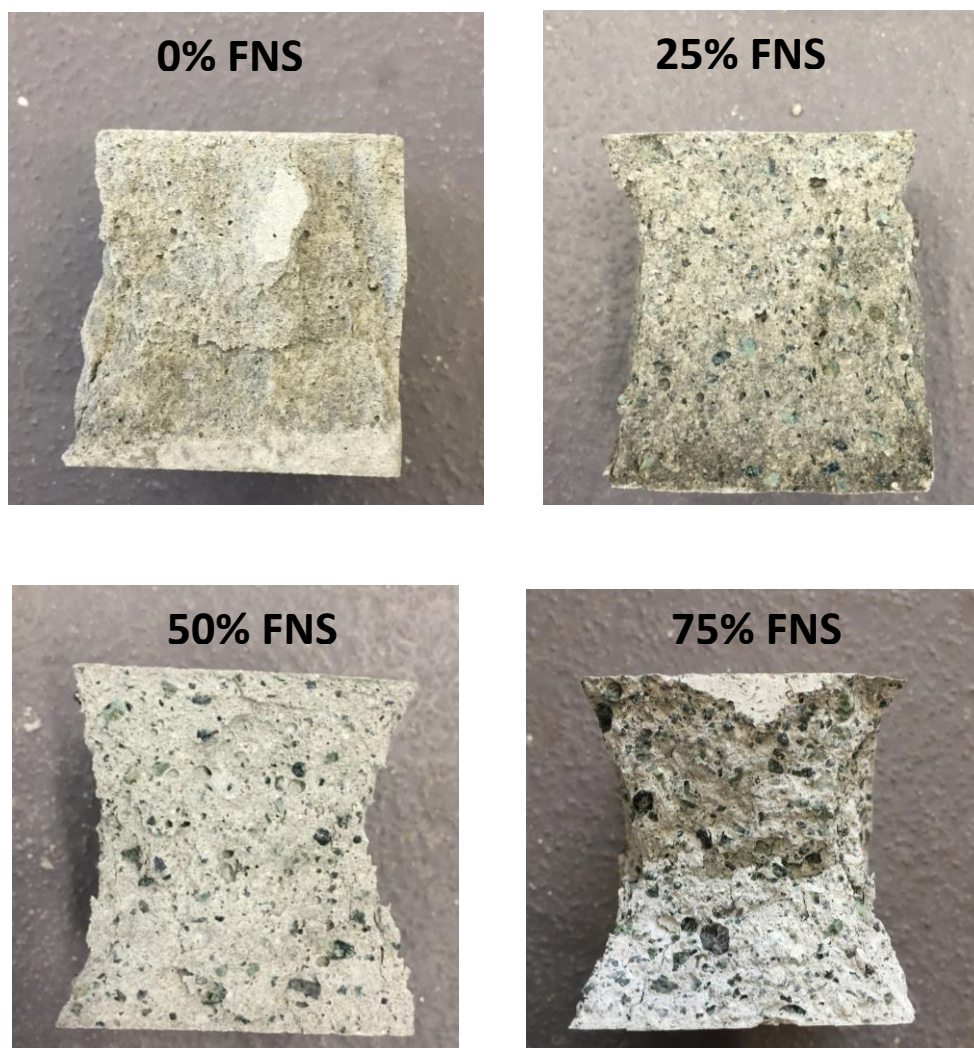


Fig. A.11 Failure pattern of mortar cubes with different proportions of FNS aggregate



Fig. A.12 Similar failure pattern of control concrete (left) and FNS concrete (right)

APPENDIX B: Mortar Results

Table B.1 Compressive strengths of mortar (PCFNS0: 100% OPC and 0% FNS aggregate)

Duration (days)	Average Strength (MPa)	Std. deviation
3	18.04	2.83
7	32.86	1.66
28	38.51	1.25
56	42.22	0.84

Table B.2 Compressive strengths of mortar (PCFNS50 :100% OPC and 50% FNS aggregate)

Duration (days)	Average Strength (MPa)	Std. deviation
3	26.27	1.95
7	47.84	2.30
28	57.04	1.76
56	61.81	2.22

Table B.3 Compressive strengths of mortar (PCFNS100: 100% OPC and 100% FNS aggregate)

Duration (days)	Average Strength (MPa)	Std. deviation
3	16.30	0.95
7	35.83	0.24
28	43.93	1.45
56	45.20	2.55

Table B.4 Wet Dry Cycle Test of mortar samples

Mix	Average wt. loss	Avg. compressive strength before (MPa)	Avg. Compressive Strength After (MPa)	Comp. strength loss (%)	FNS content (%)	Std. Dev. Comp. strength (before)	Std. Dev. Comp. strength (after)
A1	4.07	42.22	37.23	11.81	0	0.84	1.93
A2	4.58	53.37	44.95	15.79	25	1.05	3.74
A3	4.78	61.81	49.59	19.78	50	2.22	0.65
A4	5.30	56.83	44.37	21.94	75	1.28	2.51
A5	5.27	45.20	34.29	24.12	100	2.55	1.27

Table B.5 Porosity test of mortar samples

Mix ID	Avg. density (kg/m ³)	Avg. absorption (%)	Avg. permeable voids (%)	FNS content (%)
PCFNS0	2614	7.61	15.21	0
PCFNS50	2817	8.05	17.97	50
PCFNS100	2863	8.28	18.51	100

Table B.6 AMBT expansion limits for reactivity classification as per AS1141.60.1

Mean mortar bar expansion (E), (%)		Aggregate reactivity classification
Duration in 1M NaOH at 80 °C		
10 days	21 days	
—	$E < 0.10$	Non-reactive
$E < 0.10$	$0.10 \leq E < 0.30$	Slowly reactive
$E \geq 0.10$	—	Reactive
—	$0.30 \leq E$	Reactive

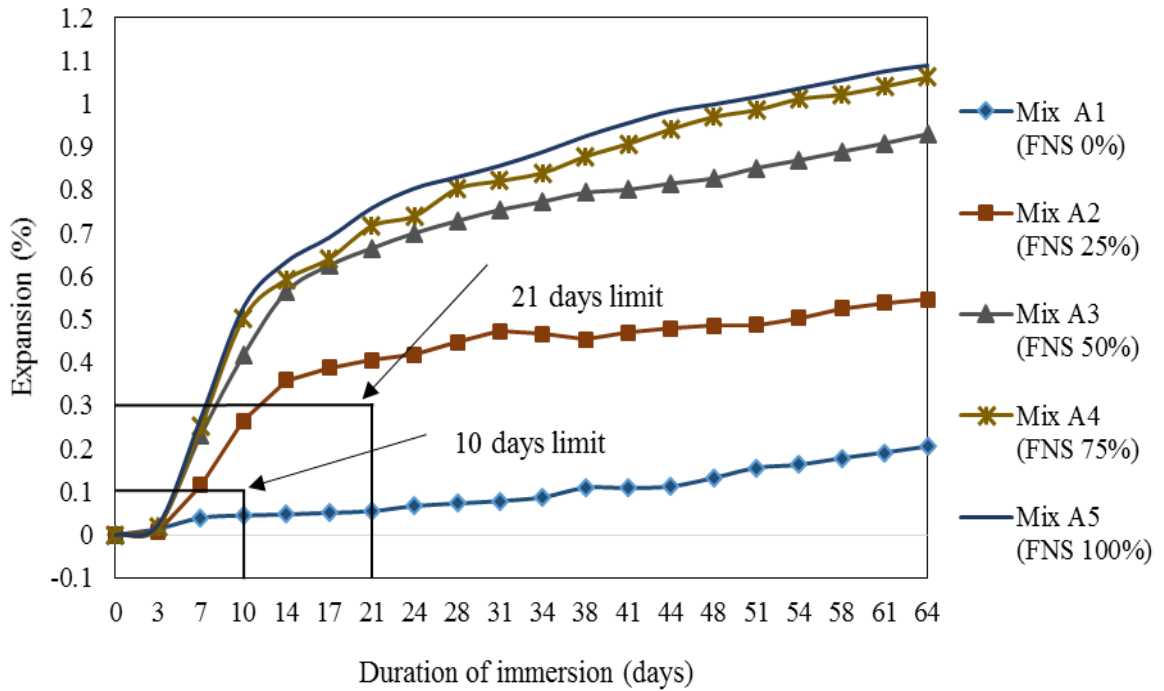


Fig. B.1 ASR expansions of the mixtures of 100% OPC

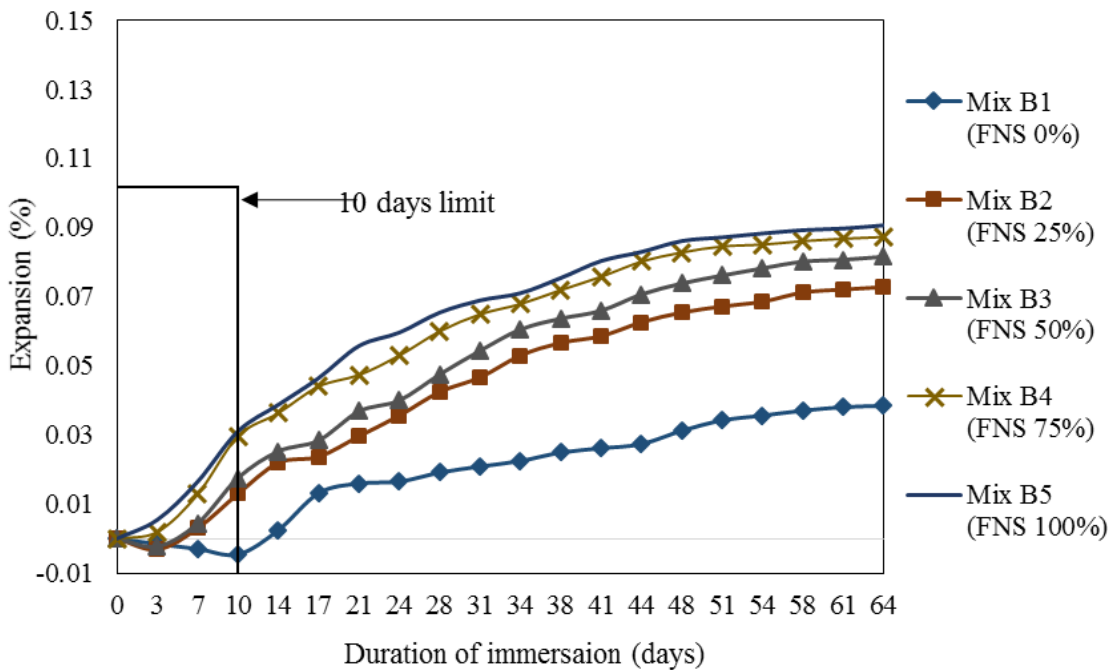


Fig. B.2 ASR expansions of the mixtures of 70% OPC and 30% fly ash

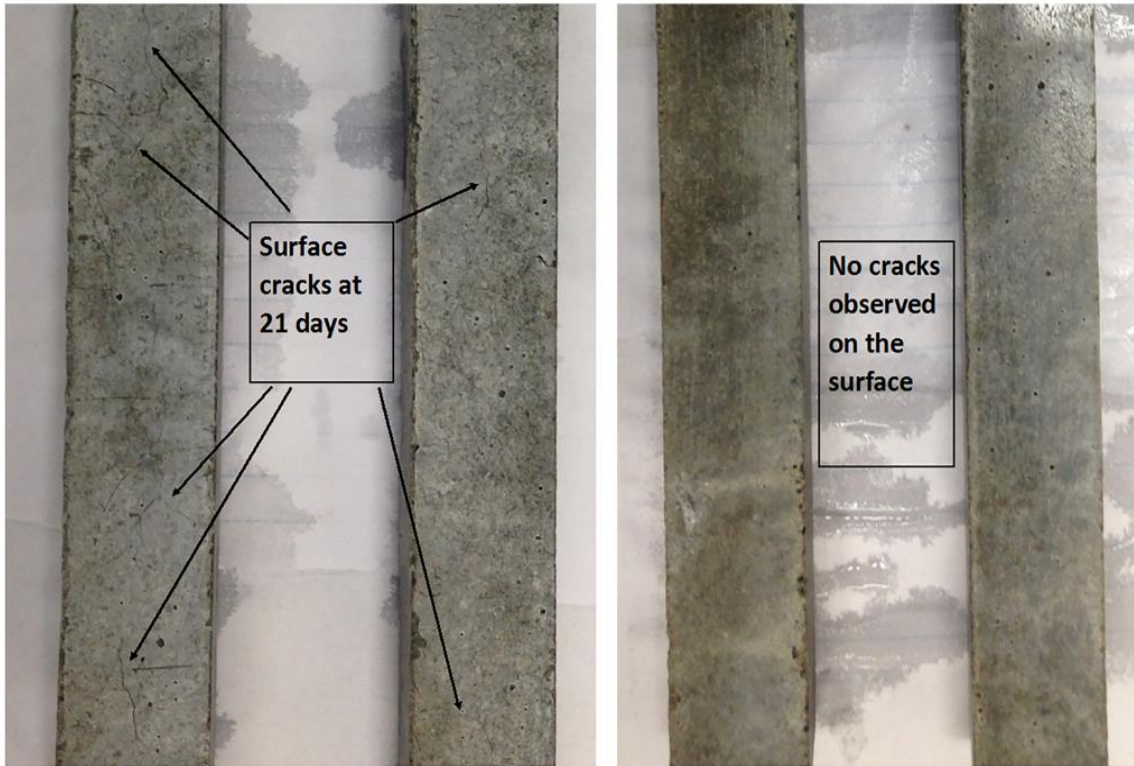
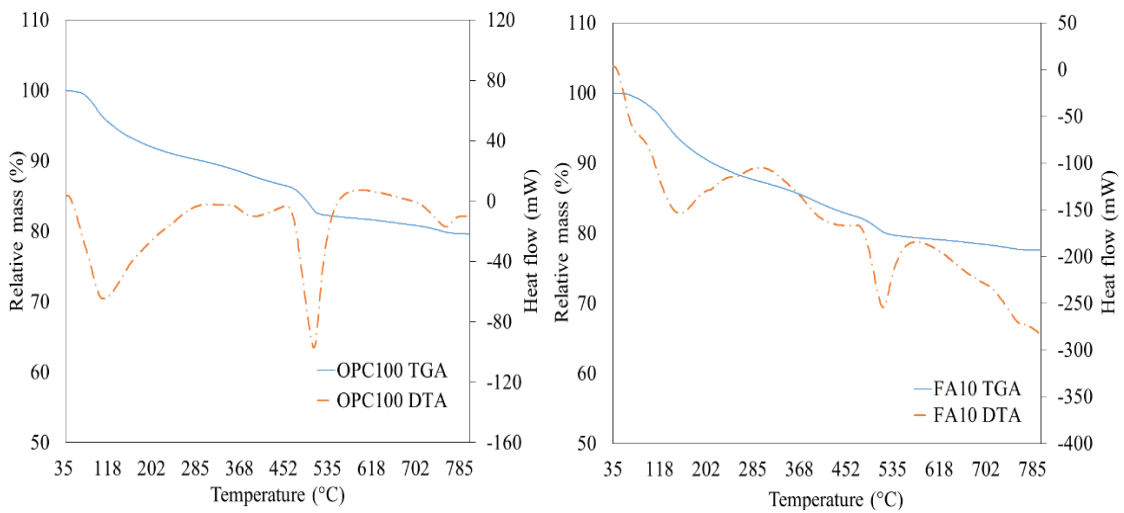


Fig. B.3 Visual inspection of AMBT samples with 50% FNS aggregate after 21 days exposure (PC100; FA10; FA20; FA30 from left to right respectively)



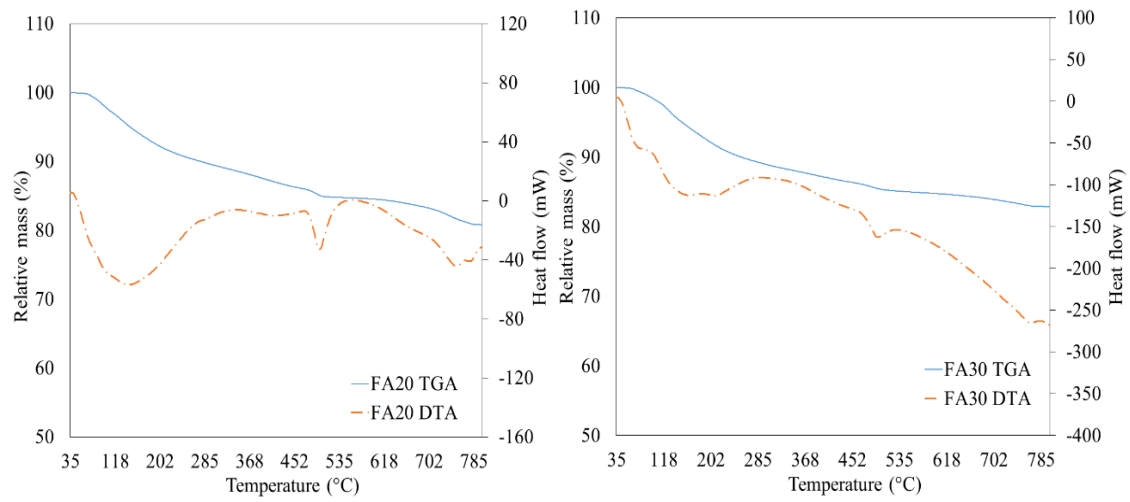


Fig. B.4 Thermogravimetric mass changes of paste samples exposed to AMBT condition

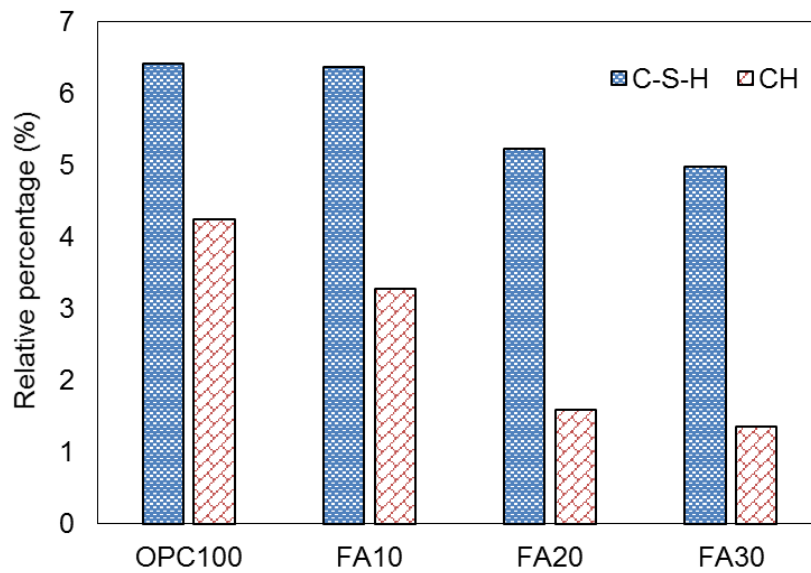


Fig. B.5 Relative C-S-H and CH content of paste samples

APPENDIX C: Concrete Results

Table C.1 Compressive strengths of Concrete (PCFNS50: 100% OPC as a binder and 50% FNS aggregates)

Duration (days)	Average (MPa)	Std. deviation
7	56.28	1.86
28	66.28	1.92
56	69.86	1.35
180	70.76	2.05

Table C.2 Compressive strengths of Concrete (FAFNS50: 30% Fly ash & 70% OPC as a binder and 50% FNS)

Duration (days)	Average (MPa)	Std. deviation
7	41.63	1.71
28	51.04	1.64
56	56.52	2.85
180	66.54	2.16

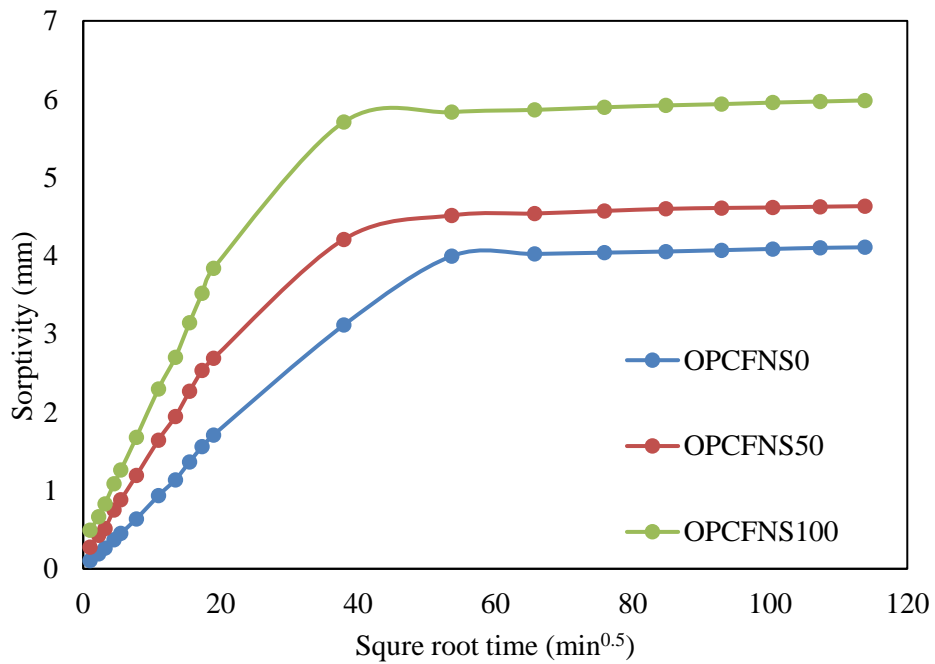


Fig. C.1 Sorptivity Test (100% OPC binder)

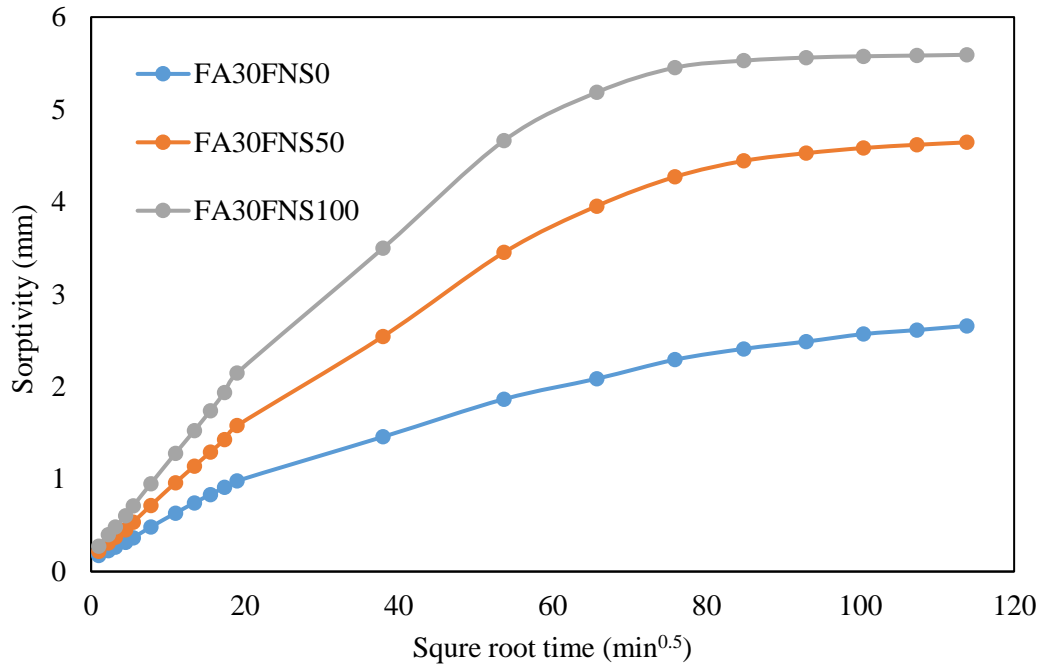


Fig. C.2 Sorptivity Test (30% fly ash and 70% OPC binder)

Table C.3 Absorption Test (100% OPC as binder)

Mix ID	Absorption (%)
PCFNS0	2.45
PCFNS50	3.74
PCFNS100	4.62

Table C.4 Absorption Test (30% fly ash 70% OPC as binder)

Mix ID	Absorption (%)
FAFNS0	2.42
FAFNS50	3.44
FAFNS100	4.09

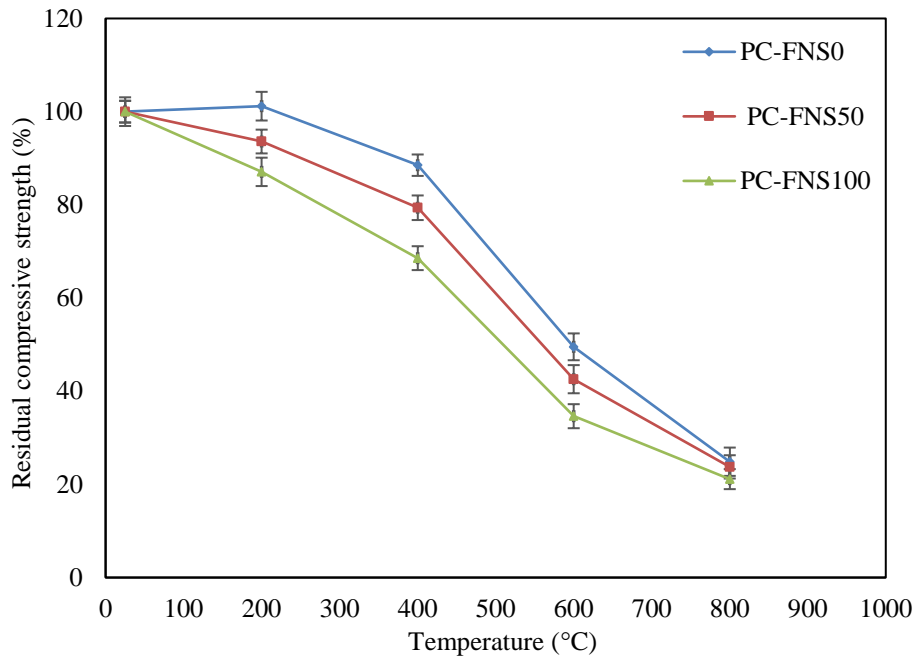


Fig. C.3 Residual strength at different temperature exposure while 100% OPC as binder

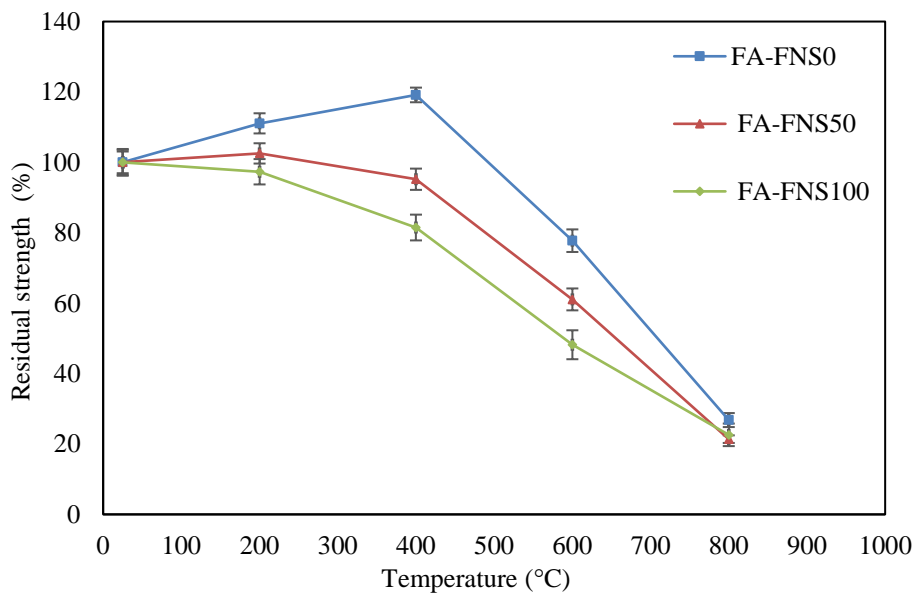


Fig. C.4 Residual strength at different temperature exposure while 30% fly ash & 70% OPC as binder

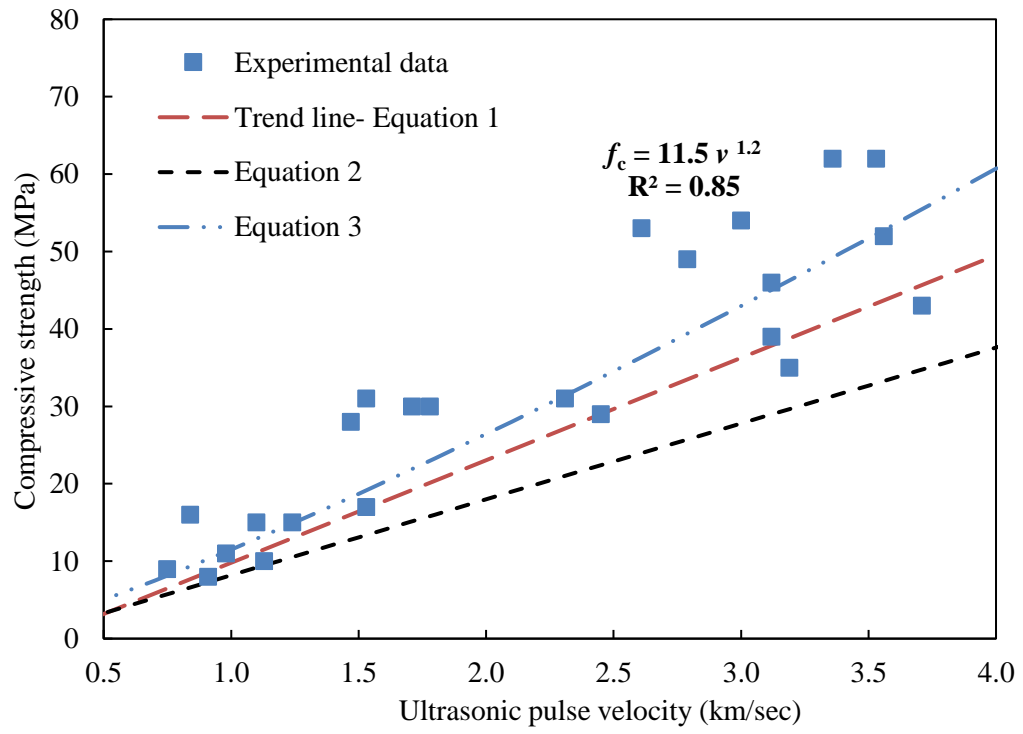


Fig. C.5 Relationship between residual compressive strength and UPV

APPENDIX D: Attribution of research outputs

Article 1.

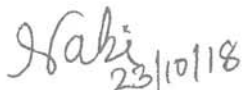
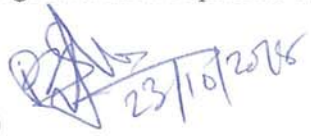
Saha, A. K., Khan, M. N. N., & Sarker, P. K. (2018). Value added utilization of by-product electric furnace ferronickel slag as construction materials: A review. Resources, Conservation and Recycling, 134, 10-24.

Authors and full affiliations:

AK Saha, PhD student, Dept. of Civil Engineering, Curtin University, WA

MNN Khan, PhD student, Dept. of Civil Engineering, Curtin University, WA

Dr PK Sarker, Associate prof., Dept. of Civil Engineering, Curtin University, WA

Name of Co-author	Literature review	Experimental design/ concept	Data collection	Discussion	Paper writing
MNN Khan				×	×
I acknowledge that these represent my contribution to the above research output.					
 (Signature) 23/10/18					
PK Sarker				×	×
I acknowledge that these represent my contribution to the above research output.					
 (Signature) 23/10/2018					

Article 2.

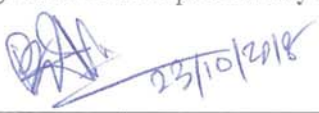

Saha, A. K., Sarker, P. K., & Majhi, S. (2018). Effect of elevated temperatures on concrete incorporating ferronickel slag as fine aggregate. Fire and Materials. Doi: 10.1002/fam.2664

Authors and full affiliations:

AK Saha, PhD student, Dept. of Civil Engineering, Curtin University, WA

Dr PK Sarker, Associate prof., Dept. of Civil Engineering, Curtin University, WA

S Majhi, PhD student, Dept. of Civil Engineering, Curtin University, WA

Name of Co-author	Literature review	Experimental design/concept	Data collection	Data analysis	Discussion	Paper writing
PK Sarker		×		×	×	×
I acknowledge that these represent my contribution to the above research output.						
(Signature)						
S Majhi			×	×		×
I acknowledge that these represent my contribution to the above research output.						
(Signature)						

Article 3 to 8.

3. Saha, A. K., & Sarker, P. K. (2018). Durability of Mortar Incorporating Ferronickel Slag Aggregate and Supplementary Cementitious Materials Subjected to Wet–Dry Cycles. *International Journal of Concrete Structures and Materials*, 12(1), 29.
4. Saha, A. K., & Sarker, P. K. (2018). Potential alkali silica reaction expansion mitigation of ferronickel slag aggregate by fly ash. *Structural Concrete*.
Doi:10.1002/suco.201700273
5. Saha, A. K., & Sarker, P. K. (2017). Sustainable use of ferronickel slag fine aggregate and fly ash in structural concrete: mechanical properties and leaching study. *Journal of Cleaner Production*, 162, 438-448.
6. Saha, A. K., & Sarker, P. K. (2017). Durability characteristics of concrete using ferronickel slag fine aggregate and fly ash. *Magazine of Concrete Research*, 70(17), 865–874
7. Saha, A. K., & Sarker, P. K. (2017). Compressive strength of mortar containing ferronickel slag as replacement of natural sand. *Procedia Engineering*, 171, 689-694.
8. Saha, A. K., & Sarker, P. K. (2016). Expansion due to alkali-silica reaction of ferronickel slag fine aggregate in OPC and blended cement mortars. *Construction and Building Materials*, 123, 135-142.

Authors and full affiliations:


AK Saha, PhD student, Dept. of Civil Engineering, Curtin University, WA

Dr PK Sarker, Associate prof., Dept. of Civil Engineering, Curtin University, WA

Co-author Attribution Dr PK Sarker,

Article number	Literature review	Experimental design/concept	Data collection	Data analysis	Discussion	Paper writing
3					×	×
4		×		×	×	×
5		×		×		×
6		×		×	×	×
7					×	×
8		×		×	×	×

I acknowledge that these represent my contribution to the above research output.


(Signature)

APPENDIX E: Copyright Permission

1. Saha, A. K., Khan, M. N. N., & Sarker, P. K. (2018). Value added utilization of by-product electric furnace ferronickel slag as construction materials: A review. *Resources, Conservation and Recycling*, 134, 10-24.

Permission:

30/05/2018

Rightslink® by Copyright Clearance Center

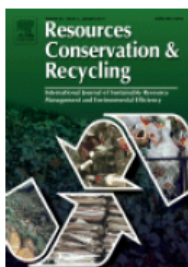


RightsLink®

Home

Create Account

Help



Title: Value added utilization of by-product electric furnace ferronickel slag as construction materials: A review

Author: Ashish Kumer Saha, M.N.N. Khan, Prabir Kumar Sarker

Publication: Resources, Conservation and Recycling

Publisher: Elsevier

Date: July 2018

© 2018 Elsevier B.V. All rights reserved.

LOGIN

If you're a **copyright.com** user, you can login to RightsLink using your copyright.com credentials. Already a **RightsLink** user or want to [learn more?](#)

Please note that, as the author of this Elsevier article, you retain the right to include it in a thesis or dissertation, provided it is not published commercially. Permission is not required, but please ensure that you reference the journal as the original source. For more information on this and on your other retained rights, please visit: <https://www.elsevier.com/about/our-business/policies/copyright#Author-rights>

2. Saha, A. K., & Sarker, P. K. (2017). Compressive strength of mortar containing ferronickel slag as replacement of natural sand. *Procedia engineering*, 171, 689-694.

Permission:

30/05/2018

Rightslink® by Copyright Clearance Center

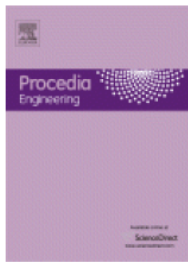


RightsLink®

Home

Create Account

Help



Title: Compressive Strength of Mortar Containing Ferronickel Slag as Replacement of Natural Sand
Author: Ashish Kumer Saha,Prabir Kumar Sarker
Publication: Procedia Engineering
Publisher: Elsevier
Date: 2017

© 2017 The Author(s). Published by Elsevier Ltd.

LOGIN
If you're a **copyright.com user**, you can login to RightsLink using your copyright.com credentials. Already a **RightsLink user** or want to [learn more?](#)

Please note that, as the author of this Elsevier article, you retain the right to include it in a thesis or dissertation, provided it is not published commercially. Permission is not required, but please ensure that you reference the journal as the original source. For more information on this and on your other retained rights, please visit: <https://www.elsevier.com/about/our-business/policies/copyright#Author-rights>

3. Saha, A. K., & Sarker, P. K. (2017). Sustainable use of ferronickel slag fine aggregate and fly ash in structural concrete: mechanical properties and leaching study. *Journal of Cleaner Production*, 162, 438-448.

30/05/2018

Rightslink® by Copyright Clearance Center

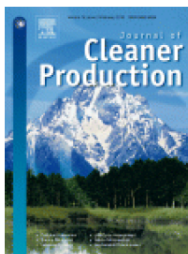


RightsLink®

Home

Create Account

Help



Title: Sustainable use of ferronickel slag fine aggregate and fly ash in structural concrete: Mechanical properties and leaching study
Author: Ashish Kumer Saha,Prabir Kumar Sarker
Publication: Journal of Cleaner Production
Publisher: Elsevier
Date: 20 September 2017

© 2017 Elsevier Ltd. All rights reserved.

LOGIN
If you're a **copyright.com user**, you can login to RightsLink using your copyright.com credentials. Already a **RightsLink user** or want to [learn more?](#)

Please note that, as the author of this Elsevier article, you retain the right to include it in a thesis or dissertation, provided it is not published commercially. Permission is not required, but please ensure that you reference the journal as the original source. For more information on this and on your other retained rights, please visit: <https://www.elsevier.com/about/our-business/policies/copyright#Author-rights>

4. Saha, A. K., & Sarker, P. K. (2018). Potential alkali silica reaction expansion mitigation of ferronickel slag aggregate by fly ash. *Structural Concrete*, 19(5), 1376-1386.

JOHN WILEY AND SONS LICENSE TERMS AND CONDITIONS

Mar 17, 2019

This Agreement between Ashish Kumer saha ("You") and John Wiley and Sons ("John Wiley and Sons") consists of your license details and the terms and conditions provided by John Wiley and Sons and Copyright Clearance Center.

License Number	4551660135516
License date	Mar 17, 2019
Licensed Content Publisher	John Wiley and Sons
Licensed Content Publication	Structural Concrete
Licensed Content Title	Potential alkali silica reaction expansion mitigation of ferronickel slag aggregate by fly ash
Licensed Content Author	Ashish K. Saha, Prabir K. Sarker
Licensed Content Date	May 2, 2018
Licensed Content Volume	19
Licensed Content Issue	5
Licensed Content Pages	11
Type of Use	Dissertation/Thesis
Requestor type	Author of this Wiley article
Format	Print and electronic
Portion	Full article
Will you be translating?	No
Title of your thesis / dissertation	Applicability of FNS aggregate in concrete
Expected completion date	Sep 2018
Expected size (number of pages)	1
Requestor Location	Ashish Kumer saha Department of civil Engg Curtin University Perth, Western Australia 6102 Australia Attn: Ashish Kumer saha
Publisher Tax ID	EU826007151

5. Saha, A. K., & Sarker, P. K. (2016). Expansion due to alkali-silica reaction of ferronickel slag fine aggregate in OPC and blended cement mortars. *Construction and Building Materials*, 123, 135-142.

30/05/2018

Rightslink® by Copyright Clearance Center

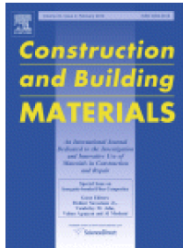


RightsLink®

Home

Create Account

Help



Title: Expansion due to alkali-silica reaction of ferronickel slag fine aggregate in OPC and blended cement mortars
Author: Ashish Kumer Saha, Prabir Kumar Sarker
Publication: Construction and Building Materials
Publisher: Elsevier
Date: 1 October 2016

LOGIN
 If you're a **copyright.com user**, you can login to RightsLink using your copyright.com credentials. Already a **RightsLink user** or want to [learn more?](#)

© 2016 Elsevier Ltd. All rights reserved.

Please note that, as the author of this Elsevier article, you retain the right to include it in a thesis or dissertation, provided it is not published commercially. Permission is not required, but please ensure that you reference the journal as the original source. For more information on this and on your other retained rights, please visit: <https://www.elsevier.com/about/our-business/policies/copyright#Author-rights>

6. Saha, A. K., & Sarker, P. K. (2017). Durability characteristics of concrete using ferronickel slag fine aggregate and fly ash. *Magazine of Concrete Research*, 70(17), 865–874.

Magazine of concrete research

Order detail ID: 71220663
Order License Id: 4360000061667
ISSN: 0024-9831
Publication Type: Journal
Volume:
Issue:
Start page:
Publisher: THOMAS/TELFORD LTD.
Author/Editor: CEMENT AND CONCRETE ASSOCIATION

Permission Status: **Granted**
Permission type: Republish or display content
Type of use: Republish in a thesis/dissertation
[Hide details](#)
Requestor type: Academic institution
Format: Print, Electronic
Portion: chapter/article
The requesting person/organization: Ashis Kumer Sha
Title or numeric reference of the portion(s): Full article
Title of the article or chapter the portion is from: Durability characteristics of concrete using ferronickel slag fine aggregate and fly ash

7. Saha, A. K., Sarker, P. K., & Majhi, S. *Effect of elevated temperatures on concrete incorporating ferronickel slag as fine aggregate. Fire and Materials*, 43(1), 8-21.

18/03/2019

RightsLink Printable License

**JOHN WILEY AND SONS LICENSE
TERMS AND CONDITIONS**

Mar 17, 2019

This Agreement between Ashish Kumer saha ("You") and John Wiley and Sons ("John Wiley and Sons") consists of your license details and the terms and conditions provided by John Wiley and Sons and Copyright Clearance Center.

License Number	4551660787898
License date	Mar 17, 2019
Licensed Content Publisher	John Wiley and Sons
Licensed Content Publication	Fire and Materials
Licensed Content Title	Effect of elevated temperatures on concrete incorporating ferronickel slag as fine aggregate
Licensed Content Author	Subhra Majhi, Prabir Kumar Sarker, Ashish Kumer Saha
Licensed Content Date	Jul 31, 2018
Licensed Content Volume	43
Licensed Content Issue	1
Licensed Content Pages	14
Type of use	Dissertation/Thesis
Requestor type	Author of this Wiley article
Format	Print and electronic
Portion	Full article
Will you be translating?	No
Title of your thesis / dissertation	Applicability of FNS aggregate in concrete
Expected completion date	Sep 2018
Expected size (number of pages)	1
Requestor Location	Ashish Kumer saha Department of civil Engg Curtin University Perth, Western Australia 6102 Australia Attn: Ashish Kumer saha
Publisher Tax ID	EU826007151